PROPERTIES OF BIODEGRADABLE DUALLY MODIFIED CASSAVA STARCH FILMS FROM CROSS-LINKING AND OXIDATION

A THESIS SUBMITTED IN PARTIAL FULFILLMENT OF THE REQUIREMENT FOR THE DEGREE OF DOCTOR OF PHILOSOPHY IN APPLIED CHEMISTRY
DEPARTMENT OF CHEMISTRY FACULTY OF SCIENCE
KING MONGKUT'S INSTITUTE OF TECHNOLOGY LADKRABANG
2019

KMITL-2019-SC-D-010-042

PROPERTIES OF BIODEGRADABLE DUALLY MODIFIED CASSAVA STARCH FILMS FROM CROSS-LINKING AND OXIDATION

YOSSATHORN TANETRUNGROJ

A THESIS SUBMITTED IN PARTIAL FULFILLMENT OF THE REQUIREMENT FOR THE DEGREE OF DOCTOR OF PHILOSOPHY IN APPLIED CHEMISTRY
DEPARTMENT OF CHEMISTRY FACULTY OF SCIENCE
KING MONGKUT'S INSTITUTE OF TECHNOLOGY LADKRABANG
2019

KMITL-2019-SC-D-010-042

Thesis Title	Properties of biodegradable dually modified cassava starch films from cross-linking and oxidation
Student Name	Mr. Yossathorn Tanetrungroj
Student ID	57605005
Degree	Doctor of Philosophy (Applied Chemistry)
Department	Chemistry
Year	2019
Thesis Advisor	Assoc. Prof. Dr. Jutarat Prachayawarakorn

Abstract

In this study, native cassava starch (NS) film was modified by both cross-linking and oxidation processes in order to improve its weak mechanical and high water absorption properties. Crosslinked-oxidized starch (COS) film and oxidized-crosslinked starch (OCS) film were prepared and compared with singly modified starch films, i.e., oxidized starch (OS) film and crosslinked (CS) starch film. The dually modified starch films were prepared by a casting technique with hydrogen peroxide as an oxidizing agent and different types of cross-linking agents, i.e., boric acid, borax and a mixture of sodium trimetaphosphate (STMP)/sodium tripolyphosphate (STPP). Several properties of the biodegradable starch films were investigated. The results revealed that the degrees of crosslinking of all COS samples were slightly lower than those of CS samples, but higher than those of OCS samples. On the contrary, the carbonyl and carboxyl contents of OCS were indentical to that of OS, but higher than those of COS. The successful cross-linking and oxidation of modified starch and modified starch films were confirmed by an FT-IR study, which showed a decrease in intensity of hydrogen bonding and additional peaks of C=O stretching, arising from carbonyl and carboxyl groups of all modified starch. The morphology of starch granules was completely destroyed in the case of OS and OCS, while a rough surface and the presence of some relatively unmolten starch granules were found for the cases of CS and COS samples. The thermal property of NS was improved by crosslinking and crosslinking-oxidation; however, the oxidation caused a decline in the thermal property of NS. For property of modified starch films, the degrees of crystallinity were reduced in the cases of OS, COS and OCS films. A rough fractured surface and the presence of some relatively unmolten starch granules were found in CS and COS films, while OS and OCS films showed smooth surface. The strength, extensibility and hydrophobic property (WVP and degree of swelling) of CS and OS films were improved by both dual modifications, especially for COS films. All modified starch films showed biodegradability by a soil burial test. The thermal

property of CS and COS films were clearly improved, and the decrease in thermal property was pronounced in OS and OCS films. All modified starch films crosslinked with borax showed the greatest overall results (highest strength and hydrophobic property). On the other hand, the lowest overall results was found in starch film crosslinked with the mixture of STMP/STPP.

Keywords : Biodegradable film, Crosslinked starch, Dual-modification, Oxidized starch

Acknowledgements

I would like to thank my advisor Assoc. Prof. Dr. Jutarat Prachayawarakorn for giving advice and positive encouragement on this work throughout the whole project. I would also like to thank Asst. Prof. Dr. Chidchanok Meechaisue, Asst. Prof. Dr. Patchanee Charoenying, Assoc. Prof. Dr. Somsak Woramongkolchai and Asst. Prof. Dr. Panpailin Seeharaj for their helpful suggestions on this thesis work. In addition, I would like to thank KMITL research and innovation services' proofreaders, Mr. Pratana Kangsadal and Assoc. Prof. Dr. John Morris, who have kindly proofread and edited the English in this thesis. I am grateful for the financial support provide by KMITL Research Fund (KREF 046108. I would like to thank all friends and staff member in the chemistry department for helping me with technical problems. Finally, I would like to express eternal gratitude to my parents for their support and helpful encouragement.

Yossathorn Tanetrungroj

Table of Contents

	Page
Abstract in English	i
Acknowledgements	iii
Table of Contents	iv
List of Tables	viii
List of Figures	x
Abbreviations/Symbols	xv
Chapter 1 Introduction	1
1.1 Research Motivation	1
1.2 Objectives of the study	3
1.3 Scope(s) of the study	3
1.4 Benefits of the study	3
Chapter 2 Theory and Literature Reviews	4
2.1 Biodegradable plastic	4
2.1.1 Applications of biodegradable plastic	4
2.1.2 Biodegradability test method of biodegradable plastic	4
2.1.2.1 Soil burial method	4
2.1.2.2 Culture of fungi or bacteria	4
2.1.2.3 Enzymatic degradation	5
2.2 Starch	5
2.2.1 The main components of starch	5
2.2.1.1 Amylose	6
2.2.1.1 Amylopectin	7
2.2.2 Crystalline form of starch	8
2.2.3 Properties of starch	9
2.2.3.1 Starch swelling and pasting	9
2.2.3.2 Starch gelatinization	11
2.2.3.3 Retrogradation of starch	13
2.3 Cassava starch	14
2.4 Modified starch	15
2.4.1 Classification of modified starch	15
2.4.1.1 Chemically modified starch	15
2.4.1.2 Physically modified starch	18
2.4.1.3 Enzymatically modified starch	19
2.4.2 Terminology and definition	19
2.4.2.1 Carbon position (C-) in AGU	19

Table of Contents (continued)

Page

2.4.2.2 Degree of polymerization (DP) 20
2.4.2.3 Dextrose equivalent (DE) or reducing value 20
2.4.2.4 Alkali number 21
2.4.2.5 Percent substitution 21
2.4.2.6 Degree of substitution (DS) 21
2.4.2.7 β-amylase digestibility 21
2.5 Dual modification 22
2.5.1 Acetylation-cross-linking 22
2.5.2 Acetylation-hydroxypropylation 22
2.5.3 Hydroxypropylation-etherification 22
2.5.4 Oxidation-cross-linking 22
2.5.5 Cross-linking-oxidation 22
2.6 Hydrogen peroxide 23
2.7 Borax 26
2.7.1 Applications of borax 27
2.8 Boric acid 29
2.8.1 Applications of boric acid 29
2.9 Sodium trimethaphosphate (STMP) 31
2.10 Sodium tripolyphosphate (STPP) 33
2.10.1 Functions of STPP in food and commercial applications 33
2.11 Plasticization 35
2.11.1 Glycerol 35
2.12 Literature Reviews 37
Chapter 3 Research methodology 42
3.1 Materials 42
3.2 Instruments 43
3.3 Method 46
3.3.1 Preparation of singly modified starch 46
3.3.1.1 Preparation of crosslinked starch (CS) 46
3.3.1.2 Preparation of oxidized starch (OS) 46
3.3.2 Preparation of dually modified starch 47
3.3.1.1 Preparation of crosslinked-oxidized starch (COS) 47
3.3.1.2 Preparation of oxidized-crosslinked starch (OCS) 47
3.3.3 Preparation of biodegradable film by different types of modified starch 47

Table of Contents (continued)

Page

3.4 Characterization 48
3.4.1 Average molecular weight 48
3.4.2 Carbonyl content (%) 48
3.4.3 Carboxyl content (%) 49
3.4.4 Degree of cross-linking 50
3.4.5 Fourier-transform infrared spectroscopy (FT-IR) 50
3.4.6 X-ray diffraction technique (XRD) 50
3.4.7 Scanning electron microscopy (SEM) 51
3.4.8 Swelling behavior 51
3.4.9 Water vapor permeability test (WVP) 51
3.4.10 Mechanical properties 51
3.4.11 Thermogravimetric analysis (TGA) 52
3.4.12 Biodegradability 52
Chapter 4 Main results and discussion 53
4.1 Properties of differently modified starch 54
4.1.1 Schematic reactions of differently modified starch 54
4.1.2 Degree of cross-linking, carbonyl content and carboxyl content of differently modified starch 58
4.1.3 FT-IR study 61
4.1.4 Morphological properties 67
4.1.5 Intrinsic viscosity and molecular weight 71
4.1.6 Thermogravimetric analysis 72
4.2 Properties of different modified starch films 79
4.2.1 FT-IR study 79
4.2.2 X-ray diffraction 84
4.2.3 Morphological properties 89
4.2.4 Degree of swelling 94
4.2.5 Water vapor permeability (WVP) 97
4.2.6 Mechanical properties 100
4.2.7 Biodegradability properties 105
4.2.8 Thermal property 113
Chapter 5 Conclusions and suggestions 120
5.1 Conclusions 120
5.1.1 Properties of different modified starch 120
5.1.2 Properties of different biodegradable modified starch films 121

Table of Contents (continued)

Page

5.2 Suggestions 122
References 123
Appendices 128
Appendix A 129
Appendix B 140
Appendix C 151
Appendix D 157
Appendix E 159
Appendix F 160
Author biography 162

List of Tables

Table		Page
2.1	Differences in various characteristics between amylose and amylopectin	6
2.2	Components of starch: the percentage of major components amylose and amylopectin (A) and minor components (B)	8
2.3	Starch gelatinization temperature range	12
2.4	The components of cassava starch	15
2.5	Properties of hydrogen peroxide	24
2.6	MSDS of hydrogen peroxide	25
2.7	Properties of borax	28
2.8	MSDS of borax	28
2.9	Properties of boric acid	30
2.10	MSDS of boric acid	30
2.11	Properties of STMP	32
2.12	MSDS of STMP	32
2.13	Properties of STPP	34
2.14	MSDS of STPP	34
2.15	Properties of glycerol	36
2.16	MSDS of glycerol	36
3.1	The components of cassava starch	42
3.2	Compositions of different modified starch	48
4.1	Abbreviations and symbols	53
4.2	Degree of cross-linking and carbonyl and carboxyl contents of differently modified starch	59
4.3	Peak assignment of the characteristic bands of the FT-IR spectrum of differently modified starch	61
4.4	Peak heights and ratios of peak height of NS and different singly modified starch	62
4.5	Peak heights and ratios of peak height of NS and different COS samples	63
4.6	Peak heights and ratios of peak heights of different OCS samples	64
4.7	Peak heights and ratios of peak heights of differently modified starch crosslinked with borax and oxidized with hydrogen peroxide	66
4.8	Intrinsic viscosity and MW of NS and differently modified starch	71
4.9	Degradation temperatures of NS and differently modified starch determined from TG and DTG thermograms	76

List of Tables (continued)

Table **Page**

4.10 Degradation temperatures of NS and differently modified starch crosslinked with borax and oxidized with hydrogen peroxide determined from TG and DTG thermograms 79
4.11 Peak heights and ratios of peak heights of various singly modified starch films 80
4.12 Peak heights and ratios of peak heights of various COS films 82
4.13 Peak heights and ratios of peak heights of various OCS films 83
4.14 Peak heights and ratios of peak heights of various modified starch films crosslinked with borax and oxidized with hydrogen peroxide 84
4.15 Degree of crystallinity of various modified starch films 86
4.16 Degree of crystallinity of various modified starch films crosslinked with borax and oxidized with hydrogen peroxide 88
4.17 WVP values of various modified starch films 98
4.18 WVP values of NS film and various modified starch films crosslinked with borax and oxidized with hydrogen peroxide 99
4.19 Percentage reductions of mechanical properties of various modified starch films after 5 and 10 days of biodegradation in soil 109
4.20 Percentage reductions of the mechanical properties of various modified starch films crosslinked with borax and oxidized with hydrogen peroxide after 5 and 10 days of biodegradation in soil 112
4.21 Degradation temperatures of NS film and various modified starch films 116
4.22 Degradation temperatures of NS film and various modified starch films crosslinked with borax and oxidized with hydrogen peroxide 119

List of Figures

Figure	Page
2.1 The chemical structure of amylose	7
2.2 The chemical structure of amylopectin	7
2.3 X-ray diffraction patterns of starch	9
2.4 Swelling of starch granules	10
2.5 Gelatinization and retrogradation of starch	12
2.6 Schematic structure of crosslinked polymer	17
2.7 Numbering system for carbons position in AGU	20
2.8 Dextrose equivalents (DE) of dextrose and maltose	20
2.9 Preparation of OS by hydrogen peroxide	24
2.10 Chemical structure of borax	26
2.11 The formation of a tetrahydroxy borate crosslink from borax	27
2.12 Chemical structure of boric acid	29
2.13 Preparation of starch borate by boric acid	29
2.14 Chemical structure of STMP	31
2.15 Preparation of distarch phosphate by STMP	31
2.16 Chemical structure of STPP	33
2.17 Chemical reaction of preparation of distarch phosphate with STPP	33
2.18 Chemical structure of glycerol	35
3.1 Flowchart of preparation of different modified starch	44
3.2 Flowchart of preparation of different modified starch films	45
4.1 Schematic structure of CS crosslinked with borax	55
4.2 Schematic structure of CS crosslinked with boric acid	55
4.3 Schematic structure of CS crosslinked with STMP/STPP	56
4.4 Chemical reaction of OS oxidized with hydrogen peroxide	56
4.5 Schematic structures of COS and OCS crosslinked with borax and oxidized with hydrogen peroxide	57
4.6 Schematic structures of COS and OCS crosslinked with boric acid and oxidized with hydrogen peroxide	57
4.7 Schematic structures of COS and OCS crosslinked with the mixture of STMP/STPP and oxidized with hydrogen peroxide	58
4.8 FT-IR spectra of NS and different singly modified starch (a) NS (b) CS-BO (c) CS-BA (d) CS-ST and (e) OS	61
4.9 FT-IR spectra of NS and different COS samples crosslinked with different cross-linking agents and oxidized with hydrogen peroxide (a) NS (b) COS-BO (c) COS-BA and (d) COS-ST	63

List of Figures (continued)

Figure **Page**

4.10 FT-IR spectra of NS and different OCS samples crosslinked with different types of cross-linking agent and oxidized with hydrogen peroxide and (a) NS (b) OCS-BO (c) OCS-BA and (d) OCS-ST 64

4.11 FT-IR spectra of differently modified starch crosslinked with borax and oxidized with hydrogen peroxide (a) NS (b) CS-BO (c) OS (d) COS-BO and (e) OCS-BO 65

4.12 SEM micrographs at 4000X magnification of NS and different singly modified starch (a) NS (b) CS-BO (c) CS-BA (d) CS-ST and (e) OS 67

4.13 SEM micrographs at 4000X magnification of NS and different COS crosslinked with different types of cross-linking agents and oxidized with hydrogen peroxide (a) NS (b) COS-BO (c) COS-BA and (d) COS-ST 68

4.14 SEM micrographs at 4000X magnification of NS and different OCS crosslinked with different types of cross-linking agents and oxidized with hydrogen peroxide (a) NS (b) OCS-BO (c) OCS-BA and (d) OCS-ST 69

4.15 SEM micrographs at 4000X magnification of differently modified starch crosslinked with borax and oxidized with hydrogen peroxide (a) NS (b) CS-BO (c) OS (d) COS-BO and (e) OCS-BO 70

4.16 Thermograms of NS and different singly modified starch (a) TGA and (b) DTG 73

4.17 Thermograms of NS and different COS crosslinked with different types of cross-linking agents and oxidized with hydrogen peroxide (a) TGA and (b) DTG 74

4.18 Thermograms of NS and different OCS crosslinked with different types of cross-linking agents and oxidized with hydrogen peroxide (a) TGA and (b) DTG 75

4.19 Thermograms of NS and differently modified starch crosslinked with borax and oxidized with hydrogen peroxide (a) TGA and (b) DTG 78

4.20 FT-IR spectra of NS film and various singly modified starch films: (a) NSF, (b) CS-BOF, (c) CS-BAF, (d) CS-STF and (e) OSF 80

4.21 FT-IR spectra of NS film and various COS films crosslinked with different cross-linking agents and oxidized with hydrogen peroxide (a) NSF, (b) COS-BOF, (c) COS-BAF and (d) COS-STF 81

4.22 FT-IR spectra of NS film and various OCS films crosslinked with different cross-linking agents and oxidized with hydrogen peroxide (a) NSF, (b) OCS-BOF, (c) OCS-BAF and (d) OCS-STF 82

List of Figures (continued)

Figure **Page**

4.23 FT-IR spectra of various modified starch films crosslinked with borax and oxidized with hydrogen peroxide (a) NS, (b) CS-BO, (c) OS, (d) COS-BO, and (e) OCS-BO 83

4.24 X-ray diffraction patterns of NS film and various singly modified starch films (a) NSF, (b) CS-BOF, (c) CS-BAF, (d) CS-STF and (e) OSF 85

4.25 X-ray diffraction patterns of NS film and various COS films crosslinked with different cross-linking agents and oxidized with hydrogen peroxide (a) NSF, (b) COS-BOF, (c) COS-BAF and (d) COS-STF 85

4.26 X-ray diffraction patterns of NS film and various OCS films crosslinked with different cross-linking agents and oxidized with hydrogen peroxide (a) NSF, (b) OCS-BOF, (c) OCS-BAF and (d) OCS-STF 86

4.27 X-ray diffraction patterns of various modified starch films crosslinked with borax and oxidized with hydrogen peroxide (a) NSF (b) CS-BOF (c) OSF (d) COS-BOF and (e) OCS-BOF 88

4.28 SEM micrographs at 4000X magnification of NS film and various singly modified starch films (a) NSF, (b) CS-BOF, (c) CS-BAF, (d) CS-STF and (e) OSF 89

4.29 SEM micrographs at 4000X magnification of NS film and various COS films crosslinked with different types of cross-linking agents and oxidized with hydrogen peroxide (a) NSF, (b) COS-BOF, (c) COS-BAF and (d) COS-STF 91

4.30 SEM micrographs at 4000X magnification of NS film and various OCS films crosslinked with different types of cross-linking agents and oxidized with hydrogen peroxide (a) NSF, (b) OCS-BOF, (c) OCS-BAF and (d) OCS-STF 92

4.31 SEM micrographs at 4000X magnification of various modified starch films crosslinked with borax and oxidized with hydrogen peroxide (a) NSF, (b) CS-BOF, (c) OSF, (d) COS-BOF, and (e) OCS-BOF 93

4.32 Degree of swelling at 100% RH versus immersion time of NS and various singly modified films 94

4.33 Degree of swelling at 100% RH versus immersion time of NS film and various COS films crosslinked with different types of cross-linking agents and oxidized with hydrogen peroxide 95

4.34 Degree of swelling at 100%RH versus immersion time of NS film and various OCS films crosslinked with different types of cross-linking agents and oxidized with hydrogen peroxide 96

List of Figures (continued)

Figure **Page**

4.35 Degree of swelling at 100%RH versus immersion time of NS film and various modified starch films crosslinked with borax and oxidized with hydrogen peroxide 97

4.36 Mechanical properties of NS film and various singly modified starch films (a) stress at maximum load, (b) Young's modulus and (c) strain at maximum load 100

4.37 Mechanical properties of various COS films crosslinked with different types of cross-linking agent and oxidized with hydrogen peroxide (a) stress at maximum load, (b) Young's modulus and (c) strain at maximum load..... 102

4.38 Mechanical properties of various OCS films crosslinked with different types of cross-linking agent and oxidized with hydrogen peroxide (a) stress at maximum load, (b) Young's modulus and (c) strain at maximum load..... 103

4.39 Mechanical properties of various modified films crosslinked with borax and oxidized with hydrogen peroxide (a) stress at maximum load, (b) Young's modulus and (c) strain at maximum load 104

4.40 Mechanical properties after biodegradation in soil of various singly modified films (a) stress at maximum load, (b) Young's modulus and (c) strain at maximum load 106

4.41 Mechanical properties after biodegradation in soil of various COS films crosslinked with different types of cross-linking agents and oxidized with hydrogen peroxide (a) stress at maximum load, (b) Young's modulus and (c) strain at maximum load..... 107

4.42 Mechanical properties after biodegradation in soil of various OCS films crosslinked with different types of cross-linking agents and oxidized with hydrogen peroxide (a) stress at maximum load, (b) Young's modulus and (c) strain at maximum load..... 108

4.43 Mechanical properties after biodegradation in soil of various modified starch films crosslinked with borax and oxidized with hydrogen peroxide (a) stress at maximum load, (b) Young's modulus and (c) strain at maximum load 111

4.44 Thermograms of NS film and various singly modified starch films (a) TGA and (b) DTG..... 113

4.45 Thermograms of NS film and various COS films crosslinked with different types of cross-linking agents and oxidized with hydrogen peroxide (a) TGA and (b) DTG 114

List of Figures (continued)

Figure **Page**

4.46 Thermograms of NS film and various OCS films crosslinked with different types of cross-linking agents and oxidized with hydrogen peroxide (a) TGA and (b) DTG 115

4.47 Thermograms of NS film and different modified starch films crosslinked with borax and oxidized with hydrogen peroxide (a) TGA and (b) DTG 118

Abbreviations/Symbols

NS	: Native starch
CS	: Crosslinked starch
OS	: Oxidized starch
COS	: Crosslinked-oxidized starch
OCS	: Oxidized-crosslinked starch
STMP	: Sodium trimetaphosphate
STPP	: Sodium tripolyphosphate
BO	: Borax
BA	: Boric acid
ST	: The mixture of sodium trimetaphosphate and sodium tripolyphosphate
HCl	: Hydrochloric acid
NaOH	: Sodium hydroxide
RVA	: Rapid visco analyzer
FT-IR	: Fourier-transform infrared spectroscopy
XRD	: X-ray diffraction
SEM	: Scanning electron microscopy
TGA	: Thermo gravimetric analysis
WVP	: Water vapor permeability
MW	: Molecular weight

Chapter 1
Introduction

1.1 Research Motivation

Currently, many synthetic polymers are utilized for food, household and foodstuff packaging, with a subsequent massive accumulation of non-degradable waste materials. Many researchers have focused on solving the problem of plastic waste by producing an alternative and environmentally friendly material. Usage of biodegradable biopolymer films can lead to lower environmental risk, hence these materials are of interest to many researchers due to their abundance, eco-friendly nature, renewability and low cost [1].

Among biopolymers, starch is one of the lowest-cost biodegradable polymers. It has already been academically researched and applied in a film packaging industry for a long period of time. Nevertheless, a native starch (NS) film has several limitations such as poor mechanical properties, high water affinity and low thermal stability that need to be improved [2].

Chemical modification of starch is one of the most widely used procedures for improving physicochemical properties of NS film. This method can be achieved by a variety of different chemical reactions such as acetylation, grafting, etherification, hydroxypropylation, oxidation and cross-linking [2-7]. Among these procedures, cross-linking has been utilized to improve starch granule stability with new covalent bonds and improve tensile strength of NS film. Crosslinked starch (CS) has been used in many applications, especially for thickening in many kinds of foods. Cross-linking agents such as epichlorohydrin and glutaraldehyde are highly toxic and unsuitable for use in food packaging applications. In this study, less toxic cross-linking agents—boric acid, borax and a mixture of sodium trimetaphosphate and sodium tripolyphosphate (STMP/STPP)—were investigated for modifying NS film because they were effective agents that did not pollute in the environment. Moreover, these chemicals are beneficial to plant growth [3-4]. Generally, different types of cross-linking agent affected different physiochemical and functional properties of the produced CS film. Typically, CS film exhibits high brittleness and water absorption but low flexibility [5].

Oxidation is a good method for altering the molecular structure of starch, reducing the viscosity and adding new functional groups (such as a carbonyl or carboxyl group) to NS film. Oxidized starch (OS) is normally prepared by reacting starch with an oxidizing agent under a controlled pH and temperature. OS is extensively utilized in paper, textile and food industries. OS film is highly flexible. Its

tensile strength was found to decrease after NS is processed by an oxidation method [6]. Hydrogen peroxide is one of the most interesting oxidizing agents because it does not form any harmful by-products as it readily decomposes into oxygen and water hence does not cause a high environmental impact [7]. However, OS film still does not have suitable properties such as proper mechanical properties and thermal stability for some applications.

To further improve some properties of NS, dual modification such as cross-linking-oxidizing or oxidizing-cross-linking is an effective method. Compared to a singly modified starch, a dually modified starch exhibits better tensile properties and thermal stability for a biodegradable film application. X. Xiao. *et al.* (2012) examined the physicochemical properties of NS, two singly modified starch (CS and OS) and two dually modified starch: crosslinked-oxidized starch (COS) and oxidized-crosslinked starch (OCS). They found that COS showed lower degree of swelling and lower solubility in water compared to NS. COS also exhibited the lowest tendency to retrograde and the highest shear resistant [8]. OCS and COS from elephant foot yam starch using sodium hypochlorite and the mixture of STMP/STPP were also prepared. It was found that both dual modifications caused the decrease in degree of crystallinity of starch; whereas, water absorption capacity, solubility and colour value (whiteness) were significantly increased [9]. G. Karmvlr *et al.* (2018) prepared COS and OCS from sodium hypochlorite and the mixture of STMP/STPP. The result showed a reduction in swelling power together with the enhancement in solubility and thermal property after the dual modification [10]. Dual modified starch from lotus rhizome starch using sodium hypochlorite and STMP exhibited the improvement of the water binding capacity, swell power, paste clarity and colour value (whiteness) of starch as compared to NS [11]. Most of the works on starch modification were focused on single modification of starch film and the effects of dual modification to starch granules. Nevertheless, a study on dual modification by cross-linking and oxidation as well as properties of the resulting biodegradable starch film has not been reported.

Therefore, the aim of this present research was to prepare and characterize dually modified starch films i.e., COS film and OCS film by using hydrogen peroxide as an oxidizing agent and three cross-linking agents—boric acid (BA), borax (BO) and a mixture of STMP and STPP (ST). The physicochemical properties of different modified starch films were comparatively investigated by Fourier transform infrared spectroscopy (FT-IR), X-ray diffractometry (XRD), scanning electron microscopy (SEM). In particular, the degree of swelling, water vapor permeability (WVP) as well as mechanical and thermal properties were evaluated. The film biodegradability was also determined by a soil burial test.

1.2 Objectives of the study

1) To experiment on a previous preparation process of a modified cassava starch regarding using different types of cross-linking agents.

2) To characterize singly and dually modified starch by cross-linking and oxidation.

3) To investigate the properties of biodegradable singly and dually modified starch films.

1.3 Scope of the study

This scope of this study is limited to preparation of singly and dually modified starch films with hydrogen peroxide and several cross-linking agents including boric acid, borax and STMP/STPP, characterization of biodegradable starch films by Fourier-transform infrared spectroscopy (FT-IR), X-ray diffractometry (XRD) and scanning electron microscopy (SEM) and measurement of several properties including water vapor permeability (WVP), percentage of swelling, tensile, thermal and biodegradable properties.

1.4 Benefits of the study

1) Higher tensile strength and lower water absorption tendency of biodegradable dually modified starch film.

2) Increased economic value of locally grown cassava.

3) Reduction of plastic waste disposal problems.

Chapter 2
Theory and Literature Reviews.

2.1 Biodegradable plastic

Biodegradable plastic is a degradable plastic that can be produced using oil or from plant-based items. They are assaulted by bacteria, parasites, yeasts or other micro-organisms which use them as sustenance. Certainly, edible bio-based materials are acceptable for producing of biodegradable plastics such as cellulose ethers, starch, hydroxypropylated starch, chitin, chitosan, zein, wheat gluten, soy proteins, milk proteins, etc. [12].

2.1.1 Applications of biodegradable plastic

1. Agriculture: container for transplanting seedlings, trees and other plants, seed cases, mulches, microencapsulations for the slow release of fertilizers, insecticides, fungicides, nematocides.

2. Medicine: surgical sutures, implants delivering medications in controlled manner.

3. Packaging: discardable containers and wrapping foils.

4. Miscellaneous: foils for prevention of erosion at freshly cultivated hill sides, sandbags for controlling floods [13].

2.1.2 Biodegradability test method of biodegradable plastic

There are three main groups of procedures for studying biological decomposition of plastic material [13].

2.1.2.1 Soil burial method

Standard samples of the material are buried in various soils, in outdoor location or under laboratory condition. From time to time, samples are withdrawn and analyzed for signs and quantitative characteristics of decomposition, such as weight loss, mechanical properties or a SEM examination. This method lacks reproducibility because of originality of soil (from garden soil to sewage sludge) and the difficulties in controlling climatic factors (temperature and humidity).

2.1.2.2 Culture of fungi or bacteria

More reproducible results can be obtained by using cultured fungi or bacteria. Commonly, the microbial degradability of synthetic polymers is studied by growth tests on solid agar media. Nutrient-salt agar is poured onto the sterile dishes and after the agar solidified, the medium is inoculated by spreading the fungus or bacteria

spore suspension throughout the surface of the agar. The polymer material is deposited on the inoculated agar surface. The test is run over a definite time (usually 3 weeks). The growth rate of inoculated fungi or bacteria is measured after incubation for a period of time.

2.1.2.3 Enzymatic degradation

Biodegradation proceeds in many cases via chemical reaction catalyzed by enzymes which are synthesized by microorganisms and have very specific action. Testing of biodegradation can be accelerated by using isolated and purified enzymes instead of the microbes themselves. Thus, the study of the detail of degradation is possible and reaction condition such as temperature, pH, pressure and irradiation may be easily varied.

2.2 Starch

Starch is a carbohydrate found principally in some algae and in all parts of higher plants including leaves, stems, shoots, rhizomes, tubers, bulbs and seeds. The empirical formula of the starch is $(C_6H_{10}O_5)_n$. Starch is an essential polysaccharide consisting of anhydroglucose monomer units, which connect to α-D-1,4 and 1,6 glucosidic linkages. The sizes of starch granules are ranging from about 1 to 1000 μm diameter depending on the starch sources. For cassava starch, the granular size range from 5 to 35 μm. In particular, the largest size is normally 25 to 35 μm and the smallest size is 5 to 15 μm [14].

2.2.1 The main components of starch

Starch mainly consists of two polymers, amylose and amylopectin. Most starch contains about 10 to 20% weights of amylose and 80 to 90% weights of amylopectin. Also, starch granules contain minor part of 0.10 to 0.14% weights of proteins, 0.03 to 0.20% weights of lipids, 0.09 to 0.63% weights of mineral and water. The lipids are found in corn, waxy rice, rice, wheat, maize, waxy maize and the phosphate are the part of phospholipids in starch. The storage starch in tuber (potato and cassava) has the phosphate attaching to the primary alcohol in glucose residues of amylopectin [15]. Starch contains varied ratio of amylose and amylopectin in different plants, resulting in different properties of plant starch. Table 2.1 presents the differences in various characteristics between amylose and amylopectin.

Table 2.1 Differences in various characteristics between amylose and amylopectin [15]

Property	Amylose	Amylopectin
Structure	Linear structure with D-glucose units	Linear and branched structure with D-glucose units
Chemical bond	α-D-1,4 glucosidic linkages	α-D-1,4 and 1,6 glucosidic linkages
Anhydroglucose units (AGU)	200-2000	More than 10000
Solubility in water	Less soluble in water	More soluble in water
Color change with iodine	Dark blue	Reddish brown
Hydrolysis with enzymes	Cannot be hydrolyzed with α and β-amylase enzymes	Can be hydrolyzed with α and β-amylase enzymes
Formation a gel	Does not form a gel with hot water	Form a gel with hot water

2.2.1.1 Amylose

Amylose is an essentially linear polysaccharide with glucose units connected through α-D-1,4 glucosidic linkage (often called AGU) as shown in Figure 2.1. Amylose is largely crystalline structure and normally comprises 1200 D-glucopyranoside units. Average molecular weight of amylose is reported to be in order to of 10^4 to 10^5. It can form a double helical structure, which stable formation in the solid state. In aqueous solution, it seems to be an expanded helix that behaves as a random coil structure. This polymer may be separated from the starch by completed gelatinization and vigorous dispersion of the hot starch solution with a reagent such as butanol in water. An amylose-butanol complex crystalline may be extracted by centrifugation. Amylose can form a complex with iodine giving a deep blue color which is used to identify amylose-containing starch. The level of amylose found in starch varies depending upon the starch source. Most starch such as regular corn, wheat, potato and cassava contains about 18 to 28% amylose. Corn and wheat are at the high end of the range, while potato and cassava are at the lower value about 16 to 22% amylose [15].

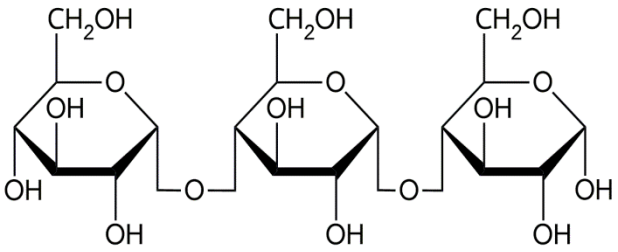

Figure 2.1 The chemical structure of amylose [15]

2.2.1.2 Amylopectin

Amylopectin is a branched polysaccharide of glucose residue containing AGU connected together with α-D-(1,4) glucosidic linkage with branching occurs with α-D-(1,6) glucosidic linkage at the C-6 position as shown in Figure 2.2. In most cases, amylopectin is much larger than amylose. Average molecular weight values of amylopectin are $61x10^6$-$112x10^6$ $g.mol^{-1}$. Amylopectin solutions are characterized by paste clarity, gelling resistance and stability on aging. For iodine test, amylopectin does not form an iodine complex with its associated deep blue coloration [15]. The amylose and amylopectin contents of different types of starch are presented in Table 2.2.

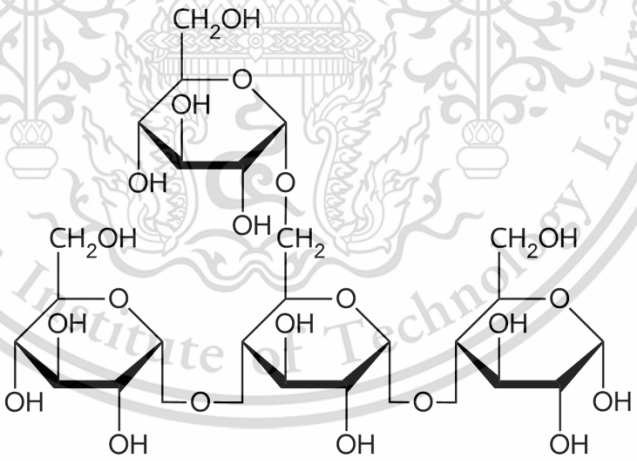

Figure 2.2 The chemical structure of amylopectin [15]

Table 2.2 Components of starch: the percentage of major components amylose and amylopectin (A) and minor components (B) [15]

Starch	Amylose[A] (%)	Amylopectin[A] (%)	Lipid[B] (%)	Protein[B] (%)	Phosphate[B] (%)
Potato	22	78	0.01	0.10	0.210
Maize	25	75	0.80	0.35	0.100
Waxy maize	0	100	0.32	0.15	0.032
Wheat	23	77	0.90	0.40	0.180
Rice	19	81	0.59	0.30	0.090
Cassava	18	82	0.02	0.10	0.009

2.2.2 Crystalline form of starch

The crystalline structure of starch is divided into A-, B- and C-types as shown in Figure 2.3. A- and B-types differ from each other by forming of double helical structures. For A-type, polymorphic structure orthogonal forming of more dense double helices occurs, while less dense hexagonal forming of double helices appears in B-type polymorphic structure. Typically, C-type contains both A- and B-type polymorphs. Another new types of crystalline structure, based on single helices of amylose are formed a period of time after thermoplastic starch is prepared and processed. These types are V_a (non-hydrated), V_h (hydrated) and E_h. The E_h type is not stable and is transformed to V_h by the effect of water. Furthermore, starch sources, the moisture conditions and contents of the plasticizer affect an important role in the recrystallization rate.

A-, B- or C-types of the starch depend on the origin of plant sources. In general, A-type appears in cereal starch (rice and maize), whereas B-type appears mostly in potato and other tuber starch. For C-type, most starch sources are found in pea starch. There are three different types of crystalline structure (A, B and C) for amylopectin within the crystalline lamellae. A-chains are related with one cluster while B-chains are involved in one, two or three clusters. A-chains are connected to the molecule only by their reducing ends. B-chains are connected to the molecule via their reducing ends. Furthermore, they are branched at a C-6 position in one or more of the D-glucopyranosyl residues. C-chains are the reducing end group [16].

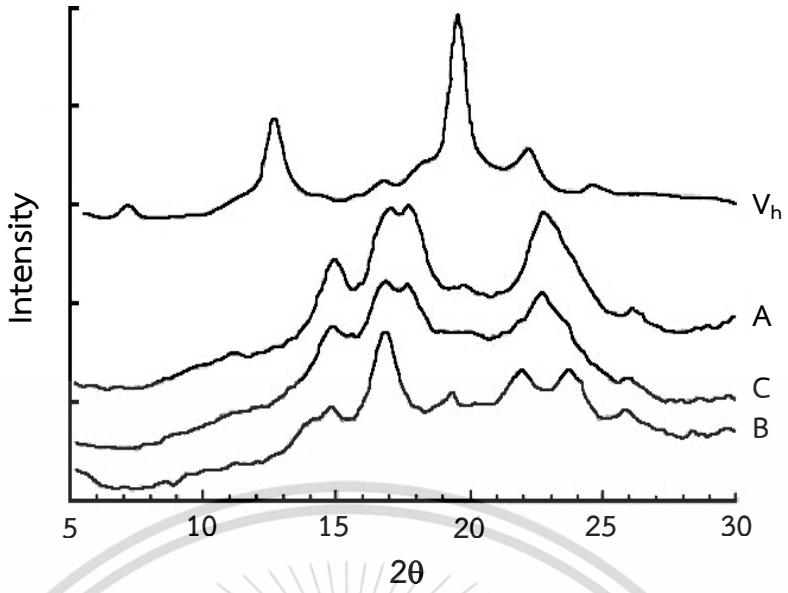

Figure 2.3 X-ray diffraction patterns of starch [17]

2.2.3 Properties of starch

2.2.3.1 Starch swelling and pasting

Several phenomena accompanied the heating of starch aqueous suspensions are observed from the loss of birefringence and partial solubilization of starch granules. As starch granules are heated in water, water molecules will penetrate into the amorphous regions to initiate starch swelling, nevertheless, which is restricted as the failure of water penetration into the crystalline regions. Starch swelling has been investigated to be mainly a property of amylopectin, while amylose and lipids affect for suppressing of starch swelling. Negative relationship is found between the amylose content and starch swelling; whereas, the lipid content does not negatively associate with starch swelling.

Measurements of the swelling power have been investigated as percentage of volume increases as well as percentage of weight increases. Relationship between degree of swelling and heating temperature has been studied by incubating starch and water suspensions at different temperatures for various periods of time. This observation was found that swelling factor increases with the increasing water/starch ratio. As the progressive increase in the incubation temperature such as 30-85°C and 60-95°C, increase in swelling power is also noticed, and the different magnitudes of increase among various starch have been related with the amylose to amylopectin ratio and amount of lipid-complex amylose chains. Moreover, at specific heating temperature, when various incubation times are employed to starch, swelling exhibits several phases.

As starch swelling proceeds the hydrogen bonds that hold the integrity of starch granules are disrupted by water molecules, which cause leaching of starch and further increase in granule swelling. Starch solubilization by leaching during starch swelling, or gelatinization, has largely been expressed as the measurement of solubilized starch content and amylose leaching, On the water-insoluble nature of amylose-lipid complex, the complexing of amylose and starch lipids during granule swelling can prevent partial amylose leaching, leading to decrease in the solubilization of water soluble carbohydrates. As an observation of the degree of starch chain interactions, starch swelling power and solubility will be affected by conditions that influence these chain interactions such as amylose/amylopectin ratio, characteristics of amylose and amylopectin as well as the aforementioned amylose-lipid complexing. When the temperature applied to heat of starch dispersions increases, swelling of starch granule causes the thickening of the suspension.

And further increase in heating temperature will disintegrate starch granules, especially in the presence of shear force, resulting in a continuous phase of solubilized polysaccharides (amylose/amylopectin) filling an interpenetrating discontinuous phase of swollen starch granules and fragments. Starch is pasted as a highly viscous paste due to the disruption of most starch granules under high temperature shearing. Accompanied starch pasting is the alteration in viscosity, measured by Rapid Visco Analyzer (RVA). Factors are used to characterize starch pasting behavior such as the peak viscosity, pasting temperature, breakdown, setback and cold or hot paste viscosity. Apart from the factors influencing starch swelling, pasting of starch-water suspension under constant shear force is also affected by the initial temperature, the heating rate and the final holding time [17]. The representation of swelling of starch granules is shown in Figure 2.4.

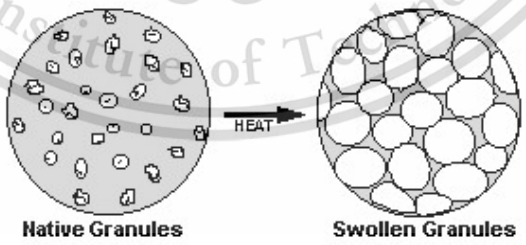

Figure 2.4 Swelling of starch granules [18]

2.2.3.2 Starch gelatinization

Starch can adsorbs and swells in water, yet it does not dissolve in water until it is heated over gelatinized or pasting temperature which starch slurry begins to have viscosity because hydrogen bond of starch is disrupted by heating, then starch slurry becomes more clear in color and viscous to be starch paste. When the starch slurry is heated, water absorption capability of starch increases as granule swelling occurs, however, which is hindered at low heating temperature by the ending of amorphous region in more ordered crystalline domains. Increase in heating temperature until a level (onset of gelatinization), the water uptake of granules is reversible, but further increase in heating temperature approaching the onset of gelatinization will cause the disruption or melting of crystallites due to thermal motion and swelling force, and the water uptake becomes irreversible. Changes in starch granule throughout gelatinization involve loss of birefringence, loss of crystallinity, morphological changes, granule swelling, solutes leaching, alterations in rheology and susceptibility toward enzymatic hydrolysis/digestibility. Differential scanning calorimetry (DSC) has become the most extensively utilized tool to investigate the gelatinization phenomenon of starch on account of the intended melting transition parameters provided by it: onset (T_o), peak (T_p), conclusion (T_c) temperatures of gelatinization, gelatinization temperature range (ΔT_g) and gelatinization enthalpy (ΔH_g). The gelatinization temperatures of different types of starch are shown in Table 2.3.

Factors affecting starch gelatinization by DSC include starch granule structure organization, water absorption, etc. Starch from various botanical sources will exhibit different gelatinization characteristics even under same testing conditions. Starch crystallinity has displayed close correlation with gelatinization parameters (gelatinization temperatures, T_m, ΔT_g and ΔH_g). Since starch crystallinity is associated with amylopectin, a higher degree of crystallinity is expected from maize starch with higher amylopectin content and this is evidenced by a higher ΔH_g and narrower found that gelatinization temperatures positively correlate with relative crystallinity of starch from normal rice. Apart from starch crystallinity, molecular structures of amylopectin and starch composition have also shown effects on starch gelatinization. Furthermore, comparison between A- and B-type of starch demonstrates that the former presents a higher ΔH_g, while the latter displays a lower T_o but higher T_p and T_c.

Biphasic endothermic transitions during starch gelatinization have been observed from both single starch melting in the presence of limited water content and mixed starch from rice, wheat potato, waxy maize and barley. The overlapped two melting endotherms occurred at low moisture content is due to the limited extent of granule swelling and melting of crystallites as water become a limiting

factor, whereas, in the case of mixed starch, granule melting position in the DSC trace is governed by the distinct granular stabilities of mixing counterparts resulting in independent gelatinization. The extent of overlapping or superimposing of these two melting endotherms is dependent on the similarities of the gelatinization temperatures of each starch [18]. The representation of gelatinization and retrogradation is displayed in Figure 2.5.

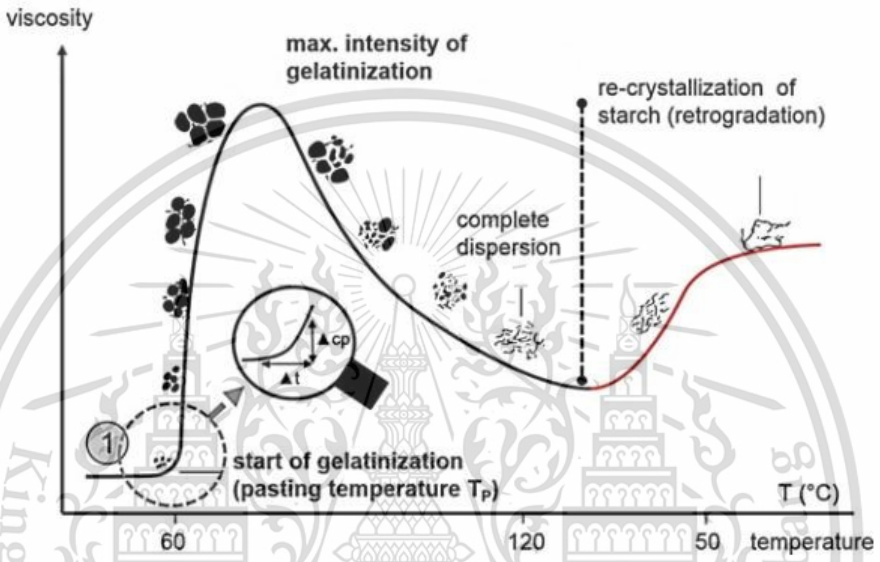

Figure 2.5 Gelatinization and retrogradation of starch [19]

Table 2.3 Starch gelatinization temperature range [19]

Starch	Gelatinization temperature range (˚C)
Potato	57-87
Maize	70-89
Waxy maize	68-90
Wheat	50-86
Cassava	64-92

2.2.3.3 Retrogradation of starch

On account of the non-thermodynamic equilibrium state of starch paste obtained from starch gelatinization, structural transition of gelatinized starch from an amorphous phase to a crystalline phase will occur during cooling process and storage of gelatinized starch. This phenomenon is collectively termed retrogradation.

Amylose and amylopectin differ in their retrogradation behaviors; retrogradation of amylose proceeds rapidly with the melting enthalpy of recrystallized amylose approaching toward maximum value within short time; the extent of the retrogradation of amylopectin, however, increases with storage along with an increment in the melting enthalpy of recrystallized amylopectin. Furthermore, when melting transition and thermal reversibility are taken into consideration, recrystallized amylose is disordered by heating at temperature above 100˚C and shown to be thermally reversible, but melting of recrystallized amylopectin occurs at lower temperature (<100˚C) and thermal reversibility is noticed. Transitional temperatures and melting enthalpies of retrograded starch (<100˚C, disintegration of recrystallized amylopectin) show to be lower than those of NS gelatinization, which has been ascribed to the weaker crystallinity of retrograded starch resulting from the less ordered manner in amylopectin chain associations, prolonged storage (under the same low temperature) only increases the melting enthalpies of recrystallized amylopectin, but preferable retrogradation conditions (low temperature for nucleation followed by high temperature for propagation) will facilitate the recrystallization of amylopectin resulting in perfect crystallites and increase in melting transition temperatures.

Chain structure of amylopectin plays a significant role in amylopectin recrystallization reassociation of amylopectin chains during retrogradation depends on the crystallization of the outermost short branch chains with a degree of polymerization (DP) of 15. Study on the retrogradation behavior of waxy cereal starch shows that amylopectin retrogradation is specifically corresponded to mole fraction of unit chains with DP 14-24; chains of DP 6-9, however, amylopectin will hinder starch retrogradation. Study on the retrogradation of amylopectin isolated from corn and wheat starch demonstrates that higher proportion of chains of DP 15-20 of corn amylopectin facilitates its recrystallization process resulting in higher retrograded crystallinity, while wheat amylopectin of greater proportions of short chains (DP 9-13) retards its retrogradation.

A small fraction in retrograded starch that has demonstrated resistance to the hydrolysis by amylolytic enzymes, along with the melting transition similar to that of recrystallized amylose, is corporately recognized as resistant starch that mainly comprises retrograded amylose also reports that during starch retrogradation, the

presence of lipids will reduce the yield of recrystallized amylose by complexation with amylose. This is based on a competitive mechanism between amylose recrystallization and amylose-lipid complexing that crystallization of amylose and lipids precedes amylose reassociation. Although reduction in enzymatic susceptibility of amylose by complexing with lipids is observed, amylose-lipid complex is enzymatically degradable.

The aforementioned recrystallization process of starch retrogradation also involves changes in X-ray crystallography. The V_h pattern for the starch after one-day aging, exhibits a mixed V_h and B structure, while the degree of crystallinity is increased. Starch gels from maize and potato both present a V_h pattern immediately after gelatinization; while the developing recrystallization renders a gradual recovery of B pattern. Thus, starch retrogradation process regarding changes in X-ray pattern is expressed as a gradual decrease in V_h structure and an increase in B structure [20-21].

2.3 Cassava starch

Cassava is a very cheap source of carbohydrate and is the main carbohydrate source in the diet of the population of the third world countries, such as Brazil, America and Southeast Asia, where it is largely grown. It is also known as Manioc (*Manihot esculentz)*, yucca, tapioca or guacamate. Cassava starch is prepared for consumption by pouring it slowly into a pot of boiling water over a fire and stirring it on the fire until it forms a brownish, viscous paste. The paste is allowed to cool and harden. Cassava starch is used to manufacture many chemical products such as citric acid and is also used in papermaking, food processing, lubricants, adhesives and textiles. Cassava is a supplementary staple food of more than 200 million in Africans aside from its uses as livestock feed, particularly for monogastrics. Cassava starch is the most major food plant with a high amount of cyanogenic glycosides. Amylose content of cassava starch, as compared with some cereal starch, has been shown less variation ranging from 17-24%, and other significant features found for cassava starch is its low contents of lipid (0.1%), protein/nitrogen (around 6.5% and 0.01%) and phosphorous (0.008-0.01%) [22]. The components of cassava starch are displayed in Table 2.4.

Table 2.4 The components of cassava starch [15]

Component	Weight percentage (%)
Amylose	18.60-23.60
Amylopectin	76.40-81.40
Lipid	0.10-0.20
Protein	6.50-7.50
Nitrogen	0.009-0.013
Phosphorous	0.008-0.01

2.4 Modified starch

Modified starch is developed to overcome one or more of these shortcomings and thus improve the properties of starch for various commercial applications. While in the broadest sense any product in which the physicochemical properties of NS have been altered might be considered to be modified, the range of modifications covered in this volume will be limited to those in which the physicochemical properties of NS are modified by chain scission, molecular rearrangements or addition of new chemical groups into the starch. Modified products which will be covered include converted starch such as acid fluidities or chlorination, crosslinked starch and all derivatives in which substituent groups have been introduced onto the starch molecules [21].

2.4.1 Classification of modified starch

2.4.1.1 Chemically modified starch

This chemical procedure generates new additional functional groups into the starch molecule and alters important properties of starch. The chemical modification of starch alters the available three hydroxyl groups at C-2, C-3 and C-6 positions. This modified method promotes either intra- or inter-molecular bonds at random positions in the starch structure. For example of chemically modified starch for many applications such as [21]:

1. Hydroxypropylated starch

The modified starch is produced by reacting with propylene oxide at high pH to introduce hydroxypropyl group on the starch under strongly alkaline conditions Hydroxypropyl starch is widely used in cosmetics and beauty products because of its ability to serve as a surfactant and emulsifier [21].

2. Acetylated starch

These are prepared by reacting water suspensions of starch granules with acetic anhydride or vinyl acetate under alkali conditions. After the reaction is completed, the slurry of starch is neutralized, washed and dewatered to remove most of the by products. Acetic anhydride is extremely unstable in water. When it reacts with starch, acetic anhydride is hydrolyzed to acetic acid and water. The vinyl acetate also hydrolyzed readily. The obtained properties of acetylated starch are reduced gelatinized temperatures, decreased retrogradation and tendency to form gels as well as improved paste clarity [21].

3. Carboxymethyl Starch

The carboxymethyl starch is produced by modifying starch with sodium monochloroacetate under alkaline condition. Carboxylation of starch progressively increases water solubility as the DS increases and they are cold-water soluble at higher substitutions and the solution is colorless. Carboxymethyl starch in many applications becomes a waste product in textile sizing and desizing operations. Carboxymethyl starch is also compatible with many hydrophilic sizing agents, such as polyvinyl alcohol used in paper sizing, in which oil resistance and water insolubility (multivalent-ion salt form) are important contributions [21].

4. Acid-modifed starch

These are made by hydrolyzing aqueous suspensions of starch granules with hydrochloric and/or sulfuric acid, keeping the temperature well within the gelatinization temperature. Since these treatments are normally run on aqueous suspensions, the extent of conversion is limited to avoid degrading the starch to the point where it starts to swell due to solubilization. The basic reaction is hydrolysis of the α-D-(1,4) or α-D-(1,6) linkages. As a result, acid-modified starch is chemically identical to unmodified starch except for the lower molecular weight [21].

5. Crosslinked starch

The aim of cross-linking is to reinforce the hydrogen bonds in the granules with chemical bonds linking together nearby molecules within the granules. These chemical bridges are much stronger than hydrogen bonds and will help retain the integrity of the swollen granules after the bonds have been destroyed. Crosslinks may be introduced in the granules by reacting glucosidic hydroxyls on nearby molecules with bifunctional chemicals capable of adding adipate or phosphate

crosslinks. Mixed adipic-acetic anhydride is used to introduce adipate crosslinks and phosphorous oxychloride or sodium trimetaphosphate used to add phosphate crosslinks. Since cross-linking reactions are run on starch suspension, it takes relatively few crosslinks to have a major impact since each granule contains millions of AGU. All residues are water soluble and largely removed during the subsequent washing and dewatering processes. The extent of cross-linking varies depending upon the food system in which they will be used. CS for a given application will provide greater thickening power on a viscosity and resistance to acidic conditions than unmodified starch. However, CS should be made of special applications not covered in the major fields of usage such as food, paper, textile and adhesives. Usage in the granule from in surgical dusting powder, as an anti-blocking dusting agent for blown films, as an absorbent in the purification of α-amylases by affinity chromatography and in combination with treatment of CS with allyl isothiocyanate as an enzyme carrier. Cross-linking agents have been widely used to crosslink starch such as STPP, glutaraldehyde, epichlorohydrin, methylene bisacrylamide, borax, di-carboxylic acid and STMP [21]. Schematic structure of crosslinked polymer is presented in Figure 2.6.

Figure 2.6 Schematic structure of crosslinked polymer [21]

6. Oxidized starch

For some applications, such as high shear coatings, a low viscosity of starch solutions is required. For this purpose, the molecular weight of NS is decreased via oxidation. By using some oxidation agents, e.g., sodium hypochlorite, hydrogen peroxide, nitric and ozone, hydroxyl groups on the starch molecules are firstly oxidized to form the carbonyl groups and then further form carboxyl groups at the hydroxyl groups at the C-2, C-3 and C-6 positions. Degree of oxidation depends on the average content of carbonyl and carboxyl groups introduced per AGU [21].

For the oxidized solutions, the associative tendencies of starch molecules are hindered, which result from the steric effect of introduced carbonyl and carboxyl groups. Therefore, compared to NS, OS has a much lower viscosity and chain lengths, and higher slurry stability, which makes it useful for many industrial applications. OS is extensively used as paper sizing agent, adhesive or additive in food application [21].

Oxidation of the aldehydic reducing end groups to carboxyl groups. Generally, aldehydes will be oxidized more readily than hydroxyls. As a result, it is possible that initially, the aldehydic end groups in starch are oxidized to carboxyl groups. The aldehydic end groups in NS will be very small. However, as hydrolysis or oxidative rupture occurs, additional aldehydic groups will be formed and be available for oxidation to carboxyls. There may be variations in the relative predominance of one type of reaction over another, but it appears that hypochlorite oxidations are random and take place at the same sites as oxidations. The relative importance of each type of reaction in terms of the final product properties varies. Thus, oxidation reaction is relatively few C-1 and C-4 hydroxyls compared to the number at C-2, C-3 and C-6 hydroxyls, it is logical to assume that the oxidations occurring at C-2, C-3 and C-6 hydroxyls probably play a dominant role in determining the properties of the resulting OS.

Oxidation of the primary hydroxyl at C-6 position to carboxyls forms glucoronic acid units. It seems likely that oxidation at the primary hydroxyls proceeds through formation of aldehydic groups initially and then carboxyl groups.

Oxidation of the secondary hydroxyls at C-2, C-3 and C-4 to ketone groups is investigated through measurements of reducing value.

Oxidation of glycol groups to aldehydic and then carboxylic groups The hydroxyls on C-2 and C-3 function as glycol groups and may be oxidized with scission of the bond between C-2 and C-3 to form aldehydic groups which may then be further oxidized to carboxyl groups. This reaction may occur when starch is oxidized through the separation of barium salts of dibasic acids of less than six carbon atoms [21].

2.4.1.2 Physically modified starch

Physical modification is extensively utilized to alter the granular structure of starch and to enhance the cold water solubility. They do not relate with any chemical modification and this technique is low-cost and simple [21].

1. Pre-gelatinized starch

Pregelatinized type is particularly useful in instant gravies, instant pudding and in dry cake mixes for freshness retention. The inherent lumping tendency of these materials is usually reduced by shipping them in form of coarse powder from which fines have been removed. Another method involves incorporation of small amounts of additives such as orthophosphate salts or polyphosphate salts is claimed to be helpful, probably by sequestering with heavy metal ions. Pregelatinized starch is used in many industrial applications wherever cooking facilities are not available or rapid hydration is desired. The properties of the cold water swelling product depend greatly on the pregelatinizing process and equipment used [21].

2. Heat-treatment starch

Heat-treatment process relating with heat–moisture both of which leads to a physical modification of starch without any gelatinization, disruption to granular integrity, or destruction of birefringence [21].

3. Annealing

Annealing modification is the process that relates to the heating of starch granules in water under a temperature below the gelatinized temperature and above the glass transition temperature. The annealing causes alterations in structure of starch granules, increase in granular stability, interactions between amorphous and crystalline phases of the starch granule, formation of crystalline, packing of double helices and reduction of swelling behavior [21].

2.4.1.3 Enzymatically modified starch

Enzymatic modification is the one of method type, which is used to hydrolysis of some part of starch into a low molecular weight of starch using enzymes. Enzymatically modified starch is extensively utilized for food and pharmaceutical industries [21].

2.4.2 Terminology and definition

2.4.2.1 Carbon position (C-) in AGU

This is used to designate the position in the monomeric AGU of the carbon or hydroxyl involved in a reaction. Numbering starts at the carbon involved in the hemi-acetal structure and ends at the carbon with the primary hydroxyl as shown in Figure 2.7.

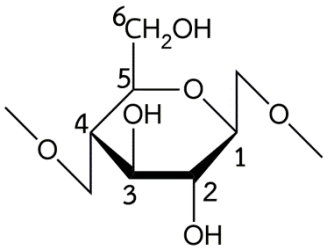

Figure 2.7 Numbering system for carbons position in AGU [21]

2.4.2.2 Degree of polymerization (DP)

The DP of a product is the average number of monomeric units in the molecule. In this case, it will be the average number of AGU.

2.4.2.3 Dextrose equivalent (DE) or reducing value

DE is an indication of the overall reducing value of a converted starch determined dextrose and exhibited DE of 1; maltose has a DE of 2 as shown in Figure 2.8. A molecule of hydrolyzed amylose or amylopectin containing 100 AGU will contain reducing end group and will thus have a DE of 1. Reference to DE is usually limited to depolymerized or converted starch such as dextrin or to syrups and sugars as a percentage of total dry substances.

Dextrose DP = 1

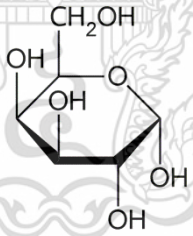

Maltose DP = 2

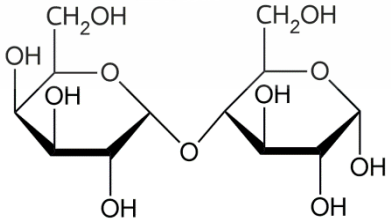

Figure 2.8 Dextrose equivalents (DE) of dextrose and maltose [21]

2.4.2.4 Alkali number

This is an approximate measure correlating with the reducing end groups in a starch product. It is determined by an empirical method involving the digestion of a starch product with alkali under controlled conditions and determining the milliliters of 0.1 M alkali consumed during the digestion by a gram of dry basis starch. During the alkaline digestion, the terminal aldehydic groups undergo progressive destruction to yield, among other products and organic acids. When done under carefully controlled conditions, the amount of acid produced provides a relative measure of the number of aldehydic groups and, hence, molecular size. It is used primarily on NS, on lightly converted starch such as acid fluidities, and on some dextrin which is too high in molecular weight to permit meaningful measurements of their DE or reducing power by conventional means. Alkali numbers are not applicable to starch esters, ethers or OS [21].

2.4.2.5 Percent substitution

This is the level of substitution expressed as the weight of the substituent percent of the total starch dry substance.

2.4.2.6 Degree of substitution (DS)

The DS refers to the average numbers per AGU on which there are substituent groups. Most of the commercially available modified starch has low DS values ranging up to about DS 0.1, which will represent on average 1 substituent group per every 10 AGU [21].

2.4.2.7 β-amylase digestibility

β-amylase digestibility is an indication of the extent to which starch, amylose, amylopectin, or modified starch is digested by this enzyme. β-amylase is a plant enzyme which hydrolyzes α-D-(1,4) glucosidic linkages in amylaceous polymers. It attacks such polymers from the non-reducing end of the polymer, removing maltose units. A purely linear polymer of glucosidic linkages such as amylose will be essentially completely hydrolyzed by β-amylase to maltose. On the contrary, the action of β-amylase is blocked by branched points such as α-D-(1,6) glucosidic bonds, which can be found in amylopectin. Consequently, β-amylase will only remove the outer branches of amylopectin so its β-amylase digestibility will be significantly less than that of amylose. Thus, the β-amylase digestibility is an indication of the linearity of the glucose polymer or hydrolyzate [21].

2.5 Dual modification

Dual modification is two steps of modification method for improving properties of starch granules, which relates to a combination of physical, chemical or enzymatic methods. The dual modification method has been reported in previous researches e.g. cross-linking-oxidation, cross-linking–acetylation, cross-linking-hydroxypropylation , acetylation–oxidation and acid hydrolysis-cross-linking. The dual-modified starch is widely utilized in food and pharmaceutical application such as thickener, emulsifier, controlled released carrier of drugs and other bioactive compounds, and also in non-food industries as adsorbent for heavy metals. For examples of dually modified starch in previous literatures, are listed below [22-23].

2.5.1 Acetylation-cross-linking

Starch was modified by acetylation with acetic anhydride. Then, acetylated starch was then modified by cross-linking with phosphoryl chloride. Acetylated-crosslinked starch presented the increased pasting viscosity and solubility of pasting of NS granules [23].

2.5.2 Acetylation-hydroxypropylation

Starch was modified by acetylation with acetic anhydride and hydroxypropylation with propylene oxide. Acetylation-hydroxypropylation modification increased swelling capacity, water absorption capacity and decreased pasting temperature and pasting viscosity [24].

2.5.3 Hydroxypropylation-etherification

Starch was modified by hydroxypropylation with phosphorus oxychloride and followed by etherification with propylene oxide. This method was clearly improved hydrophobicity and the gelatinized temperature of NS granules [25].

2.5.4 Oxidation-cross-linking

Starch was modified by oxidation with sodium hypochlorite or hydrogen peroxide and, then, crosslinked with either sodium phytate or STMP/STPP. OCS exhibited greater adhesive property and stable viscosity than NS [9].

2.5.5 Cross-linking-oxidation

Starch was crosslinked with STMP/STPP or sodium phytate and followed by oxidation with hydrogen peroxide or sodium hypochlorite. COS presented lower solubility and swelling power than that of NS and good resistant to shear and retrogradation [10].

2.6 Hydrogen peroxide

Hydrogen peroxide contains an empirical formula of H_2O_2. It is commercially available in aqueous solutions. The characteristic of hydrogen peroxide is a colorless liquid and is stabilized against decomposition, which occurs in the presence of traces of iron, copper, aluminum, platinum and other transition metals. A solution of anhydrous hydrogen peroxide in ether (2.5 M) is obtained by drying of the ether extracts with anhydrous magnesium sulfate. The hydrogen peroxide content is determined by iodometric titration. Molecular complexes can be prepared from some tertiary amines and 30 or 90% solutions of hydrogen peroxide, 1,4-Diazabicyclooctane (forms an adduct with two molecules of hydrogen peroxide. The adduct consists of hygroscopic crystals melting at 112˚C, which is stable for a limited time at room temperature and can be used as a source of hydrogen peroxide in oxidations [26].

The hydrogen peroxide does not mix with nonpolar organic compounds. To increase its solubility, ethanol, tert-butyl alcohol, trifluoroethanol, tetrahydrofuran, acetonitrile, formic acid and, especially, acetic acid are used. When formic or acetic acid is used the reacting species is the corresponding peroxy acid. Under such conditions, the products of oxidation by hydrogen peroxide resemble those obtained with peroxy acids. Different products may result from oxidation by hydrogen peroxide in alkaline medium, such as in pyridine, ammonia and sodium or potassium hydroxide. Applications of hydrogen peroxide have been widely used as an oxidizing agent in starch (Figure 2.9), mild antiseptic, disinfectant, antimicrobial agents, whitening agents of teeth, bleaching agents in textile, paper, sizing, mining industries and cleaning agent in electronic industry [27]. The properties and material safety data sheet (MSDS) of hydrogen peroxide are shown in Tables 2.5-2.6.

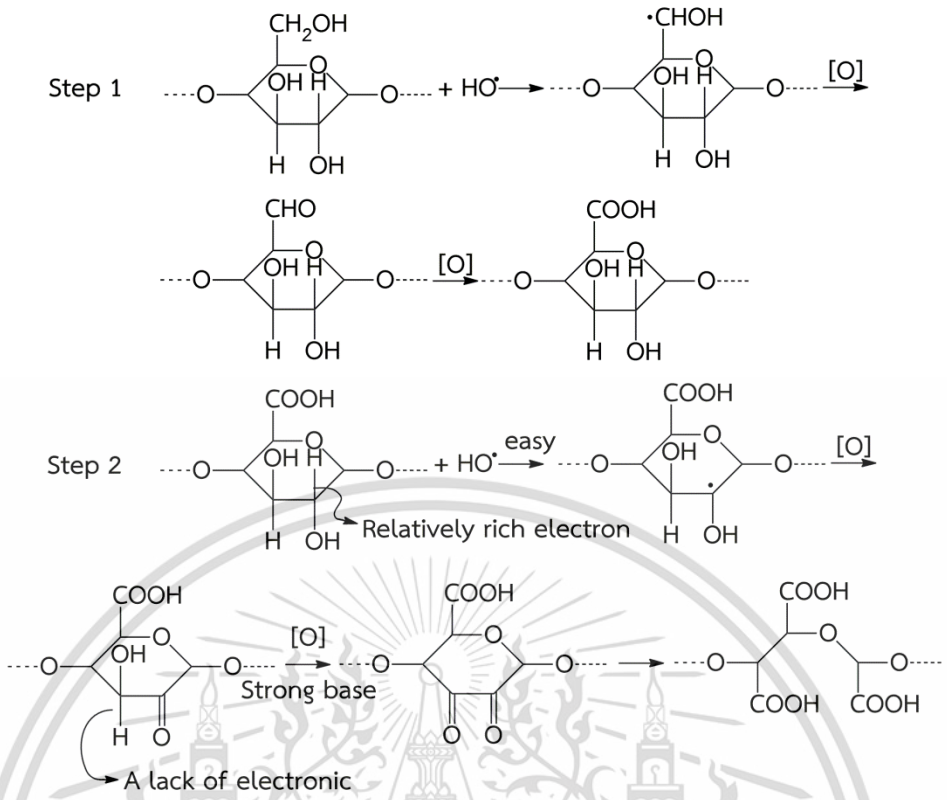

Figure 2.9 Preparation of OS by hydrogen peroxide [28]

Table 2.5 Properties of hydrogen peroxide [26]

Property	Detail
Appearance	Colorless liquid
Odor	Odorless
Molecular weight	34.02 g/mol
Boiling point	152.0°C
Water solubility	Soluble
pH	4.6

Table 2.6 MSDS of hydrogen peroxide [29]

Data	Detail
IUPAC name	Hydrogen peroxide
Chemical name	Hydrogen peroxide
CAS No.	7722-84-1
RTECS code	LC 15430
Hazard labels (DOT)	 5.1 - Oxidizer 8 - Corrosive
NFPA number	 NFPA health hazard: 3 - Materials that, under emergency conditions, can cause serious or permanent injury. NFPA fire hazard: 1 - Materials that must be preheated before ignition can occur. NFPA reactivity: 3 - Materials that in themselves are capable of explosive decomposition or explosive reaction but that require a strong initiating source or must be heated under confinement before initiation. NFPA specific hazard: OX - Materials that posses oxidizing properties.

2.7 Borax

Borax (or sodium borate or sodium tetraborate) contains an empirical formula of $Na_2B_4O_7$ (Figure 2.10). It is a crucial compound of boron and a salt of boric acid. Appearance of borax is white solid powder that completely soluble in water. Borax is not a deeply toxic substance. Borax contains the $[B_4O_5(OH)_4]^{2-}$ ion. In this structure, there are two four-coordinate boron atoms (two BO_4 tetrahedra) and two three-coordinate boron atoms. Borax is also easily converted to boric acid and other borates, which have been used for many applications. Borax is completely soluble in ethylene glycol and water [30].

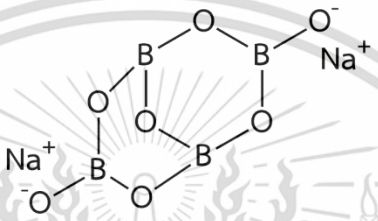

Figure 2.10 Chemical structure of borax [30]

Borax is an effective cross-linking agent for starch as well as other polymers such as polyvinyl alcohol, natural gums, etc. It imparts major changes to the properties of starch solutions. Perhaps the most noticeable one is the increase in viscosity which occurs as borax is added. As borax is introduced, the viscosity will continue to increase until the borax concentration increase. Further levels of borax addition will not change the viscosity. Although borax will affect the viscosity of all forms of starch, the increase in degree of viscosity will vary with the molecular weight and the relative concentrations of amylose and amylopectin present. Thus, if by adding a given amount of borax to a solution of cornstarch the viscosity is increased from 1000 to 5000 centipoise (cps), a solution of enzyme-converted cornstarch at the same 1000 cps starting point (the enzyme-converted starch will be present at substantially higher solids content than the unmodified starch to produce equal starting viscosities might undergo a viscosity increase only to 2000 centipoise with the same content of borax. Viscosity increase is far from the only effect of borax. Cohesiveness is increased. Starch such as root starch and waxy corn starch which are already cohesive in nature and cereal starch will become more cohesive in texture. Substrates to be bonded will be held together much more tenaciously with a high stronger bond than observed with NS. This effect is more pronounced when adding borax to cereal starch which exhibits very poor cohesiveness or tack in simple

water cooks. Borax has a stabilizing effect upon starch which normally gel upon cooling [30]. The properties and MSDS of borax are displayed in Tables 2.7-2.8.

2.7.1 Applications of borax

1. Borax is utilized in household laundry and cleaning product.

2. Borate ions are utilized in laboratory to made buffers.

3. It is utilized as a cooking ingredient for adding a firm thick texture to the food, or as a preservative.

4. Anti-fungal compound for cellulose insulation.

5. Borax is utilized as a thickening agent in many kinds of food such as yoghurt, meat ball, jelly, etc.

6. Good cross-linking agent for various substances such as starch (Figure 2.11), chitosan or other biopolymers [31].

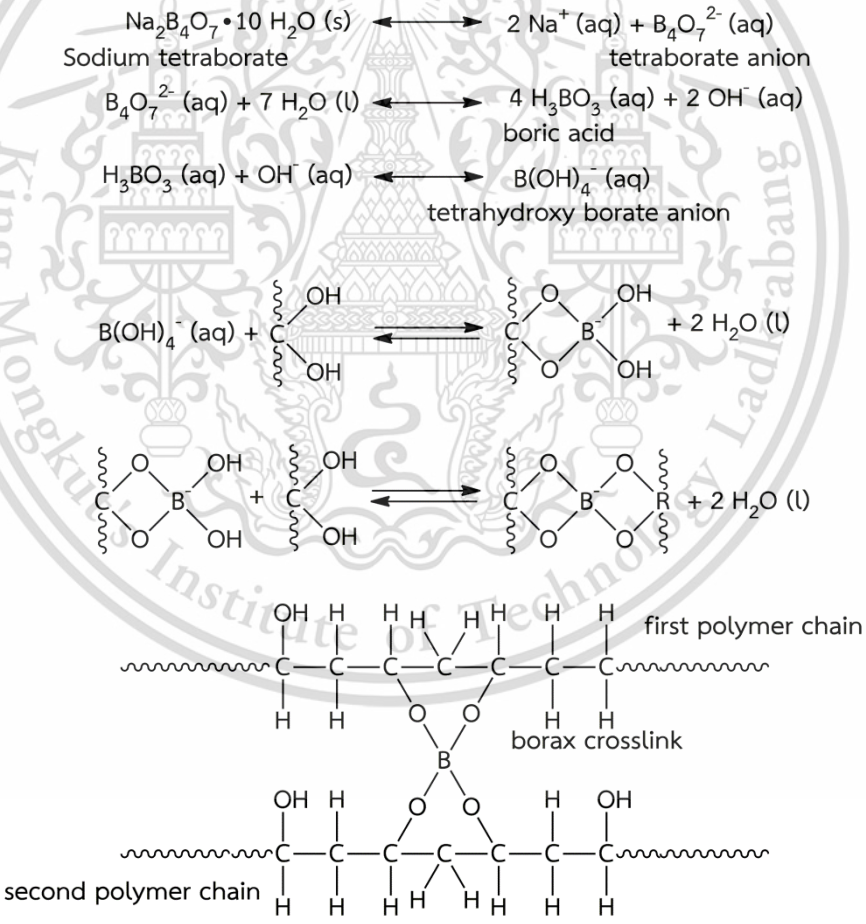

Figure 2.11 The formation of a tetrahydroxy borate crosslink from borax [32]

Table 2.7 Properties of borax [30]

Property	Detail
Appearance	White solid powder
Molecular weight	237.24 g/mol
Density	1.73 g/cm^3
Melting point	743.0°C
Boiling point	1575.0°C
Water solubility	Soluble
pH	9.3

Table 2.8 MSDS of borax [29]

Data	Detail
IUPAC name	Sodium borate, sodium tetraborate
Chemical name	Sodium tetraborate decahydrate
CAS No.	12267-73-1
RTECS code	VZ2275000
NFPA number	 NFPA health hazard: 1 - Materials that cause irritation upon exposure, but only minor injury is sustained even if no medical treatment is provided. NFPA fire hazard: 0 - Materials that will not burn. NFPA reactivity: 0 - Materials that are stable even under exposure to fire.

2.8 Boric acid

Boric acid or hydrogen borate, is a weak monobasic lewis acid of boron. It has the empirical formula of H_3BO_3 (or $B(OH)_3$) as shown in Figure 2.12 and can be appeared in the form of colorless crystals or a white solid powder that is soluble in water. In general, boric acid is highly soluble in boiling water (Tables 2.9-2.10). Boric acid is produced by reacting of borax (sodium tetraborate decahydrate) with a hydrochloric acid [33]:

$$Na_2B_4O_7{\cdot}10\ H_2O + 2\ HCl \longrightarrow 4\ B(OH)_3\ [or\ H_3BO_3] + 2\ NaCl + 5\ H_2O$$

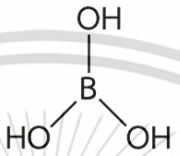

Figure 2.12 Chemical structure of boric acid [33]

2.8.1 Applications of boric acid

1. Boric acid is utilized as a mild antiseptic, an antifungal, an antibacterial and an antiviral agent. It is used in the treatment of yeast infections and cold sores.

2. Boric acid is utilized as a preservative of cereal grains such as rice and wheat.

3. Boric acid can be utilized as an antiseptic for minor burns or cuts.

4. Boric acid is utilized as an acne treatment.

5. Yeast infections can be treated with the use of boric acid.

6. Effective cross-linking agents in chemically modified starch such as starch borate (Figure 2.13) [33].

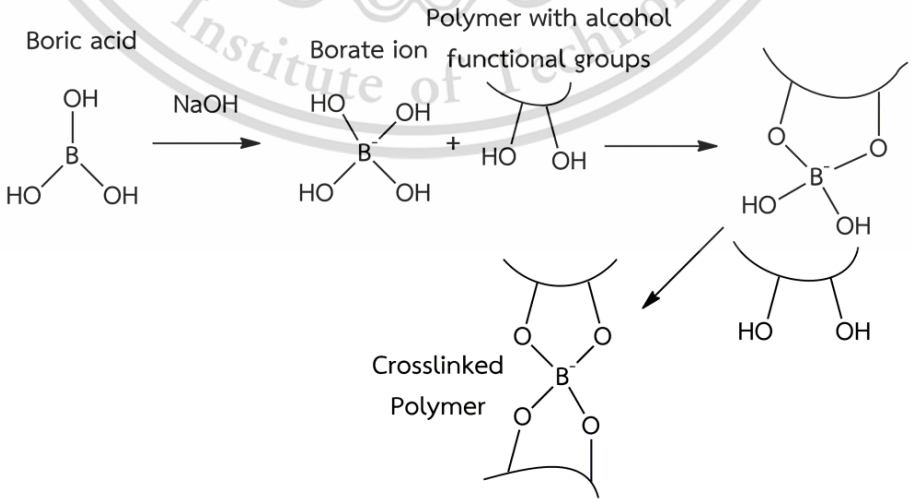

Figure 2.13 Preparation of starch borate by boric acid [34]

Table 2.9 Properties of boric acid [33]

Property	Detail
Appearance	White solid powder
Molecular weight	62.02 g/mol
Density	1.43 g/cm^3
Melting point	171.0°C
Boiling point	300.0°C
Water solubility	Soluble
pH	3.8-4.8

Table 2.10 MSDS of boric acid [29]

Data	Detail
IUPAC name	Boric acid
Chemical name	Boric acid
CAS No.	12258-53-6
RTECS code	ED4550000
NFPA number	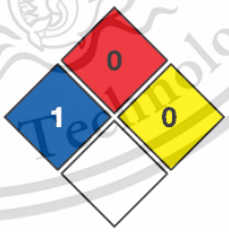 NFPA health hazard: 1 - Materials that cause irritation upon exposure, but only minor injury is sustained even if no medical treatment is provided. NFPA fire hazard: 0 - Materials that will not burn. NFPA reactivity: 0 - Materials that are stable even under exposure to fire.

2.9 Sodium trimethaphosphate (STMP)

Sodium trimetaphosphate (STMP), with formula of $Na_3P_3O_9$. It is the sodium salt of trimetaphosphoric acid. STMP is produced by heating sodium polyphosphate at a few hundred degrees. It is a white granular or powdered material that finds specialized applications in food and construction industries [35]. The chemical structure of STMP is presented in Figure 2.14.

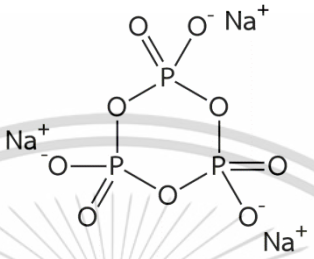

Figure 2.14 Chemical structure of STMP [35]

STMP is an efficient cross-linking agent for modifying of starch granules (Figure 2.15), chitosan and other polymers. For CS, distarch phosphates and distarch adipates are the most widely crosslinked starch in industry field, which contains a phosphate bridge. The distarch phosphates contain the two hydroxyl groups on neighboring starch molecules, while distarch adipate contains a longer bond, causing the presence of cross-linking or a covalent bond. Because of the more permanent nature of the covalent bonded bridge or crosslink, only a small DS, typically one crosslink per 100–3000 AGU of the starch, is necessary to produce sufficient effects [35]. In addition, the properties and MSDS of STMP are presented in Tables 2.11-2.12.

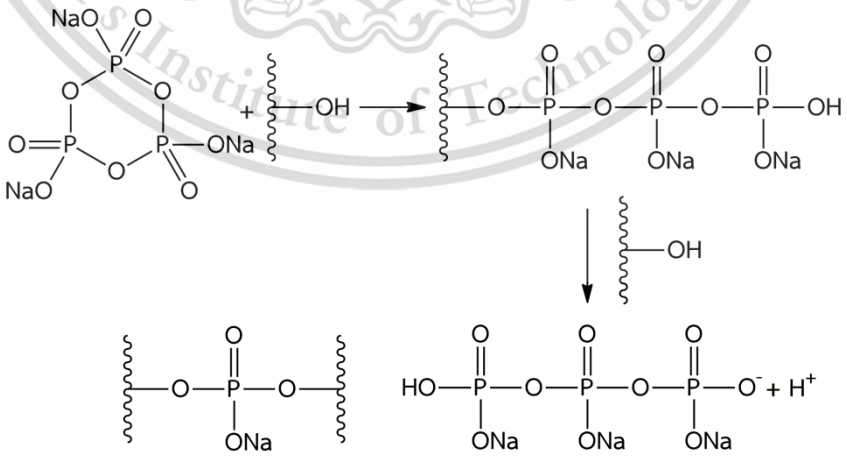

Figure 2.15 Preparation of distarch phosphate by STMP [36]

Table 2.11 Properties of STMP [35]

Property	Detail
Appearance	White solid powder
Molecular weight	305.88 g/mol
Density	2.49 g/cm^3
Melting point	53.0°C
Water solubility	Soluble
pH	9.1-10.2

Table 2.12 MSDS of STMP [29]

Data	Detail
IUPAC name	Sodium trimetaphosphate
Chemical name	Sodium trimetaphosphate
CAS No.	7785-84-4
RTECS code	CB4287241
NFPA number	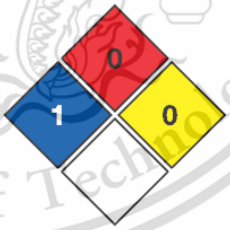 NFPA health hazard: 1 - Materials that cause irritation upon exposure, but only minor injury is sustained even if no medical treatment is provided. NFPA fire hazard: 0 - Materials that will not burn. NFPA reactivity: 0 - Materials that are stable even under exposure to fire.

2.10 Sodium tripolyphosphate (STPP)

Sodium tripolyphosphate (STPP) is an inorganic compound with empirical formula of $Na_5P_3O_{10}$ (Figure 2.16 and Tables 2.13-2.14). It is the polyphosphate penta anion salt. It is extensively utilized for many industrial applications, especially detergent. It is prepared from heating a mixture of disodium phosphate, $Na_2H_PO_4$ and monosodium phosphate, NaH_2PO_4, under controlled conditions [35].

$$2\ Na_2H_PO_4 + NaH_2PO_4 \longrightarrow Na_5P_3O_{10} + 2\ H_2O$$

STPP is a white powder salt, which can appear in anhydrous form and as the hexahydrate. The chemical structure of STPP is presented in Figure 2.16. It is easily dissolved in water and can soften hard water to make suspension solution become into clear solution. It has weak alkalinity but it is not harmful to a human [35].

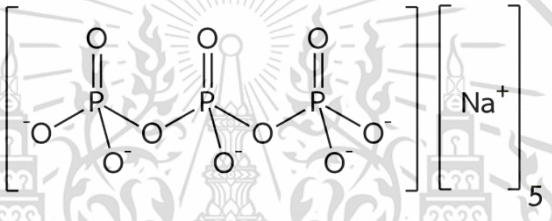

Figure 2.16 Chemical structure of STPP [35]

2.10.1 Functions of STPP in food and commercial applications

1. To decrease amount of cooked-out juice.
2. To decrease growth of microbes and loss of carbonation in beverages.
3. To decrease turbidity in wines/ciders and vinegars.
4. To crosslink with starch or other polymers (Figure 2.17) [35].

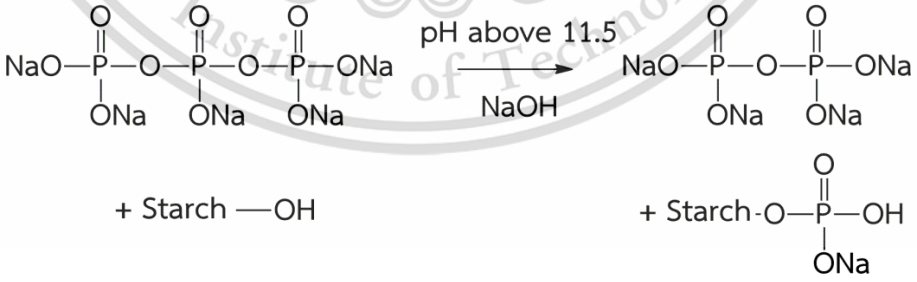

Figure 2.17 Chemical reaction of preparation of distarch phosphate with STPP [36]

Table 2.13 Properties of STPP [35]

Property	Detail
Appearance	White solid powder
Molecular weight	367.86 g/mol
Density	2.52 g/cm^3
Melting point	622.0°C
Water solubility	Soluble
pH	9.1-10.2

Table 2.14 MSDS of STPP [29]

Data	Detail
IUPAC name	pentasodium phosphoryl phosphate
Chemical name	Sodium trimetaphosphate
CAS No.	7785-29-4
RTECS code	YK4570000
NFPA number	 NFPA health hazard: 1 - Materials that cause irritation upon exposure, but only minor injury is sustained even if no medical treatment is provided. NFPA fire hazard: 0 - Materials that will not burn. NFPA reactivity: 0 - Materials that are stable even under exposure to fire.

2.11 Plasticization

Plasticizer is substance which improves the flexibility and processability of polymeric materials. Plasticizers play a role to decrease the intermolecular secondary bond forces between polymer chains, with the result that the plastic becomes more flexible. The plasticizer acts as an internal lubricant and permits the polymers to slip past one another. In free volume theories, the incorporation of a plasticizer increases a free volume of a polymer and that the free volume is identical for polymer at glass transition temperature (T_g). Plasticizer extends the lower temperature range for use of materials since they discourage polymer chain associative behavior and encourage segmental flexibility, thus increasing the rotational freedom and effectively decreasing the material's typical T_g. The plasticizers are classified into two major categories: internal and external plasticizer. The plasticization of polymers by added plasticizers is called external plasticization. An internal plasticization can be achieved by copolymerization of the parent monomer with comonomers that provide flexible chain units [37].

2.11.1 Glycerol

Glycerol is a trihydric alcohol with an empirical chemical formula of $C_3H_5(OH)_3$. Its IUPAC name is propanol-1,2,3-triol (Figure 2.18). It is colorless, odorless, sweet taste, very viscous and absorptive. It is easily soluble in water due to its polar structure containing three hydroxyl groups. Glycerol is made from a byproduct of separation process from attached fatty acid molecules. This is the main component of fats and oils which is commonly found in plants and animals. Glycerol is an intermediate in carbohydrate and lipid metabolism. It is utilized as a plasticizer, emulsifier, pharmaceutical agent and sweetener [38]. The properties and MSDS of glycerol are illustrated in Tables 2.15-2.16.

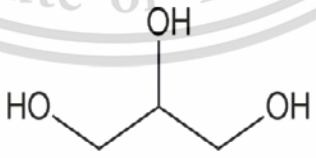

Figure 2.18 Chemical structure of glycerol [38]

Table 2.15 Properties of glycerol [38]

Property	Detail
State	Colorless and odorless liquid
Molecular weight	34.02 g/mol
Density	1.26 g/cm^3
Melting point	17.9°C
Boiling point	290.0°C
Water solubility	Soluble

Table 2.16 MSDS of glycerol [29]

Data	Detail
IUPAC name	Propane-1,2,3-Triol
Chemical name	Glycerol, Glycerin
CAS No.	56-81-5
RTECS code	MA 8050000
NFPA number	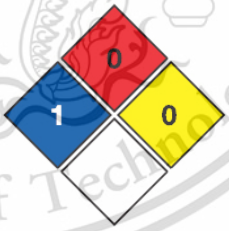 NFPA health hazard: 1 - Materials that cause irritation upon exposure, but only minor injury is sustained even if no medical treatment is provided. NFPA fire hazard: 0 - Materials that will not burn. NFPA reactivity: 0 - Materials that are stable even under exposure to fire.

2.12 Literature Reviews

S. H. Koo *et al.* (2010) conducted a study on preparation of CS from corn starch with different amounts of STMP/STPP—5, 10 and 12% (w/w)— on a dry basis of starch. The resulting CS showed low to high degree of cross-linking: 51.3%, 98.1% and 99.1%, respectively. It was observed that cross-linking corn starch with STMP/STPP reduced its solubility, swelling factor and paste clarity. The swelling factor and paste clarity were associated with the degree of cross-linking. XRD patterns of all prepared CS exhibited a similar A-type pattern and the cross-linking process did not cause any change in the crystallinity of corn starch. Morphology of CS granules exhibited rough fracture and formations of deep groove [39].

R. Wongsagonsupa *et al.* (2014) investigated several properties of CS from tapioca starch prepared with different contents of a mixture of STMP/STPP cross-linking agent. CS was crosslinked with a 99:1 (w/w) mixture of STMP and STPP at pH 11. The amounts of STMP/STPP used were varied from 0.25% to 6.0% (w/w of dry starch). They found that swelling, solubility, paste clarity were reduced with increasing amount of STMP/STPP. Thermal gravimetric analysis (TGA) showed higher thermal stability of CS granules as compared to that of NS. Among the obtained samples, CS obtained from using 1.0% STMP/STPP formed the strongest gel and presented the highest shear resistance [40].

K. Sangseethong *et al.* (2010) investigated the preparation and properties of OS from cassava starch oxidized with hypochlorite (at 3% active chlorine) and hydrogen peroxide. Copper sulfate (0.1 wt% of starch) was used as a catalyst. The blend was mixed and stirred to the end of a reaction time of 30, 60, 120 and 300 min. It was found that two reagents could create OS with a comparative range of viscosity and particle size distribution; however, peroxide was able to oxidize the starch at a faster rate. There were no significant changes on the surface of OS granules at a reaction time of 30 min. Nevertheless, a rough surface was observed after a reaction time of 60 min. At an oxidation time of 120 or 300 min, the starch granules showed rough surface. After having been cooled, the peroxide-OS produced firmer gel than the hypochlorite-OS. A DSC analysis revealed that the two types of oxidation did not affect amylopectin retrogradation. It was also found that the oxidation might apply only to the amylose part [7].

X. Dang *et al.* (2019) prepared OS from potato starch by using hydrogen peroxide at different concentrations (0.8, 1.7, 3.3, 6.6 and 9.9 ml to 50 g of dry starch) and a complex of sodium citrate and Fe^{2+} as a catalyst. Carbonyl contents were found to be 0.11, 0.25, 0.45, 0.67 or 0.81 per 100 AGU, respectively. FT-IR, XRD, DSC and SEM techniques were used to investigate the physiochemical and thermal

properties of OS. FT-IR results for OS showed a new carbonyl peak (C=O stretching) at 1722.1 cm^{-1}. A loss of the crystal phase of starch molecules was observed with an increasing content of carbonyl content, leading to a decrease in the degree of crystallinity. From SEM micrographs, it was observed that the starch surface was destroyed producing smaller starch granules, especially for carbonyl content at 0.45 and 0.81. An increase in the thermal property of OS granules was also detected by DSC which might come from a new arrangement of starch molecules into a crystalline structure [28].

Y. Yin *et al.* (2005) investigated corn starch blend with polyvinyl alcohol (PVA) that was crosslinked with boric acid at different concentrations—0, 0.5, 1, 1.5 and 2 wt% of dried starch—by a casting method and plasticized with glycerol. An increase in viscosity of CS blend with boric acid was observed. O-H stretching of IR peak was found to shift to lower wave number. With an increasing content of boric acid, the maximum stress of the starch/PVA blend increased, but the elongation at break value decreased. Good mechanical properties were observed for the starch/PVA blended crosslinked film with boric acid at 2 wt%. In the same manner, the blended film exhibited good transparency, mechanical properties and water resistance. With an increase in the boric acid content, the film became brittle with high tensile strength and low elongation at break [41].

B. Sreedha *et al.* (2005) performed a characterization of mechanical, thermal properties and morphology of starch–PVA blends crosslinked with borax. The blend films were plasticized with glycerol and cast. Several contents of borax—4, 8 and 12 wt%—were studied. It can be seen that stress at maximum load of the starch–PVA blend films improved after they were crosslinked with borax. With an increase in cross-linking agent content, stress at maximum load of the starch-PVA blend films increased. T_g of a crosslinked blend film was higher than that of the pure blend film. TGA analysis revealed that the thermal stability of the blend films crosslinked with borax was higher than that of the starch-PVA blend film without borax [42].

N. Detduangchan *et al.* (2014) attempted to improve the mechanical and thermal properties as well as the hydrophobicity of NS film from rice starch by cross-linking. NS film was prepared into CS film with a mixture of STMP/STPP (4, 8 and 12 wt%) by a casting technique using sorbitol as a plasticizer. It was found that the pasting viscosity of solutions of CS granules in water reduced as the content of the cross-linking agent increased. The degree of cross-linking seemed to increase with an increasing content of the cross-linking agent. Higher tensile strength together with lower elongation at break and lower hydrophilicity of CS film were noticed after the film was crosslinked. In addition, lower crystalline peak and lower degree of crystallinity were observed in CS films. Thermal properties of CS films were

conducted by dynamic mechanical thermal analysis (DMTA) and DSC. They presented that T_g of CS film was shifted to higher temperature than that of NS film and the storage modulus of CS film was significantly increased [43].

L. M. Foncesa *et al.* (2015) reported the influence of different contents of sodium hypochlorite (at active chlorine of 0.5, 1.0 and 1.5 g/100 g) on properties of OS film from potato starch. The carbonyl and carboxyl contents of OS were 0.068, 0.111 and 0.139 per 100 AGU and 0.039, 0.052 and 0.067 per 100 AGU, respectively. A rise in the carbonyl and carboxyl contents of OS was observed when the active chlorine concentration was increased. The oxidation resulted in decrease in viscosity and swelling capacity of NS. After the films were crosslinked, not only the water solubility of the obtained OS films was decreased, but WVP was also decreased as well as the hardness and tensile strength. The highest extendibility and lowest hydrophilicity were obtained in OS film with the highest of degree of oxidation [44].

S.D. Zhang *et al.* (2009) prepared thermoplastic oxidized starch (TPOS) by mixing OS from corn starch with glycerol plasticizer from compression molding technique. Different degree of oxidation (DO) of 0.385, 0.495 and 0.554 were obtained from reacting with different molar ratios of hydrogen peroxide to starch at 0.7, 1 and 2. The influence of DO on several properties of TPOS was studied. FT-IR analysis confirmed that at hydrogen peroxide/starch molar ratios of 0.7, OS contained higher aldehyde groups than carboxyl groups, while peroxide oxidation generated mainly carboxyl groups at molar proportions up to 2.0, SEM micrograph showed that the particles of OS (at DO 0.385) presented a porous structure. With the increase of DO, crystallinity, intrinsic viscosity, tensile strength and thermal property of OS significantly reduced. Moreover, water uptake value of OS decreased in the case of low DO (0.385 and 0.495). From this study, TPOS with DO at 0.385 showed the highest of maximum stress, however, the highest of maximum elongation was obtained from TPOS at 0.495 [45].

H.X. Xiao *et al.* (2012) investigated the physicochemical properties of NS, two singly modified starch (CS and OS) and two dually modified starch: cross (COS and OCS from rice starch using epichlorohydrin 0.3% w/w of dry starch and sodium hypochlorite (2.5% active chlorine w/w). Degree of swelling, solubility, morphology, the tendency of retrogradation, pasting and thermal properties of different modified starch were examined. The result showed that COS exhibited lower degree of swelling and solubility in water compared to NS and OCS. COS also exhibited not only the lowest tendency to retrograde but also the highest shear resistant and thermal property. For morphology, no difference in morphology of COS and OCS was observed as compared to NS, CS and OS. Furthermore, the reduction in pasting temperature and peak viscosity were found in case of COS [8].

S. Sukhija *et al.* (2016) developed both dually modified starch (OCS and COS) from elephant foot yam starch using sodium hypochlorite (2.5% active chlorine w/w) and the mixture of STMP/STPP (0.03% w/w of dry starch). The comparative results of amylose content, degree of cross-linking, physicochemical, morphology and thermal property of singly and dually modified starch were examined. The dual modification of NS was confirmed by FT-IR and XRD results. It was found that all modifications of starch caused a decrease in amylose content and degree of crystallinity, while water binding capacity and colour value (whiteness) increased. All modified starch showed a rise in degree of swelling and solubility depending on temperature. The light transmittance of OS, COS and OCS was clearly improved compared to NS. The rough fractured surfaces of the starch granules appeared in case of CS and both dually modified starch; while, a smooth surface appeared in NS and OS. Pasting properties of OS and COS from using RVA demonstrated a decrease in viscosity as compared to NS [9].

G. Karmvlr *et al.* (2018) prepared modified NS from white sorghum starch by dual modification (oxidation-cross-linking) by sodium hypochlorite 0.8% active chlorine and the mixture of STMP/STPP (99:1) at 25% wt. of dried starch. Amylose content, degree of swelling, solubility and textural properties of different modified starch were evaluated. The starch was also analysed for thermal properties by DSC and crystallinity by XRD technique. The amylose contents of all modified starch were lower than when compared to NS and varied from 4.11 to 22.4%. All of modified starch exhibited an A-type XRD pattern. Oxidation and dual modification not only decreased the degree of swelling, but also increased the solubility of the starch. A substantial increase in hardness value of starch pastes was detected after modification. Cross-linking and dual modification could also improve thermal stability of NS [10].

S. Sukhija *et al.* (2016) focused on the dual modification of lotus rhizome starch using sodium hypochlorite and STMP with different contents of cross-linking agent (1%, 2% and 3%w/w of dry weight of starch) and oxidizing agent (0.5, 1 and 1.5% w/w active chlorine). Morphological, thermal, FT-IR and XRD analyses of different dually modified starch were investigated further upon varying degrees of cross-linking (4.31-58.28%), carbonyl (0.03-0.07%) and carboxyl content (0.07-0.15%). Dual modification obviously improved the water binding capacity, swell power, paste clarity and colour value (whiteness) of starch. With the increase in degree of cross-linking, the degree of carboxyl content and carbonyl content of dually modified starch tended to decrease. The decrease in intensity peak at 1644 cm^{-1} corresponding to the intramolecular hydrogen bond could support the success of cross-linking by STMP. A rise in degree of crystallinity for oxidized and dually modified starch was

observed when the degree of oxidation increased. The morphology of OS and OCS granules presented damaged surface or fissures, while the smooth surface of NS, CS and COS was observed and CS or COS also exhibited no change in the morphology of starch granules after modification [11].

Chapter 3

Research methodology

3.1 Materials

1. Cassava starch; from Chaopraya Phuchrai 1999 Co., Ltd., Thailand.

Table 3.1 The components of cassava starch

Component	Weight percentage (%)
Amylose	16.4±3
Amylopectin	83.6±2
Lipid	0.25±0.1
Protein	6.50-7.50
Humidity	<13
Ash	0.23±0.1
Size	<160 μm
pH	6-7

Remark: Data of the manufacturer.

2. Borax; food grade from Union Chemical 1986 Co., Ltd., Thailand.
3. Boric acid; food grade from Italmar Co., Ltd., Thailand.
4. Sodium tripolyphosphate or STPP; food grade from Chemipan Co., Ltd., Thailand.
5. Sodium trimetaphosphate or STMP; food grade from Chemipan Co., Ltd., Thailand.
6. Hydrogen peroxide; 30%w/v analysis grade from Chem-Supply Co, Ltd., Australia.
7. Hydrochloric solution; analysis grade from Carlo Erba Co., Ltd., France.
8. Sodium hydroxide; analysis grade from Carlo Erba Co., Ltd., France.
9. Hydroxalamine hydrochloride; analysis grade from Carlo Erba Co., Ltd., France.
10. Methyl orange indicator; analysis grade from Carlo Erba Co., Ltd., France.

11. Phenolphthalein; analysis grade from Carlo Erba Co., Ltd., France.
12. Dimethyl sulfoxide or DMSO; analysis grade from Carlo Erba Co., Ltd., France.
13. Glycerol; from Lab System Co., Ltd., Thailand.
14. Ethanol; analysis grade from Carlo Erba Co., Ltd., France.
15. Distilled water.

3.2 Instruments

1. Beaker; 250, 500 and 1000 ml
2. Three-neck round-bottom; 500 and 1000 ml
3. Heating mantle; MQ 1000 ml from FALC Co., Ltd., Italy.
4. Hot plate stirrer; CMAG HS7 5000 from IKA Co., Ltd., Thailand.
5. Mechanical stirrer; RW 20 D from IKA Co., Ltd., Thailand.
6. Water bath; WNP22 from Memmert Co., Ltd., U.S.A.
7. Analytical balance; MS204TS/00 from Mettler-Toledo Co., Ltd., Thailand.
8. Vacuum filter; A35 from Eyela Co., Ltd. U.S.A.
9. Hot air oven; UF110 from Memmert Co., Ltd. U.S.A.
10. Blender; EM 44A from SHARP Co., Ltd. Thailand.
11. Centrifuge; Universal 320 from Hettich Co., Ltd., U.S.A.
12. Granulator; ZM100 from Retsch Co., Ltd., Germany.
13. Capillary viscometer from Thomas Scientific Co., Ltd., U.S.A.
14. Rapid visco analyzer (RVA); RVA-4 from Newport Co., Ltd. U.S.A.
15. Universal testing machine); LR 5 K from Lloyd Instrument Co., Ltd., UK
16. Fourier transform infrared spectrophotometer (FT-IR); SPECTRUM GX from Perkin Elmer Co., Ltd., U.S.A.
17. Scanning Electron Microscopy (SEM); JSM-5410 from Jeol Co., Ltd., Japan.
18. X-ray diffractometer (XRD); D8 Advance from Bruker Co., Ltd., U.S.A.
19. Thermogravimetric analyzer (TGA); Pyris 1 from Perkin Elmer Co., Ltd., U.S.A.

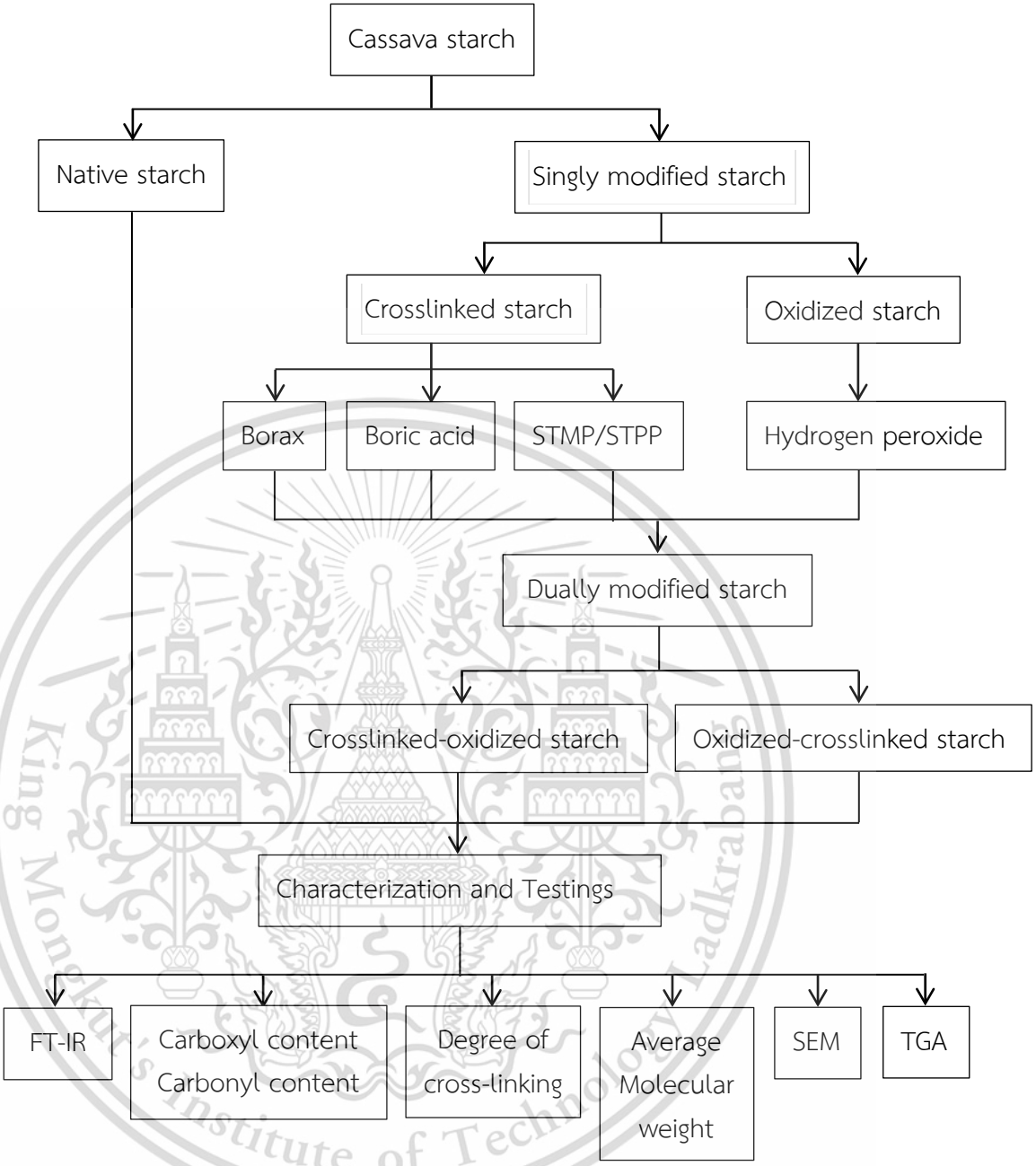

Figure 3.1 Flowchart of preparation of different modified starch

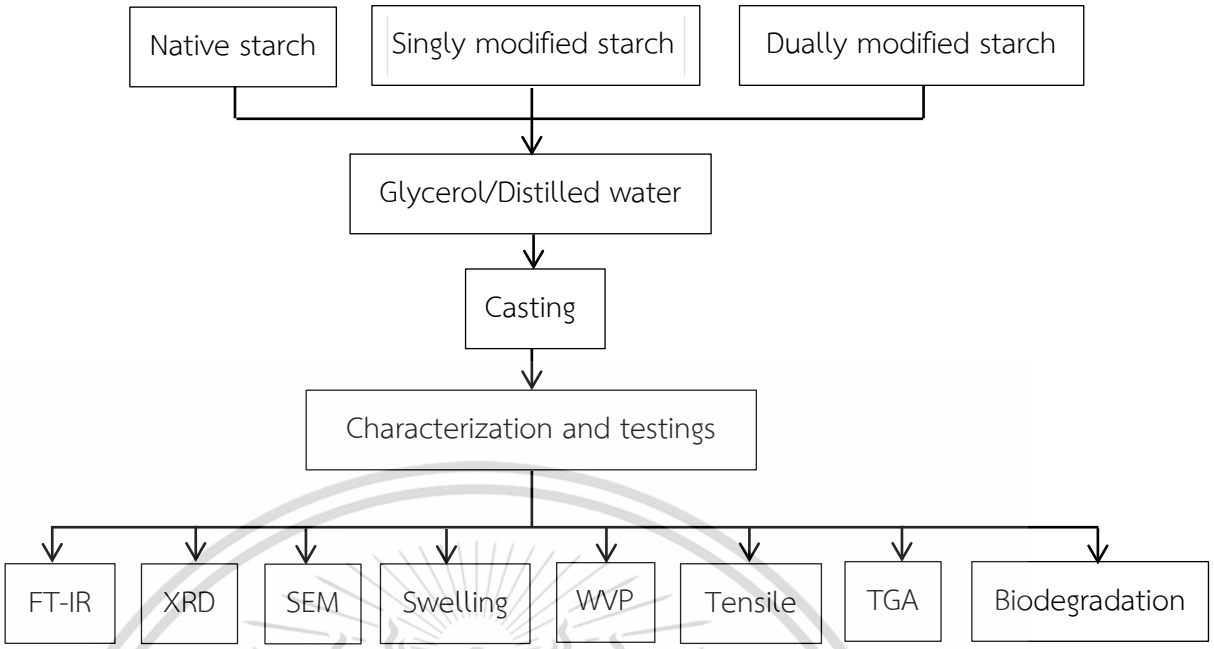

Figure 3.2 Flowchart of preparation of different modified starch films

3.3 Method

In this study, preparation flowcharts of different modified starch and modified starch films are shown in Figures 3.1-3.2.

3.3.1 Preparation of singly modified starch

3.3.1.1 Preparation of crosslinked starch (CS)

1. Cassava starch (50 g) was suspended in 70 mL of distilled water.
2. pH was adjusted to 10.0 with 0.1 M NaOH.
3. Starch slurry was mixed with each cross-linking agent: borax, boric acid and STMP/STPP at 20% w/w on a dry basis of starch according to the formulas shown in Table 3.2.
4. The temperature of the slurry was controlled at 45°C; it was continuously stirred with a magnetic stirrer at 300 rpm for 2 h.
5. pH of the suspension was neutralized to 7.0 with 0.1 M HCl; the suspension was filtrated and washed thoroughly with distilled water to remove the remaining cross-linking agent.
6. The resulting CS was dried at 50°C for 24 h in a hot-air oven.

3.3.1.2 Preparation of oxidized starch (OS)

1. Firstly, 50 g of cassava starch was suspended in 250 mL distilled water in a 1000 mL three-neck round-bottom flask and heated at 80°C for 1 h with continuous stirring at 300 rpm in order to form gelatinized starch. The pH was adjusted to 10.0 with 0.1M NaOH.
2. After the gelatinized starch was cooled to room temperature, 200 mL of distilled water containing 25.0 mL of 30% (w/v) hydrogen peroxide (20% w/w on a dry basis of starch) was added dropwise to the mixture for 15 min with continuous stirring at 300 rpm for 2 h while the temperature was controlled to be 25°C.
3. After 2 h, the pH was neutralized to 7.0 with 0.1 M HCl.
4. OS was separated from the gelatinized starch by precipitation with ethanol for 24 h.
6. OS was filtrated and washed thoroughly with distilled water to remove remaining hydrogen peroxide.
7. OS sample was then dried in a hot-air oven at 50°C for 24 h.
8. It was ground into powder with a granulator (Retsch, Germany).

3.3.2 Preparation of dually modified starch

3.3.2.1 Preparation of crosslinked-oxidized starch (COS)

1. Cassava starch was firstly crosslinked with 20% (dry basis weight of starch) in the same manner as CS described above.

2. In the second step (oxidation process), hydrogen peroxide was added by using the same procedure as that in the preparation of OS.

3.3.2.2 Preparation of oxidized-crosslinked starch (OCS)

1. Cassava starch was firstly oxidized with hydrogen peroxide in the same manner as CS was prepared.

2. After the oxidation, a cross-linking agent was added to crosslink OS as previously described in 3.3.1.1.

3.3.3 Preparation of biodegradable film by different types of modified starch

1. To prepare a starch solution at a concentration of 10% (w/v), NS or modified starch (10 g) was added into a beaker with 100 mL of distilled water followed by an addition of 30% w/w glycerol.

2. The mixture was then heated on a hot plate and magnetically stirred at a speed of 300 rpm at 65˚C until pre-gelatinization occurred.

3. After having been cooled to room temperature, the mixture was cast onto a polyethylene plate. The thickness of the film was controlled by adjusting and fixing the poured volume (70 mL) to achieve a film thickness of 0.1-0.2 mm.

4. The film was placed in a hot-air oven at 50˚C for 6 h.

5. After drying, biodegradable starch film of about 0.1-0.2 mm in thickness was obtained.

Table 3.2 Compositions of different modified starch

Sample	Cassava Starch (g)	Distilled water (mL)	Borax/Boric acid/STMP and STPP		Hydrogen peroxide	
			g	% wt	g	% wt
CS-BO	50	70	10	20	-	-
CS-BA	50	70	10	20	-	-
CS-ST	50	70	10	20	-	-
OS	50	250	-	-	10	20
COS-BO	50	320	10	20	10	20
COS-BA	50	320	10	20	10	20
COS-ST	50	320	10	20	10	20
OCS-BO	50	320	10	20	10	20
OCS-BA	50	320	10	20	10	20
OCS-ST	50	320	10	20	10	20

3.4 Characterization

3.4.1 Average molecular weight

The method of intrinsic viscosity was used to determine the average molecular weight (MW) of a sample. The test was performed at 25.0±0.1°C with an Ubbelohde Viscometer. The starch was dissolved in dimethyl sulfoxide (DMSO) solvent. The average molecular weight of starch was obtained based on intrinsic viscosity measurements. Intrinsic viscosity was calculated using Mark-Houwink equation:

$$[\eta] = KM^{a} \quad \text{(Eq.1)}$$

where $[\eta]$ is intrinsic viscosity; K and a are constants equal to 8.5×10^{-3} mL/g and 0.76, respectively; and M is the average molecular weight [46].

3.4.2 Carbonyl content (%)

The carbonyl content was examined by following the titrimetric method of R. J. Smith (1967) [47]. Starch (4 g) was dissolved with 100 mL of distilled water in a 500 mL flask and heated in the boiling water bath for 20 min, cooled to 40°C, adjusted to pH 3.2 with 0.1 M HCl and added to 15 mL of hydroxylamine reagent. The reaction mixture was continuous mechanically stirred at 300 rpm under heating within the controlled temperature of 40±5°C for 4 h. After that, the sample was rapidly titrated with 0.1 M HCl using methyl orange as an indicator until the red to

yellow end point (pH 3.2). Only hydroxylamine reagent as a blank was prepared by dissolving 25 g hydroxylamine hydrochloride in 100 mL of 0.5 M NaOH before adjusting the final volume to 500 ml. The carbonyl content was determined according to Eq. 2 below:

$$\text{Carbonyl content (\%)} = \left[\frac{(V_b\text{-}V_s)\text{mL} \times C_{HCl} \times 0.028 \times 100}{\text{Sample weight (g)}}\right] \quad \text{(Eq.2)}$$

where V_b is the titrate volume of HCl consumed by the blank (mL); V_s is the titrate volume of HCl consumed by the sample (mL); C_{HCl} is concentration of HCl (0.1 M) and 0.028 = (molar mass of carbonyl group)/1000.

3.4.3 Carboxyl content (%)

The carboxyl content of OS was examined according to the modified method of K. Sangseethong *et al.* (2010) [39]. Starch (2 g) was dissolved in 25 mL of 0.1 M HCl and the starch slurry was stirred with a magnetic stirrer at 300 rpm for 30 min. The starch solution was then filtered and washed with 400 mL of distilled water until free of chloride ions. The starch sample was then carefully moved into a 500 mL beaker and the volume was adjusted to 300 mL with distilled water. The system was stirred by using mechanical stirrer at 300 rpm under heating within the temperature range of 80±5°C for 15 min to form the gelatinized starch. The hot starch solution was then adjusted to 450 mL with distilled water and titrated with standardized 0.1 M NaOH using phenolphthalein as an indicator until a light pink color appeared (pH 8.3). A blank test was carried out with unmodified starch. The carboxyl content was determined according to Eq. 3 as follows:

$$\text{Milliequivalents of Acidity} = \left[\frac{(V_s\text{-}V_b)\text{mL} \times C_{NaOH} \times 100)}{\text{Sample weight (g)}}\right]$$

$$\text{Carboxyl content (\%)} = \frac{\text{Milliequivalent of acidity} \times 0.045}{\text{100 g starch}} \quad \text{(Eq.3)}$$

where V_s is the titrate volume of NaOH consumed by the sample (mL); V_b is the titrate volume of NaOH consumed by the blank (mL); C_{NaOH} is concentration of NaOH (0.1 M) and 0.045 = (molar mass of carboxyl group)/1000.

3.4.4 Degree of cross-linking

A Rapid Viscosity Analyser (RVA) was used to determine the change in viscosity of starch during heating and cooling. Starch (3 g) was dissolved into 25 ml of distilled water in a RVA vessel. The reaction mixture was stirred at 960 rpm for 10 s and at 160 rpm by a plastic paddle in the vessel. After incubating for 1 min at 50°C, the starch sample was heated to 95°C in 3.7 min, controlled at 95°C for 2.5 min, cooled to 50°C in 3.7 min. Peak viscosity were determined as the maximum viscosity during the heating step. Peak viscosity was determined by the average of three measurements on each starch sample. The degree of cross-linking was calculated according to Eq. 4 below:

$$\text{Degree of crosslinking} = \frac{A - B}{A} \times 100 \qquad \text{(Eq.4)}$$

where, A = the peak viscosity of NS ; B = the peak viscosity of CS [43].

3.4.5 Fourier-transform infrared spectroscopy (FT-IR)

FT-IR spectroscopic analyses were performed by using the KBr pellets with a Spectrum 2000 GX spectrometer (PerkinElmer, U.S.A.). Dried powder sample was mixed with KBr powder and then, the mixture was pressed into pellets. FT-IR spectra were performed in the range of 4000-400 cm^{-1} with a resolution of 4 cm^{-1} and 10 consecutive scans per sample. The peak height and ratio of peak height were also determined. The ratio of the peak height was calculated by the ratio of the peak height of interested peak/the peak height of referenced peak at 859 cm^{-1}, the referenced peak showed the constant peak height.

3.4.6 X-ray diffraction technique (XRD)

X-Ray diffraction patterns and degree of crystallinity of the samples were obtained by using a D8 Advance X-ray diffractometer (Bruker, Madison, U.S.A.) with CuK_α radiation operating *at* 40 kV and 35 mA. The scattering angle (2θ, θ is the Bragg angle) covered a range from 5° to 60° at a scan rate of 1°/min. Percentage crystallinity was calculated by following equation:

$$\text{Crystallinity (\%)} = \frac{A_c}{A_c + A_a} \times 100 \qquad \text{(Eq.5)}$$

where A_c and A_a refer to the area of crystalline peak diffraction and the total area of the X-ray diffractogram, respectively.

3.4.7 Scanning electron microscopy (SEM)

Samples were characterized for morphology by scanning electron microscopy (LEO 1450 VP). Each film was frozen in liquid nitrogen and fractured. The samples were coated with a thin film of gold by using the ion sputtering method in order to prevent electrical charging during observation. The SEM micrographs were configured at 15 kV with approximations in the range of 4000X.

3.4.8 Swelling behavior

The samples from each type of film (20×20 mm^2) were firstly dried at 105°C for 2 h to determine their initial dry weight and then were immersed in distilled water at temperature of 25±5°C for 2, 4, 6 and 72 h. The weight of the wet film (W_2) was recorded after removal of the water with blotting paper. Three measurements were produced for each sample. The degree of swelling was determined as follows:

$$\text{Swelling (\%)} = \frac{W_2 - W_1}{W_1} \times 100 \qquad \textit{(Eq.6)}$$

where W_2 is the wet weight of the sample and W_1 is the dried weight of the sample.

3.4.9 Water vapor permeability test (WVP)

WVP tests of the samples were performed by using the gravimetric modified cup method (the desiccant method) according to ASTM-E96 standard method. The amount of water vapor transferred through the sample area was determined from the weight gain versus time. WVP was determined according to Eq. 7 below:

$$WVP = \frac{W \times X}{t \times A \times \Delta P} \qquad \textit{(Eq.7)}$$

where W/t = the slope of sample weight vs. time (g/day); X = the average thickness of the film (mm); A = the exposed surface area of the film (32.15 cm^2) and ΔP = the difference in partial vapor pressures at the top and bottom sides of the film (KPa) [48].

3.4.10 Mechanical properties

Tensile properties of the films were evaluated according to ASTM D-882 by using a Universal Testing Machine (Lloyd Instrument, LR 5K, West Sussex, UK) at 25±1°C and 60±5%RH. A film was cut into a dimension of 100×15 mm^2 and then equipped in a desiccator containing a saturated solution of ammonium nitrate for 24 h before measurement. The measurements were performed by using a gauge length

of 50 mm, a crosshead speed of 50 mm/s and a load cell of 100 N. The mechanical properties values were determined from different ten independent measurements for each sample. Stress at maximum load, Young's modulus and strain at maximum load can be calculated by the following equations:

$$\text{Tensile strength} = F/A \quad \text{(Eq.8)}$$

$$\text{Strain at maximum load (\%)} = \frac{(L - L_0)}{L_0} \times 100 \quad \text{(Eq.9)}$$

$$\text{Young's modulus} = \frac{F/A}{(L-L_0)/L_0} \quad \text{(Eq.10)}$$

F is the force that extended the specimen (N)

A is the cross section area of the specimen (mm^2)

L is the length of the specimen after stretching (mm)

L_o is the initial length of the specimen (mm)

3.4.11 Thermogravimetric analysis (TGA)

Thermogravimetric (TGA) and derivative thermogravimetric (DTG) thermograms of the samples were evaluated with a thermogravimetric analyser (Pyris 1, Perkin Elmer, USA). The sample was performed in a temperature range from 50 to 600°C with a constant heating rate of 10°C/min under nitrogen atmosphere. Thermal decomposition temperature (T_d) was obtained from the maximum degradation temperature.

3.4.12 Biodegradability

A film was buried under a depth of approximately 10 cm from the surface of soil. pH and temperature of the soil were controlled at 7±1 and 25±2°C, respectively. The water content of the soil was controlled in the range of 5–10%. Then, the sample was thoroughly removed from the soil and their mechanical properties were recorded from ten independently tested specimens.

Chapter 4
Main results and discussion

This study focused on the effects of single and dual modifications of cassava starch films by oxidation with hydrogen peroxide and cross-linking with different types—borax, boric acid and a mixture of STMP/STPP. The physiochemical properties of the singly and dually modified cassava starch films (CS, OS, COS and OCS) were also investigated and compared. The characterization techniques included Fourier transform infrared spectroscopy (FT-IR), X-ray diffractometry (XRD) and scanning electron microscopy (SEM). In particular, the degree of swelling and water vapor permeability (WVP) as well as several mechanical and thermal properties were determined. The levels of biodegradability of the films were also determined by a soil burial test. Abbreviations and symbols of the terms used in this research are shown in Table 4.1.

Table 4.1 Abbreviations and symbols

No.	Abbreviation	Meaning
1	NS	Native cassava starch
2	CS-BO	Cassava starch crosslinked with borax
3	CS-BA	Cassava starch crosslinked with boric acid
4	CS-ST	Cassava starch crosslinked with the mixture of STMP/STPP
5	OS	Cassava starch oxidized with hydrogen peroxide
6	COS-BO	Crosslinked-oxidized cassava starch with borax and hydrogen peroxide
7	COS-BA	Crosslinked-oxidized cassava starch with boric acid and hydrogen peroxide
8	COS-ST	Crosslinked-oxidized cassava starch with the mixture of STMP/ STPP and hydrogen peroxide
9	OCS-BO	Oxidized-crosslinked cassava starch with hydrogen peroxide and borax
10	OCS-BA	Oxidized-crosslinked cassava starch with hydrogen peroxide and boric acid
11	OCS-ST	Oxidized-crosslinked cassava starch with hydrogen peroxide and the mixture of STMP/STPP
12	NSF	Native cassava starch film
13	CS-BOF	Cassava starch film crosslinked with borax

No.	Abbreviation	Meaning
14	CS-BAF	Cassava starch film crosslinked with boric acid
15	CS-STF	Cassava starch film crosslinked with the mixture of STMP/STPP
16	OSF	Cassava starch film oxidized with hydrogen peroxide
17	COS-BOF	Crosslinked-oxidized cassava starch film with borax and hydrogen peroxide
18	COS-BAF	Crosslinked-oxidized cassava starch film with boric acid and hydrogen peroxide
19	COS-STF	Crosslinked-oxidized cassava starch film with the mixture of STMP/STPP and hydrogen peroxide
20	OCS-BOF	Oxidized-crosslinked cassava starch film with hydrogen peroxide and borax
21	OCS-BAF	Oxidized-crosslinked cassava starch film with hydrogen peroxide and boric acid
22	OCS-STF	Oxidized-crosslinked cassava starch film with hydrogen peroxide and the mixture of STMP/STPP

4.1 Properties of different modified starch

In this study, the physicochemical properties of biodegradable singly and dually modified cassava starch by cross-linking with different types—borax, boric acid and a mixture of STMP/STPP as well as oxidation with hydrogen peroxide— were examined and compared as follows:

4.1.1 Schematic reactions of different modified starch

The proposed schematic reactions and possible chemical structures of different singly modified starch and different dually modified starch are displayed in Figures 4.1-4.4 and Figures 4.5-4.7, respectively.

For the synthesis of CS, the four hydroxyl groups of the starch chains at the C-2, C-3 or C-6 positions reacted with either borax or boric acid (CS-BO and CS-BA) and formed tetra-starch borate structures (Figures 4.1-4.2). In particular, when borax was added to the starch solution, it was transformed into four boric acid molecules, and then the boric acid crosslinked with the starch molecules. On the other hand, the two hydroxyl groups of the starch chains at the C-2 and C-3 positions crosslinked with STMP/STPP (CS-ST) to produce di-starch phosphate structures (Figure 4.3).

$Na_2B_4O_7 \cdot 10\ H_2O\ (s) \longleftrightarrow 2\ Na^+\ (aq) + B_4O_7^{2-}\ (aq)$

Sodium tetraborate — tetraborate anion

$B_4O_7^{2-}\ (aq) + 7\ H_2O\ (l) \longleftrightarrow 4\ H_3BO_3\ (aq) + 2\ OH^-\ (aq)$

boric acid

$H_3BO_3\ (aq) + OH^-\ (aq) \longleftrightarrow B(OH)_4^-\ (aq)$

tetrahydroxy borate anion

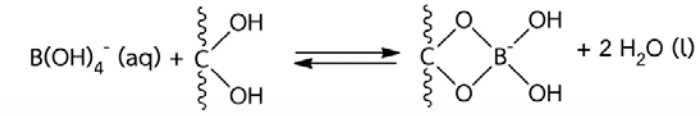

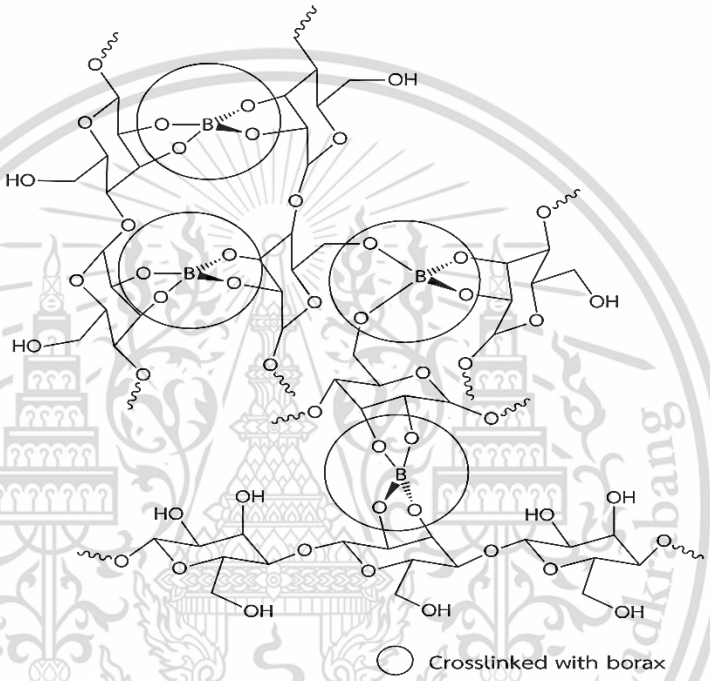

Figure 4.1 Schematic structure of CS crosslinked with borax

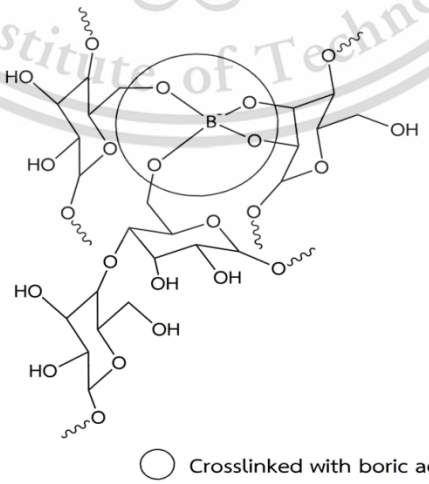

Figure 4.2 Schematic structure of CS crosslinked with boric acid

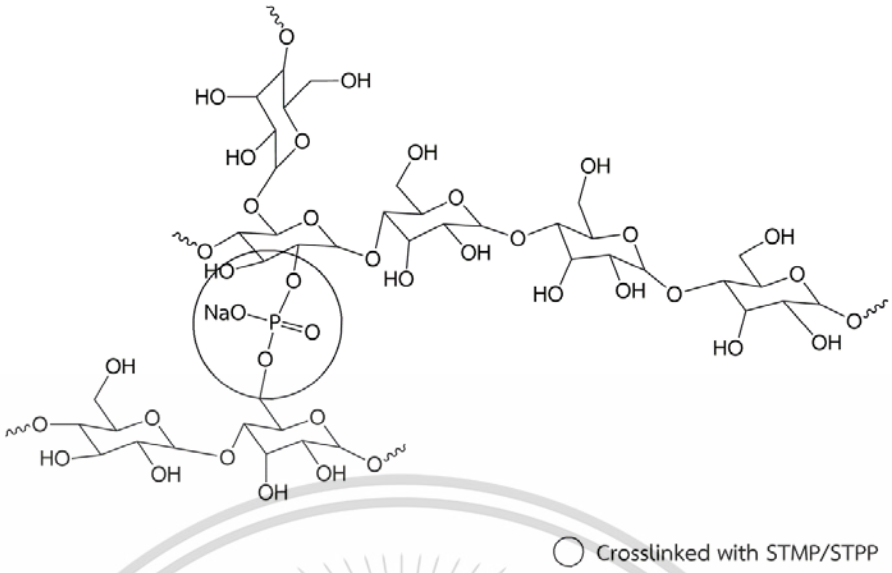

Figure 4.3 Schematic structure of CS crosslinked with STMP/STPP

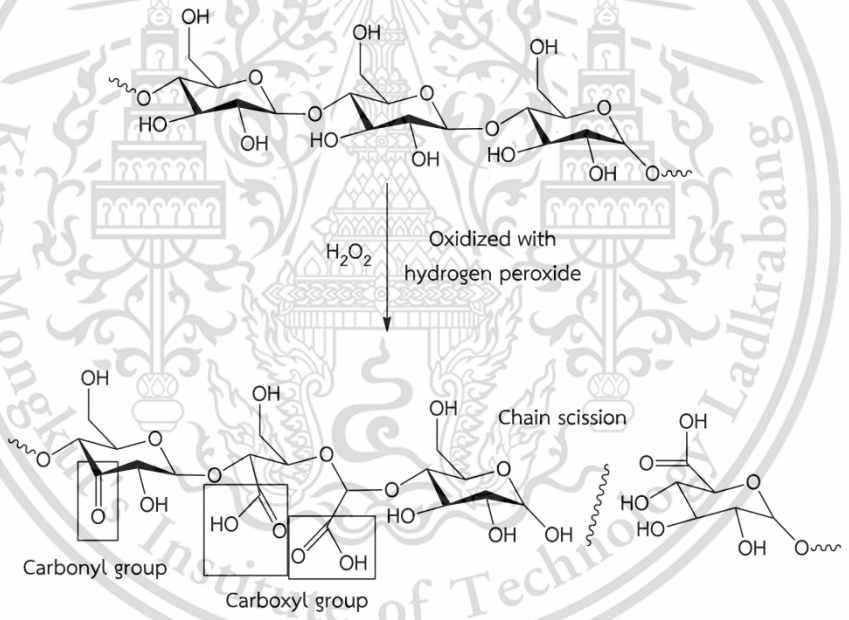

Figure 4.4 Chemical reaction of OS oxidized with hydrogen peroxide

For the preparation of OS, the hydroxyl groups of the starch at the C-2, C-3 or C-6 positions reacted with hydrogen peroxide and generated the new carbonyl and carboxyl substitution groups. A concurrent reaction of partial chain scission could also occur, which resulted in low molecular weights and shorter starch chains (Figure 4.4).

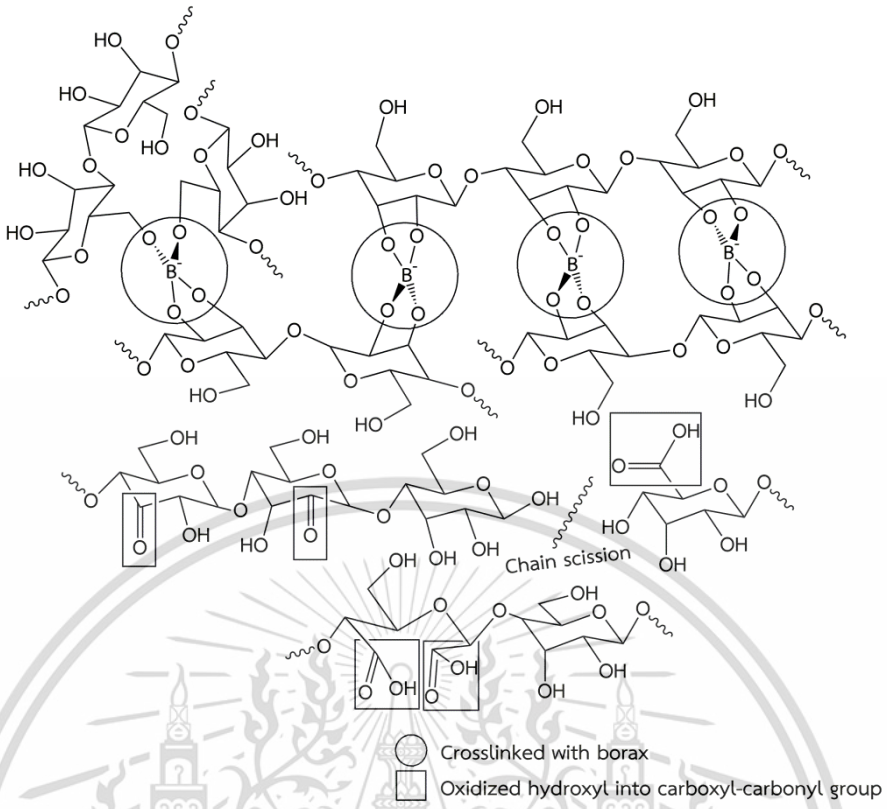

Figure 4.5 Schematic structures of COS and OCS crosslinked with borax and oxidized hydrogen peroxide

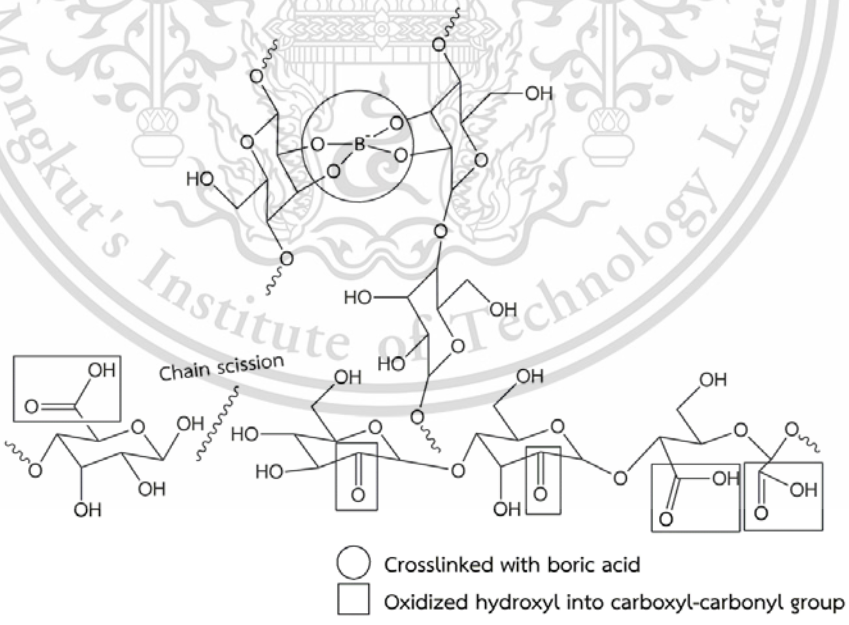

Figure 4.6 Schematic structures of COS and OCS with crosslinked with boric acid and oxidized with hydrogen peroxide

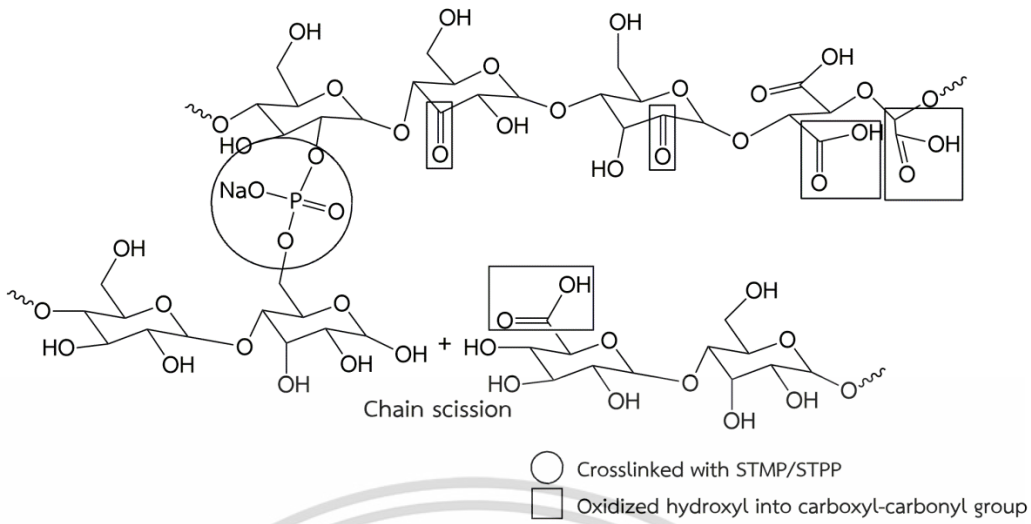

Figure 4.7 Schematic structures of COS and OCS crosslinked with the mixture of STMP/STPP and oxidized with hydrogen peroxide

Figure 4.5-4.7 represent schematic structures of COS and OCS crosslinked with different types of cross-linking agents and oxidized with hydrogen peroxide. For the synthesis of COS, the hydroxyl groups of the starch chains at the C-2, C-3 or C-6 positions primarily reacted with a cross-linking agent to form three-dimensional crosslinked network (CS) structure: di-starch phosphate or tetra-starch borate structures. After that, the remaining hydroxyl groups of CS were oxidized with hydrogen peroxide to form COS structure that contained carboxyl and carbonyl groups. A side reaction generated some shorter starch chains.

For OCS, the hydroxyl groups of the starch backbone firstly reacted with hydrogen peroxide to produce OS structure containing carboxyl and carbonyl groups. In addition, partial cleavage of the starch chains could occur during the oxidation process, leading to the formation of low molecular weight starch backbones. After that, the remaining hydroxyl groups of OS crosslinked with the molecules of cross-linking agent to produce tetra-starch borate or di-starch phosphate (OCS) structures.

4.1.2 Degree of cross-linking, carbonyl content and carboxyl content of differently modified starch

The degree of cross-linking as well as the carbonyl and carboxyl contents were used to affirm the success of the starch structure modification as shown in Table 4.2. These characteristics were strongly dependent on the type of modification procedure involved. In addition, peak viscosity measured by an RVA technique was utilized to examine the degree of cross-linking of differently modified starch, except for OS sample which was not crosslinked.

Table 4.2 Degree of cross-linking, carbonyl and carboxyl contents of differently modified starch

Sample	Peak viscosity (cps)	Degree of cross-linking (%)	Carbonyl content (%)	Carboxyl content (%)
NS	6980±0.19	-	-	-
CS-BO	2041±0.18	70.76±0.03	-	-
CS-BA	2315±0.22	66.81±0.04	-	-
CS-ST	3720±0.20	46.72±0.02	-	-
OS	-	-	0.53±0.22	0.48±0.14
COS-BO	2116±0.21	69.68±0.04	0.30±0.23	0.20±0.23
COS-BA	2378±0.18	65.93±0.03	0.35±0.12	0.27±0.18
COS-ST	3804±0.22	45.50±0.05	0.38±0.24	0.34±0.17
OCS-BO	5237±0.18	24.97±0.01	0.52±0.25	0.47±0.15
OCS-BA	5639±0.19	19.21±0.01	0.52±0.13	0.46±0.22
OCS-ST	5853±0.22	16.17±0.01	0.53±0.21	0.47±0.23

Table 4.2 shows the degree of cross-linking as well as the carbonyl and carboxyl contents of differently modified starch. It can be observed that the peak viscosities of all CS, COS and OCS samples were clearly lower than that of NS. This result confirmed the successful cross-linking reactions between NS and the tested crosslinkers. The lower peak viscosities of all CS, COS and OCS samples when compared to that of NS sample were due to the formation of intermolecular bridges in the cross-linking process that reduced the affinity between the starch molecules and water molecules [43].

When comparing the degree of cross-linking of different types of modified starch, using the same type of cross-linking agents, all COS samples exhibited slightly lower degrees of cross-linking agents than all CS samples. This was probably because the partial starch chain cleavage occurred during oxidation reaction in dual modification method (preparation of COS) that slightly decreased the formation of di-starch phosphate or tetra borate structures of all COS samples. Nevertheless, all OCS samples presented a lower degree of cross-linking values than those of CS and COS, comparing with the same type of cross-linking agents, which might be due to the lower numbers of remaining free hydroxyl groups after the oxidation process available to react with cross-linking agents from first step of OS preparation [11].

When comparing the effects of the different types of cross-linking agents of various CS, COS and OCS samples, it can be seen that the degrees of cross-linking of

CS, COS and OCS samples crosslinked with the mixture of STMP/STPP were lower than those for borax and boric acid. This could be because the lowest cross-linking efficiency among the various cross-linking agents due to STMP/STPP could react two hydroxyl groups of starch molecules, leading to lower crosslink density (Figure 4.3). When the cross-linking efficiencies of borax and boric acid were compared, all modified starch crosslinked with borax showed higher degree of cross-linking than with boric acid, which can explain that borax was a more efficient cross-linking agent. Borax was more efficient because when it was added to a starch solution, it was converted into four boric acid molecules, each of which could crosslink with starch molecules, leading to a high crosslink density and efficiency (Figure 4.1).

When the carboxyl and carbonyl contents of the differently modified starch were compared, it was found that OS presented similar carboxyl and carbonyl contents to those of all OCS samples. The carboxyl content was 0.48 and the carbonyl content was 0.53. It was suggested that cross-linking reaction did not affect the influence of oxidation reaction at first step on the preparation of OCS method. Nevertheless, all COS samples showed lower the carboxyl and carbonyl contents than that of OS and all OCS, comparing with the same type of cross-linking agent because of the smaller chance for free hydroxyl groups to react with hydrogen peroxide due to the high degree of cross-linking.

Regarding the effects of using different cross-linking agents for preparing COS, the carboxyl and carbonyl contents of prepared COS could be ranked as follows: COS-ST>COS-BA>COS-BO. This result was a consequence of the different efficiencies of the cross-linking agents and the different amounts of the remaining hydroxyl groups after cross-linking. In particular, COS-ST provided the highest number of carbonyl groups because of its lowest degree of cross-linking, hence more remaining hydroxyl groups were available to react with the hydrogen peroxide (Figure 4.7). COS-BA contained higher carboxyl and carbonyl contents than those of COS-BO because of a lower degree of cross-linking and a higher number of remaining hydroxyl groups from the lower degree of cross-linking in the first step of cross-linking-oxidizing method. This result agrees with a result reported by S. Sukhija *et. al* (2016) that COS from lotus rhizome starch could be prepared by using a smaller quantity of the oxidizing agent (NaOCl) after cross-linking with STMP. Cross-linking could also restrain the rearrangement of starch molecules, leading to a lower chance of oxidation [11].

4.1.3 FT-IR study

In general, FT-IR is a method for identifying functional groups of a substance. Table 4.3 summarizes the peak assignments of the characteristic bands of the FT-IR spectrum of differently modified starch.

Table 4.3 Peak assignment of the characteristic bands of the FT-IR spectrum of differently modified starch

Wave number (cm^{-1})	Characteristic band
3600 – 3200	O-H stretching
3000 – 2800	Alkane C-H stretching
1750 – 1730	Carboxyl and Carbonyl C=O stretching
1645 – 1640	Hydrogen bonding
1630 – 1600	Bounded water
1485 – 1420	O-H bending
1300 – 1100	C-O-C stretching
1200 – 1000	C-O-H bending
900 – 940	C-H out-of-plane bending
800 – 860	C-H out-of-plane bending
737 – 770	C-H out-of-plane bending

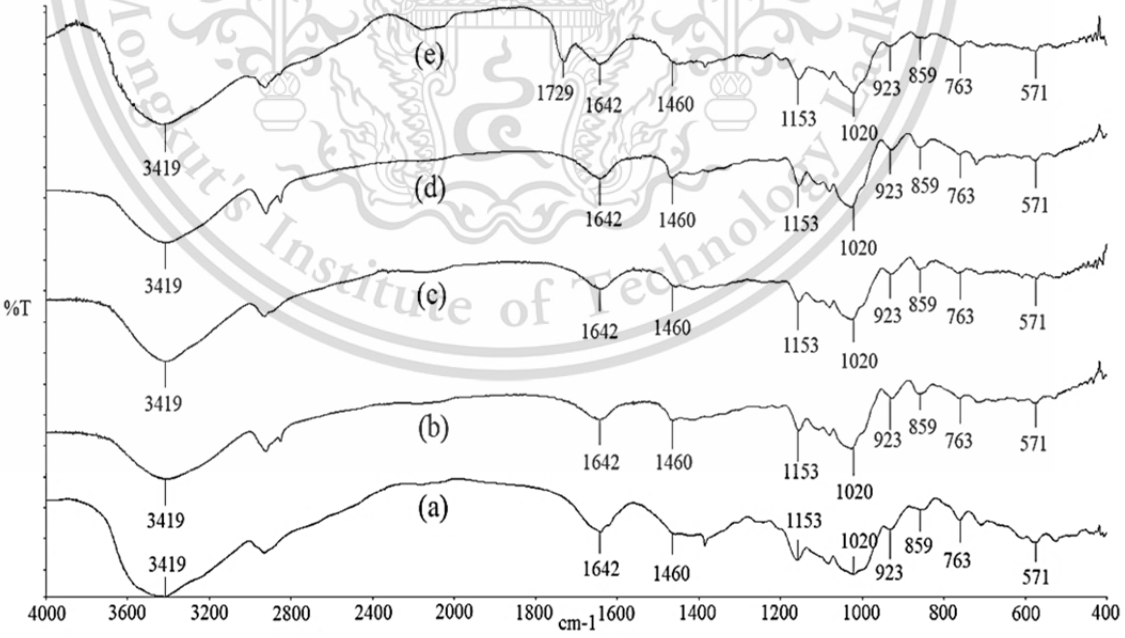

Figure 4.8 FT-IR spectra of NS and different singly modified starch **(a)** NS **(b)** CS-BO **(c)** CS-BA **(d)** CS-ST and **(e)** OS

Table 4.4 Peak heights and ratios of peak height of NS and different singly modified starch

Sample	Peak height			Ratio of peak height	
	1729 cm^{-1}	1642 cm^{-1}	859 cm^{-1}	1729 cm^{-1} /859 cm^{-1}	1642 cm^{-1} /859 cm^{-1}
NS	-	50.23	29.50	-	1.70
CS-BO	-	40.87	27.21	-	1.50
CS-BA	-	43.78	26.58	-	1.64
CS-ST	-	47.75	28.67	-	1.66
OS	36.54	37.87	24.23	1.52	1.56

Remark: ratio of peak height = peak height of interested peak/peak height of referenced peak of 859 cm^{-1}

FT-IR spectra of NS and all CS samples in Figure 4.8 show a broad absorption band of O-H stretching in the range of 3200-3400 cm^{-1}. A peak in the range of 2800-3000 cm^{-1} was assigned to C–H asymmetric stretching of $–CH_2–$. The bands in the range of 1630-1600 cm^{-1} and 1450-1475 cm^{-1} were assigned to the bound water existed in the starch and O-H bending, respectively. The peaks in the range of 1100-1300 cm^{-1} and 1000-1200 cm^{-1} were characteristic of C–O–C stretching and C-O-H bending, respectively [9, 11]. Figure 4.8 shows that the unmodified and modified starch exhibited similar IR peak positions since they possessed a similar polysaccharide structure. Regarding the FT-IR absorption peaks of all CS samples (Figures 4.8(b)-(d)), the heights of the peak at 1642 cm^{-1} of intermolecular hydrogen bonding were lower than that of NS (Table 4.4) because of the lower amounts of available hydroxyl groups after cross-linking, especially for CS-BO. This result confirmed successful cross-linking of all CS samples. Furthermore, the spectrum of OS in Figure 4.8(e) exhibited a new characteristic peak of C=O stretching at 1729 cm^{-1}, arisen from the oxidation of the starch structure that generated carbonyl and carboxyl groups [11, 28].

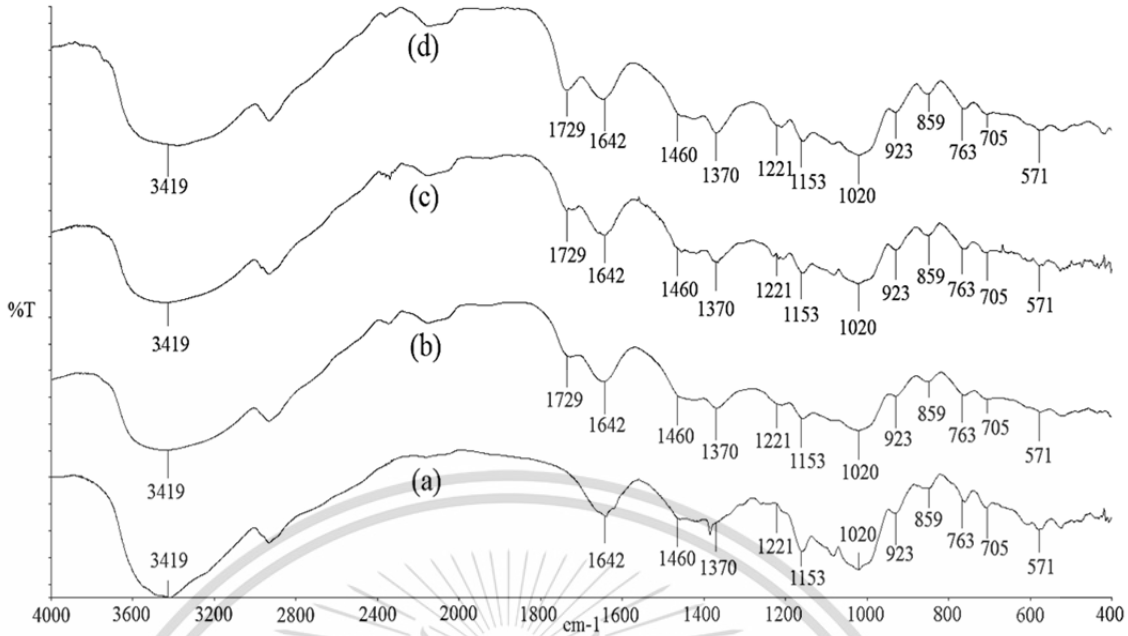

Figure 4.9 FT-IR spectra of NS and different COS samples crosslinked with different cross-linking agents and oxidized with hydrogen peroxide (a) NS (b) COS-BO (c) COS-BA and (d) COS-ST

Table 4.5 Peak heights and ratios of peak height of NS and different COS samples

Sample	Peak height			Ratio of peak height	
	1729 cm^{-1}	1642 cm^{-1}	859 cm^{-1}	1729 cm^{-1} /859 cm^{-1}	1642 cm^{-1} /859 cm^{-1}
NS	-	50.23	29.50	-	1.70
COS-BO	24.15	28.79	22.15	1.09	1.30
COS-BA	27.23	29.46	22.32	1.21	1.32
COS-ST	34.56	30.15	22.50	1.53	1.34

Remark: ratio of peak height = peak height of interested peak/peak height of referenced peak of 859 cm^{-1}

The FT-IR spectra presented in Figure 4.9 can be used to detect the specific function groups of NS and dually modified starch (COS). The spectra of all COS samples exhibited the similar characteristic peaks when compared with the spectrum of NS. Similar to the spectrum results of OS, all COS samples showed a new peak at 1729 cm^{-1} attributable to vibration of C=O stretching of carboxyl and carbonyl groups caused by the oxidation reaction and the diminished peak of hydrogen bonding at

1642 cm^{-1} was clearly observed (Table 4.5) due to the effect of cross-linking. These results affirmed the achievement of COS synthesis [11, 28]. The heights of the C=O stretching peak are ranked as followed: COS-ST>COS-BA>COS-BO (Table 4.5). These heights depended directly on the carbonyl and carboxyl contents of COS samples (Table 4.2).

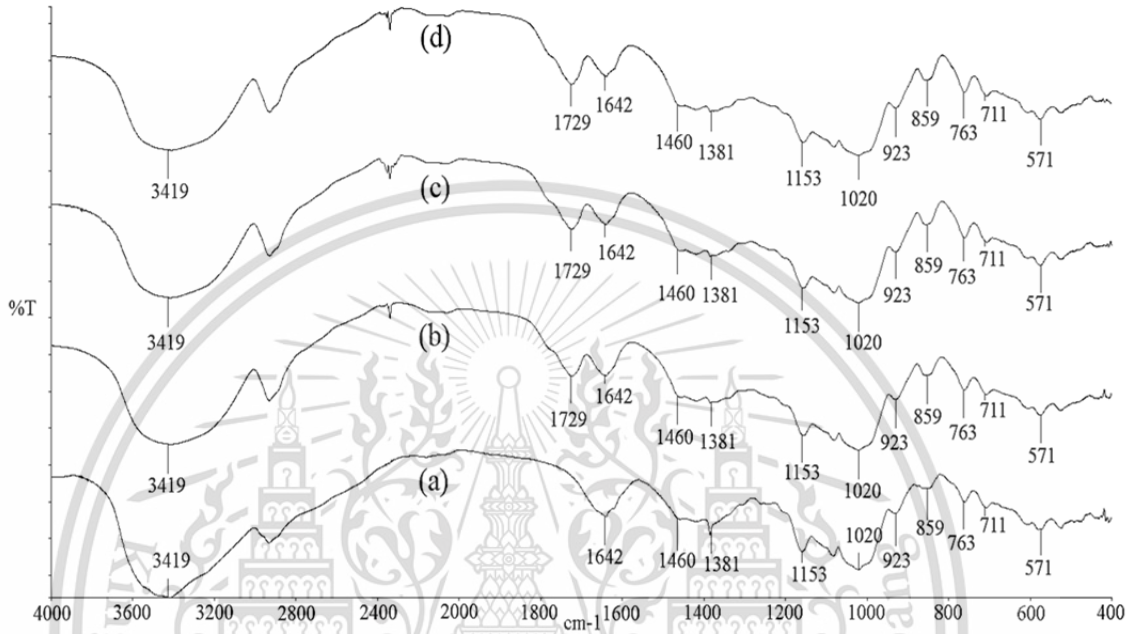

Figure 4.10 FT-IR spectra of NS and different OCS samples crosslinked with different types of cross-linking agent and oxidized with hydrogen peroxide and (a) NS (b) OCS-BO (c) OCS-BA and (d) OCS-ST

Table 4.6 Peak heights and ratios of peak heights of different OCS samples

Sample	Peak height			Ratio of peak height	
	1729 cm^{-1}	1642 cm^{-1}	859 cm^{-1}	1729 cm^{-1} /859 cm^{-1}	1642 cm^{-1} /859 cm^{-1}
NS	-	50.23	29.50	-	1.70
OCS-BO	36.69	33.29	24.30	1.50	1.37
OCS-BA	37.58	34.59	24.89	1.51	1.39
OCS-ST	38.76	35.94	25.67	1.51	1.40

Remark: ratio of peak height = peak height of interested peak/peak height of referenced peak of 859 cm^{-1}

FT-IR spectra for NS and different OCS samples are displayed in Figure 4.10. It was found that various OCS samples exhibited similar characteristic peaks when compared with those for NS, CS and COS. Nevertheless, all OCS samples showed a new peak at 1729 cm^{-1}, attributable to C=O stretching of carboxyl and carbonyl groups that was similar to a peak that OS and COS samples exhibited. The heights of the peak of C=O stretching of all OCS samples were almost equal (Table 4.6). Additionally, it should be noted that the decrease in intensity of the peak at 1642 cm^{-1} (Table 4.6), which was attributed to hydrogen bonding, also confirmed the success of the cross-linking process [9, 11]. The cross-linking agent was able to react successfully with the hydroxyl groups of the starch backbone.

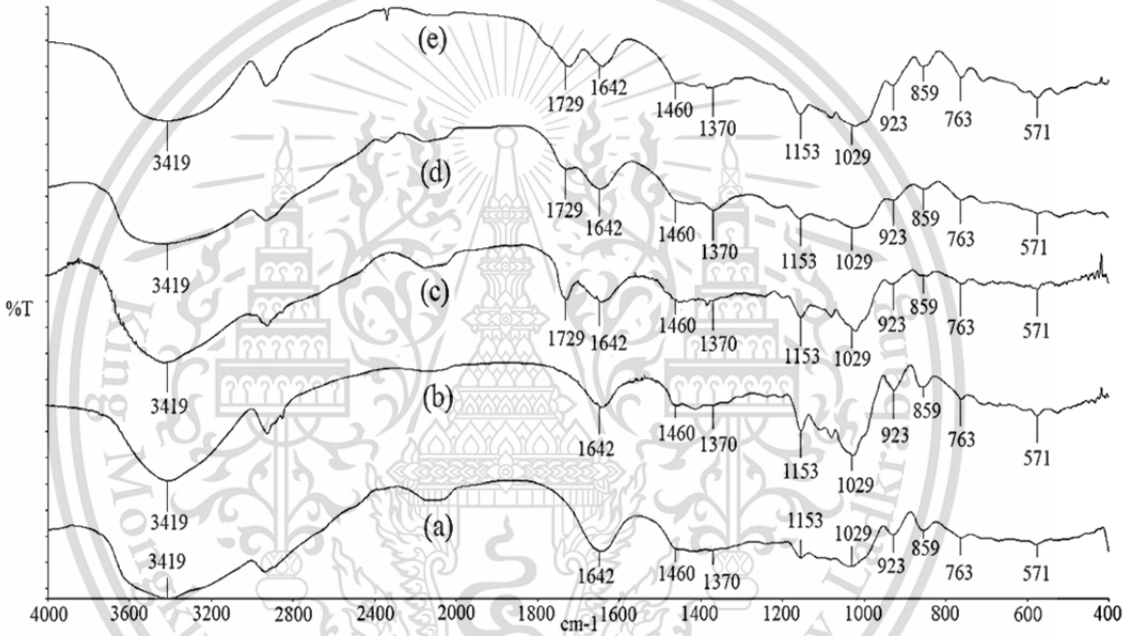

Figure 4.11 FT-IR spectra of differently modified starch crosslinked with borax and oxidized with hydrogen peroxide (a) NS (b) CS-BO (c) OS (d) COS-BO and (e) OCS-BO

Table 4.7 Peak heights and ratios of peak heights of differently modified starch crosslinked with borax and oxidized with hydrogen peroxide

Sample	Peak height			Ratio of peak height	
	1729 cm^{-1}	1642 cm^{-1}	859 cm^{-1}	1729 cm^{-1} /859 cm^{-1}	1642 cm^{-1} /859 cm^{-1}
NS	-	50.23	29.50	-	1.70
CS-BO	-	40.87	27.21	-	1.50
OS	36.54	37.87	24.23	1.52	1.56
COS-BO	24.15	28.79	22.15	1.09	1.30
OCS-BO	36.69	33.29	24.30	1.50	1.37

Remark: ratio of peak height = peak height of interested peak/peak height of referenced peak of 859 cm^{-1}

Figure 4.11 depicts FT-IR spectra of NS as well as singly and dually modified starch from crosslinked with borax and oxidized with hydrogen peroxide. It can be seen that the FT-IR spectra of all samples showed similar characteristic peaks. This was because all of the samples consisted of the same polysaccharide chemical structure. All modified starch showed a diminished peak at 1642 cm^{-1}, which was attributed to the decrease in available hydroxyl groups after completion of cross-linking and oxidation reactions. This result confirmed the change in starch chains from cross-linking and oxidation modifications. For OS, COS-BO and OCS-BO, the FT-IR spectra showed an additional peak at 1729 cm^{-1}, attributable to C=O stretching of carboxyl and carbonyl groups [11, 28]. The highest intensity of C=O stretching peak (Table 4.7) was exhibited by OS and OCS-BO because of their highest carboxyl and carbonyl contents (Table 4.2). The modified starch with boric acid and the mixture of STMP/STPP showed a similar FT-IR result to that of the modified starch with borax.

4.1.4 Morphological properties

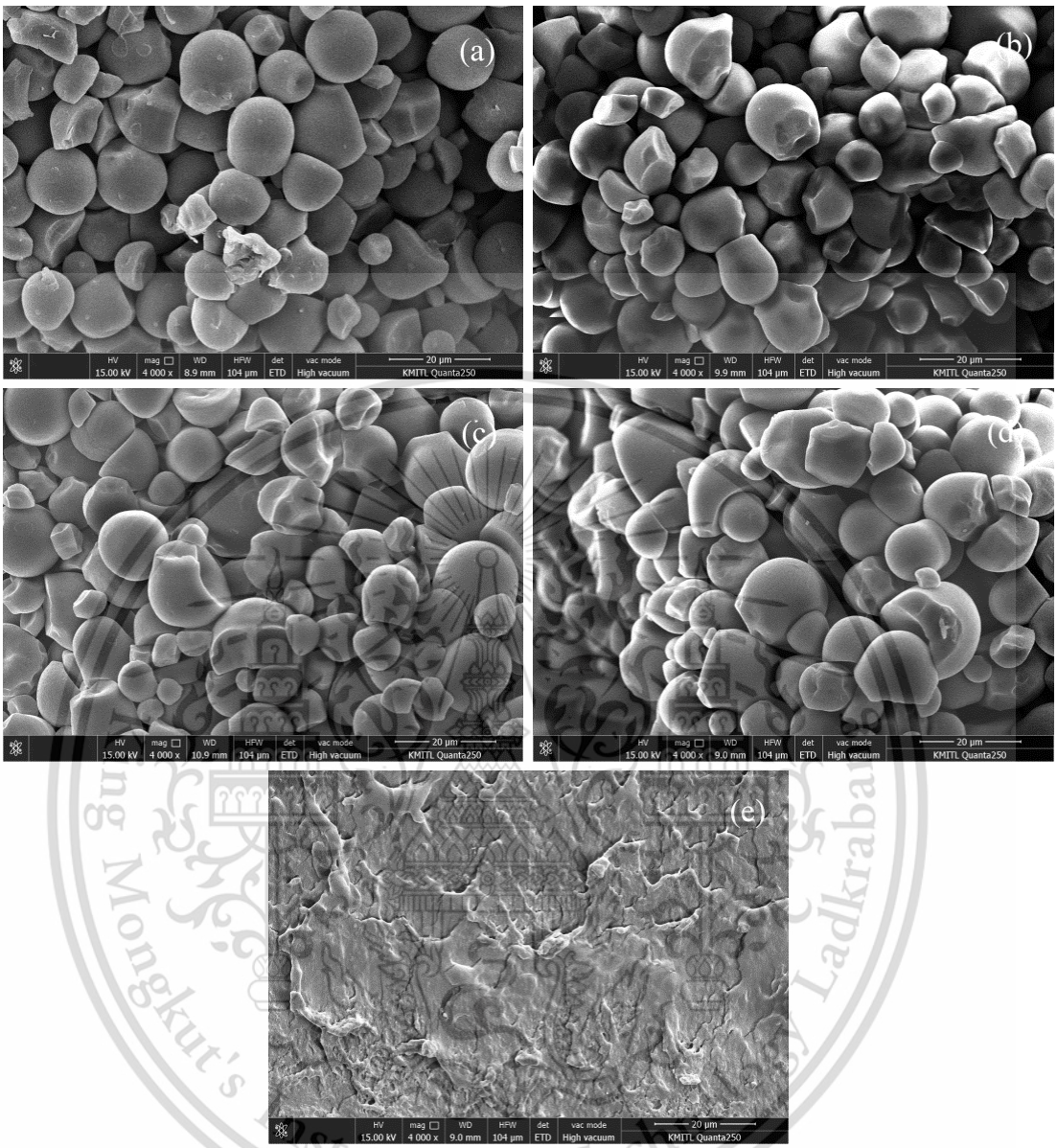

Figure 4.12 SEM micrographs at 4000X magnification of NS and different singly modified starch **(a)** NS **(b)** CS**-**BO **(c)** CS**-**BA **(d)** CS**-**ST and **(e)** OS

SEM micrographs of NS and various singly modified starch at 4000X magnification are shown in Figure 4.12**.** The SEM micrographs of NS (Figure 4.12(a)) showed separated spherical starch granules, but those of all CS samples in Figures 4.12**(**b**)-(**d**)** showed less spherical granules that agglomerate into bunches like a bunch of grapes**.** In particular, the surface of CS sample was apparently less smooth, especially in the case of CS**-**BO sample**.** A comparison of the morphologies of various CS samples revealed that they were not significantly different**.** Similar morphology

was also expressed in earlier result for CS from rice starch crosslinked with STMP/STPP [8].

On the other hand, OS sample exhibited a substantial change in morphology after oxidation and its granular starch structure was completely destroyed by the oxidation process as shown in Figure 4.12(e). This result agrees well with a morphological result of a study by Z. Dang *et al.* (2019). They reported that a change in morphology was observed when potato starch was oxidized with hydrogen peroxide [28].

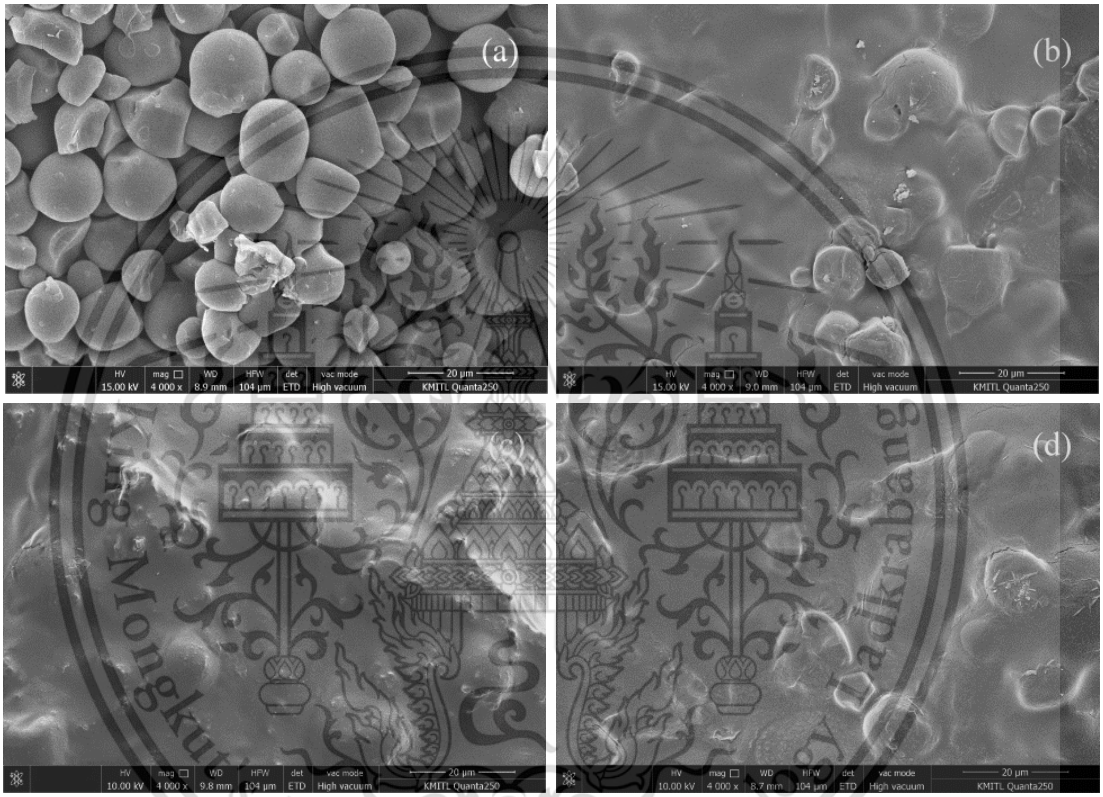

Figure 4.13 SEM micrographs at 4000X magnification of NS and different COS crosslinked with different types of cross-linking agents and oxidized with hydrogen peroxide (a) NS (b) COS-BO (c) COS-BA and (d) COS-ST

Figure 4.13 displays SEM micrographs at 4000X magnification of NS and various COS samples. After cross-linking-oxidization-method, it can be seen that all COS samples showed different morphology compared to NS film with consisting of some non-separated spherical starch granules. In particular, some starch granules were destroyed or breaking by the oxidation process with hydrogen peroxide as an oxidizing agent. In addition, COS-BO showed the lower smooth fractured surface than those of COS-BA and COS-ST. Moreover, COS-BO presented some unmolten starch granules. This result was probably because it contained the highest degrees of cross-

linking and the lowest degree of oxidation, respectively. On the contrary, COS-ST presented the highest smooth fractured surface and some unmolten starch granules due to the maximum degree of oxidation and the minimum degree of cross-linking among all COS samples (Table 4.2).

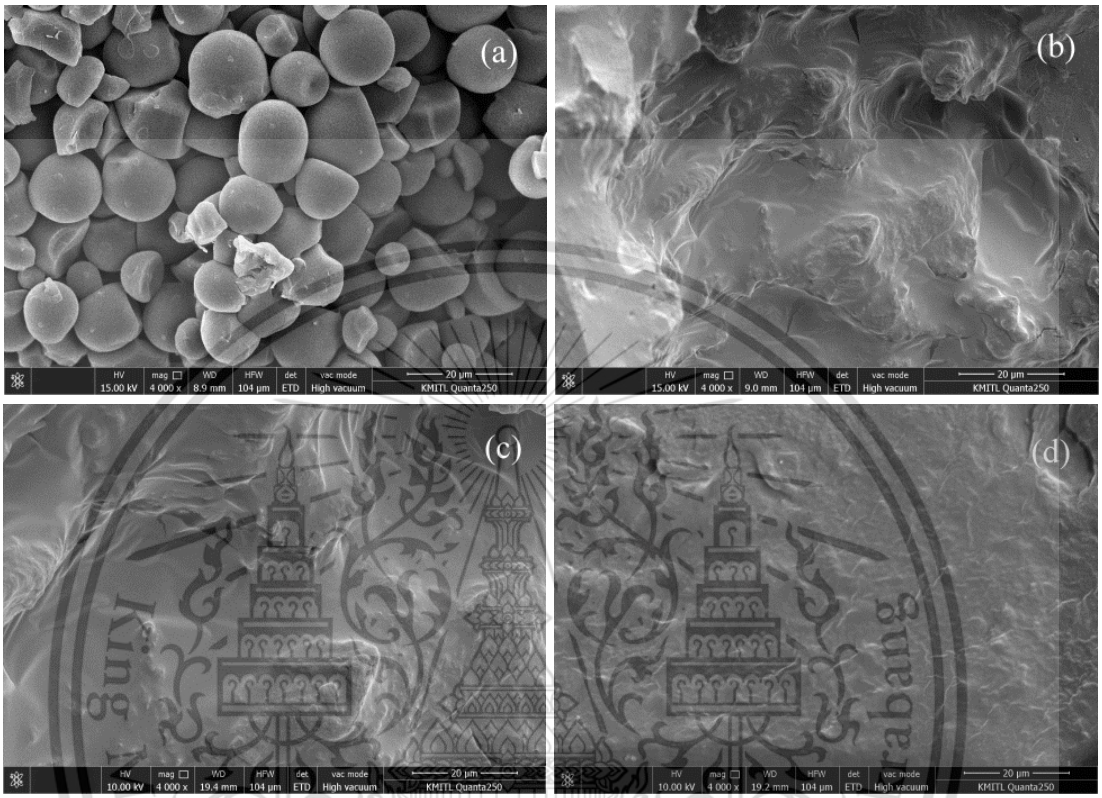

Figure 4.14 SEM micrographs at 4000X magnification of NS and different OCS crosslinked with different types of cross-linking agents and oxidized with hydrogen peroxide (a) NS (b) OCS-BO (c) OCS-BA and (d) OCS-ST

SEM micrographs at 4000X magnification of unmodified starch and various OCS samples with different types of cross-linking agents are shown in Figure 4.14. The SEM micrographs of all OCS samples showed different morphologies when compared to morphology of NS that exhibited almost no appearances of granules, only smooth surface with some protrusions that resembled flattened surface. This appearance was caused by destruction of starch granules via the high degree of oxidation [28, 45]. Among OCS samples, the surface of OCS-BO (Figure 4.14(b)) was the least smooth; its highest surface roughness was due to its highest degree of cross-linking. In contrast, the surface of OCS-ST (Figure 4.14(d)) was the smoothest; its lowest surface roughness was due to its lowest degree of cross-linking (Table 4.2).

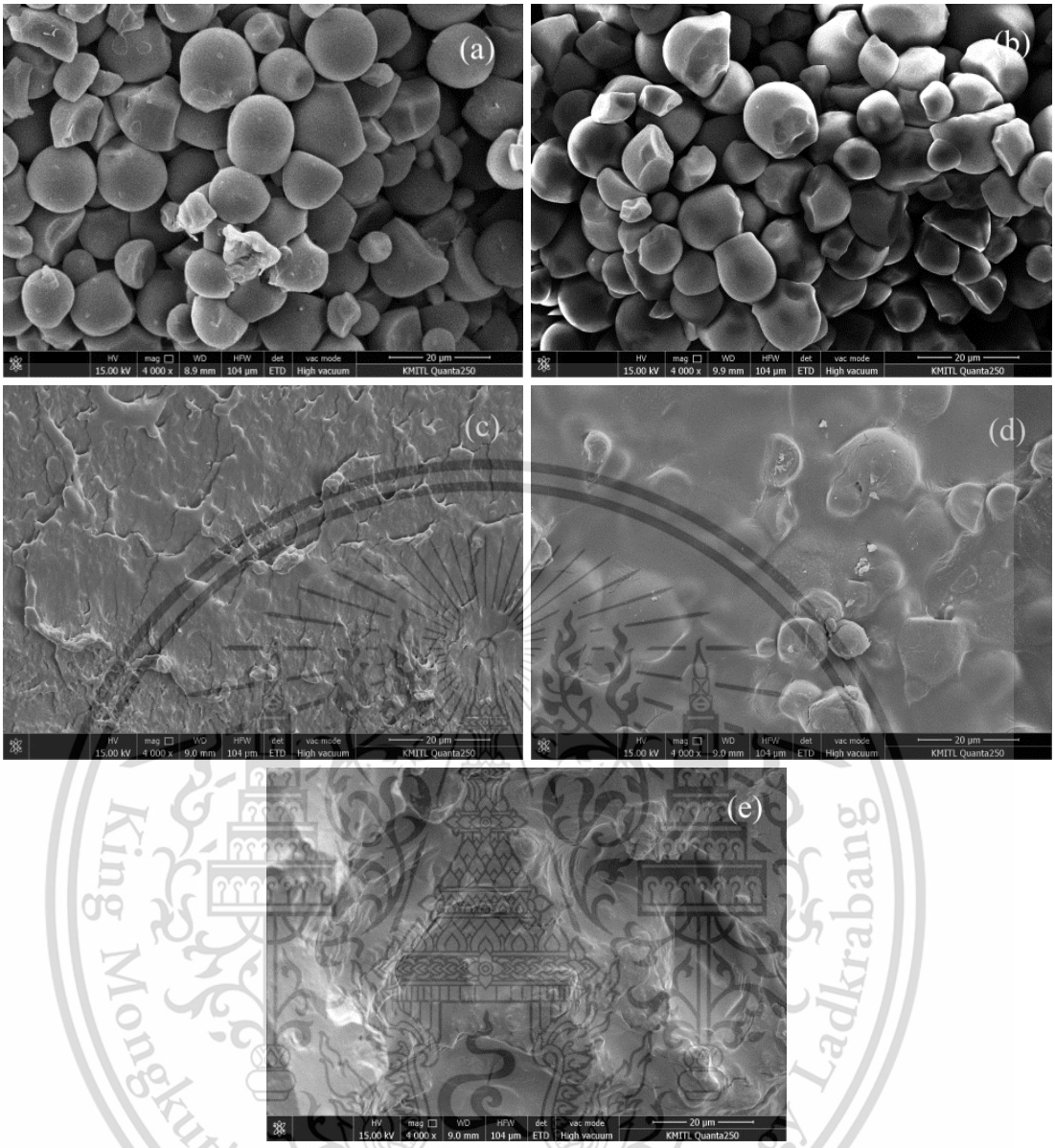

Figure 4.15 SEM micrographs at 4000X magnification of differently modified starch crosslinked with borax and oxidized with hydrogen peroxide (a) NS (b) CS-BO (c) OS (d) COS-BO and (e) OCS-BO

A comparison of SEM micrographs at 4000X magnification of NS with various singly and dually modified starch crosslinked with borax and oxidized with hydrogen peroxide (Figure 4.15) showed that the morphology of CS-BO was slightly different from that of NS, which could be described above regarding the morphologies of CS sample compared to that of NS (Figure 4.12). In addition, OS, OCS-BO and COS-BO showed a highly different morphology, smooth surface with almost no appearance of granules were observed for OCS-BO and OS, from that of NS, however, OCS-BO represented more surface roughness than that of OS, which might be due to the

effect of cross-linking with borax for the synthesis of OCS. On the contrary, COS-BO exhibited not only the smooth fractured surface but also the presence of some unmolten starch granules. These results of smooth fractured surface were attributed to a disruption of starch granules by oxidation with hydrogen peroxide [28], but the occurrences of unmolten starch granules and rough surface were due to the effect of cross-linking with borax [49]. These result indicated that all types of modification method affected the morphology of NS granules. Based on these morphology results, SEM micrographs were also correlated with the degree of cross-linking and the carboxyl and carbonyls contents of various modified starch (Table 4.2). This finding could be explained that starch granules were not disrupted and showed the rough surface because of high degree of cross-linking, whereas the smooth surface and the disrupted surface were clearly observed, caused by high degree of oxidation.

4.1.5 Intrinsic viscosity and MW

The method of intrinsic viscosity was used to obtain MW of a sample and intrinsic viscosity was determined using the Mark-Houwink equation. The intrinsic viscosity and MW of differently modified starch are tabulated in Table 4.8.

Table 4.8 Intrinsic viscosity and MW of NS and differently modified starch

Sample	Intrinsic viscosity (mL/g)	MW (g/mol)
NS	250.7±0.1	(75.0±0.5)×10^4
CS-BO	1439.9±0.2	(758.2±0.4)×10^4
CS-BA	1280.1±0.2	(650.0±0.5)×10^4
CS-ST	1112.6±0.3	(540.5±0.3)×10^4
OS	16.0±0.4	(2.0±0.4)×10^4
COS-BO	548.8±0.2	(213.3±0.4)×10^4
COS-BA	513.7±0.4	(195.5±0.6)×10^4
COS-ST	439.6±0.3	(159.3±0.2)×10^4
OCS-BO	199.9±0.3	(56.5±0.3)×10^4
OCS-BA	179.7±0.3	(49.1±0.5)×10^4
OCS-ST	155.5±0.5	(40.6±0.4)×10^4

Intrinsic viscosity and MW of NS and various types of modified starch are shown in Table 4.8. The intrinsic viscosities and MW of all CS and COS samples were higher than those of NS because of their higher cross-linking density and the formation of

three-dimensional crosslinked structure of starch chains as shown in Figures 4.1-4.3 and Figures 4.5-4.7. On the other hand, the intrinsic viscosities and MW of OS and OCS were markedly lower than those of NS. This result could be due to disruption of starch granules and hydrogen bonding between starch chains as well as progressive substitution of hydroxyl groups by carbonyl and carboxyl groups in the oxidation reaction. Similar observations were also reported for CS crosslinked with L-Ascorbic acid and OS oxidized with periodate [50-51]. Regarding dually modified starch and singly modified starch, all COS samples exhibited lower intrinsic viscosity and MW than CS samples. This could be explained that hydrogen peroxide cleaved the C_2-C_3 bonds of the glucose units of cassava starch backbone [28]. Furthermore, OCS samples exhibited higher intrinsic viscosity and MW than OS samples due to the effect of cross-linking. When COS and OCS samples were compared, it was found that all COS samples showed higher intrinsic viscosity and MW than OCS samples because of higher degree of cross-linking (Table 4.2).

When considering the influence of cross-linking agents on intrinsic viscosity and MW of various modified starch, all singly and dually modified starch crosslinked with borax and the mixture of STMP/STPP showed the highest and lowest intrinsic viscosity and MW, respectively. This result correlated well with the degree of cross-linking (Table 4.2). All of these results indicated that highly crosslinked network structure of modified starch led to an increase in their high intrinsic viscosity and MW. This phenomenon was also related to the work of M. Majzoobi *et.al.* (2014) who reported an increasing trend of intrinsic viscosity of wheat starch crosslinked with L-ascorbic acid [50].

Based on these results, the highest intrinsic viscosity and MW obtained in this present study were observed in CS-BO which provided the highest degree of cross-linking. In contrast, the lowest intrinsic viscosity and MW were observed in OS.

4.1.6 Thermogravimetric analysis

Thermal property of unmodified starch and differently modified starch were investigated by using TGA technique in the temperature range of 50-600°C under nitrogen atmosphere at the heating rate of 10°C/min in order to investigate thermal degradation temperature, which was obtained from the maximum decomposition temperature as shown in Figures 4.16-4.19 and the degradation temperatures are reported in Table 4.9.

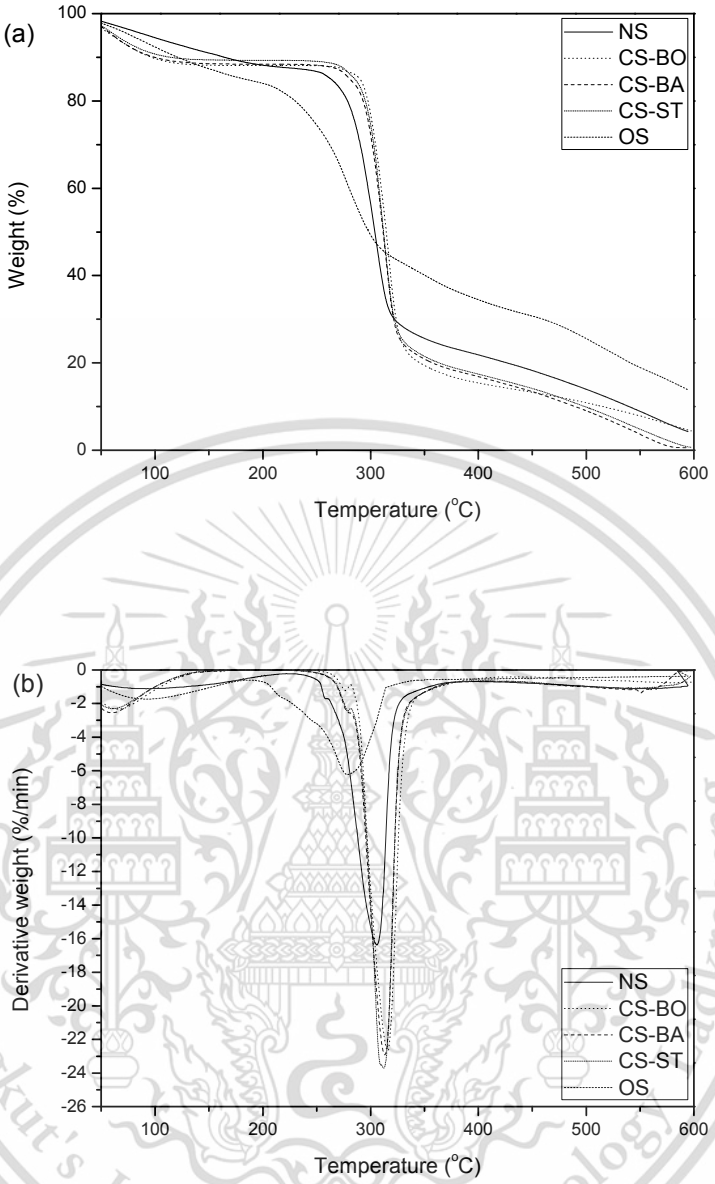

Figure 4.16 Thermograms of NS and different singly modified starch **(a)** TGA and **(b)** DTG

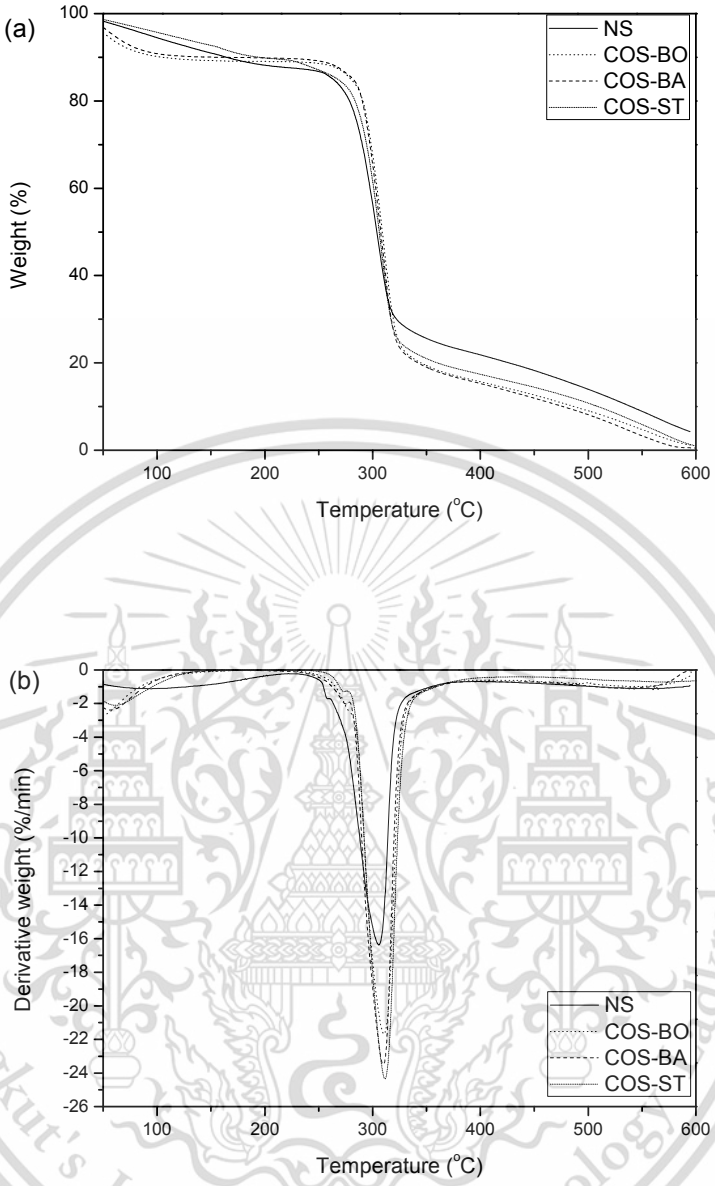

Figure 4.17 Thermograms of NS and different COS crosslinked with different types of cross-linking agents and oxidized with hydrogen peroxide **(**a**)** TGA and **(**b**)** DTG

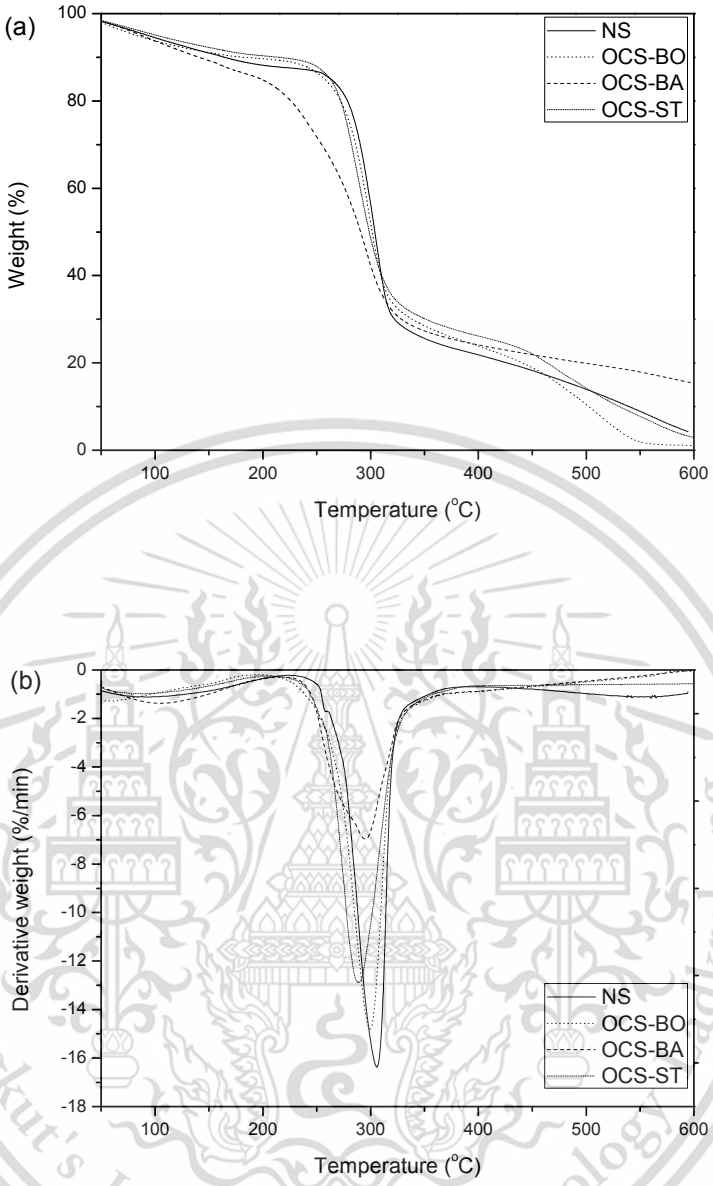

Figure 4.18 Thermograms of NS and different OCS crosslinked with different types of cross-linking agents and oxidized with hydrogen peroxide **(**a**)** TGA and **(**b**)** DTG

Table 4.9 Degradation temperatures of NS and differently modified starch determined from TG and DTG thermograms

Sample	Main degradation temperature (Starch) (°C)
NS	302.3
CS-BO	315.2
CS-BA	313.0
CS-ST	311.3
OS	277.8
COS-BO	310.2
COS-BA	309.1
COS-ST	308.0
OCS-BO	298.0
OCS-BA	289.9
OCS-ST	288.4

Thermal decomposition temperatures of differently modified starch were characterized by TGA technique. As can be seen in Figures 4.16-4.18 and Table 4.9, TGA and DTG thermograms of NS and all modified starch samples exhibited degradation transition step. The main transition from 280 to 320°C was ascribed to starch decomposition [40]. All CS samples showed drastically improved thermal properties that were observed from an increase in thermal decomposition temperature of all types of CS. This result was because cross-linking enhanced the stability of starch granules [40]. The decomposition temperatures of the main transition of various CS samples crosslinked with different types of cross-linking agents were ranked as follows: CS-BO>CS-BA>CS-ST. This result was probably because a difference in cross-linking efficiency of each cross-linking agents that CS-BO and CS-ST obtained the highest and lowest degree of cross-linking (Table 4.2). On the contrary, OS exhibited lower thermal decomposition temperature than NS, which may be due to cleavage of starch chains at C-2 and C-3 positions and the presence of low molecular weight of starch chains from oxidation process (Figure 4.4) [54].

Regarding thermal properties of different COS samples, it should be noted that all COS samples (Figure 4.17 and Table 4.9) showed a higher degradation temperature than those of NS and OCS samples. This could be due to crosslinkages between starch molecules which resulted in a higher decomposition temperature. On the other hand, all COS samples showed lower thermal degradation

temperatures than all CS samples due to the effect of oxidation. The order of degradation temperatures of different COS samples with different types of cross-linking agents was as follows: COS-BO>COS-BA>COS-ST. These results were highly dependent on the degree of cross-linking of each type of modified starch (Table 4.2).

In contrast, it can be observed in Figure 4.18 and Table 4.9 that all OCS samples showed lower thermal decomposition temperature than all COS samples. This finding might be due to cleavage of starch chain by oxidation with hydrogen peroxide [28]. Nevertheless, the degradation temperatures of all OCS samples were clearly higher than that of OS due to strengthened connection between starch granules by cross-linking. The order of degradation temperatures of different OCS samples was as follows: OCS-BO>OCS-BA>OCS-ST. This result is related to the degree of cross-linking as well as the carbonyl and carboxyl contents (Table 4.2).

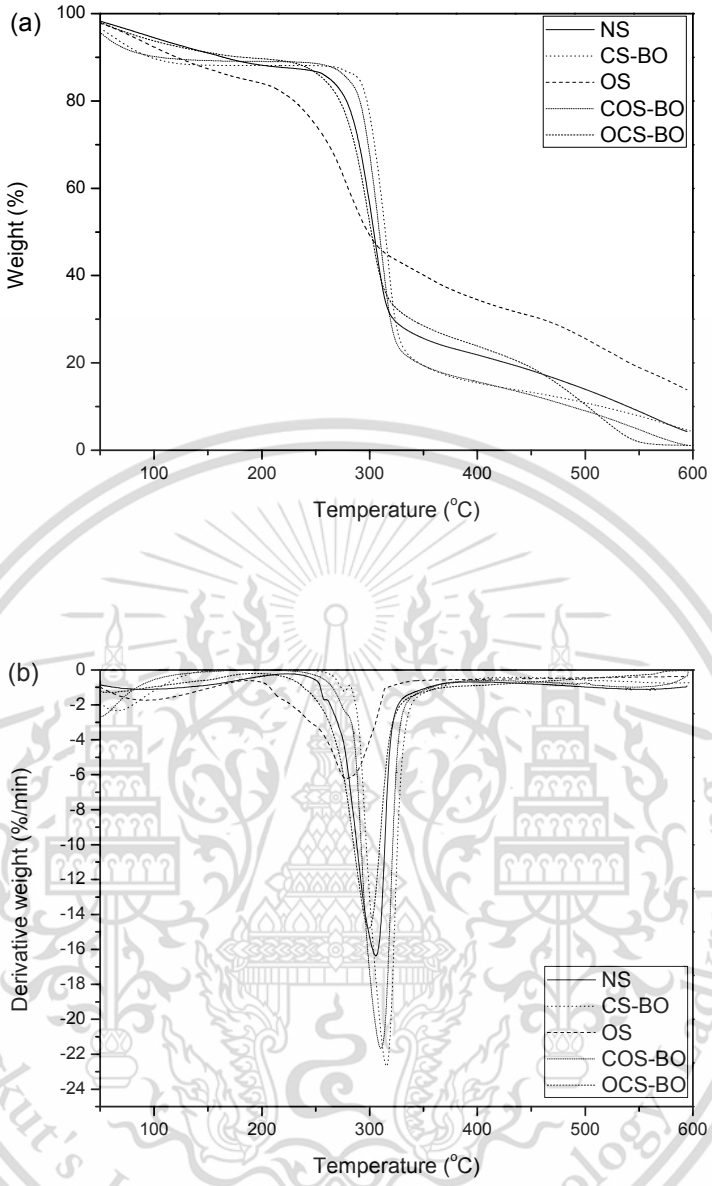

Figure 4.19 Thermograms of NS and differently modified starch crosslinked with borax and oxidized with hydrogen peroxide **(a)** TGA and **(b)** DTG

Table 4.10 Degradation temperatures of NS and differently modified starch crosslinked with borax and oxidized with hydrogen peroxide determined from TG and DTG thermograms

Sample	Main Degradation temperature (Starch) (°C)
NS	302.3
CS-BO	315.2
OS	277.8
COS-BO	310.2
OCS-BO	298.0

It can be observed in Figure 4.19 and Table 4.10 that the improved thermal property was found in CS-BO and COS-BO due to strengthened connection between starch granules by cross-linking. Conversely, the decrease in thermal property was found in OS and OCS-BO because of cleavage of starch chain by oxidation with hydrogen peroxide. In addition, OCS-BO displayed lower thermal decomposition temperature than COS-BO due to the effect of oxidation [52]. Nevertheless, the degradation temperature of OCS-BO was clearly higher than that of OS due to the stabilization of starch granules by cross-linking. Besides, the maximum and minimum thermal degradation temperatures found in this work were exhibited by CS-BO and OS samples, respectively.

4.2 Properties of different modified starch films

In this study, the physicochemical, mechanical and biodegradable properties of biodegradable singly and dually modified cassava starch films by oxidation with hydrogen peroxide and cross-linking with different types of cross-linking agents, such as BA, BO, and a mixture of STMP/STPP were investigated and compared as follows:

4.2.1 FT-IR study

Function group analysis was used to detect the specific function groups of the different biodegradable modified starch films. The FT-IR spectra of NS film and various singly, dually modified starch films are depicted in Figures 4.20-4.23.

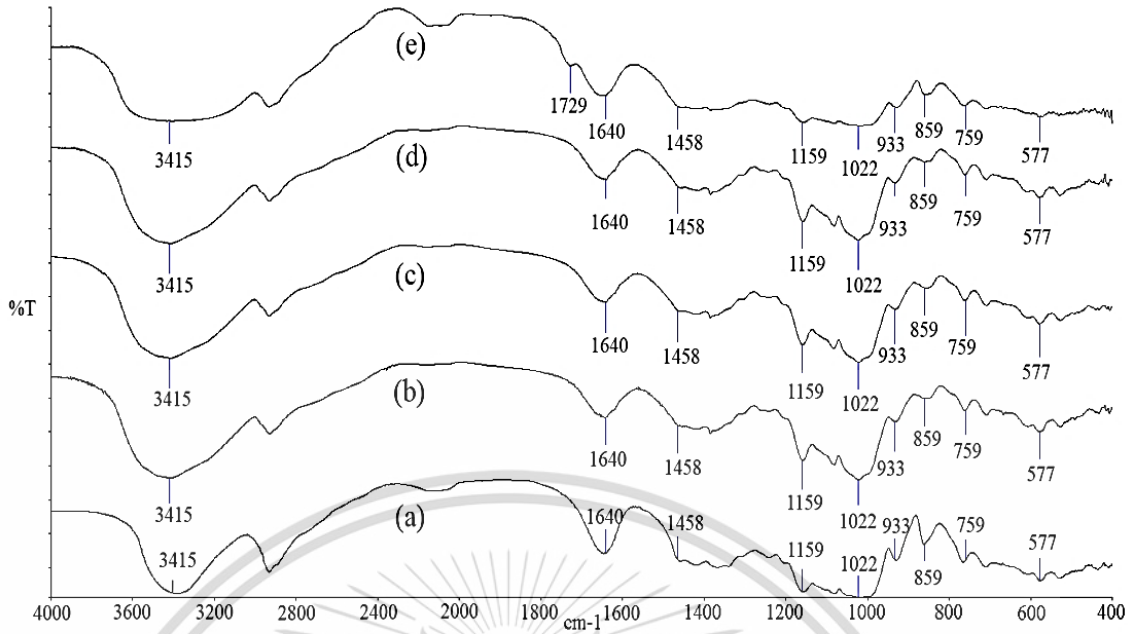

Figure 4.20 FT-IR spectra of NS film and various singly modified starch films **(a)** NSF, (b) CS-BOF, **(c)** CS-BAF, **(d)** CS-STF and **(e)** OSF

Table 4.11 Peak heights and ratios of peak heights of various singly modified starch films

Sample	Peak height			Ratio of peak height	
	1729 cm^{-1}	1640 cm^{-1}	859 cm^{-1}	1729 cm^{-1} /859 cm^{-1}	1640 cm^{-1} /859 cm^{-1}
NSF	-	48.67	21.57	-	2.25
CS-BOF	-	40.65	20.24	-	2.00
CS-BAF	-	41.23	19.67	-	2.09
CS-STF	-	41.56	19.56	-	2.12
OSF	34.56	42.53	20.45	1.54	2.08

Remark: ratio of peak height = peak height of interested peak/peak height of referenced peak of 859 cm^{-1}

As can be seen in Figure 4.20, the FT-IR spectra of NS film and various singly modified starch films exhibited a similar IR peak pattern. The characteristic broad peak at 3415 cm^{-1} arises from O-H stretching of starch and glycerol. A band of C–H asymmetric stretching appears at 2800-3000 cm^{-1}, while the peaks in the ranges of 1600-1630 cm^{-1} and 1450-1475 cm^{-1} are assigned to the bound water existed in the

starch and O-H bending, respectively. The absorption peaks in the ranges of 1070-1275 cm^{-1} and 1000-1200 cm^{-1} are characteristic of C–O–C stretching and C-O-H bending, respectively [8, 11].

Figure 4.20 shows that the unmodified and modified starch films exhibited FT-IR peaks at nearly the same positions since they possessed a similar polysaccharide structure. On comparing the spectra of various CS films and NS film in Figures 4.20(b)-(d), the heights of the peaks at 1640 cm^{-1} of all CS films was lower than that of NS film (Table 4.11) because of fewer free available hydroxyl groups since most hydroxyl groups were already reacted to form a starch borate or di-starch phosphate crosslinked structure (Figures 4.1-4.3). This observation affirmed the achievement of cross-linking of all CS films. Furthermore, the spectrum of OS film in Figure 4.20(e) shows a new characteristic peak of C=O stretching at 1729 cm^{-1} from the introduction of carbonyl and carboxyl groups into the starch structure generated by oxidation with hydrogen peroxide (Figure 4.4) [11, 28].

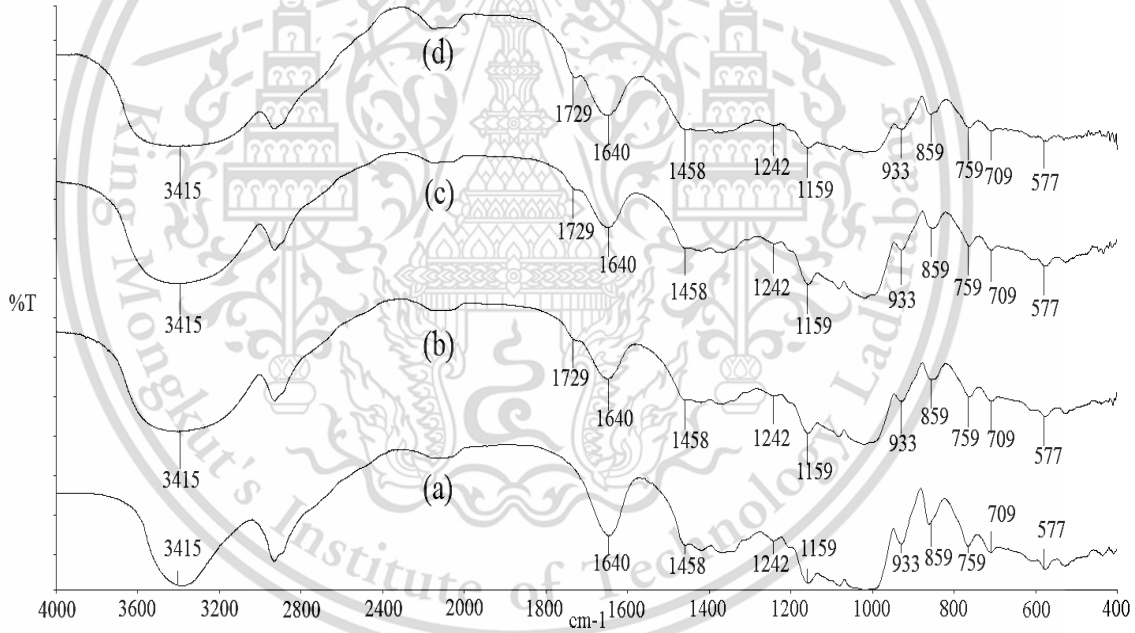

Figure 4.21 FT-IR spectra of NS film and various COS films crosslinked with different types of cross-linking agents and oxidized with hydrogen peroxide (a) NSF, (b) COS-BOF, (c) COS-BAF and (d) COS-STF

Table 4.12 Peak heights and ratios of peak heights of various COS films

Sample	Peak height			Ratio of peak height	
	1729 cm^{-1}	1640 cm^{-1}	859 cm^{-1}	1729 cm^{-1} /859 cm^{-1}	1640 cm^{-1} /859 cm^{-1}
NSF	-	48.67	21.57	-	2.25
COS-BOF	21.65	28.41	19.87	1.09	1.43
COS-BAF	21.22	27.03	18.45	1.15	1.48
COS-STF	23.21	29.20	19.34	1.21	1.51

Remark: ratio of peak height = peak height of interested peak/peak height of referenced peak of 859 cm^{-1}

As can be seen in Figure 4.21, all COS films presented the same FT-IR characteristic peaks when compared to NS film. In particular, after NS was modified by cross-linking-oxidizing, the FT-IR spectra of all COS films showed a diminished peak of hydrogen bonding at 1640 cm^{-1} and a new peak attributable to the C=O stretching of carbonyl and carbonyl groups at 1729 cm^{-1}. COS films crosslinked with different cross-linking agents presented the same FT-IR peak patterns, but they showed a difference in the intensity peak of C=O stretching of carbonyl and carbonyl groups at 1729 cm^{-1} (Table 4.12). The ratios of peak heights of C=O stretching are ranked as follows: COS-STF>COS-BAF>COS-BOF. This result depended directly upon the carboxyl and carbonyl contents of the various COS films (Table 4.2).

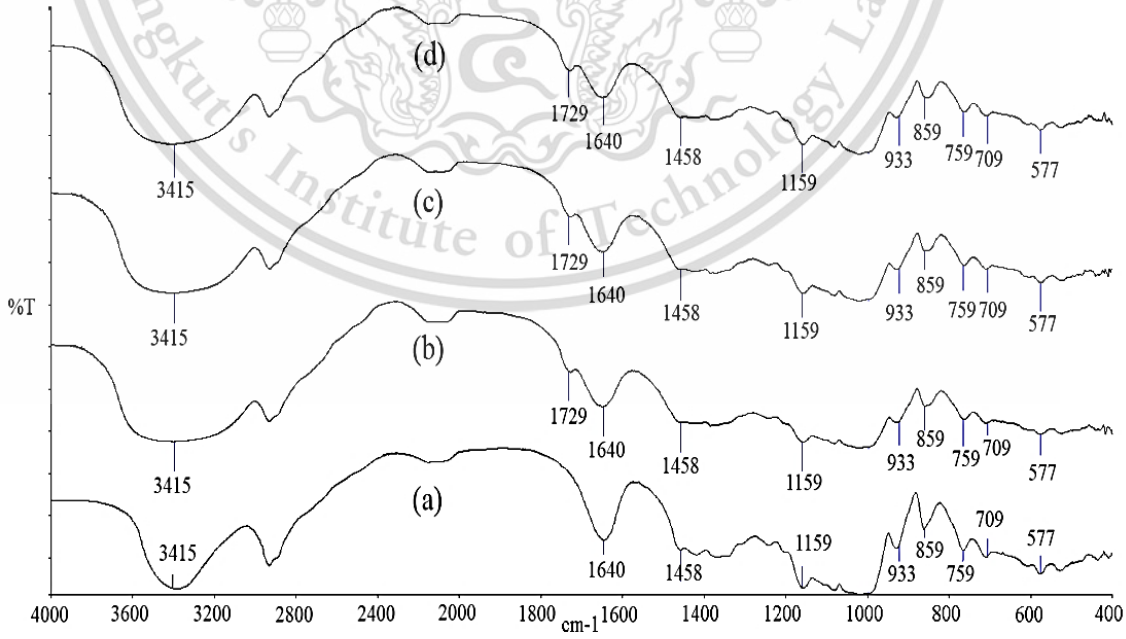

Figure 4.22 FT-IR spectra of NS film and various OCS films crosslinked with different types of cross-linking agents and oxidized with hydrogen peroxide (a) NSF, (b) OCS-BOF, (c) OCS-BAF and (d) OCS-STF

Table 4.13 Peak heights and ratios of peak heights of various OCS films

Sample	Peak height			Ratio of peak heights	
	1729 cm^{-1}	1642 cm^{-1}	859 cm^{-1}	1729 cm^{-1} /859 cm^{-1}	1640 cm^{-1} /860 cm^{-1}
NSF	-	48.67	21.57	-	2.25
OCS-BOF	31.74	31.53	21.02	1.51	1.50
OCS-BAF	31.54	31.34	20.89	1.51	1.54
OCS-STF	31.22	32.04	20.54	1.52	1.56

Remark: ratio of peak height = peak height of interested peak/peak height of referenced peak of 859 cm^{-1}

As can be seen in Figure 4.22, all OCS films exhibited similar FT-IR peaks when compared to NS film. As expected, the FT-IR spectra of all OCS films presented an additional peak attributable to the C=O stretching vibration of carbonyl and carbonyl groups at 1729 cm^{-1} and showed a decrease in the peak intensity of intra molecular hydrogen bonding at 1640 cm^{-1} (Table 4.13). Comparison of the FT-IR spectra of OCS films crosslinked with different cross-linking agents illustrated relatively similar FT-IR peak patterns and intensity peaks of the C=O stretching of carbonyl and carbonyl groups at 1729 cm^{-1}, which could be due to the similar carbonyl and carboxyl contents among OCS films (Table 4.2).

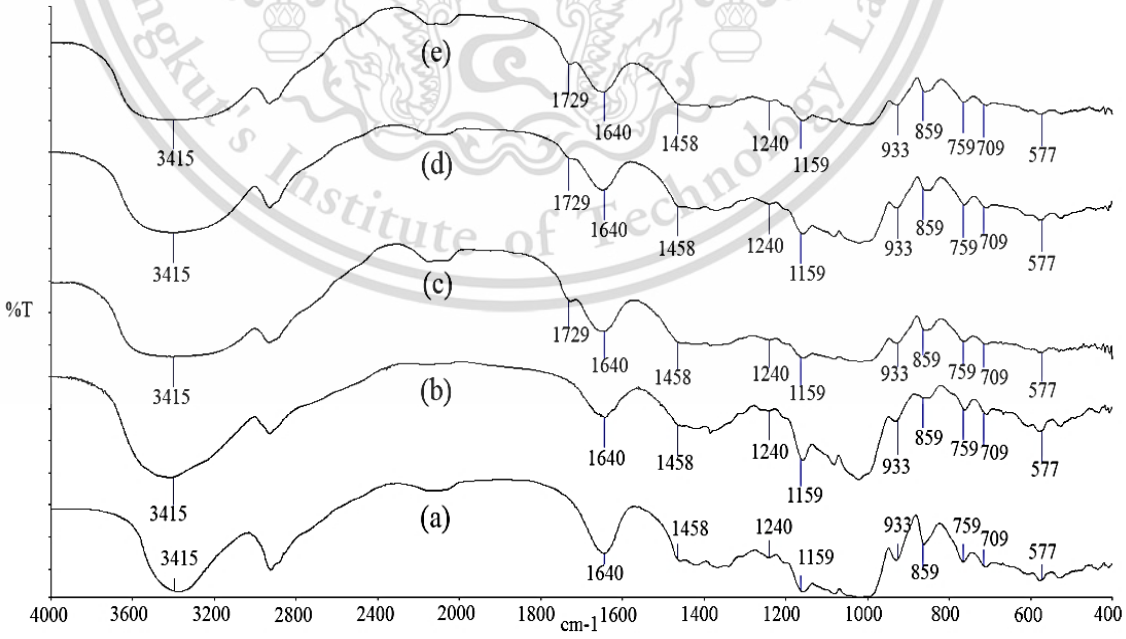

Figure 4.23 FT-IR spectra of various modified starch films crosslinked with borax and oxidized with hydrogen peroxide (a) NSF, (b) CS-BOF, (c) OSF, (d) COS-BOF and (e) OCS-BOF

Table 4.14 Peak heights and ratios of peak heights of various modified starch films crosslinked with borax and oxidized with hydrogen peroxide

Sample	Peak height			Ratio of peak height	
	1729 cm^{-1}	1640 cm^{-1}	859 cm^{-1}	1729 cm^{-1} /859 cm^{-1}	1640 cm^{-1} /859 cm^{-1}
NSF	-	48.67	21.57	-	2.25
CS-BOF	-	40.65	20.24	-	2.00
OSF	34.56	42.53	20.45	1.54	2.08
COS-BOF	21.65	28.41	19.87	1.09	1.43
OCS-BOF	31.74	31.53	21.02	1.51	1.50

Remark: ratio of peak height = peak height of interested peak/peak height of referenced peak of 859 cm^{-1}

For comparison of the FT-IR spectrum between NS, singly and dually modified starch films oxidized with hydrogen peroxide and crosslinked with borax, it can be seen in Figure 4.23 that all films showed similar peaks in their FT-IR spectrum attributable to the characteristics of the polysaccharide structure. As expected, successful syntheses of CS-BOF and OSF were observed in the decline of a hydrogen bonding peak at 1640 cm^{-1} (Table 4.14). Also, a new peak of C=O stretching of carbonyl and carbonyl groups at 1729 cm^{-1} was observed in OSF [11, 28].

For COS-BOF and OCS-BOF, a new peak of C=O stretching of carbonyl and carbonyl groups at 1729 cm^{-1} together with a decrease in the intensity of the hydrogen bonding peak at 1640 cm^{-1} were also observed [8, 11]. A comparison of the FT-IR spectra of COS-BOF and OCS-BOF revealed that OCS-BOF showed a higher intensity peak of C=O stretching than COS-BOF (Table 4.14), implying higher amounts of carbonyl and carboxyl groups (Table 4.2). All of these results confirmed the success of the dual modifications.

4.2.2 X-ray diffraction

X-ray diffraction patterns and the degree of crystallinity of various biodegradable modified films were evaluated by using the XRD technique as shown in Figures 4.24-4.27. The degrees of crystallinity of various modified starch films are presented in Table 4.15.

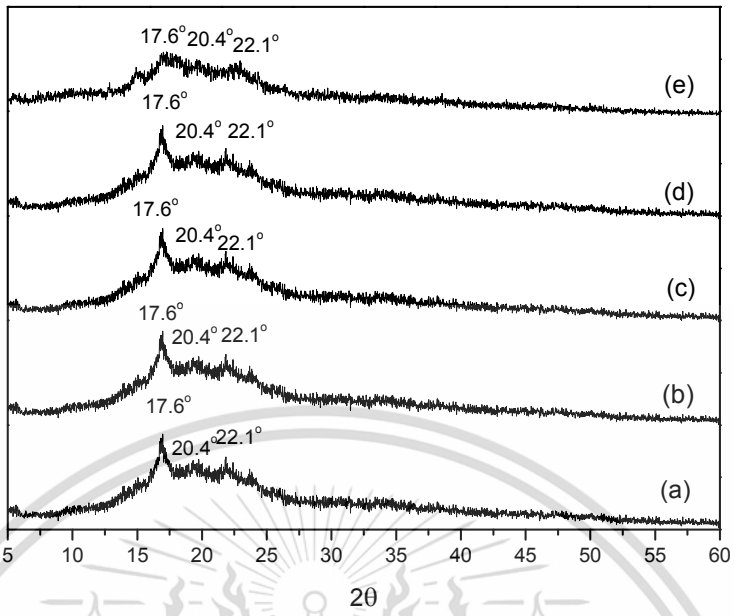

Figure 4.24 X-ray diffraction patterns of NS film and various singly modified starch films **(a)** NSF, **(b)** CS-BOF, **(c)** CS-BAF, **(d)** CS-STF and **(e)** OSF

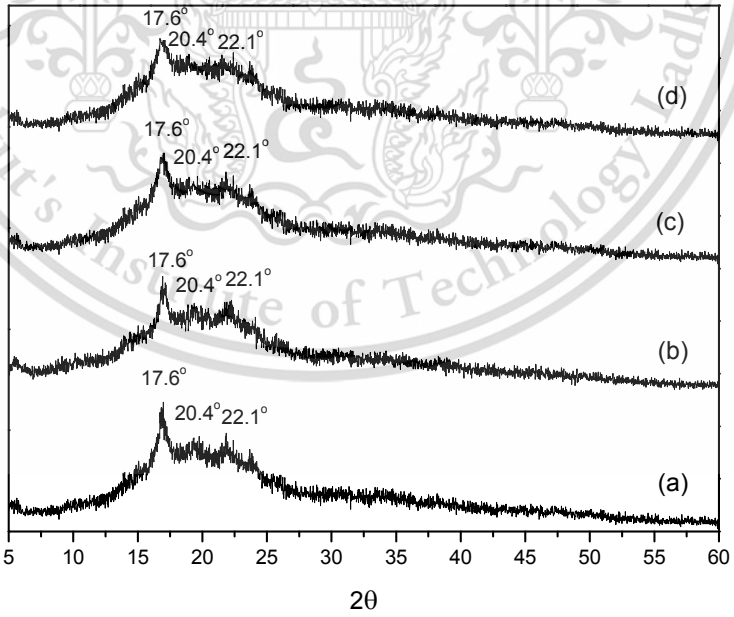

Figure 4.25 X-ray diffraction patterns of NS film and various COS films crosslinked with different types of cross-linking agents and oxidized with hydrogen peroxide **(a)** NSF, **(b)** COS-BOF, **(c)** COS-BAF and **(d)** COS-STF

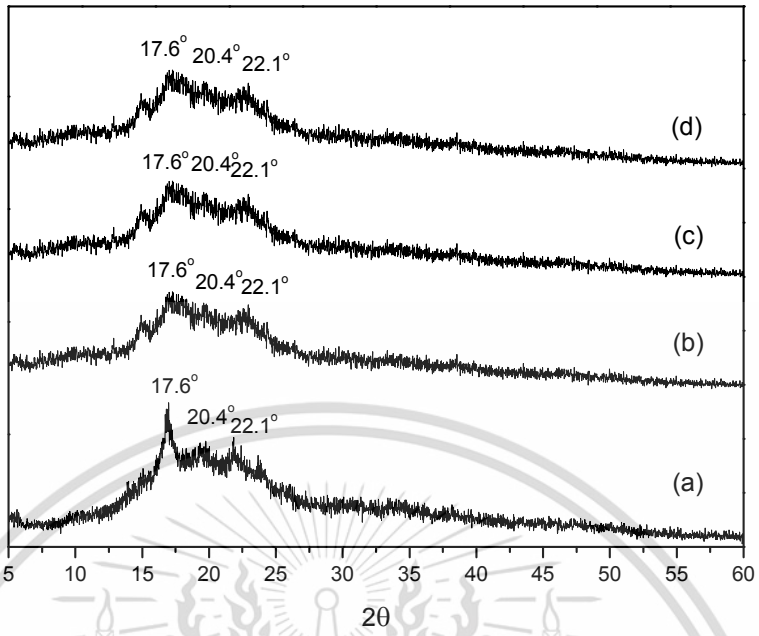

Figure 4.26 X-ray diffraction patterns of NS film and various OCS films crosslinked with different types of cross-linking agents and oxidized with hydrogen peroxide **(a)** NSF, **(b)** OCS-BOF, **(c)** OCS-BAF and **(d)** OCS-STF

Table 4.15 Degree of crystallinity of various modified starch films

Sample	Degree of crystallinity (%)
NSF	49.2±0.02
CS-BOF	49.2±0.03
CS-BAF	49.2±0.02
CS-STF	49.3±0.04
OSF	38.3±0.04
COS-BOF	46.4±0.02
COS-BAF	45.2±0.04
COS-STF	43.1±0.03
OCS-BOF	38.5±0.02
OCS-BAF	38.7±0.03
OCS-STF	38.6±0.02

X-ray diffraction patterns and the degrees of crystallinity of various modified starch films are displayed in Figures 4.24-4.26 and Table 4.15. X-ray diffractograms of all modified starch films showed combinations of B-type and V_h type X-ray diffraction

patterns, with the peak positions at 2θ of 17.6°, 20.4° and 22.1° [52]. These patterns are characteristic of pre-gelatinized starch granules that were partially disrupted by a casting method [53].

As seen in Figure 4.24, the degrees of crystallinity of all CS films were also comparable to that of NS film (Table 4.15). This was probably because cross-linking did not change the crystalline phase and only reacted to the starch in the amorphous phase [39]. However, the intensities of the peaks at 17.6°, 20.4° and 22.1° of OS decreased, indicating that the degree of crystallinity of OS film was drastically reduced and clearly lower than that of NS film, resulting from a loss in hydrogen bonding of the starch structure by the substitution of carbonyl and carboxyl groups and backbone chain cleavage (Figure 4.4) [45]. This observation confirmed that the oxidation process occurred to the starch granules. These XRD results agree well with those from previous studies of CS from corn starch crosslinked with epichlorohydrin and OS from potato starch oxidized with hydrogen peroxide [8, 28].

When COS films were compared in terms of their degree of crystallinity with NS film (Figure 4.25 and Table 4.15), all COS films showed a decrease in the degree of crystallinity. This was attributed to the cleavage of starch chains, loss of hydrogen bonding between starch molecules, and introduction of carbonyl and carboxyl groups via the oxidation process [45]. Furthermore, among COS films crosslinked with various cross-linking agents, the percentage of crystallinity of COS-STF was slightly lower than in the case of COS-BOF and COS-BAF. This result is probably because of the higher carboxyl and carbonyl contents of COS-ST left over from the cross-linking reaction and hence more readily available for further oxidation and cleavage of starch chains (Table 4.2), leading to a lower degree of crystallinity. On the other hand, the maximum percentage of crystallinity was obtained from COS-BOF due to its offering the lowest carboxyl and carbonyl contents. It was suggested that the oxidation reaction was primarily responsible for the lower degree of crystallinity.

Nevertheless, all OCS film exhibited a lower degree of crystallinity than NS film as can be seen in Figure 4.26 and Table 4.15. This was because of the cleavage of starch chains and the disintegration of hydrogen bonds in the starch molecules during oxidation [45]. This investigation confirmed that oxidation occurred in the starch backbones, causing a decrease in the degree of crystallinity of all OCS films. In addition, the degrees of crystallinity of OCS films crosslinked with various cross-linking agents were almost identical. This was because the cross-linking reaction that occurred after oxidation did not affect any change in the crystalline phase of the starch [8, 10].

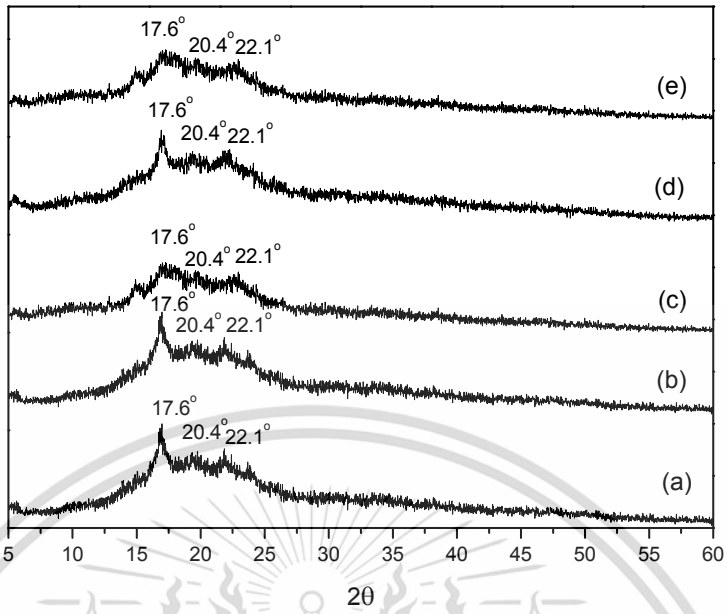

Figure 4.27 X-ray diffraction patterns of various modified starch films crosslinked with borax and oxidized with hydrogen peroxide **(a)** NSF **(b)** CS-BOF **(c)** OSF **(d)** COS-BOF and **(e)** OCS-BOF

Table 4.16 Degree of crystallinity of various modified starch films crosslinked with borax and oxidized with hydrogen peroxide

Sample	Degree of crystallinity (%)
NSF	49.2±0.02
CS-BOF	49.2±0.03
OSF	38.3±0.04
COS-BOF	46.4±0.02
OCS-BOF	38.5±0.02

Figure 4.27 and Table 4.16 depict the X-ray diffraction patterns and degree of crystallinity of various modified starch films crosslinked with borax and oxidized with hydrogen peroxide**.** It can be seen from Table 4.16 that OSF, COS-BOF and OCS-BOF showed a decrease in degree of crystallinity compared to NSF**.** This also stemmed from the cleavage of starch chains, loss of hydrogen bonding between starch molecules, and introduction of carbonyl and carbonyl groups on the starch chains by the oxidation process **[**45**].**

Furthermore, it should be noted that the crystallinity of OSF was almost identical to that of OCS-BOF since the cross-linking reaction did not alter the crystallinity of the starch film [10]. Between the two dually-modified starch films, OCS–BOF showed a lower degree of crystallinity than COS-BOF. This was ascribed to the chain cleavage of starch caused by high degree of oxidation.

4.2.3 Morphological properties

An SEM technique was utilized to investigate the morphologies at 4000X magnification of NS and modified starch films before and after their modification (Figures 4.28-4.31).

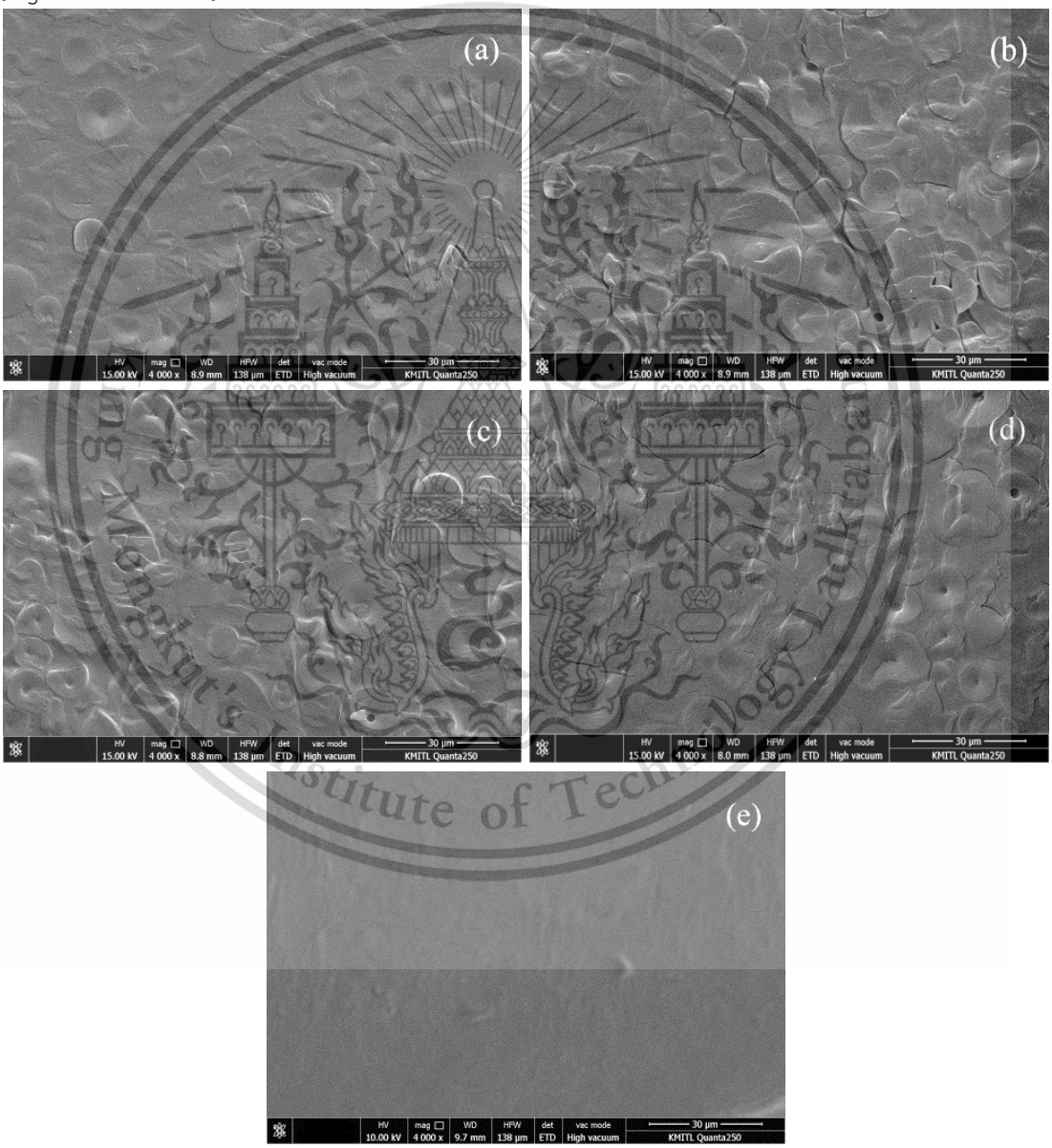

Figure 4.28 SEM micrographs at 4000X magnification of NS film and various singly modified starch films (a) NSF, (b) CS-BOF, (c) CS-BAF, (d) CS-STF and (e) OSF

SEM micrographs at 4000X magnification of NS film and different singly modified starch films are displayed in Figure 4.28. NS film revealed a rough surface that exhibited some starch granules (Figure 4.28(a)). On the other hand, SEM micrographs of all CS films (Figures 4.28(b)-(d)) showed rougher surfaces than that of NS film. Moreover, many starch granules were not destroyed after the starch was modified by cross-linking. This was caused by starch granules being highly strengthened after cross-linking, suggesting that the starch structure was difficult to break down. The results of this SEM investigation agree well with those of an earlier study on a cast biodegradable starch film from Chinese yam starch crosslinked with propylene oxide, STMP, and STPP [49]. In this study, when the morphologies of different types of CSF were compared, CS-BOF (Figure. 4.28(b)) exhibited the unmolten starch granules that were not destroyed by cross-linking and the highest surface roughness due to the highest degree of cross-linking (Table 4.2). On the other hand, the morphology of CS-STF (Figure 4.28(d)) showed the unmolten starch granules and smoother surface than that of CS-BOF due to lower degree of cross-linking. Furthermore, it can be seen in Figure 4.28(e) that not only the starch granules on the surface of OSF completely were disrupted, but the surface was also much smoother than that of NSF because of the destruction of the starch granules and the partial of cleavage of the starch chains [45]. In addition, this smoothest OSF morphology agrees well with its lowest degree of crystallinity obtained from the XRD study (Table 4.15). The smooth morphology of OSF was also reported for OS film from potato starch oxidized with sodium hypochlorite [6].

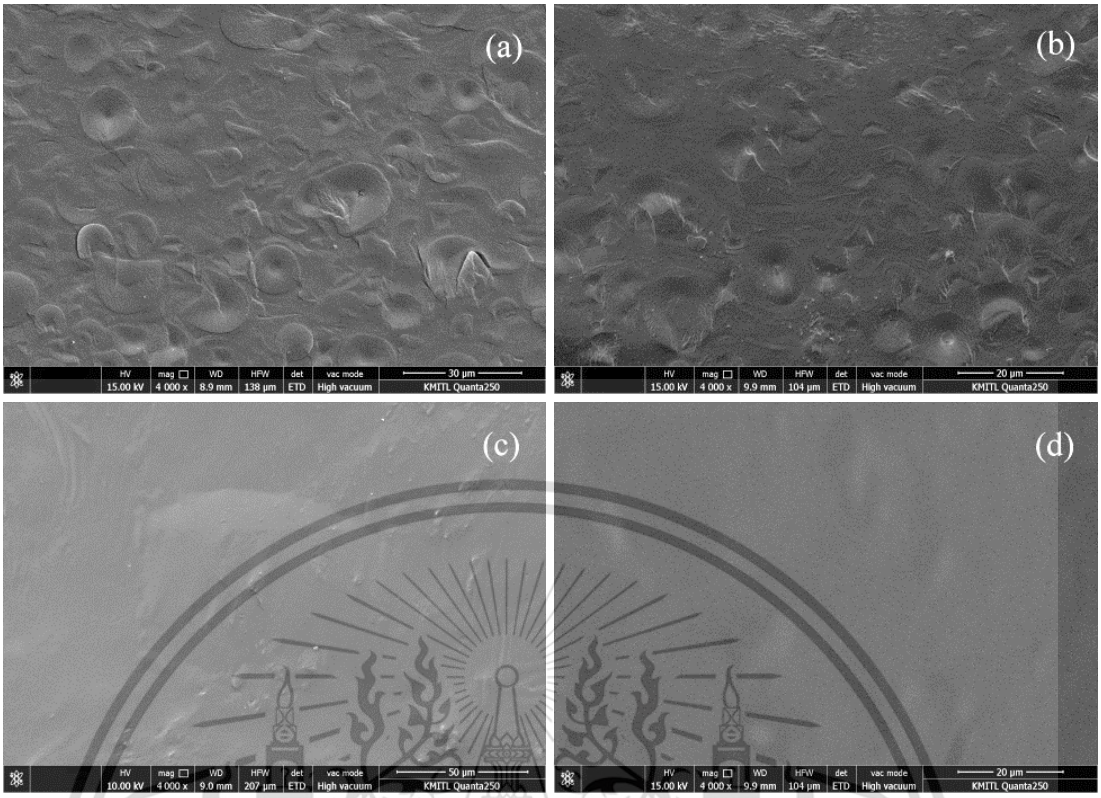

Figure 4.29 SEM micrographs at 4000X magnification of NS film and various COS films crosslinked with different types of cross-linking agents and oxidized with hydrogen peroxide **(a)** NSF, **(b)** COS-BOF, **(c)** COS-BAF and **(d)** COS-STF

Figure 4.29 displays the morphologies of NS film and COS films crosslinked with different agents at 4000X magnification**.** All COS films **(**Figures 4.29**(**b**)-(**d**))** showed lower amounts of starch granules and a smoother surface than NS film **(**Figure 4.29**(**a**)).** In particular, COS-STF **(**Figure 4.29**(**d**))** showed the smoothest surface because of the highest degree of oxidation and the lowest degree of cross-linking among all COS films. Conversely, for the case of COS-BOF **(**Figure 4.29**(**b**))**, its surface still presented some starch granules because of the highest degree of cross-linking and the lowest degree of oxidation **(**Table 4.2**).** This fact could be explained that starch granules were not completely disrupted and the surface roughly fractured because of the cross-linking, whereas the smooth surface was due to the oxidation process **[**6, 45**].**

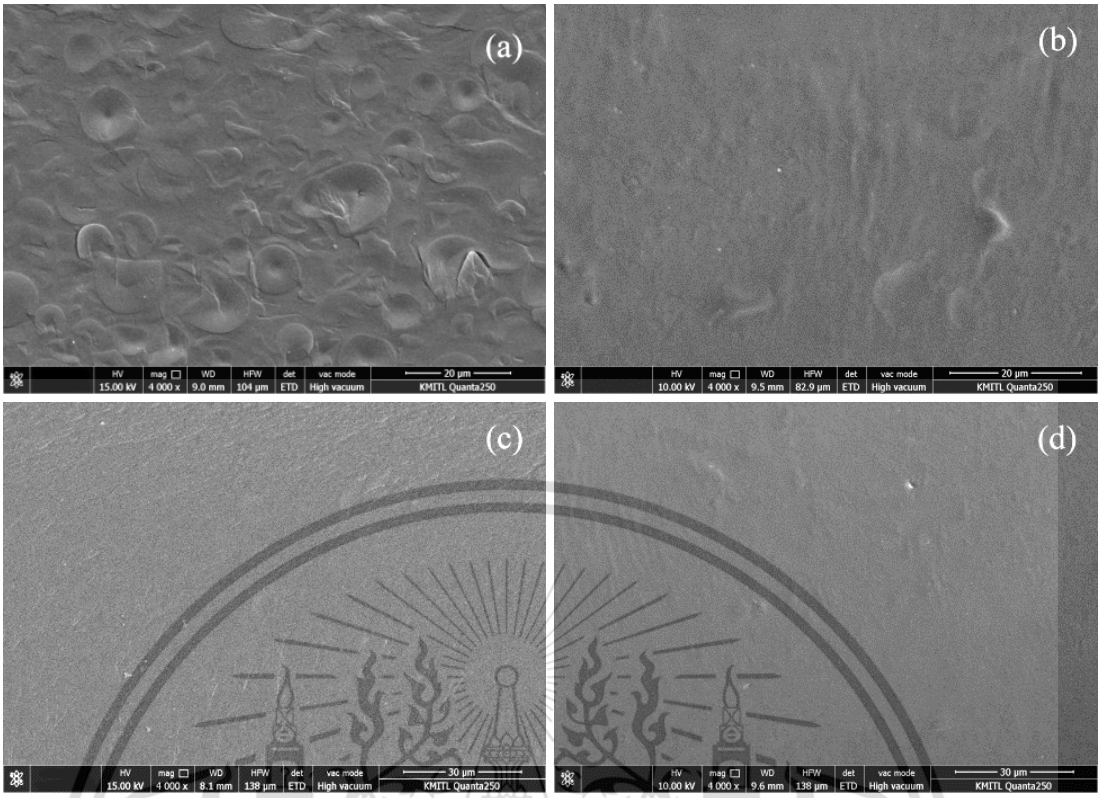

Figure 4.30 SEM micrographs at 4000X magnification of NS film and various OCS films crosslinked with different types of cross-linking agents and oxidized with hydrogen peroxide **(a)** NSF, **(b)** OCS-BOF, **(c)** OCS-BAF and **(d)** OCS-STF

SEM micrographs at 4000X magnification of NS film and various OCS films crosslinked with different types of cross-linking agents and oxidized with hydrogen peroxide are displayed in Figure 4.30. All OCS films showed a relatively smooth surface with no appearance of starch granules, while NS film exhibited a rough surface with some unmolten starch granules. This was due to the cleavage of starch chains and loss of the crystallinity phase (Table 4.15) by the substitution of hydroxyl groups by carbonyl and carboxyl groups from the oxidation process [6] (Figure 4.4), leading to the appearance of a smooth surface. A comparison between the morphologies of various OCS films crosslinked with different agents revealed that OCS-STF exhibited the smoothest fractured surface, caused by the highest degree of oxidation. On the other hand, OCS-BOF exhibited the roughest surface among all OCS films due to the lowest degree of oxidation (Table 4.2).

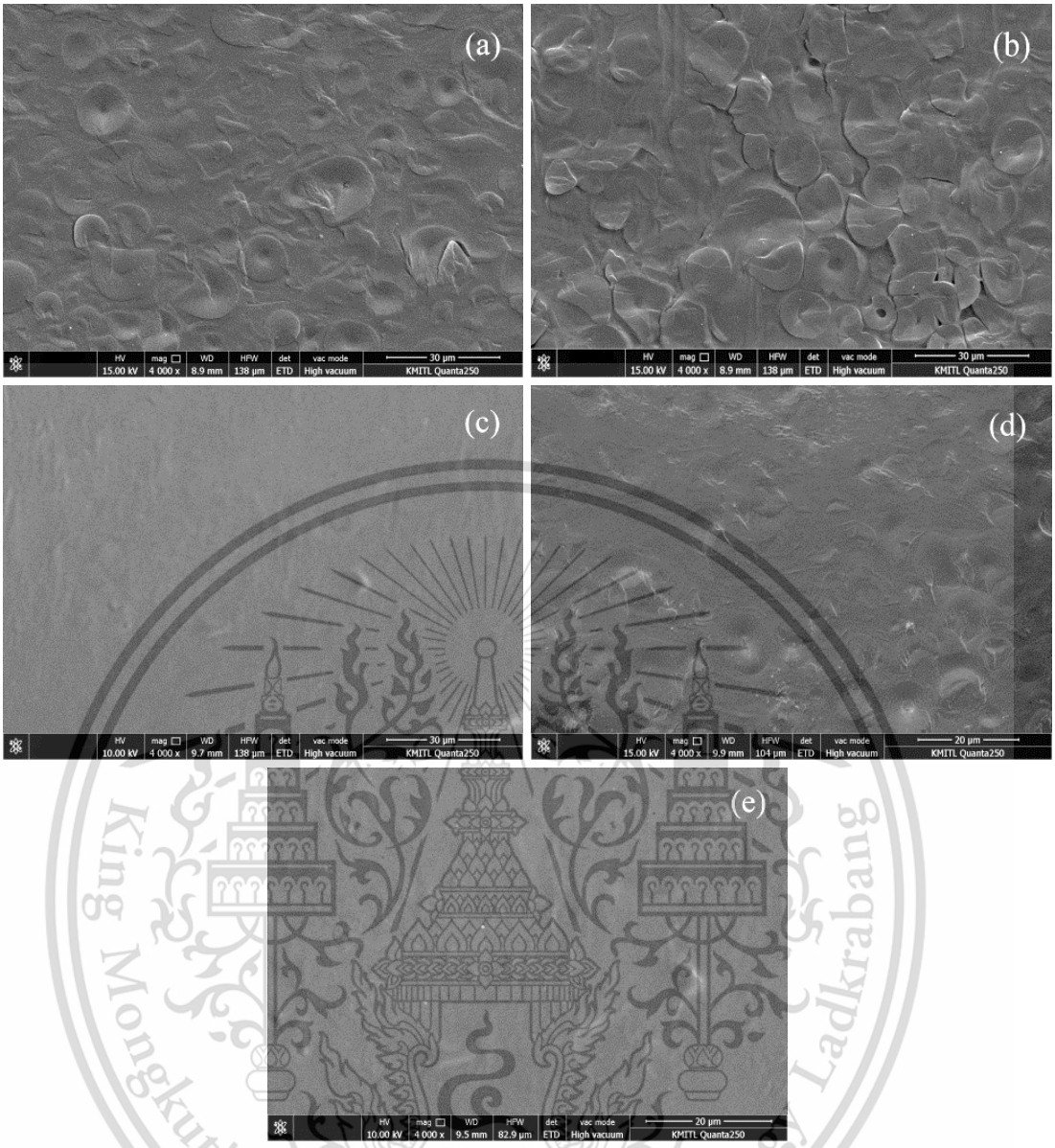

Figure 4.31 SEM micrographs at 4000X magnification of various modified starch films crosslinked with borax and oxidized with hydrogen peroxide **(**a**)** NSF, **(**b**)** CS-BOF, **(**c**)** OSF, **(**d**)** COS-BOF and **(**e**)** OCS-BOF

SEM micrographs of NS film and various modified starch films are displayed in Figure 4.31. The morphological properties of the modified starch films were highly dependent on the modification procedure. NS film (Figure 4.31(a)) showed a rather rough surface with some unmolten starch granules. On the other hand, the surface of CS-BOF (Figure 4.31(b)) was observed to be even rougher with more unmolten starch granules than the case for NSF (Figure 4.31(a)). In contrast, a relatively smooth and homogeneous surface was observed for OSF. This was because of the destruction of the granules by the oxidation process [6]. When morphologies

between singly modified and dually modified starch films were compared, the smoother fractured surface was observed in COS-BOF (as comparison to CS-BOF), which can be explained that NS granules were clearly disrupted by oxidation process [6]. Conversely, OS-BOF showed slightly rougher surface than OSF due to the effect of cross-linking [45].

Regarding the morphologies of different dually modified starch films, the surface of COS-BOF (Figure 4.31(d)) was rougher, with many starch granules, than that of OCS-BOF. This was because of a higher degree of cross-linking (Table 4.2). On the other hand, the surface of OCS-BOF was rather smooth and homogeneous (Figure 4.31(e)), which can be associated with the destruction of the starch granules by high oxidation process.

4.2.4 Degree of swelling

The degree of swelling of all biodegradable starch films was investigated by immersing a sample in distilled water at 25±5˚C for 2, 4, 6 and 72 h, weighing the swollen sample at 100% RH, then calculating the degree of swelling according to Eq. (6) in Section 3.4.8. These degrees of swelling are shown in Figures 4.32-4.35.

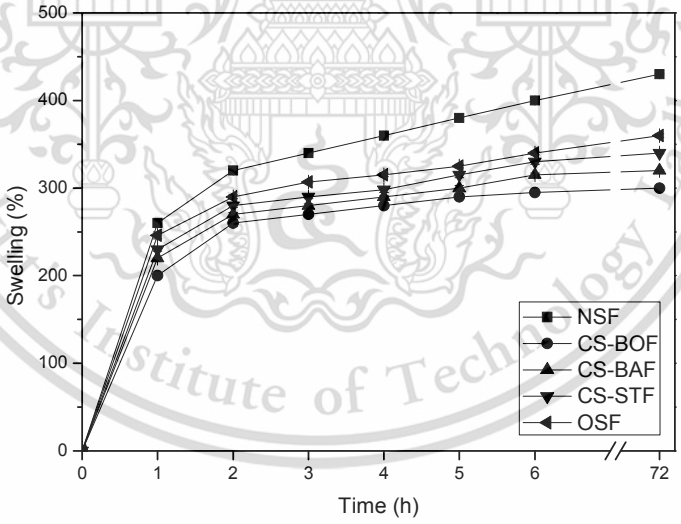

Figure 4.32 Degree of swelling at 100% RH versus immersion time of NS and various singly modified starch films

Figure 4.32 shows that the degree of swelling of all samples clearly increased with increased time. However, the degree of swelling of all singly modified starch films clearly decreased after the single modifications because the hydrophilic hydroxyl groups in the AGU of starch were depleted by the oxidation and cross-

linking processes [6, 43]. Diffusion of water molecules in the matrix of modified starch molecules was highly restricted because of the compact structure of the tetra-borate starch in CS-BOF and CS-BAF and the di-starch phosphate in CS-STF (Figures 4.1-4.3), leading to lower swelling capacity when compared to that of NSF. Regarding CSF crosslinked with different agents, the order of their degrees of swelling is as follows: CS-STF>CS-BAF>CS-BOF. This order agrees well with their degree of cross-linking: a higher degree of cross-linking resulted in a denser structure of the starch film matrix, resulting in lower swelling behavior [39]. In particular, a decrease in the swelling capacity of OSF was also accompanied by the substitution of hydroxyl groups with hydrophobic carbonyl groups [45]. Similar results of a decrease in swelling behavior were also reported for the cast CS films from rice starch with a mixture of STMP/STPP and TPOS from corn starch oxidized with hydrogen peroxide [43, 45].

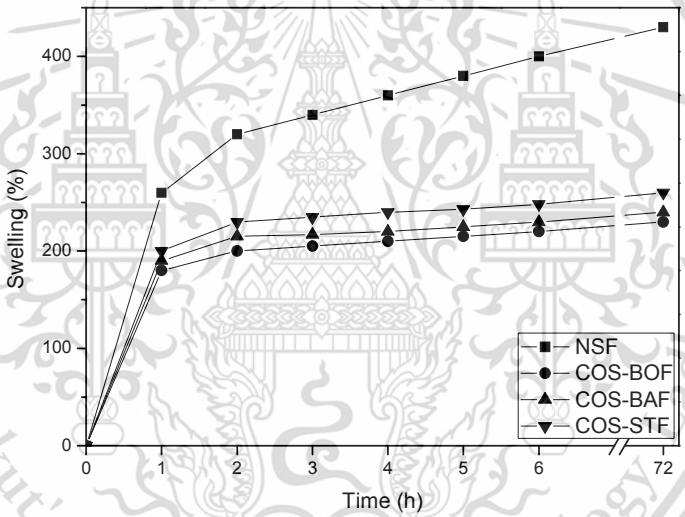

Figure 4.33 Degree of swelling at 100% RH versus immersion time of NS film and various COS films crosslinked with different types of cross-linking agents and oxidized with hydrogen peroxide

The degree of swelling results of NS film and various dually modified starch (COS) films after the starch films were immersed in water for different immersion times at 100% RH are shown in Figure 4.33. It was found that the degree of swelling of all COS films tended to decrease after the crosslinked-oxidized modification. This might be due to a reduction in hydration capacity of the starch backbones, from cross-linking and oxidation [8]. The ranked order of the degree of swelling of different COS films was COS-STF> COS-BAF> COS-BOF. This order was the inverse of the order

of degree of cross-linking; i.e., COS-STF and COS-BOF showed the minimum and maximum degrees of cross-linking, respectively (Table 4.2).

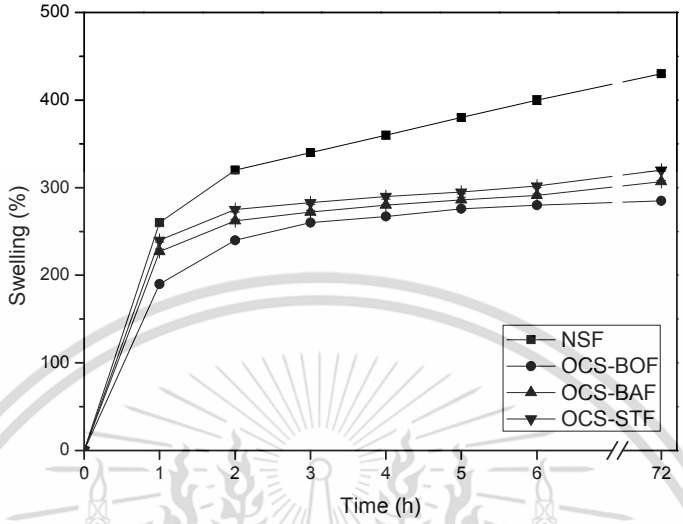

Figure 4.34 Degree of swelling at 100% RH versus immersion time of NS film and various OCS films crosslinked with different types of cross-linking agents and oxidized with hydrogen peroxide

It was observed that all OCS films represented lower degree of swelling than that of NS film (Figure 4.34). This might be due to the decrease in hydrophilic groups in the starch backbones after dual modification. When the degrees of swelling of OCS films crosslinked with different types of cross-linking agents were compared, their ranking order turned out to be OCS-STF>OCS-BAF>OCS-BOF. As expected, OCS-BOF exhibited the lowest degree of swelling because of its highest degree of cross-linking (Table 4.2) that produced the most hydrophobicity among OCS films. On the other hand, the highest degree of swelling was observed in OCS-STF from the lowest degree of cross-linking and the highest degree of oxidation (Table 4.2), leading it to be the most hydrophilic.

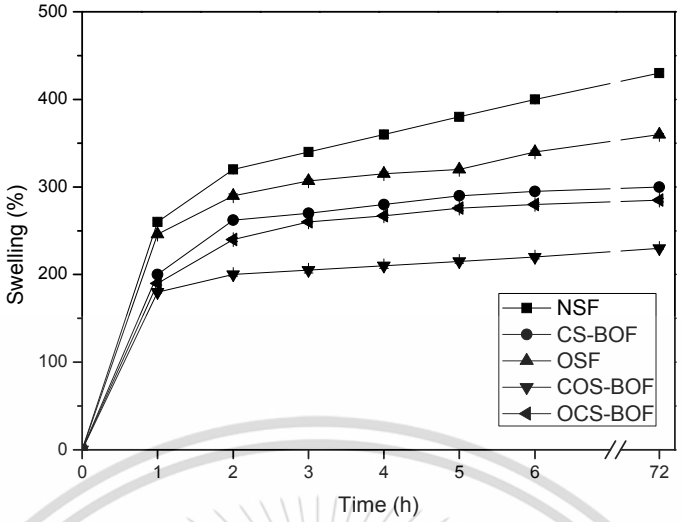

Figure 4.35 Degree of swelling at 100% RH versus immersion time of NS film and various modified starch films crosslinked with borax and oxidized with hydrogen peroxide

It can be observed in Figure 4.35 that all types of modification led to a lower degree of swelling capacity for all modified starch films than that of NS film, suggesting that the modifications of starch improved the hydrophobicity of NS film. In addition, OSF showed higher degree of swelling than CS-BOF, which was probably caused by the partial cleavage of starch chains during the oxidation process, leading to higher diffusion of water molecules into the matrix of starch backbones. It should be noted that both types of dually modified starch films (COS-BOF and OCS-BOF) showed lower degrees of swelling than their singly modified counterparts (CS-BOF and OS-BOF). This might be due to the diminished hydrophilic groups in the starch backbones after both types of modification, leading to an improvement in hydrophobicity. A similar swelling capacity result was reported for dually modified sorghum starch with NaOCl and STMP [10].

Interestingly, COS-BOF showed the lowest degree of swelling capacity in this work, attributable to the high degree of cross-linking and the decrease in numerous hydrophilic hydroxyl groups that created a dense structure of starch chains, blocking water molecules from penetrating into the starch matrix.

4.2.5 Water vapor permeability (WVP)

WVP tests of various biodegradable modified starch films were performed by using a gravimetric modified cup method (desiccant method) in accordance with the

ASTM-E96 standard. The WVP values of various modified starch films are presented in Table 4.17

Table 4.17 WVP values of various modified starch films

Sample	WVP ($g.mm/m^2.day.KPa$)
NSF	22.2±0.04
CS-BOF	17.0±0.03
CS-BAF	19.1±0.03
CS-STF	19.9±0.03
OSF	20.5±0.04
COS-BOF	14.2±0.04
COS-BAF	15.9±0.03
COS-STF	16.3±0.02
OCS-BOF	15.8±0.02
OCS-BAF	16.8±0.02
OCS-STF	17.3±0.05

The result of the WVP test is the most important indicator of the useful properties of biodegradable starch films. WVP values of various modified starch films were not only influenced by the type of cross-linking agent but also by the different starch treatment methods. WVP values of various modified starch films are listed in Table 4.17. All CS films exhibited lower WVP than that of NS film caused by the reinforcement of the structure of the starch granules and the formation of tetra-starch borate and di-starch phosphate structures via cross-linking (Figures 4.1-4.3). This phenomenon limited water vapor permeability and restricted the mobility of the starch chains in the amorphous region [39]. The ranking order of WVP values of CS films crosslinked with various agents was: CS-BOF<CS-BAF<CS-STF. This result was markedly correlated with the degree of cross-linking (Table 4.2). When NS was modified by an oxidation method (OSF), its WVP value clearly decreased. The decrease in WVP was the result of the decrease in the number of hydrophilic groups (-OH) of starch molecules together with higher numbers of more substituted hydrophobic carbonyl groups in the starch chains after the oxidation process [6, 45]. This decrease in WVP agrees well with the decrease in water absorption properties of CSF blend with PVA crosslinked with borax and OSF oxidized with sodium hypochlorite [6, 42]

As expected, the WVP values of all COS films were lower than that of NS film because of the reduction in hydrophilicity from hydroxyl groups altered by the dual modifications. In general, both modification procedures restricted the water vapor absorption capacity of modified starch films. Among COS films crosslinked with various agents, COS-BOF showed the lowest WVP because of its high degree of cross-linking, while the WVP of COS-STF was higher than that of COS due to the lower degree of cross-linking (Table 4.2).

Furthermore, the same trend was observed in OCS films crosslinked with all types of cross-linking agents; WVP values of all OCS films also decreased from the enhancement of hydrophobicity by the oxidized-crosslinked method. As available hydrophilic hydroxyl groups were reduced by increasing the substitution of hydrophobic carbonyl groups [45]. On comparing among OCS films, borax provided the most significant cross-linking effect on the WVP results of OCS films that presented the lowest WVP values due to lower water vapor absorption caused by a high degree of cross-linking. In contrast, OCS-STF exhibited higher WVP values than those of other OCS films because of its minimal degree of cross-linking (Table 4.2). As a result, OCS-STF could absorb more water molecules. The WVP results of all modified starch films in this study were also positively correlated with the degree of swelling results (Figures. 4.32-4.34).

Table 4.18 WVP values of NS film and various modified starch films crosslinked with borax and oxidized with hydrogen peroxide

Sample	WVP ($g.mm/m^2.day.KPa$)
NSF	22.2±0.04
CS-BOF	17.0±0.03
OSF	20.5±0.04
COS-BOF	14.2±0.04
OCS-BOF	15.8±0.02

WVP values of unmodified and variously modified starch films crosslinked with borax and oxidized with hydrogen peroxide are represented in Table 4.18. It should be noted that both singly and dually modified starch films demonstrated an improvement in the resistance of WVP caused by a decrease in the number of free hydrophilic hydroxyl groups. In addition, OSF exhibited higher WVP than that of CS-BOF, which could be attributed to partial starch chain scission and the decrease in

crystallnity of starch that led to the higher hydrophilicity of starch granules; therefore, it was able to easily absorb more water molecules.

A comparison of the WVP values of dually modified starch films and singly modified films showed that both dually modified starch films exhibited lower WVP values than those of both singly modified starch films because a large number of hydrophilic hydroxyl groups were altered by both the cross-linking agent and the oxidizing agent, reducing the hydrophilicity of the starch chains [8].

A lower WVP value was found in COS-BOF than in OCS-BOF because of its higher degree of cross-linking (Table 4.2). In general, WVP value was positively influenced by degree of cross-linking. A high degree of cross-linking created a considerably compact tetra-starch borate structure and substantially reduced the number of hydroxyl groups, leading to a decrease in WVP value.

4.2.6 Mechanical properties

The mechanical properties of the various modified starch films were investigated according to ASTM D-882 at 25±1°C and 60±5% RH. In addition, stress at maximum load, Young's modulus, and strain at the maximum load of NS film and different singly modified starch films are illustrated in Figure 4.36.

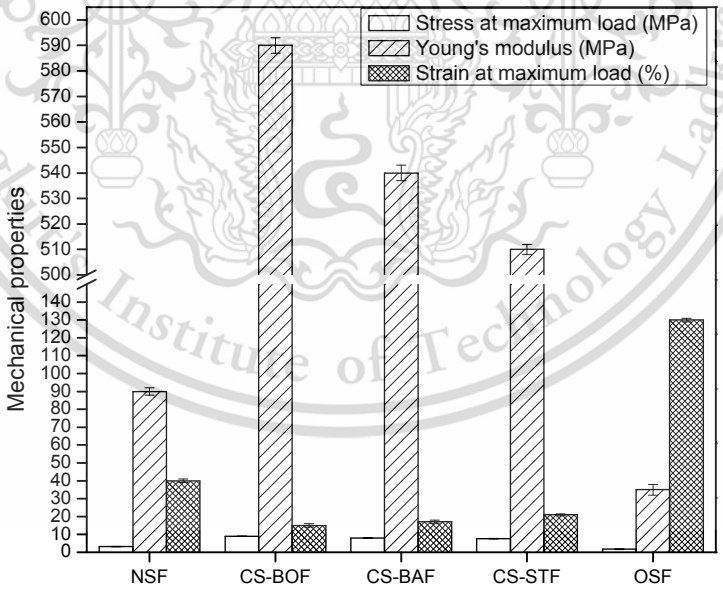

Figure 4.36 Mechanical properties of NS film and various singly modified starch films (a) stress at maximum load, (b) Young's modulus and (c) strain at maximum load

The mechanical properties mentioned as stress at maximum load, Young's modulus, and strain at maximum load of NS film and various singly modified starch

films are displayed in Figure 4.36. It was suggested that all CS films clearly showed greater stress at maximum load and Young's modulus than NS film, but lower strain at maximum load. This result could explain that cross-linking reinforced the strength and stability of the starch molecules and consequently more energy would be required to break down, leading to higher resistance to mechanical shearing of the starch chain. For comparison among CS films crosslinked with different types of cross-linking agent, the ranking order in stress at maximum load and Young's modulus was CS-BO>CS-BA>CS-ST. This result was related to the order of degree of cross-linking of each CS film (Table 4.2). The cross-linking reagents could react with the hydroxyl groups in the starch backbones and produced strong bond linkages and a compact structure of tetra-starch borate or di-starch phosphate (Figures 4.1-4.3). This phenomenon facilitated an improvement in the strength of CS film. The results of mechanical properties agree well with previous research on a cast biodegradable starch film from Chinese yam starch crosslinked with propylene oxide, STMP, and STPP [48].

On the other hand, the decrease in stress at maximum load and Young's modulus of OS film and the enhancement in strain at maximum load were clearly observed. This observation indicated that the oxidation reaction played a role in the destruction of hydrogen bonds and crystal structures of starch together with an increase in motional freedom of the starch chain in the amorphous region, presenting lower strength and higher flexibility of OS film [45]. This result was positively correlated with the degree of crystallinity and morphology (Table 4.15 and Figure 4.28). Similar observations were also reported for TPOS film from corn starch oxidized with hydrogen peroxide [45].

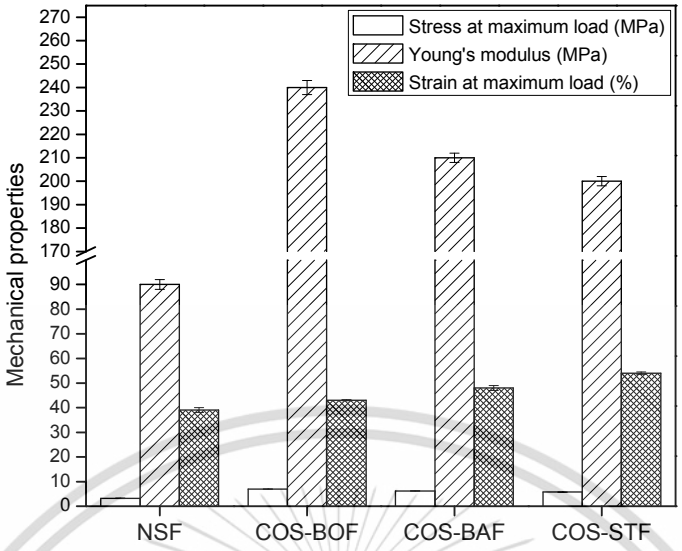

Figure 4.37 Mechanical properties of various COS films crosslinked with different types of cross-linking agent and oxidized with hydrogen peroxide (a) stress at maximum load, (b) Young's modulus and (c) strain at maximum load

The mechanical properties of various COS films are displayed in Figure 4.37; the results exhibited the enhancement of stress at maximum load and Young's modulus when compared to NS film. This was because cross-linking strengthened the starch molecules by strong bond interaction and the formation of a compact crosslinked network structure, and restricted the molecular motion of the starch chains [48], leading to higher strength in COS film. Furthermore, strain at maximum load values of all COS films were also higher than NS film. The result was ascribed to the disruption in hydrogen bonding between the starch backbones and the loss of degree of crystallinity as observed in the XRD study (Table 4.15), resulting in the starch molecules moving more easily. It was suggested that the crosslinked-oxidized method could improve not only the strength but also the flexibility of NS film. When comparing the mechanical properties between various COS films with different cross-linking agents, COS-BOF presented higher stress at maximum load and Young's modulus when compared to those of COS films, but strain at maximum load was slightly lower. This may be due to the fact that the high strength and stiffness of COS-BOF corresponded to the high degree of cross-linking. However, COS-STF presented the highest strain at maximum load value but the lowest stress at maximum load and Young's modulus values, which was due to the lowest degree of cross-linking and the highest degree of oxidation (Table 4.2).

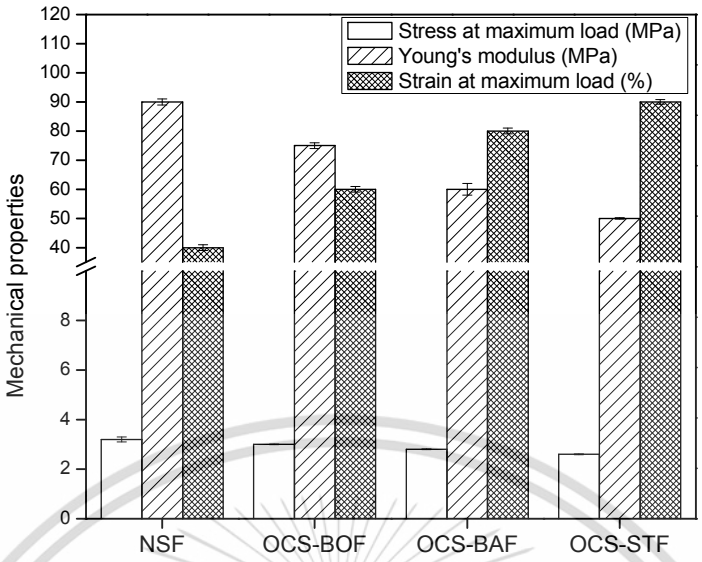

Figure 4.38 Mechanical properties of various OCS films crosslinked with different types of cross-linking agent and oxidized with hydrogen peroxide (a) stress at maximum load, (b) Young's modulus and (c) strain at maximum load

As observed in various types of OCS film from Figure 4.38, the improved extendibility observed from strain at maximum load was clearly pronounced in all OCS films. This result might be due to the effect of oxidation whereby the crystalline phases in the starch structure were disrupted [45]. When OCS films with different types of cross-linking agents were compared, OCS-BOF showed the highest stress at maximum load and Young's modulus, followed by OCS-BAF and OCS-STF. This result is related to the degree of cross-linking of different OCS samples (Table 4.2). As expected, OCS-BOF showed the maximum degree of cross-linking, which could be explained that the borax cross-linking agent reacted with -OH groups in the starch molecules and consequently generated a high quantity of tetra-starch borate structures that were more difficult to break.

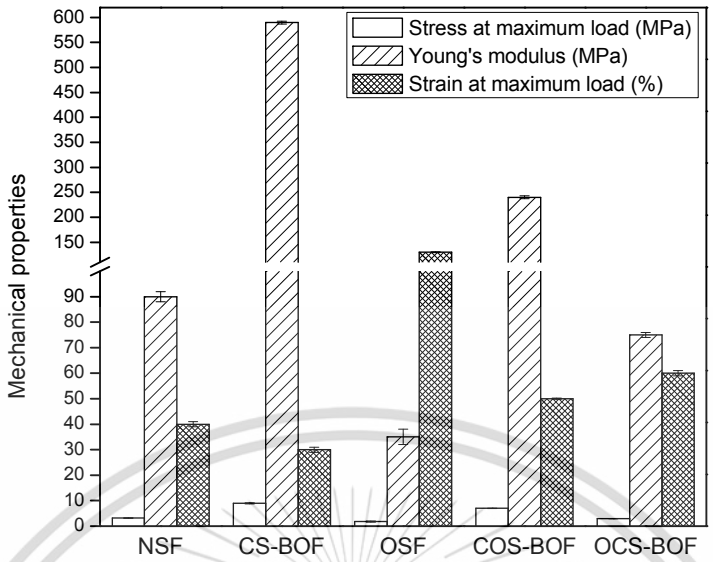

Figure 4.39 Mechanical properties of various modified starch films crosslinked with borax and oxidized with hydrogen peroxide (a) stress at maximum load, (b) Young's modulus and (c) strain at maximum load

Tensile strength, Young's modulus, and strain at maximum load of various modified starch films using hydrogen peroxide and borax as an oxidizing agent and cross-linking agent are presented in Figure 4.39. It was observed that a rise in stress at maximum load in the case of CS-BOF was observed, which was responsible for the increase in strong bond interaction and the formation of tetra-starch borate structures arising from cross-linking with borax (Figure 4.1). However, an increase in flexibility was observed in OSF due to the consequence of starch structural weakening by the oxidation process [45]. This result could be explained that the degraded starch chains could not resist the mechanical shearing force, thereby resulting in lower tensile strength and Young's modulus.

Interestingly, it was suggested that COS-BOF demonstrated enhanced flexibility and excellent tensile properties including high strength and flexibility. This result was attributed to the stabilization of starch as a result of cross-linking process. In addition, OCS-BOF showed the enhancement of strength compared to OSF, caused by the effect of cross-linking. Higher strength and extensibility of the modified starch films as well as lower swelling capacity and hydrophilicity of the starch molecules (Table 4.18 and Figure 4.39) after cross-linking and oxidation were the major reasons for the better mechanical properties of COS-BOF and OCS-BOF.

In comparison of the mechanical properties of COS-BOF and OCS-BOF, it was revealed that COS-BOF was found to show higher tensile strength and Young's modulus than OCS-BOF due to the higher degree of cross-linking and lower carbonyl

and carbonyls contents (Table 4.2). Basically, cross-linking could reinforce the strong intermolecular bonding between starch backbones [39]. In the same way, the lower stiffness of OCS-BOF was probably due to the disintegration of the structure of the starch granules and the disruption of hydrogen bonding between starch molecules by the oxidation process [45].

4.2.7 Biodegradability properties

Biodegradability tests of various differently modified starch films from the soil burial test were investigated for 5 and 10 days in the range of 5–10% moisture. Consequently, the mechanical properties of the various modified starch films, mentioned as stress at maximum load, Young's modulus and strain at maximum load, were evaluated after a soil burial test and presented in Figures 4.40-4.43, while the percentages of the reduction in mechanical properties after 5 and 10 days of biodegradation in soil are shown in Table 4.19.

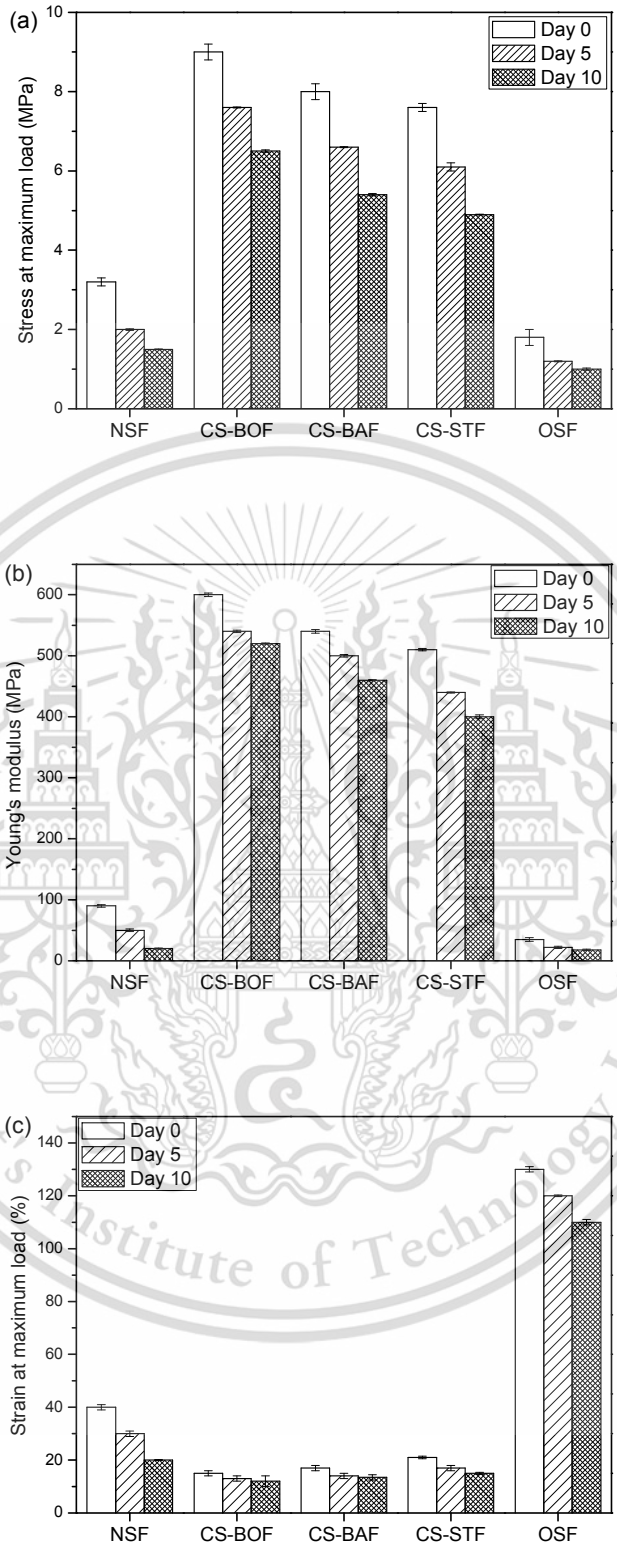

Figure 4.40 Mechanical properties after biodegradation in soil of various singly modified starch films **(a)** stress at maximum load, **(b)** Young's modulus and **(c)** strain at maximum load

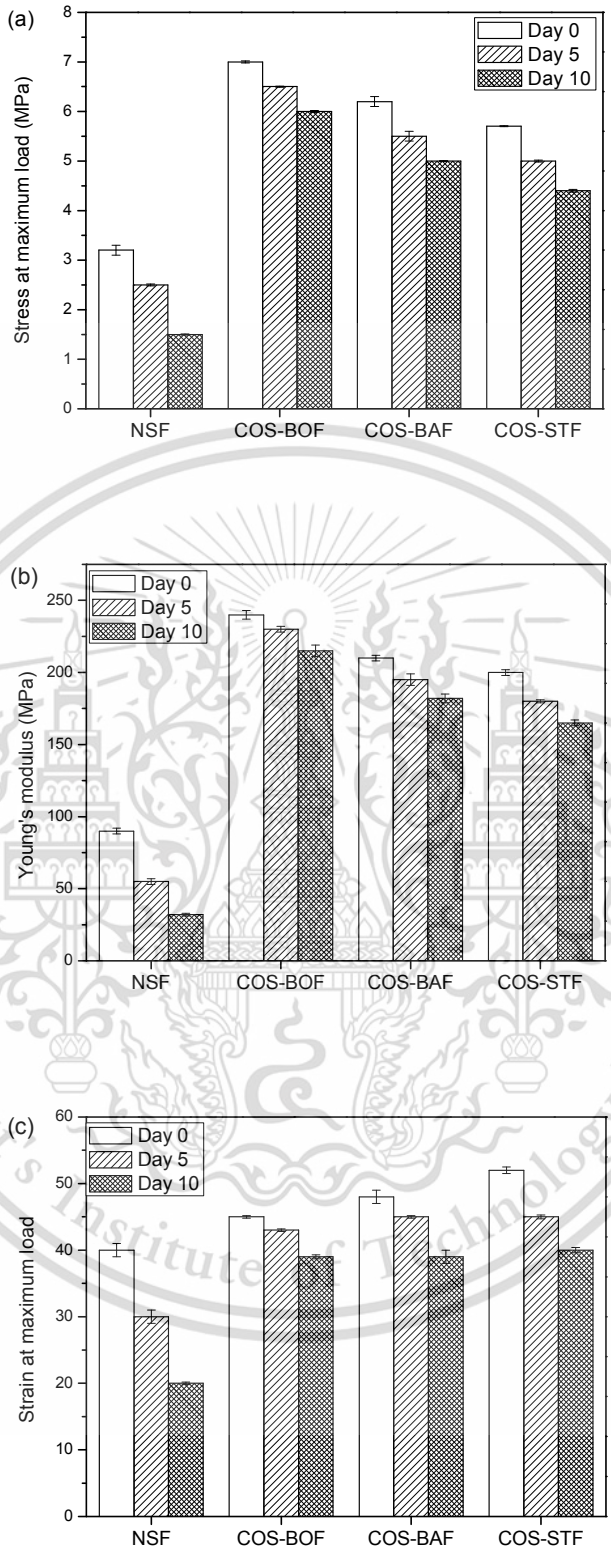

Figure 4.41 Mechanical properties after biodegradation in soil of various COS films crosslinked with different types of cross-linking agents and oxidized with hydrogen peroxide (a) stress at maximum load, (b) Young's modulus and (c) strain at maximum load

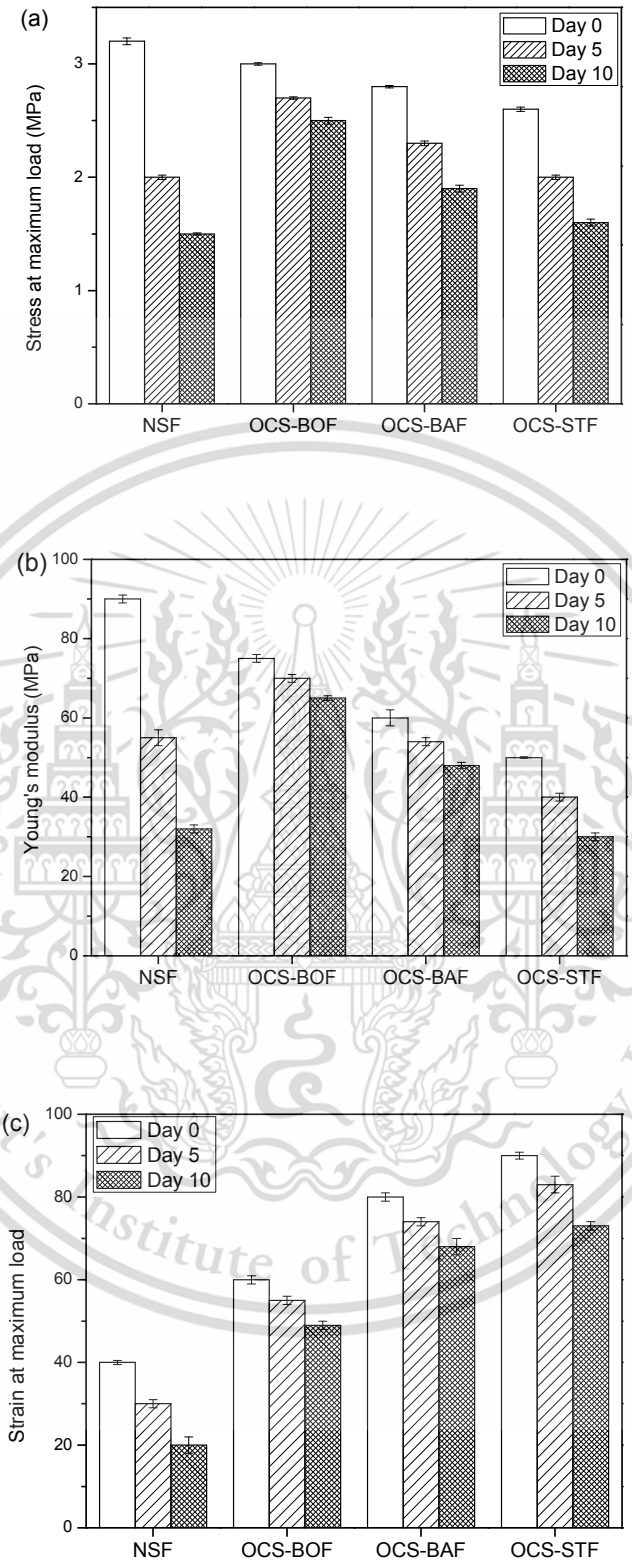

Figure 4.42 Mechanical properties after biodegradation in soil of various OCS films crosslinked with different types of cross-linking agents and oxidized with hydrogen peroxide **(**a**)** stress at maximum load, **(**b**)** Young's modulus and **(**c**)** strain at maximum load

Table 4.19 Percentage reductions of mechanical properties of various modified starch films after 5 and 10 days of biodegradation in soil

Sample	Percentage of a reduction in mechanical properties for 5 days (%)			Percentage of a reduction in mechanical properties for 10 days (%)		
	Stress at maximum load	Young's modulus	Strain at maximum load	Stress at maximum load	Young's modulus	Strain at maximum load
NSF	37.5	44.4	25.0	53.1	66.6	50.0
CS-BOF	15.5	11.8	13.3	27.7	16.9	20.0
CS-BAF	17.5	12.9	17.6	32.5	18.5	20.5
CS-STF	19.7	13.7	19.0	35.5	21.5	28.5
OSF	33.3	37.1	20.7	44.4	48.5	23.0
COS-BOF	7.1	4.1	4.4	14.2	10.4	11.1
COS-BAF	11.2	5.2	6.2	16.1	13.3	12.5
COS-STF	12.2	6.5	7.6	19.3	17.5	13.4
OCS-BOF	10.0	6.0	8.3	16.6	12.0	13.3
OCS-BAF	17.8	8.3	10.0	21.4	13.3	15.0
OCS-STF	19.2	10.0	11.1	23.0	16.0	18.8

The declines in the mechanical properties of stress and strain at maximum load and Young's modulus after the soil burial test were the indicators of soil burial efficiency. As the results from Figures 4.40-4.42 and Table 4.19, unmodified starch and all modified starch films showed a decrease in stress at maximum load, Young's modulus, and strain at maximum load after 5 and 10 days of the biodegradation test. This observation claimed that all starch films could biodegrade by a soil burial test. This occurrence might be because the water absorption of the films triggered the microorganisms in soils to grow, utilizing the material as food [54]. Nevertheless, all modified starch films illustrated lower biodegradability than NS film, but it still could biodegrade according to the biodegradation test caused by the lower water absorption capacity of starch film.

With a comparison of COS and OCS films crosslinked with different types of cross-linking agents (Figures 4.41-4.42), it was found that OCS and COS films crosslinked with STMP/STPP showed more rapid biodegradation than those of borax and boric acid on the basis of the observation of a decrease in mechanical properties after the soil burial test resulting from higher hydrophilicity. On the contrary, COS and OCS films crosslinked with borax showed lower biodegradability than when

crosslinked with other cross-linking agents. This fact was related to the results of hydrophilicity observed in terms of degree of swelling (Figures 4.33-4.34) and the WVP results (Table 4.17). This result explained that COS-STF and OCS-STF could more readily absorb water molecules and exhibited higher hydrophilicity than those of COS and OCS films crosslinked with borax and boric acid. The water absorption in soil resulted in a hydrolysis reaction and a weak effect on the tensile properties of the starch films, causing a rapid biodegradation in the soil. All of these results implied that the hydrophilicity of different modified starch films positively affected the biodegradability properties.

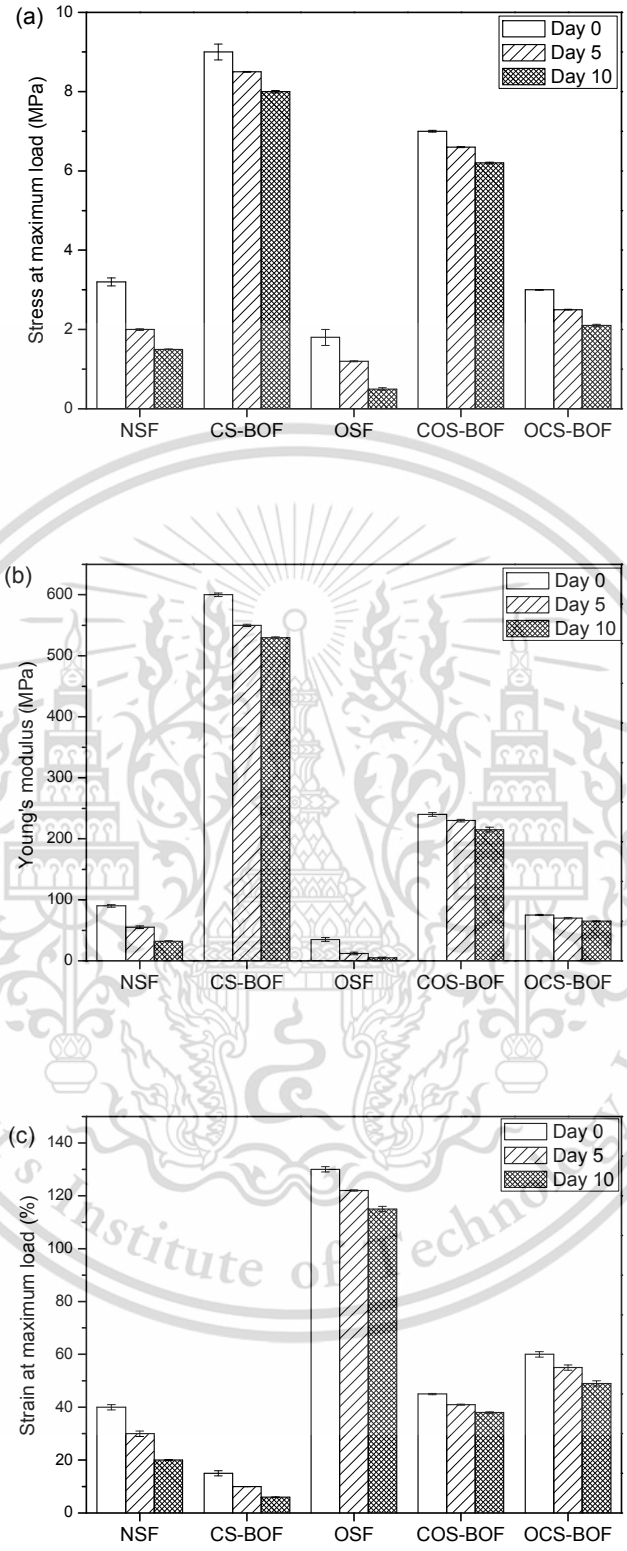

Figure 4.43 Mechanical properties after biodegradation in soil of various modified starch films crosslinked with borax and oxidized with hydrogen peroxide **(a)** stress at maximum load, **(b)** Young's modulus and **(c)** strain at maximum load

Table 4.20 Percentage reductions of the mechanical properties of various modified starch films crosslinked with borax and oxidized with hydrogen peroxide after 5 and 10 days of biodegradation in soil

Sample	Percentage of a reduction in mechanical properties for 5 days (%)			Percentage of a reduction in mechanical properties for 10 days (%)		
	Stress at maximum load	Young's modulus	Strain at maximum load	Stress at maximum load	Young's modulus	Strain at maximum load
NSF	37.5	44.4	25.0	53.1	66.6	50.0
CS-BOF	15.5	11.8	13.3	27.7	16.9	20.0
OSF	33.3	37.1	20.7	44.4	48.5	23.0
COS-BOF	7.1	4.1	4.4	14.2	10.4	11.1
OCS-BOF	10.0	6.0	8.3	16.6	12.0	13.3

Figure 4.43 and Table 4.20 illustrate the mechanical properties of NS film and various modified starch films crosslinked with borax and oxidized with hydrogen peroxide before and after biodegradation in the soil burial test. After the samples were buried in soil, all of them showed a significant reduction in their tensile strength, Young's modulus, and elongation values. This result claimed biodegradability of all starch films, which resulted from hydrolysis of the starch backbones by moisture absorption from the soil and attacks from microorganisms in the soil [54]. However, all modified starch films presented a smaller change in tensile properties after the biodegradability test than NS film due to a reduction in water absorption capacity caused by the modification as observed from the WVP and swelling results (Figure 4.35 and Table 4.18).

In addition, both dually modified starch films (COS-BOF and OCS-BOF) exhibited lower biodegradability than both singly modified starch films (CS-BOF and OSF). This implies that the rapid degradation of the polysaccharide chains was mainly due to the absorption capacity of the different modified starch films since both singly modified starch films exhibited higher hydrophilicity than both dually modified starch films.

Regarding the biodegradability of COS-BOF and OCS-BOF, it was found that OCS-BOF showed more rapid biodegradation than COS-BOF, which could be due to the higher hydrophilicity of OCS-BOF. The hydrophilicity led to a strong affinity for water molecules in the soil. These results are consistent with the higher degree of swelling and WVP results of various modified starch films.

4.2.8 Thermal property

The thermal properties of NS film and various modified starch films were investigated by the TGA technique in the temperature range of 50-600˚C under a nitrogen atmosphere at the heating rate of 10˚C/min in order to determine the maximum degradation temperature as shown in Figures 4.44-4.47. The degradation temperatures are presented in Table 4.21.

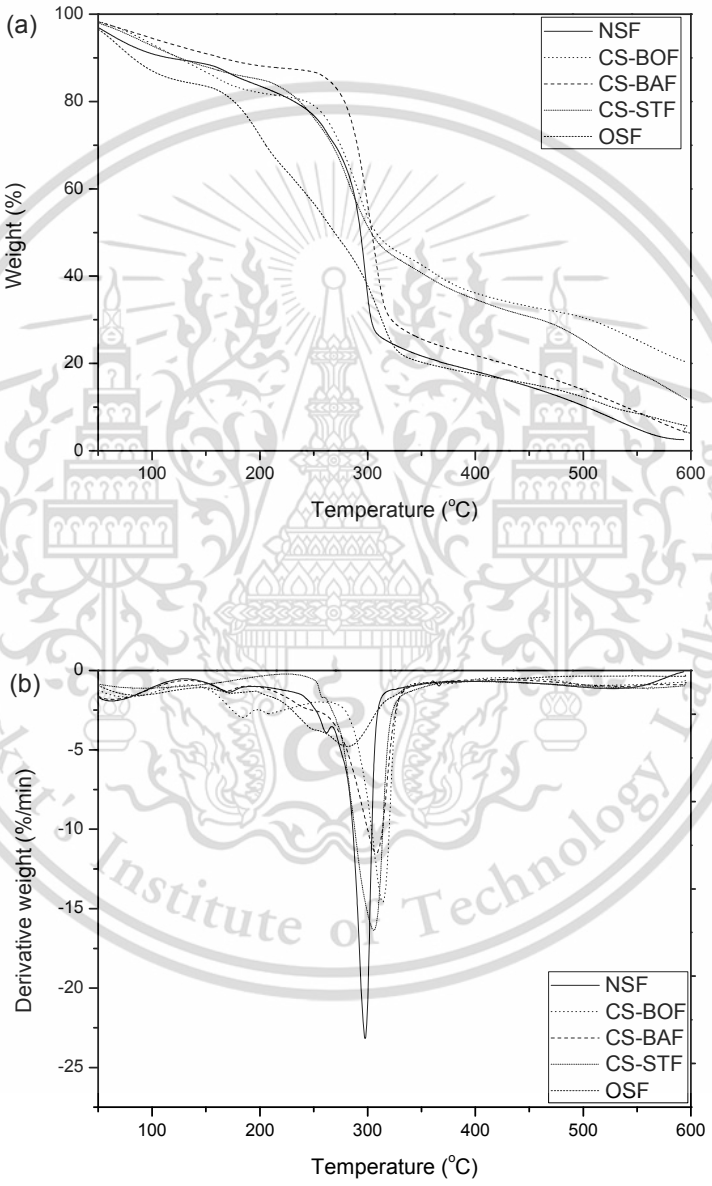

Figure 4.44 Thermograms of NS film and various singly modified starch films **(a)** TGA and **(b)** DTG

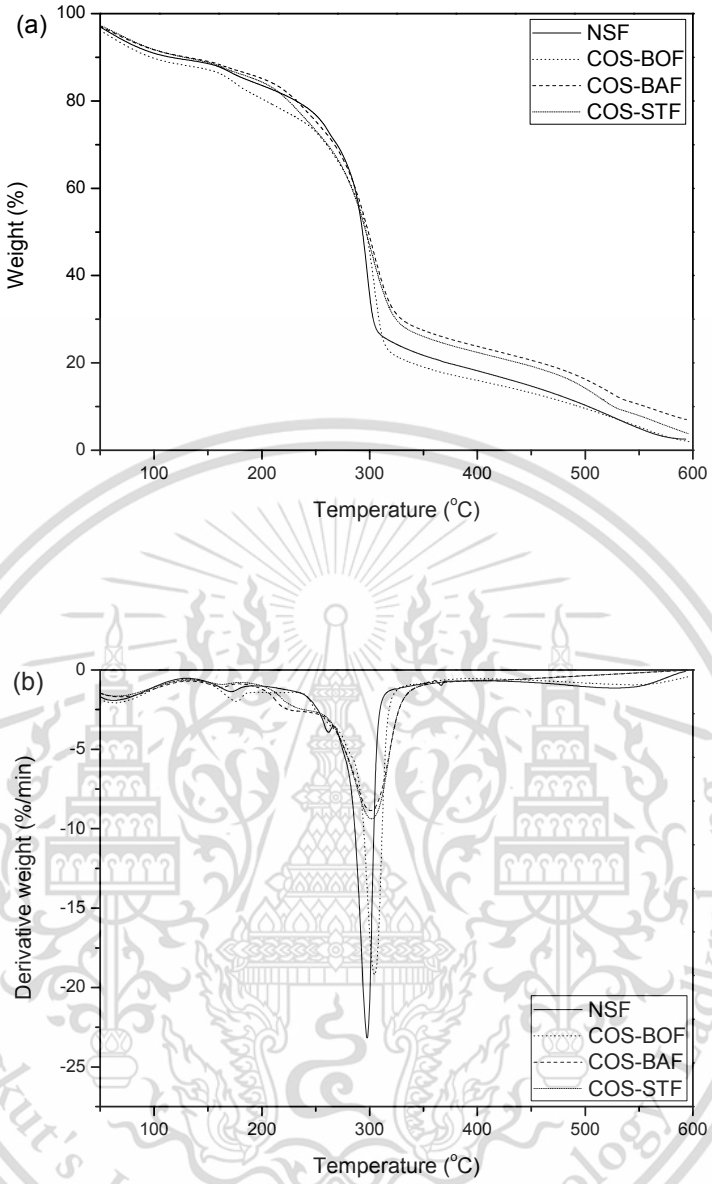

Figure 4.45 Thermograms of NS film and various COS films crosslinked with different types of cross-linking agents and oxidized with hydrogen peroxide **(a)** TGA and **(b)** DTG

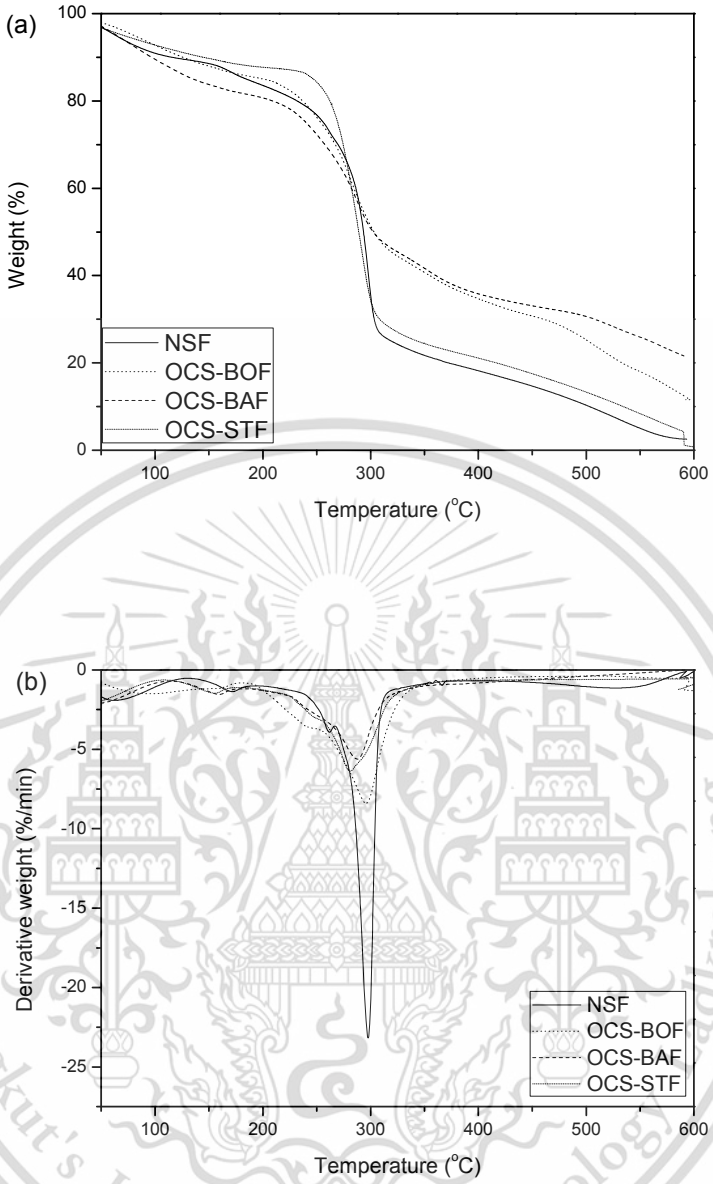

Figure 4.46 Thermograms of NS film and various OCS films crosslinked with different types of cross-linking agents and oxidized with hydrogen peroxide **(a)** TGA and **(b)** DTG

Table 4.21 Degradation temperatures of NS film and various modified starch films

Sample	Degradation temperature (°C)	
	Step 1 (Glycerol)	Step 2 (Starch)
NSF	171.9	297.5
CS-BOF	180.7	316.9
CS-BAF	183.8	313.8
CS-STF	169.4	308.0
OSF	185.6	287.2
COS-BOF	169.4	307.7
COS-BAF	162.3	305.2
COS-STF	176.1	304.3
OCS-BOF	161.6	295.2
OCS-BAF	175.6	292.0
OCS-STF	170.3	289.8

The TGA and DTG curves of NS film and various modified starch films are shown in Figures 4.44-4.46 and the degradation temperature were determined from the maximum degradation temperatures as shown in Table 4.21. For all of the starch films, there were 2 stages of decomposition. The initial step in the ranges of 160-190°C was attributed to glycerol plasticizer. The main second stage in the range of 280-320°C was merely due to the degradation of the starch [55]. The results revealed that all CS films illustrated noticeably higher degradation temperatures for starch than that of NS film. This was due to the linkages between starch molecules via the cross-linking reaction providing higher thermal stability for all CS films [43]. In addition, the thermal degradation of starch of various types of CS film was ranked as follows: CS-BOF>CS-BAF>CS-STF. These results were related to the degree of cross-linking. In general, high degree of cross-linking could improve the stabilization of starch granules to a greater extent than a low degree of cross-linking [43]. In contrast, a lower degradation temperature of starch in comparison to NS film was exhibited in the case of OSF. This might be due to the partial cleavage of starch backbones and the loss of hydrogen bonding between the starch chains by the substitution with carbonyl and carboxyl groups via the oxidation reaction. This result was in good agreement with earlier works concerning CS film from rice starch crosslinked with epichlorohydrin and OS from yam starch oxidized with sodium periodate [43, 55].

When considering the thermal properties of different COS films, all COS films showed slightly higher thermal degradation temperatures than NS film. This might be explained that cross-linking could enhance the strong bond interaction between starch chains and the formation of crosslinked network structures, resulting in high stabilization of the starch structure. When comparing the degradation temperatures in the second transition of COS films with different types of cross-linking agents, it was suggested that COS-BOF showed the highest thermal properties that provided the highest degradation temperature, caused by the maximum degree of cross-linking. Conversely, COS-STF illustrated lower degradation temperatures than those of COS films due to the highest degree of oxidation (Table 4.2).

As observed in the case of various types of OCS film, the results showed that all OCS films showed lower degradation temperatures than NS film, especially OCS-STF. This was probably because of the high degree of carbonyl and carboxyl groups of OCS-STF resulting from higher opportunity for the oxidation reaction to take place (Table 4.2). This characteristic caused the interruption of the starch chain, leading to the weakening of the thermal properties of starch film. Nevertheless, OCS-BOF showed higher degradation temperatures than other OCS films because of the higher degree of cross-linking and lower degree of oxidation (Table 4.2).

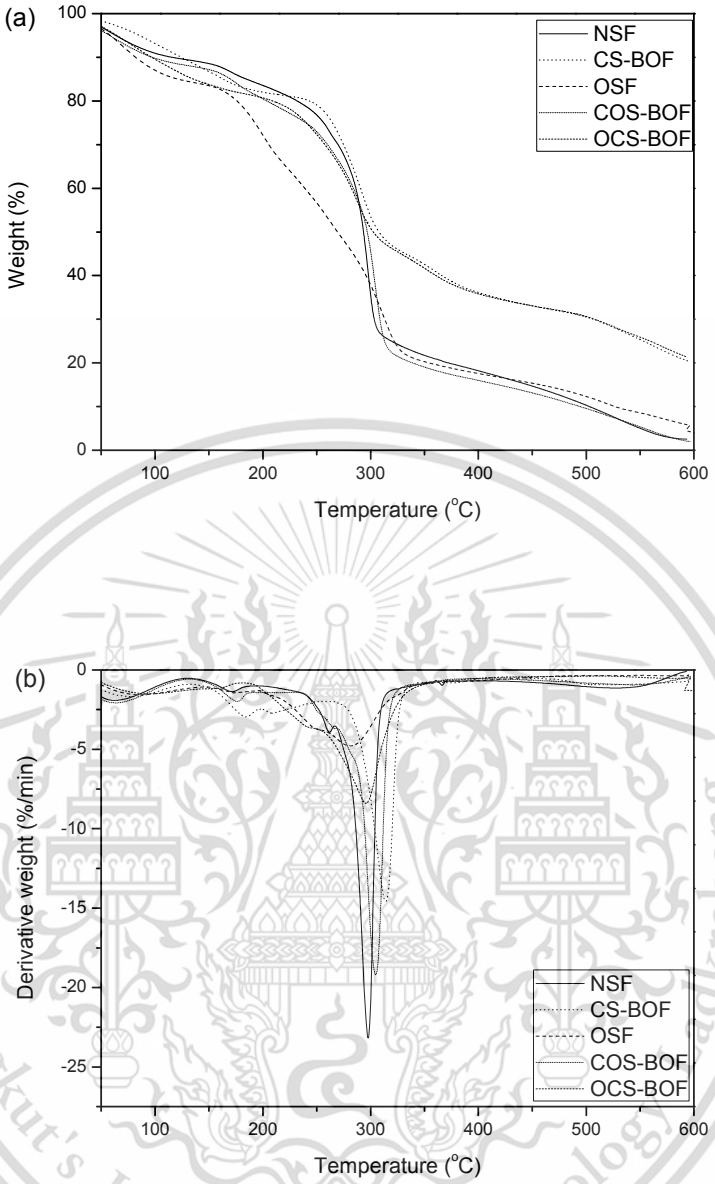

Figure 4.47 Thermograms of NS film and different modified starch films crosslinked with borax and oxidized with hydrogen peroxide (a) TGA and (b) DTG

Table 4.22 Degradation temperatures of NS film and various modified starch films crosslinked with borax and oxidized with hydrogen peroxide

Sample	Degradation temperature (°C)	
	Step 1 (Glycerol)	Step 2 (Starch)
NSF	171.9	297.5
CS-BOF	180.7	316.9
OSF	185.6	287.2
COS-BOF	169.4	307.7
OCS-BOF	161.6	295.2

The TGA and DTG graphs of NS, singly, and dually modified starch films crosslinked with borax and oxidized with hydrogen peroxide are presented in Figure 4.47 and the maximum degradation temperatures of different modified starch films are tabulated in Table 4.22.

Interestingly, the improvement of the thermal properties was observed in the case of CS-BOF and COS-BOF. This was caused by the stabilization of the starch chain and the formation of tetra-starch borate via cross-linking [43]. However, the thermal degradation temperature of COS-BOF was lower than that of CS-BOF, resulting from the partial chain scission and the loss of hydrogen bonding between starch chains. On the other hand, the decrease in thermal properties was pronounced in the cases of OSF and OCS-BOF, caused either by the loss in hydrogen bonding or the cleavage of starch chains by the oxidation process [55]. Interestingly, OCS-BOF showed higher decomposition temperature than OSF. It should be noted that the dual modification by the oxidized-crosslinked method could improve the thermal properties of single modified films (OSF) due to the effect of cross-linking in creating strong linkages between starch molecules.

When comparing thermal properties between COS-BOF and OCS-BOF, it was suggested that COS-BOF showed higher degradation temperatures than OCS-BOF, caused by a higher degree of cross-linking including a lower degree of oxidation of COS-BOF (Table 4.2). Among all of these results, the highest degradation temperature was found in CS-BOF and the lowest degradation temperature was presented in OSF.

Chapter 5
Conclusions and suggestions

5.1 Conclusions

Various properties of different modified starch and different biodegradable modified starch films by single modification (CS and OS) and dual modification (COS and OCS) were investigated. The sample results are concluded as follows:

5.1.1 Properties of different modified starch

5.1.1.1 There was a slightly lower degree of cross-linking for all COS presented than for all CS samples but all COS samples contained higher degrees of cross-linking than OCS samples. The carboxyl and the carbonyl content of OS sample was similar to all OCS samples, which in turn showed higher carbonyl and carboxyl contents than that all COS samples. Borax was found to be the most efficient cross-linking agent, which provided the highest degree of cross-linking, followed by boric acid and the STMP/STPP mixture. The highest amount of cross-linking in the present study was found in CS-BO; while the highest carbonyl and carboxyl contents was found in OS and all OCS samples.

5.1.1.2 The FT-IR study displayed a decrease in the intensity peak of hydrogen bonding at 1642 cm^{-1} and the new characteristic peaks of 1729 cm^{-1} assigned to C=O stretching of carbonyl and carboxyl groups, confirming the successful modification by the cross-linking and oxidation of differently modified starch. In addition, all OCS samples presented higher intensities of C=O stretching peaks of carbonyl and carbonyl groups than all COS samples.

5.1.1.3 The SEM study showed that all CS samples illustrated relative morphology similar to NS and there was the presence of some starch granules. The morphology of OS and OCS samples exhibited relatively smooth fractured surfaces and disruption of the starch granules. On the contrary, all COS showed a combination of the mixture of smooth surfaces and the presence of some starch granules.

5.1.1.4 The cross-linking reaction increased the intrinsic viscosity and MW but the oxidation decreased the intrinsic viscosity and MW of the modified starch. The intrinsic viscosity and MW of CS and COS were increased, while OS and OCS showed lower intrinsic viscosities viscosity and MW than NS.

5.1.1.5 From the TGA techniques, the increase in thermal property was observed in all the case of all CS and COS samples. On the other hand, thermal property was decreased for OS and all OCS samples. Moreover, all COS samples displayed lower thermal property than all CS samples, although it was higher but

higher than OS and OCS samples and the improved thermal properties were observed for property of OS after the oxidation-cross-linking method (OCS).

5.1.2 Properties of different biodegradable modified starch films

5.1.2.1 The FT-IR spectra of all types of CS, COS and OCS films showed the diminished hydrogen bonding peaks at 1640 cm^{-1}; while, the FT-IR spectra of OS, OCS and COS films presented new additional peaks of C=O stretching of carbonyl and carboxyl groups at 1729 cm^{-1}. Besides, all OCS films showed higher intensities peaks of C=O stretching at 1729 cm^{-1} of carbonyl and carboxyl groups than all COS samples.

5.1.2.2 For the XRD study, oxidation reduced the degree crystallinity for the biodegradable modified starch films including OS, all COS and OCS films, while cross-linking was not found to affect the degree of crystallinity for all the modified starch films.

5.1.2.3 The morphology revealed that all CS and COS films displayed rough fractured surfaces and the presence of some unmolten starch granules, but smooth surfaces was found in OS film and all OCS films.

5.1.2.4. The degree of swelling for all modified starch films clearly reduced after starch modification. Both dually modified starch films (COS and OCS films) presented lower degrees of swelling in comparison to both singly modified starch films (CS and OS films), while all COS films showed lower degrees of swelling than all OCS films, while the lowest degree of swelling was found in COS-BOF.

5.1.2.5 All the types of starch modification decreased the WVP values of the biodegradable starch films, all COS and OCS films were found to lower WVP than all CS and OS films. All COS films showed lower WVP values than all OCS films. Additionally, the minimum WVP value was observed in COS-BOF.

5.1.2.6 Stress at the maximum load and Young's modulus were enhanced by the cross-linking and the crosslinked-oxidized methods; whereas, strain at the maximum load or flexibility was increased by the oxidation and the oxidation-cross-linking methods. All COS and OCS films showed both excellent strength and extensibility, while all COS films showed higher tensile strength and Young's modulus compared to all OCS films. The maximum tensile strength and Young's modulus was found in CS-BOF.

5.1.2.7 All the modified starch films were able to degrade in the soil burial test. All the modified starch films exhibited lower biodegradability compared to the unmodified starch film, however, they could still biodegrade.

5.1.2.8 For thermal properties, the thermal degradation temperatures for all CS and COS films were clearly enhanced when compared to NS film, especially

for CS-BO and COS-BO. In contrast, OS and all OCS films displayed significantly decreased thermal degradation temperatures.

5.1.2.9 The dual modification could improve hydrophobicity together with the enhanced mechanical properties of both single modified films (all CS films and OS film) in terms of high strength and flexibility.

5.1.2.10 When comparing the efficiency of the different types of cross-linking agents, all the modified starch films crosslinked with borax presented the greatest overall results (strength and hydrophobic property). Meanwhile, the lowest overall results were found in those crosslinked with the STMP/STPP mixture. Finally, the least effective cross-linking agent was found to be the STMP/STPP mixture.

5.1.2.11 The best overall properties of biodegradable starch films in this study was found in COS-BOF, which showed both good tensile strength and flexibility including the lowest hydrophilic properties (degree of swelling and WVP).

5.2 Suggestions

The present research was focused on improving the physicochemical properties of biodegradable dually modified starch films based on different types of modified starch, including OCS and COS. The dually modified starch films can be further improved and developed using the following suggestions:

5.2.1 Blending with other types of dually modified starch such as acetylated-crosslinked starch to enhance various properties for packaging applications.

5.2.2 Further test for flocculation capacity of modified starch films for water waste treatment application.

5.2.3 The obtained film in the present study showed higher thickness than commercial film for using in packaging application, the thickness of the starch film could be reduced by decreasing the volume of the starch solution for during casting.

References

[1] Chua, H. Yu H.F. and Ma, C.K. 1999. "Accumulation of Biopolymers in Activated Sludge Biomass." *Applied Biochemistry and Biotechnology.* 78(1) : 389-399.

[2] Bemiller, J.N. 1997. "Starch Modification: Challenges and Prospects." *Starch-Stärke.* 49(4) : 127-131.

[3] Radley, J.A. 1976. "Chemical Analysis of Raw and Modified Starches." 133-166. in Lyne, F.A. **Examination and Analysis of Starch and Starch Products**, London : Applied science publisher.

[4] Ayoub, A. and Rizvi, S.S.H. 2009. "An Overview on the Technology of Cross-Linking of Starch for Nonfood Applications."*Journal of Plastic Film and Sheeting*. 25(1) : 25-45.

[5] Colivet, J. and Carvalhoa, R.A. 2016. "Hydrophilicity and Physicochemical Properties of Chemically Modified Cassava Starch Films." *Industrial Crop and Products.* 95 : 599-607.

[6] Zavareze, E.D.R. Pinto, V.Z. Klein, B. El Halal, S.L.M. Elias, M.C. Prentice-Hernández, C. and Dias, A.R.G. 2012. "Development of Oxidised and Heat–Moisture Treated Potato Starch Film." *Food Chemistry*. 132(1) : 344-350.

[7] Sangseethong K. Termvejsayanon, N. and Sriroth K. 2010. "Characterization of Physicochemical Properties of Hypochlorite and Peroxide Oxidized Cassava Starches." *Carbohydrate Polymers*. 82(2) : 446-453.

[8] Xiao ,H.X., Lin, Q.L., Liu, G.Q. and Yu, F.X. 2012. "A Comparative Study of the Characteristics of Cross-linked, Oxidized and Dual-Modified Rice Starches." *Molecules.* 17(9) : 10946-10957.

[9] Sukhija, S. Singh, S. and Riar, C.S. 2016. "Effect of Oxidation, Cross-linking and Dual Modification on Physicochemical, Crystallinity, Morphological, Pasting and Thermal Characteristics of Elephant Foot Yam (*Amorphophallus Paeoniifolius*) Starch."*Food Hydrocolloids*. 55 : 56-64.

[10] Karmvir, G. Ritika, B.Y. Baljeet, S.Y. and Roshanlal, Y. 2018. "Physico-Chemical, Textural and Crystallinity Properties of Oxidized, Crosslinked and Dual- Modified White Sorghum Starch." *International Journal of Food Properties*. 25(5) : 2104-2111.

[11] Sukhija, S. Singh, S. and Riar, C.S. 2017. "Molecular Characteristics of Oxidized and Cross-linked Lotus (*Nelumbo Nucifera*) Rhizome Starch." *International Journal of Food Properties*. 20(1) : S1065-S1081.

[12] Ebnajjed, S. 2012. **Handbooks of Biopolymers and Biodegradable Plastics, Properties, Processing and Applications.** Oxford : William Andrew Publishing.

[13] Ashter, S.A. 2016. **Bioplastics Engineering**. Oxford : William Andrew Publishing.

[14] Manners, D.J. 1968. **Starch and Its Derivatives**. London : Chapman and Hall.

[15] Galliard, T. 1987. **Starch: Properties and Potential**. Chichester : The Society of Chemical Industry by John Wiley and Sons.

[16] Rees, D.A. 1977. **Polysaccharide Shapes**. London : Chapman and Hall.

[17] Radley, J.A. 1976. **Examination and Analysis of Starch and Starch Product**. London : Applied science publishers.

[18] Whistler, R.L. Remiller, J.N. and Paschall, E.F. 1984. **Starch Chemistry and Technology**. 2nd ed. Amsterdam : Elsevier Academic press.

[19] Schirmer, M. Jekle, M. and Becker, T. 2015. "Starch Gelatinization and Its Complexity for Analysis." *Starch-Starke*. 67(1-2) : 30-41.

[20] Chinma, C.N. Ariahu, C.C. and Abu, J.O. 2013. "Chemical Composition, Functional and Pasting Properties of Cassava Starch and Soy Protein Concentrate Blends." *Journal of Food Science and Technology*. 50(6) : 1179–118.

[21] Wurzburg, O.B. 1986. **Modified Starches: Properties and Uses**. Boca Raton, Florida : CRC Press.

[22] Smiley, R.A. and Jackson, H.L. 2002. **Chemistry and the Chemistry Industry : A Practical Guide for Nom-Chemists**. Boca Raton : CRC Press.

[23] Mirmoghtadaie, L. Kadivar, M. and Shahedi, M. 2009. "Effects of Cross-Linking and Acetylation on Oat Starch Properties." *Food chemistry*. 116(3) : 709-713.

[24] Das, A.B. Singh, G. Singh, S. and Riar, C.S. 2010. "Effect of Acetylation and Dual Modification on Physico-Chemical, Rheological and Morphological Characteristics of Sweet Potato (*Ipomoea Batatas*) Starch." *Carbohydrate Polymers*. 80(3) : 725–732.

[25] Granza, A.G. Travalini, A.P. Farias, F.O. Colman, T.A.D. Schnitzler, E. and Demiate, I.M. 2015. "Effects of Acetylation and Acetylation–Hydroxypropylation (Dual-

Modification) on the Properties of Starch from Carioca Bean (*Phaseolus Vulgaris L).*" *Journal of Thermal Analysis and Calorimetry*. 119(1) : 769-777.

[26] Georg, B. 1963. **Handbook of preparative inorganic chemistry 1**. Translated by Reed, F. 2nd ed. New York : N.Y. Academic Press.

[27] Lukasiewicz, M. Achremowicz, B. and Bednarz, S. 2005. "Microwave-Assisted Oxidation of Starch using Hydrogen Peroxide" in **29th International Electronic Conference on Synthetic Organic Chemistry**. Basel : Switzerland

[28] Dang, Z. Chen, H. Shan, Z. Zhen, W. and Yang, M. 2019. "The oxidation of Potato Starch by Electro-Fenton System in the Presence of Fe(II) Ions." *International Journal of Biological Macromolecules*. 121 : 113-119.

[29] Search by Catalog Number: [Online].
Available : http://www.labchem.com/tools/msds/index.php?all=true.

[30] Haynes, W.M. 2016. **Handbook of Chemistry and Physics**. 97th ed. Boca Raton : CRC Press.

[31] Skeist, I. 1990. **Handbook of Adhesives**. 3rd ed. New York : Springer.

[32] GK-12 Project. 2011. **Hands-on Activity: Let's Make Silly Putty**. [Online].
Available : https://www.teachengineering.org/activities.

[33] Helvaci, C. 1994. "Boron and Borates". In Carr, D. D. **Industrial Minerals and Rocks.** 6th ed. Colorado : Society of Mining, Metalurgy and Exploration.

[34] Awada, H. Montplaisir, D. and Daneault, C. 2014. "The Development of a Composite Based on Cellulose Fibres and Polyvinyl Alcohol in the Presence of Boric Acid." *Bioresources*. 9(2) : 3439-3448.

[35] Schrödter, K. Bettermann, G. Staffel, T. Wahl. F. Klein, T. and Hofmann, T. 2008. **Phosphoric Acid and Phosphates. Ullmann's Encyclopedia of Industrial Chemistry**. Weinheim : Wiley-VCH.

[36] Sechi, N.S.M. and Marques, P.T. 2017. "Preparation and Physicochemical, Structural and Morphological Characterization of Phosphorylated Starch." *Materials Research*. 20(2) : 174-180.

[37] Pandey, J.K. Reddy, K.R. Mohanty, A.K. and Misra, M. 2015. **Handbook of Polymer nanocomposites. Processing, Performance and Application**. New York : Springer.

[38] Lide, D. R. 1994. **Handbook of Data on Organic Compounds**. 3rd ed. Boca Raton : CRC Press.

[39] Koo, S.H. Lee, K.Y. and Lee, H.G. 2010. "Effect of Cross-linking on the Physicochemical and Physiological Properties of Corn Starch." *Food Hydrocolloids.* 24(6-7) : 619–625.

[40] Wongsagonsupa, R. Pujchakarn, T. Jitrakbumrung, S. Chaiwat, W. Fuongfuchat, A. Varavinit, S. Dangtipe, S. and Suphantharika, M. 2014. "Effect of Cross-Linking on Physicochemical Properties of Tapioca Starch and Its Application in Soup Product." *Carbohydrate Polymers*. 101 : 656-665.

[41] Yin, Y. Li, J. Liu, Y. and Li, Z. 2005. "Starch Crosslinked with Poly(Vinyl Alcohol) by Boric Acid." *Journal of Applied Polymer Science*. 96(4) : 1394–1397.

[42] Sreedhar, B. Sairam, M. Chattopadhyay, D.K. Syamala Rathnam, P.A. and Mohan Rao, D.V. 2005. "Thermal, Mechanical, and Surface characterization of Starch–Poly(Vinyl Alcohol) Blends and Borax-Crosslinked Films."*Journal of Applied Polymer Science*. 96(4) : 1313–1322.

[43] Detduangchan, N. Sridach, W. and Wittaya, T. 2014. "Enhancement of the Properties of Biodegradable Rice Starch Films by Using Chemical Crosslinking Agents." *International Food Research Journal*. 21(3) : 1225-1235.

[44] Fonseca, L.M. Gonçalves, J.R. El Halal, S.L.M. Pinto, V.Z. Dias, A.R.G. Jacques, A.C. and Zavareze, E.R. 2015. "Oxidation of Potato Starch With Different Sodium Hypochlorite Concentrations and Its Effect on Biodegradable Films." *LWT - Food Science and Technology*. 60 : 714-720.

[45] Zhang, S.D. Zhang, Y.R. Wang, X.L. and Wang. Y.Z. 2009. "High Carbonyl Content Oxidized Starch Prepared by Hydrogen Peroxide and Its Thermoplastic Application."*Starch-Starke*. 61(11) : 646-655.

[46] Sherma, J. 2008. "Principles of Gel Permeation Chromatography". *Journal of AOAC International.* 91(4) : 113A-118A.

[47] Smith, R.J. 1967. "Characterization and Analysis of Starches". 620-625. in Whistler, R.L. and Paschall, E. F. **Starch Chemistry and Technology.** 2nd ed. New York : Academic Press.

[48] Gutierrez, T.J. Tapia, M.S. Perez. E. and Fama, L. 2015. "Structural and Mechanical Properties of Edible Films Made from Native and Modified Cush-Cush yam and cassava starch." *Food Hydrocolloids*. 45 : 211-217.

[49] Salisu, A.A. Musa, H. Abba, H. and Kogo, A.A. 2013. "Preparation and Characterization of Dialdehyde Starch Urea (DASU) and, It`s Sorption Potential

for Co(ii), Pb(ii) and Zn(ii) Ions from Aqueous Solution." *Journal of Chemical and Pharmaceutical Research.* 5(5) : 153-158.

[49] Wang, L. Liu, X. and Wang, J. 2017. "Structural Properties of Chemically Modified Chinese Yam Starches and Their Films." *International Journal of Food Properties*. 20(6) : 1239-1250.

[50] Majzoobi, M. Beparva, P. Farahnaky, A. and Badii, F. 2014. "Physicochemical Properties of Cross-linked Wheat Starch Affected by L-Ascorbic Acid." *Journal of Agricultural Science and Technology.*16(2) : 355-364.

[51] Wongsagon, R. Shobsngob, S. and Varavinit, S. 2005. "Preparation and Physicochemical Properties of Dialdehyde Tapioca Starch." *Starch-Starke.* 57 : 166-172.

[52] Stephen, A.M. Phillips, G.O. and Williams, P.A. 2006. **Food Polysaccharides and Their Applications.** 2nd ed. New York: Taylor and francis, CRC Press.

[53] Tapia, M.S. Perez, E. Rodriguez, P.E. Guzman, R. Collin, M.N.D. Tran, T. and Rolland-Sabate, A. 2012. "Some Properties of Starch and Starch Edible Films from Under-Utilized Roots and Tubers from the Venezuelan Amazons." *Journal of Cellular Plastics*. 48 : 526–544.

[54] Obasi, H.C. Onuoha, F.N. Eze, I.O. Nwanonenyi, S.C. Arukalam I.O. and Uzoma, P.C. 2013. "Effect of Soil Burial on Properties of Polypropylene (PP)/Plasticized Potato Starch (PPS) Blends." *The International Journal of Engineering and Science.* 2 : 14–18.

[55] Zhang, L. Liu, P. Wang, Y. and Gao, W. 2012. "Study on Physico-Chemical Properties of Dialdehyde Yam Starch with Different Aldehyde Group Contents." *Thermochimica Acta.* 512(1-2) : 196–201.

Appendices

Appendix A

FT-IR study

FT-IR spectra of NS, various modified starch, NS film and various modified starch films

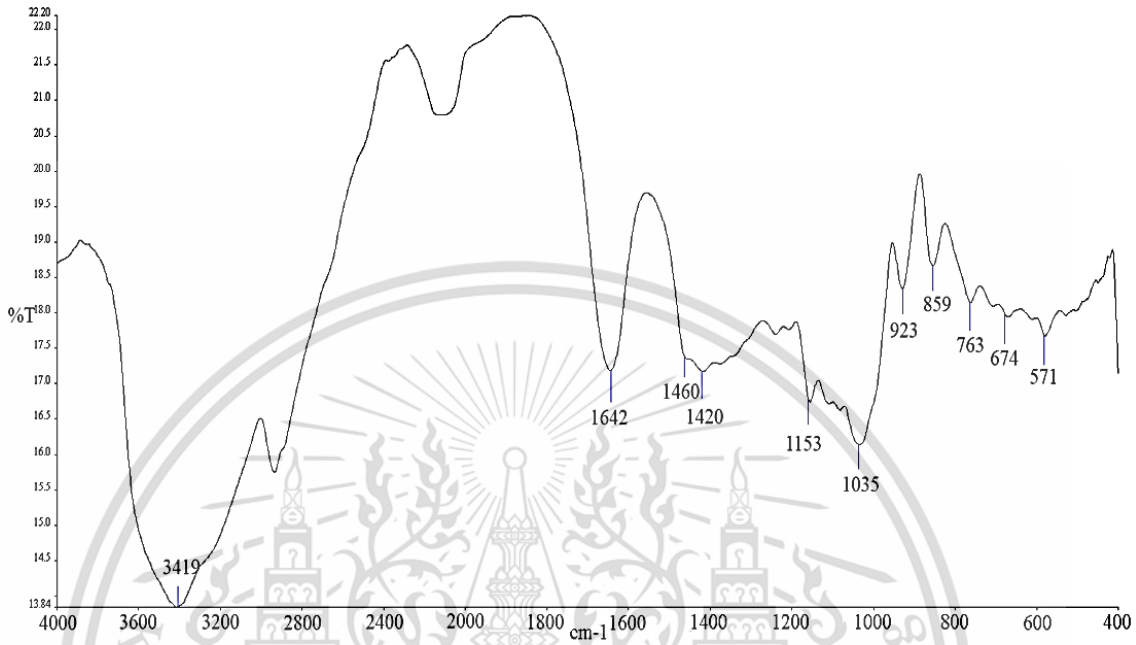

Figure A-1 FT-IR spectrum of NS

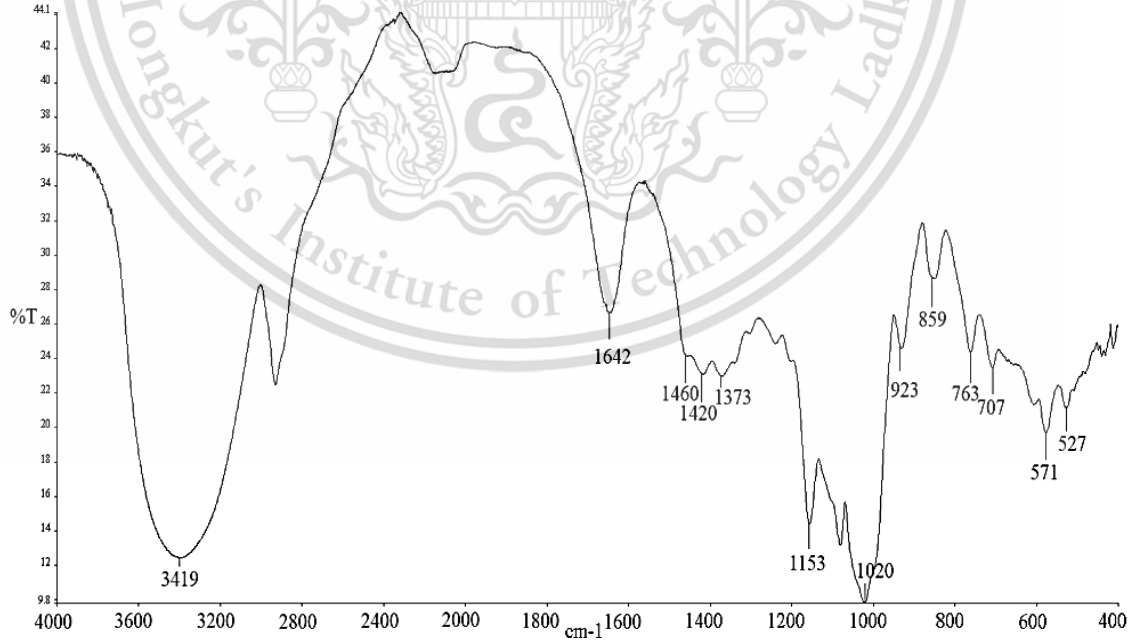

Figure A-2 FT-IR spectrum of CS-BO

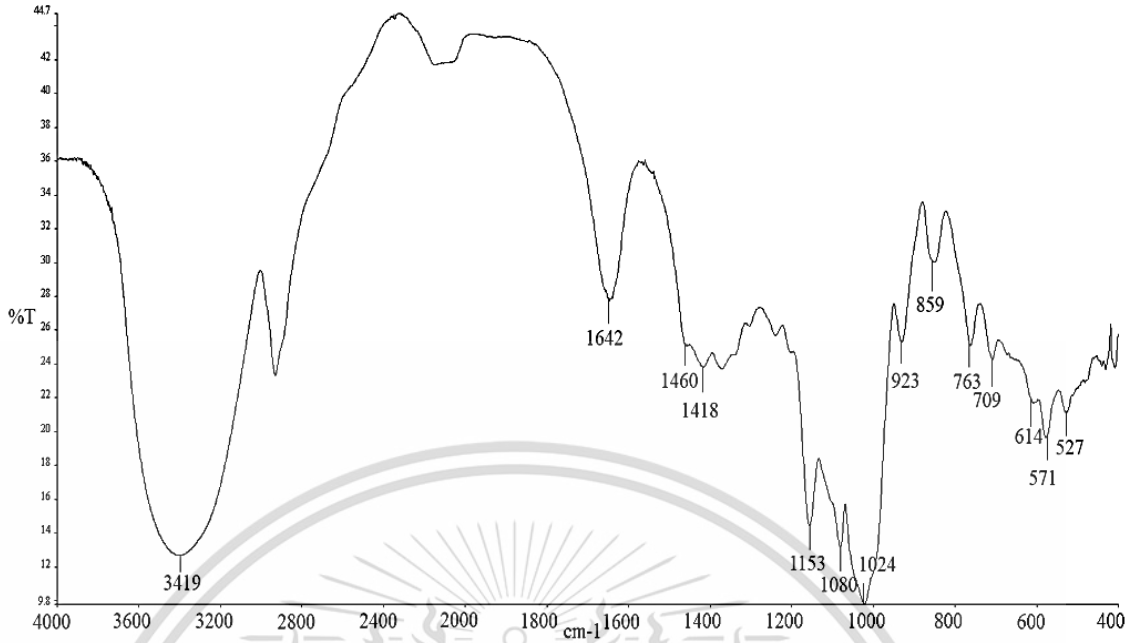

Figure A-3 FT-IR spectrum of CS-BA

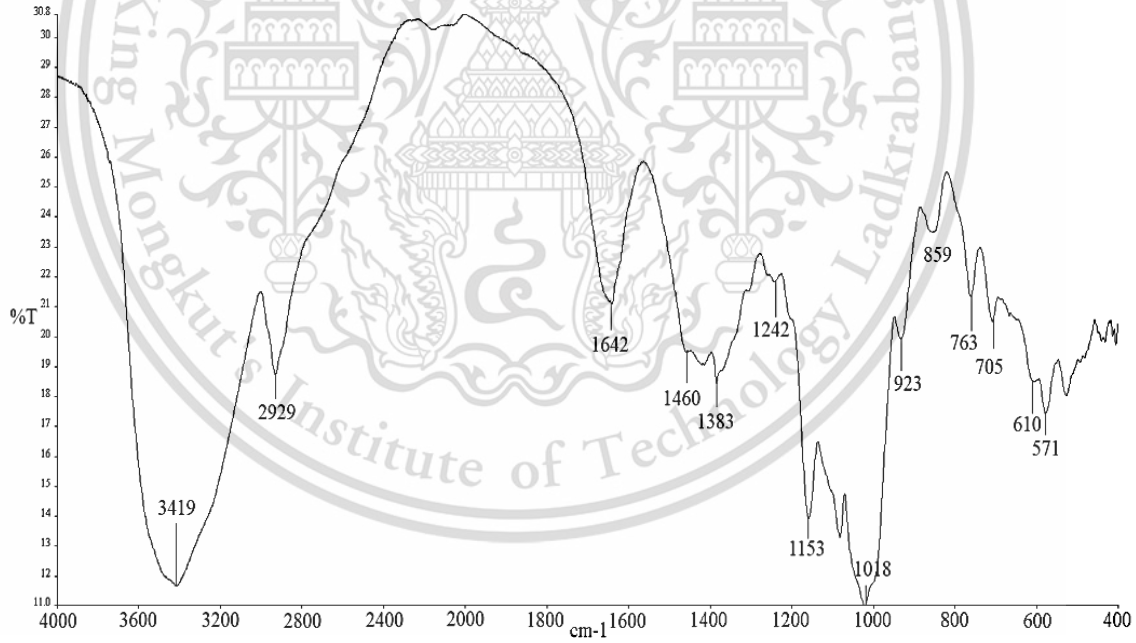

Figure A-4 FT-IR spectrum of CS-ST

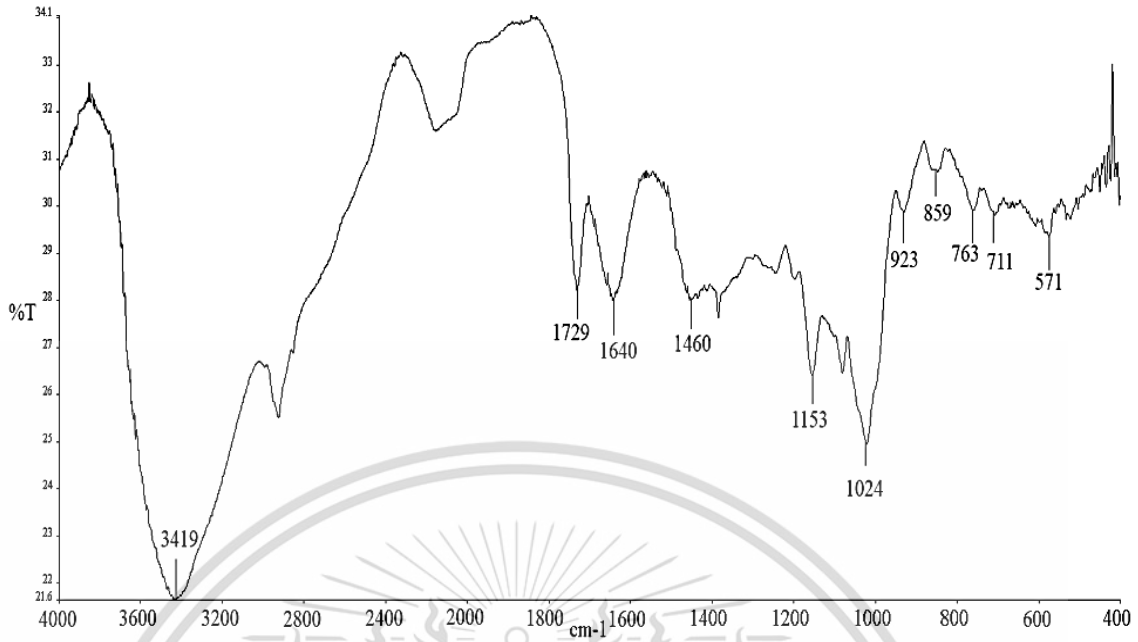

Figure A-5 FT-IR spectrum of OS

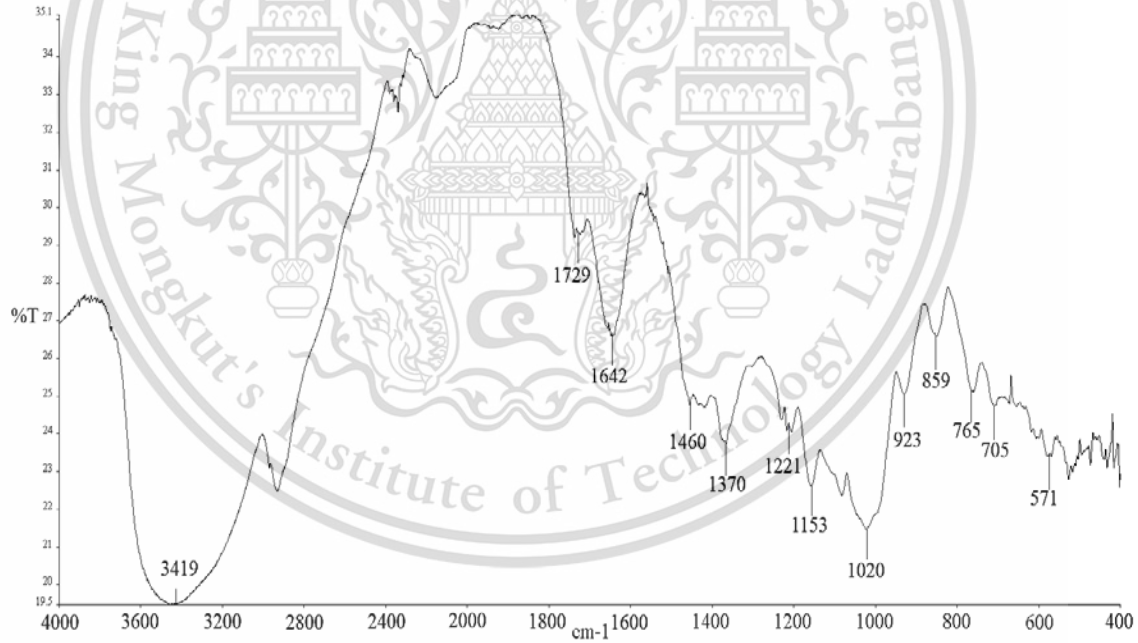

Figure A-6 FT-IR spectrum of COS-BO

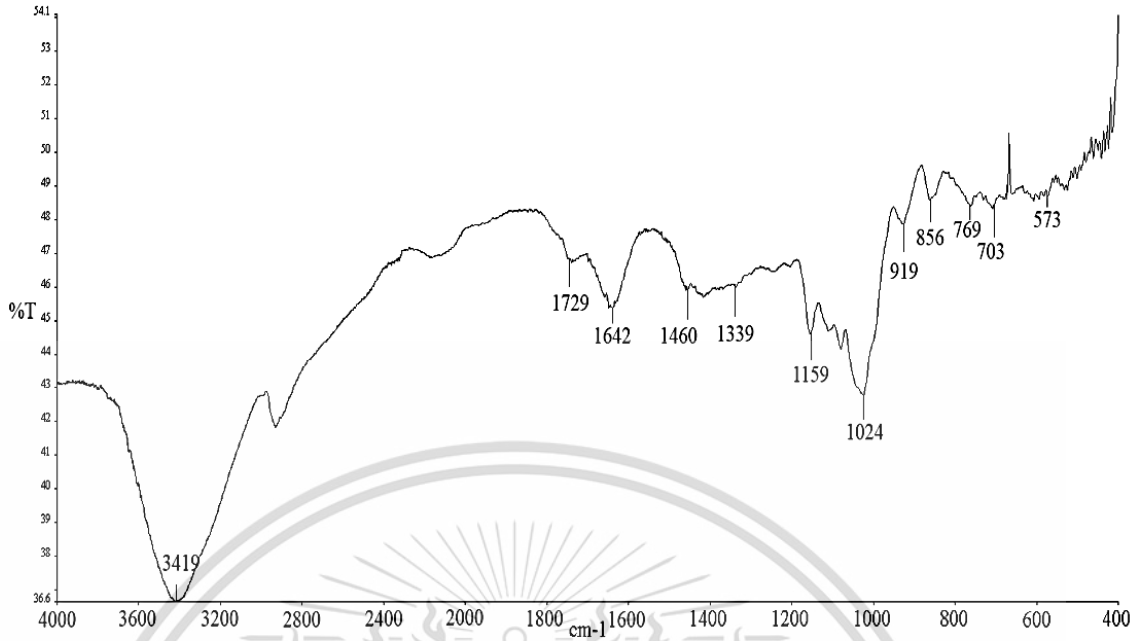

Figure A-7 FT-IR spectrum of COS-BA

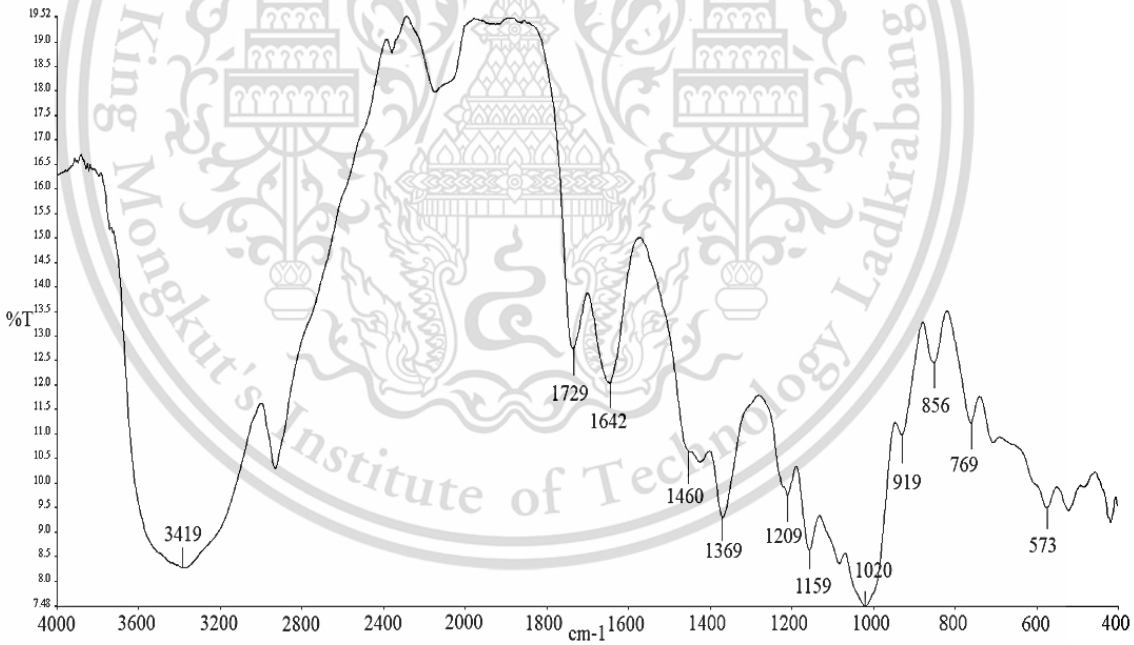

Figure A-8 FT-IR spectrum of COS-ST

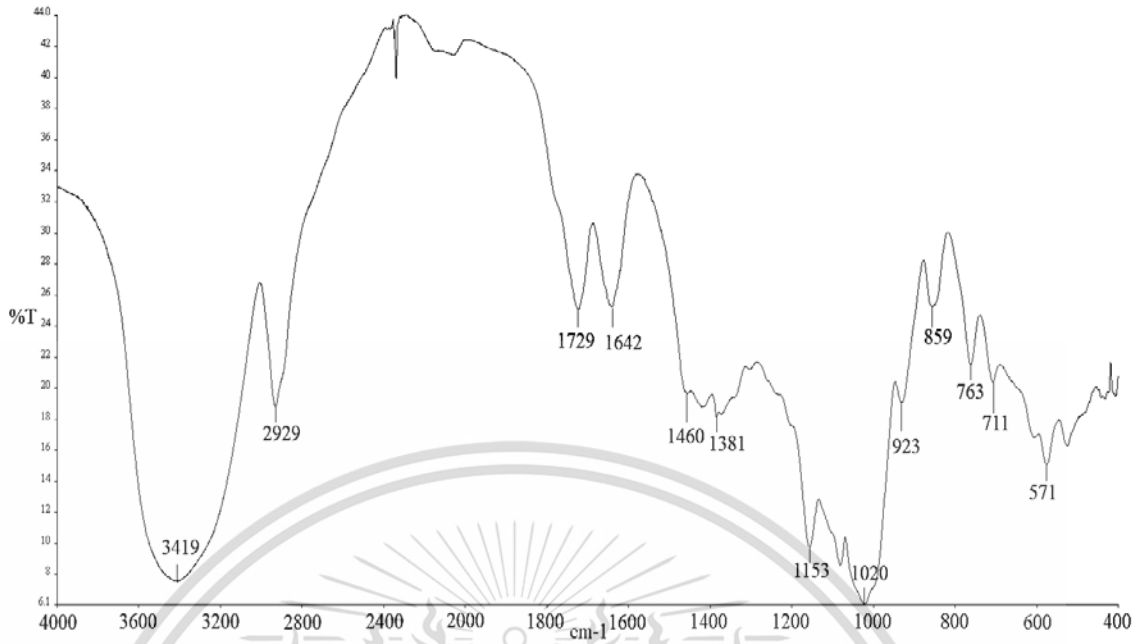

Figure A-9 FT-IR spectrum of OCS-BO

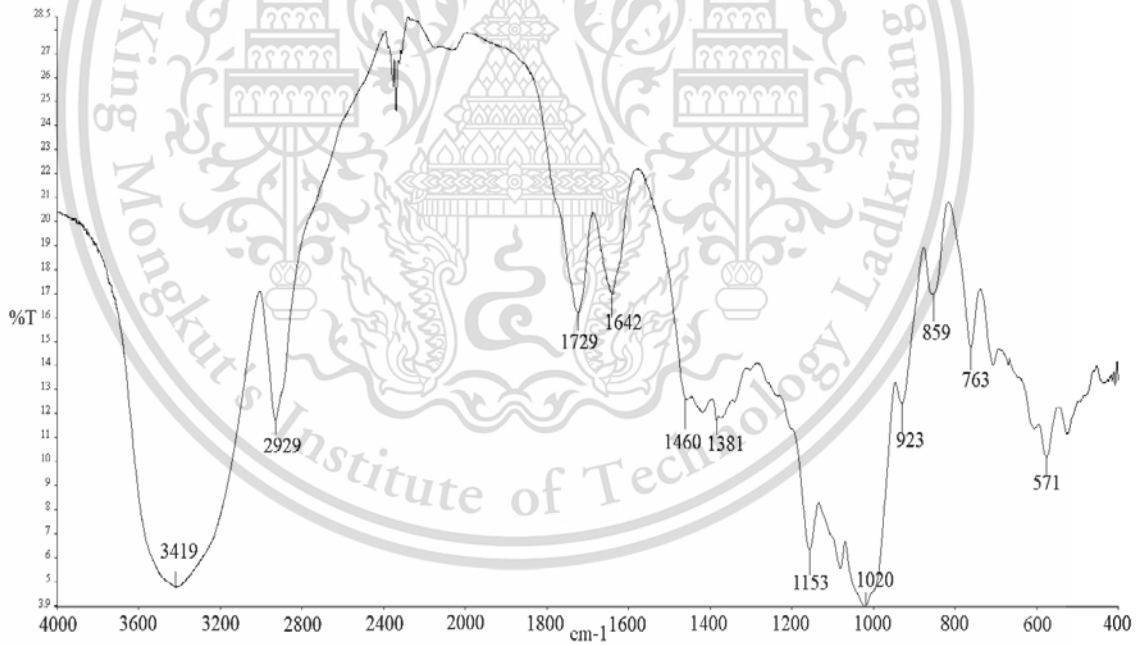

Figure A-10 FT-IR spectrum of OCS-BA

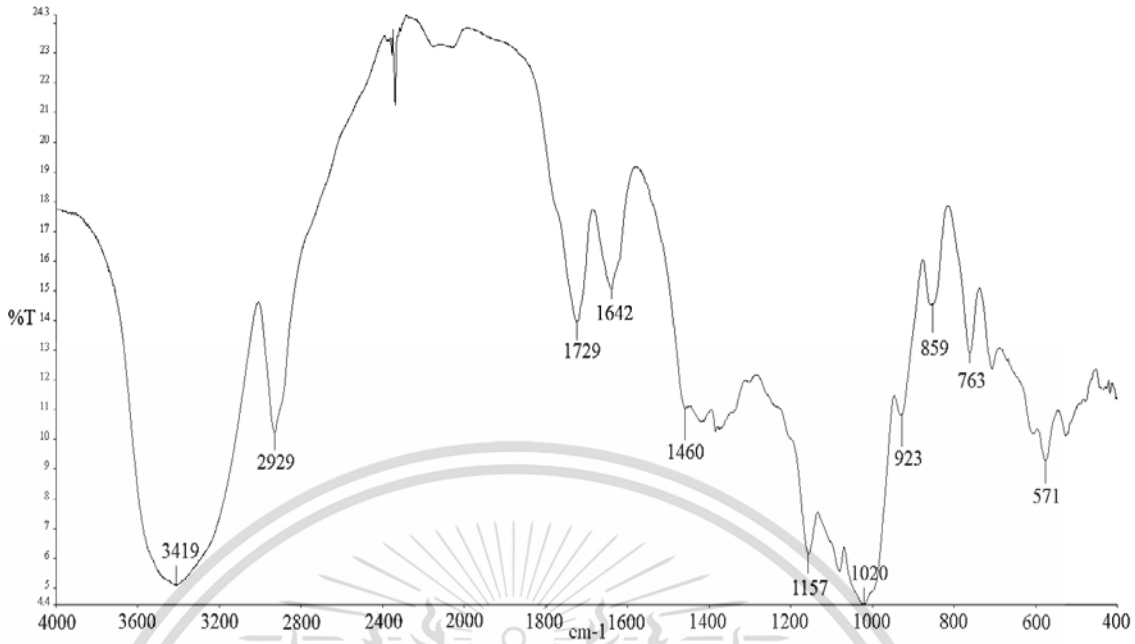

Figure A-11 FT-IR spectrum of OCS-ST

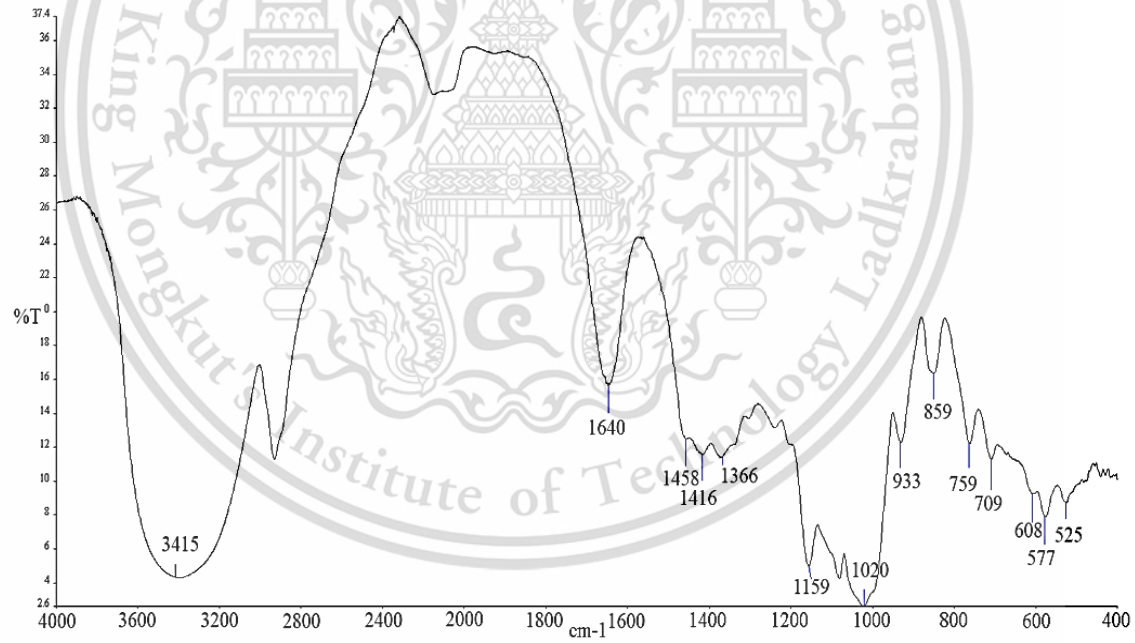

Figure A-12 FT-IR spectrum of NSF

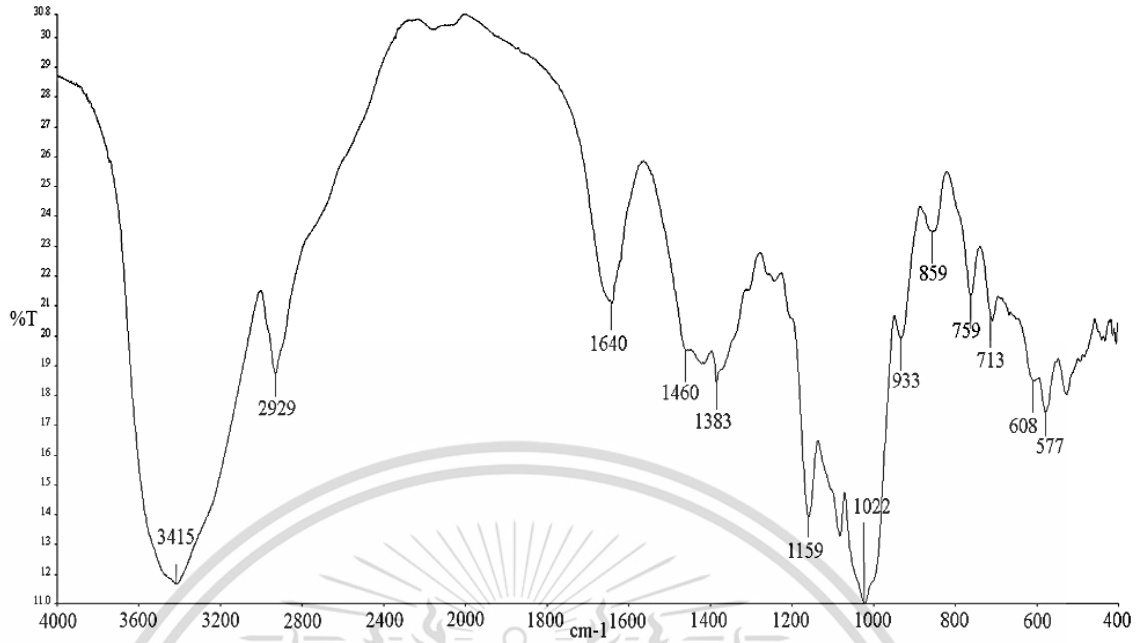

Figure A-13 FT-IR spectrum of CS-BOF

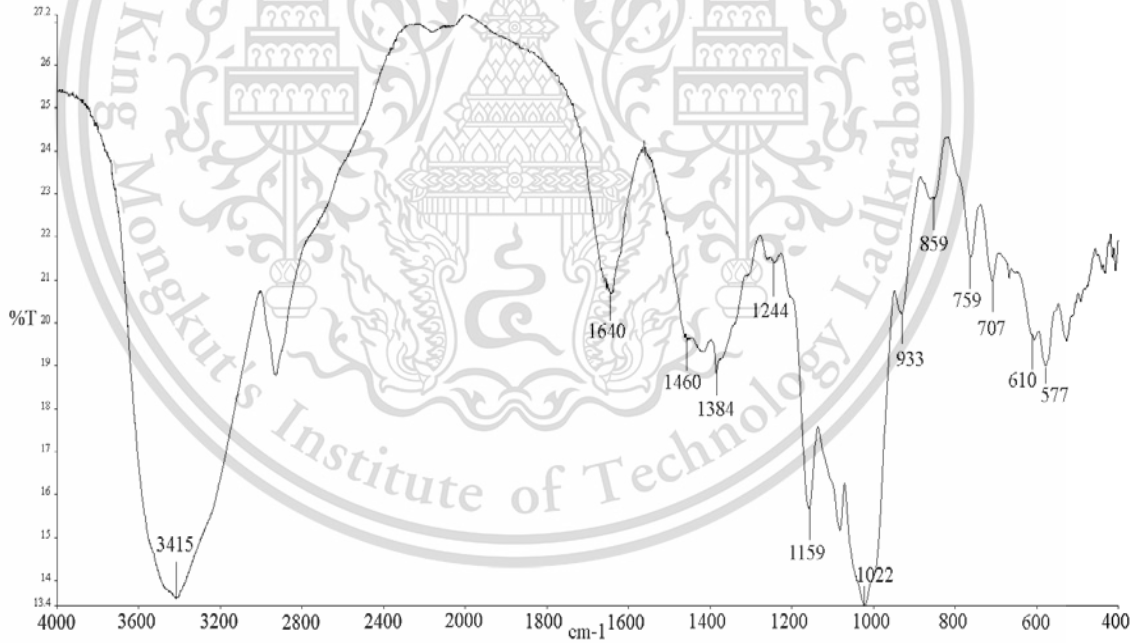

Figure A-14 FT-IR spectrum of CS-BAF

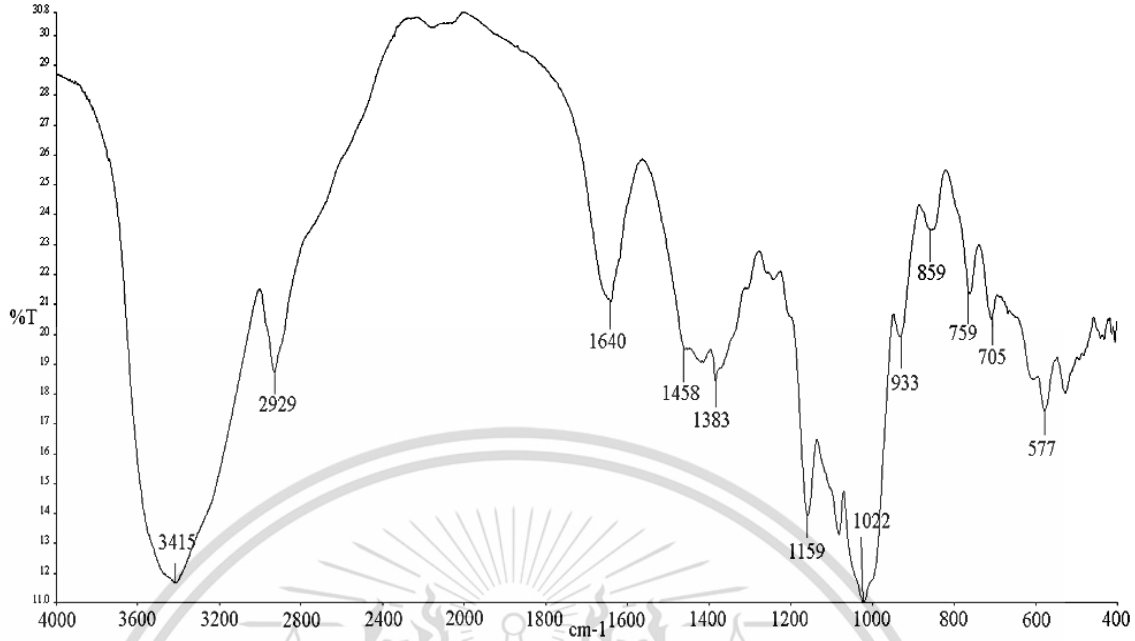

Figure A-15 FT-IR spectrum of CS-STF

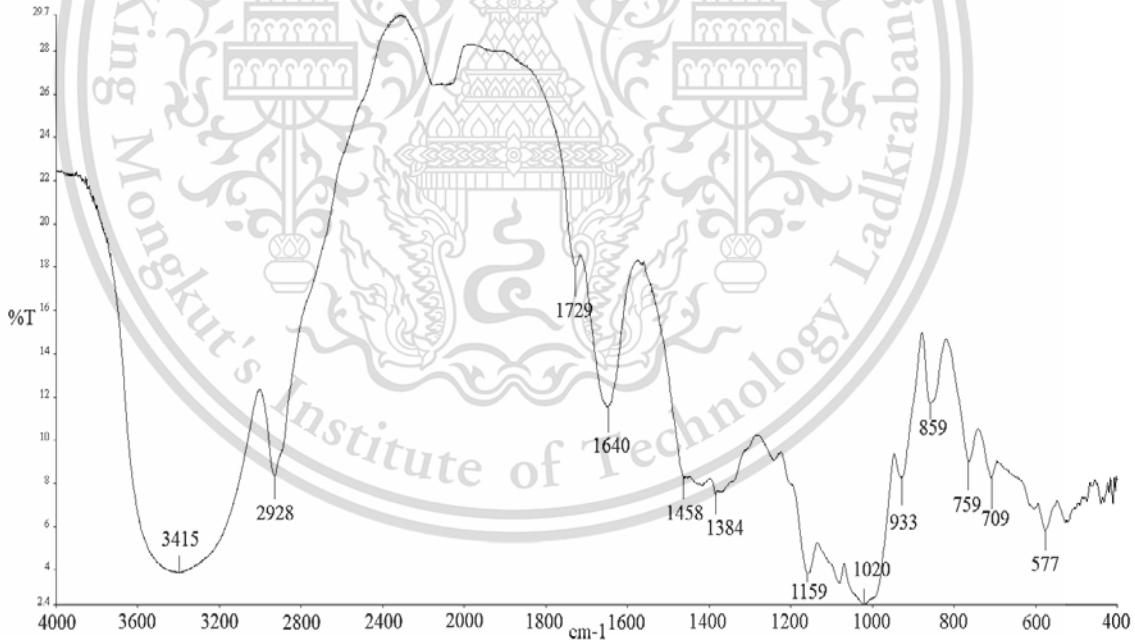

Figure A-16 FT-IR spectrum of OSF

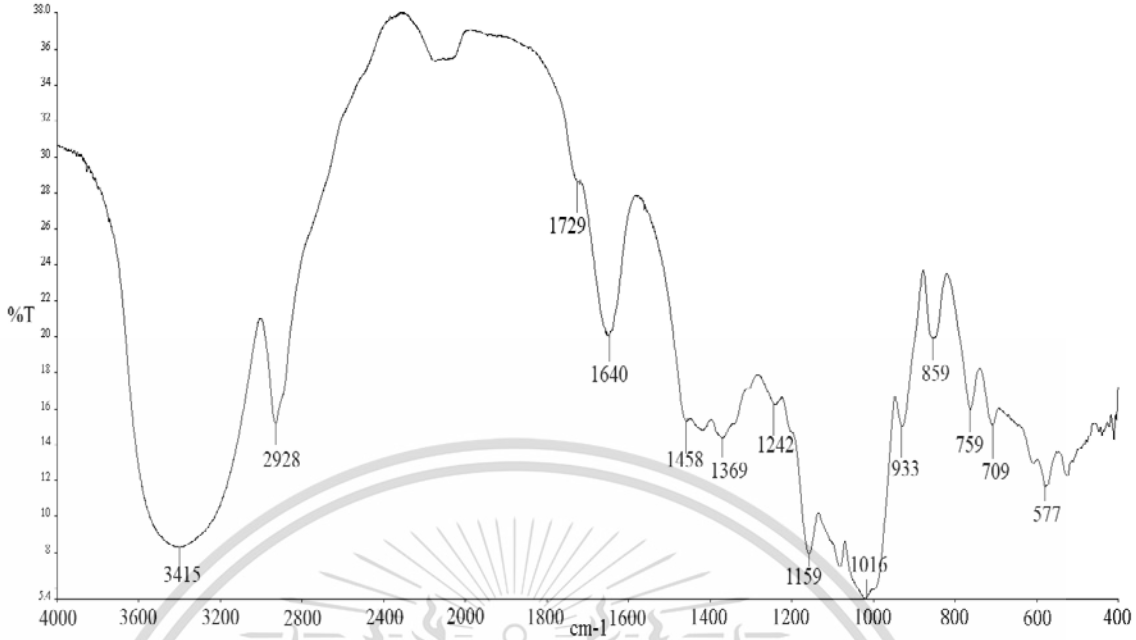

Figure A-17 FT-IR spectrum of COS-BOF

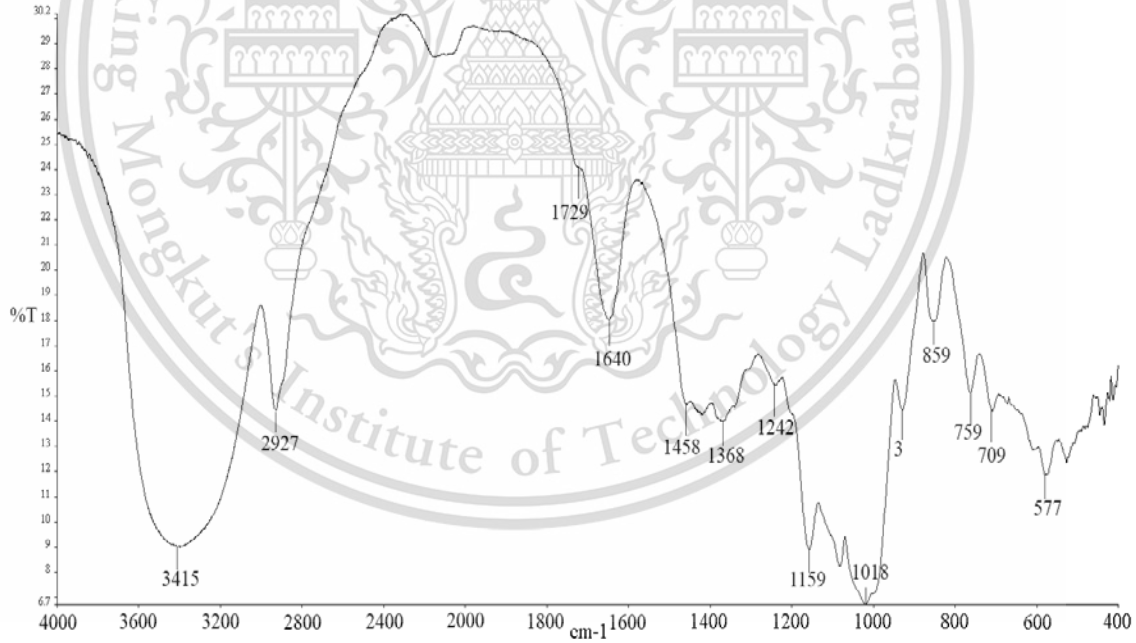

Figure A-18 FT-IR spectrum of COS-BAF

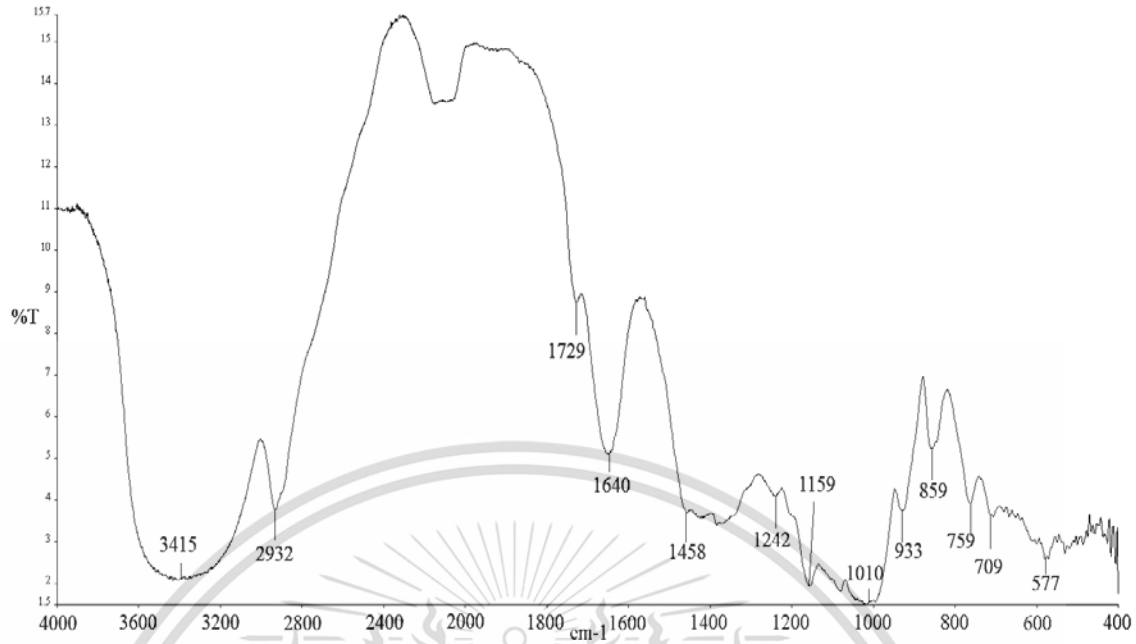

Figure A-19 FT-IR spectrum of COS-STF

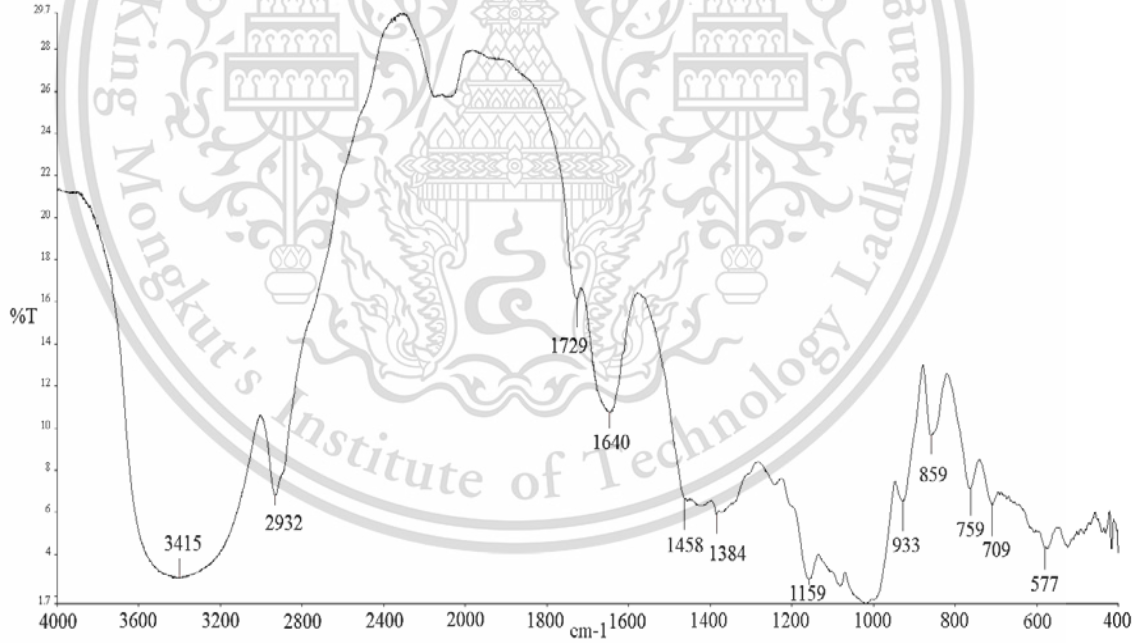

Figure A-20 FT-IR spectrum of OCS-BOF

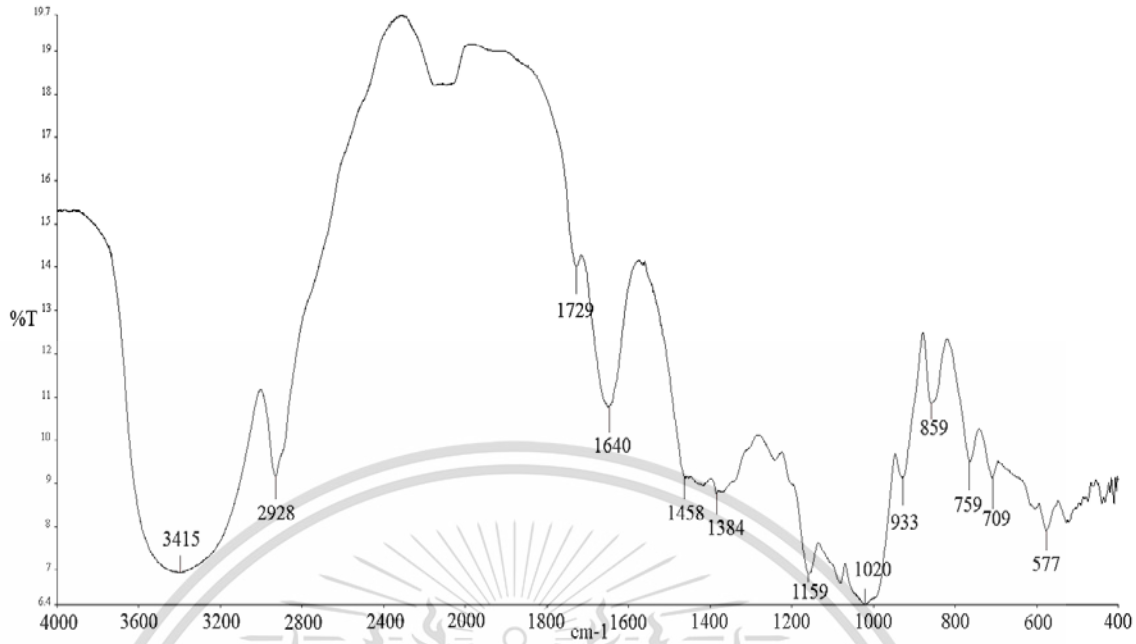

Figure A-21 FT-IR spectrum of OCS-BAF

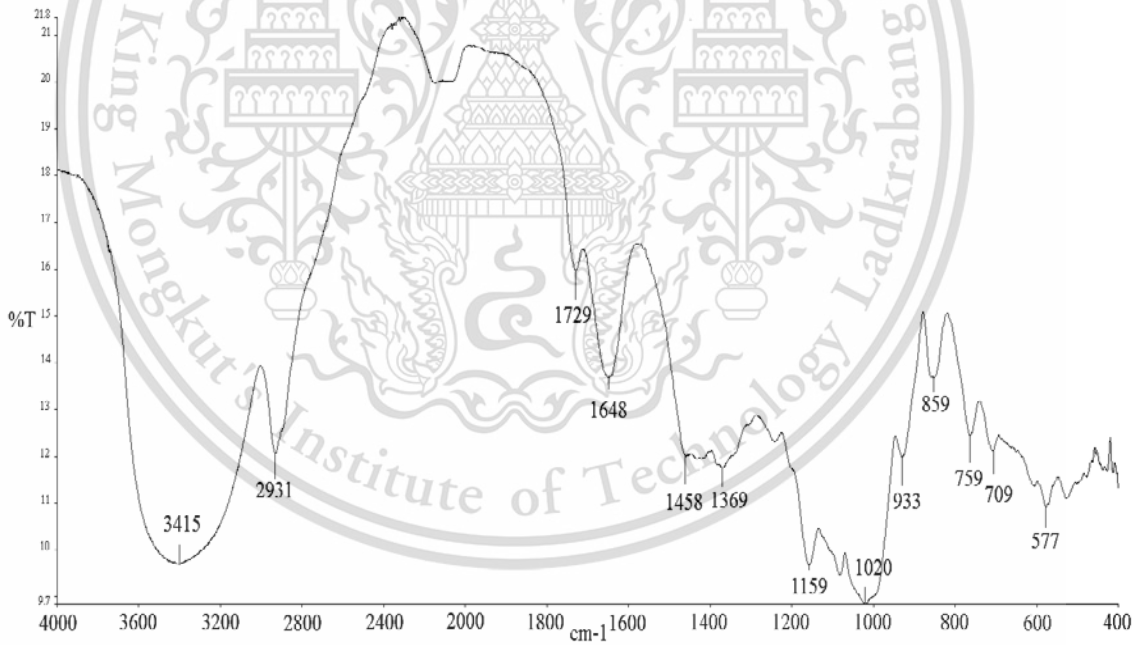

Figure A-22 FT-IR spectrum of OCS-STF

Appendix B

Thermal property by TGA technique

TGA thermograms of NS, various modified starch, NS film and various modified starch films

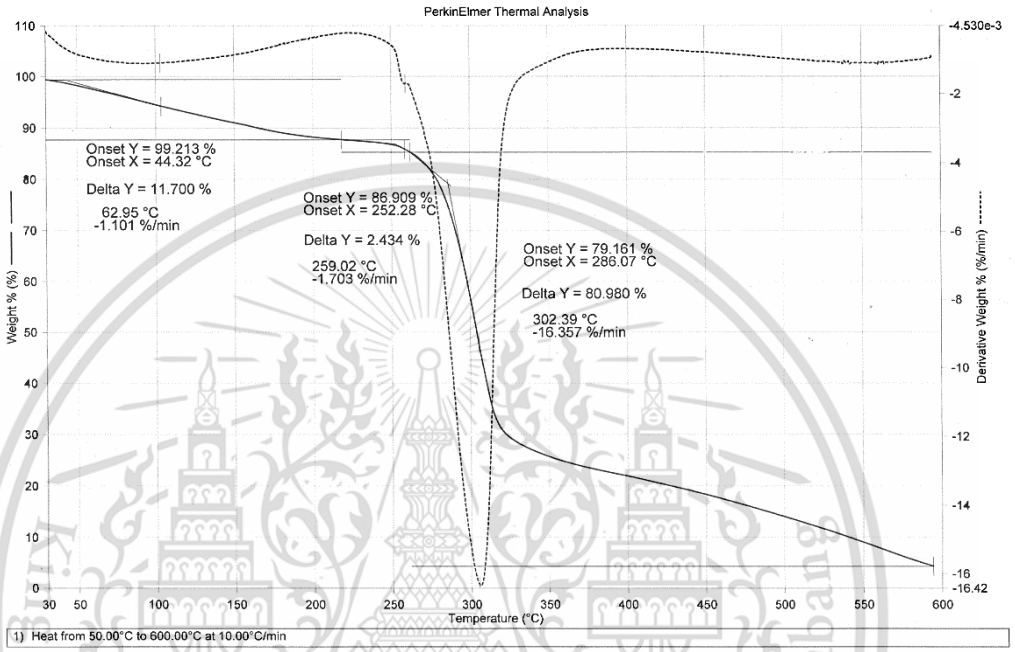

Figure B-1 TGA thermogram of NS

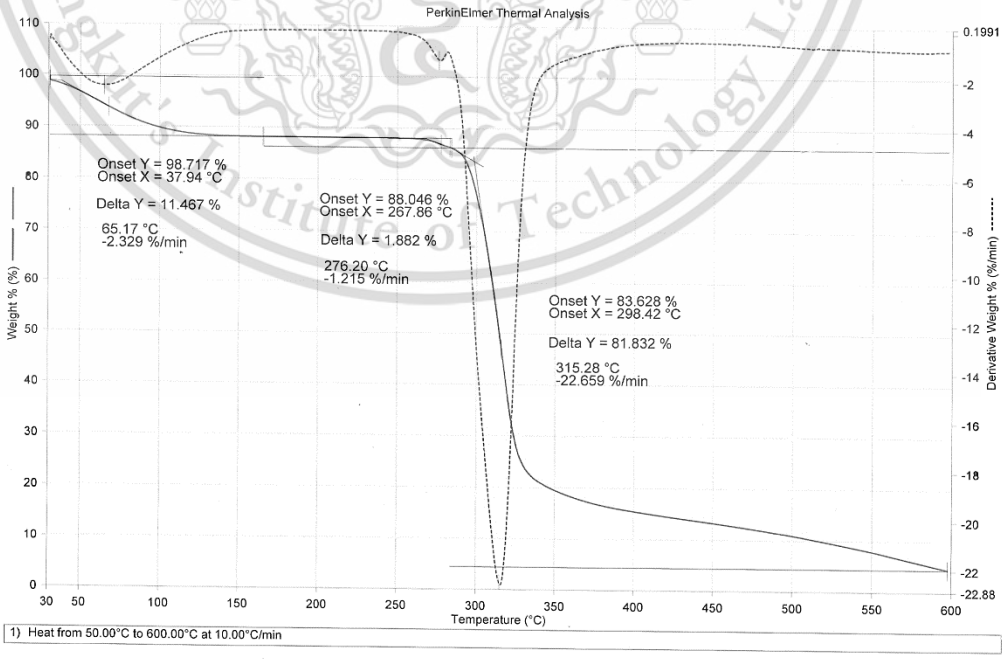

Figure B-2 TGA thermogram of CS-BO

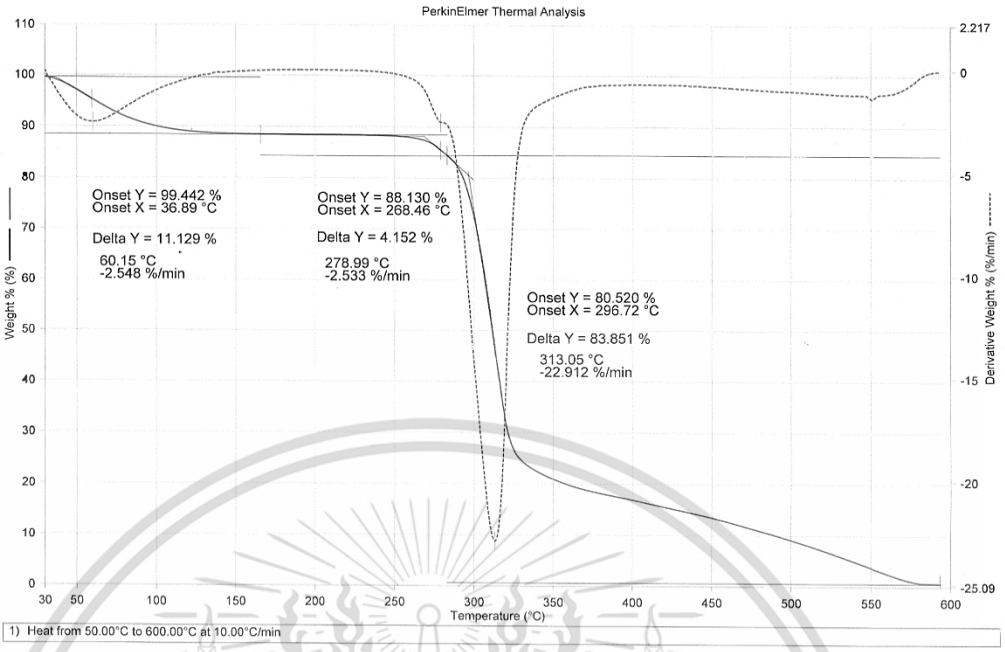

Figure B-3 TGA thermogram of CS-BA

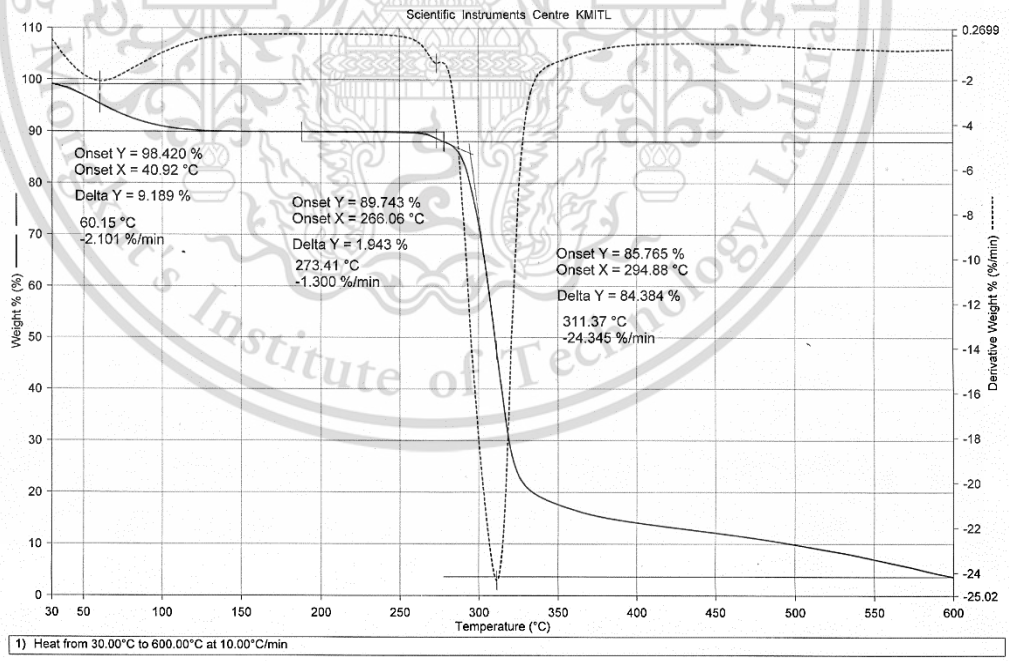

Figure B-4 TGA thermogram of CS-ST

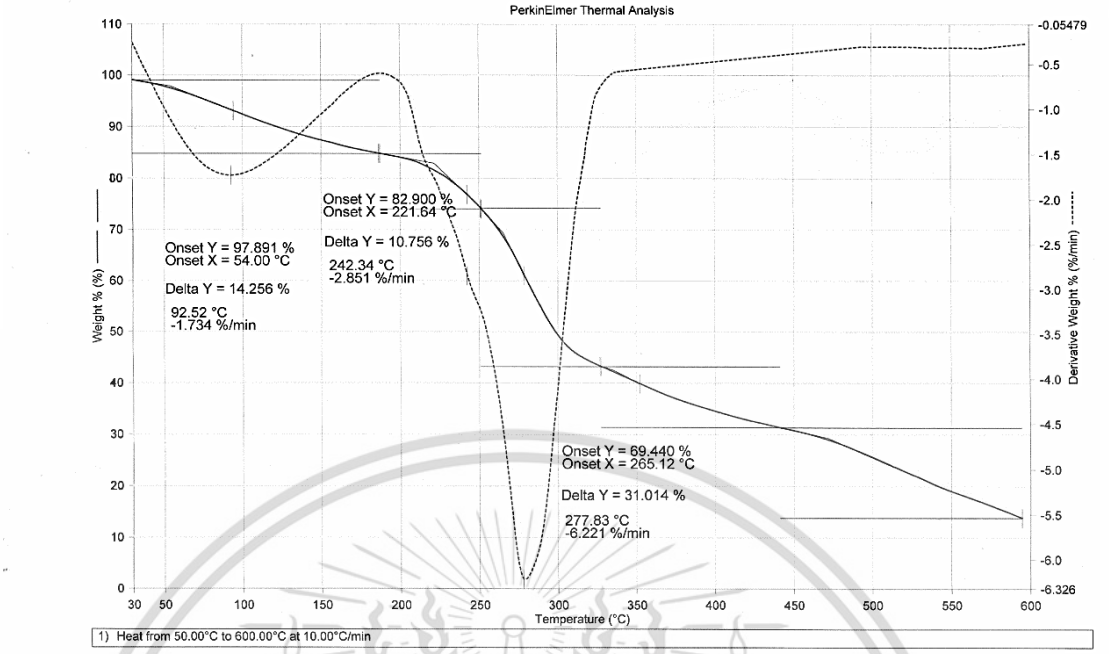

Figure B-5 TGA thermogram of OS

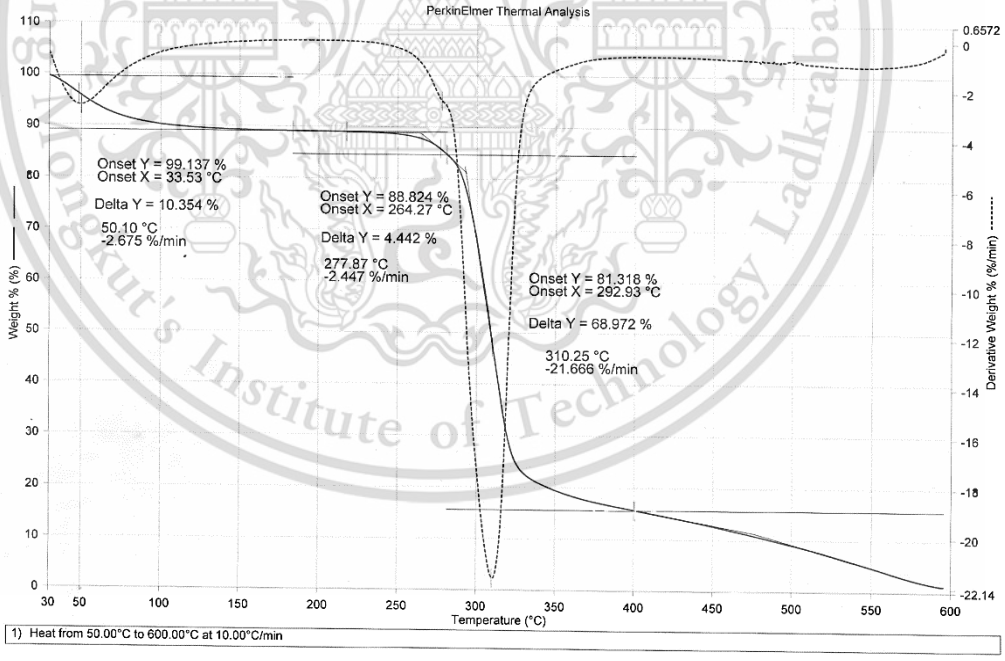

Figure B-6 TGA thermogram of COS-BO

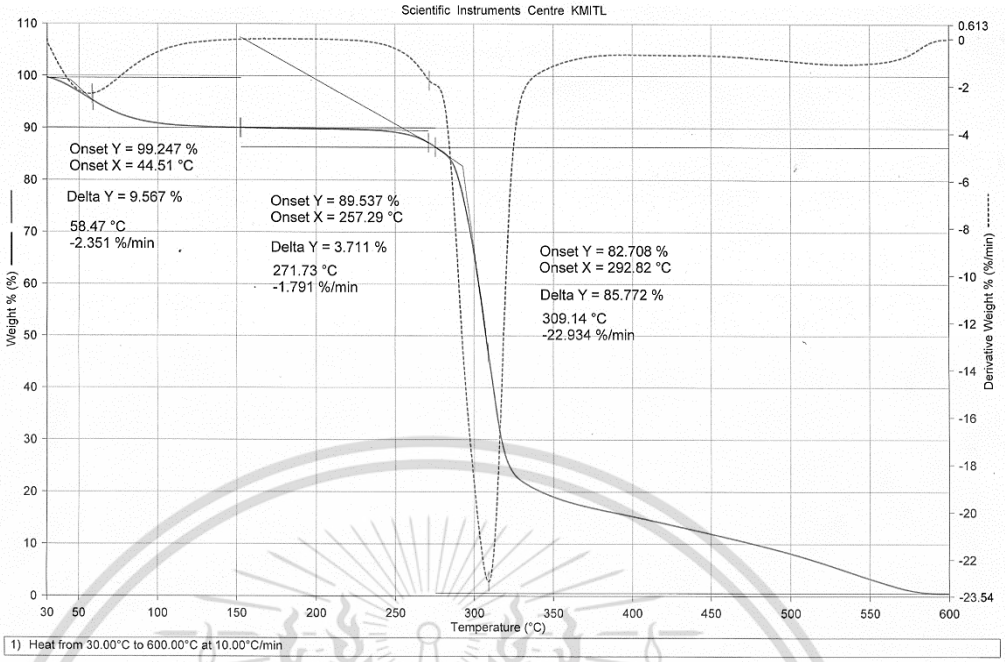

Figure B-7 TGA thermogram of COS-BA

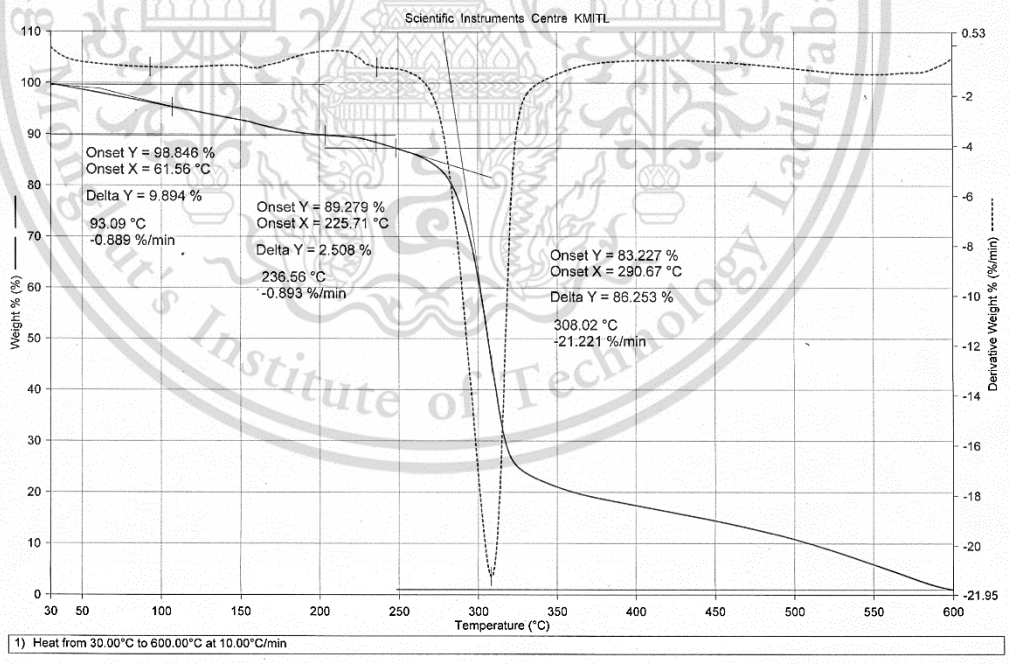

Figure B-8 TGA thermogram of COS-ST

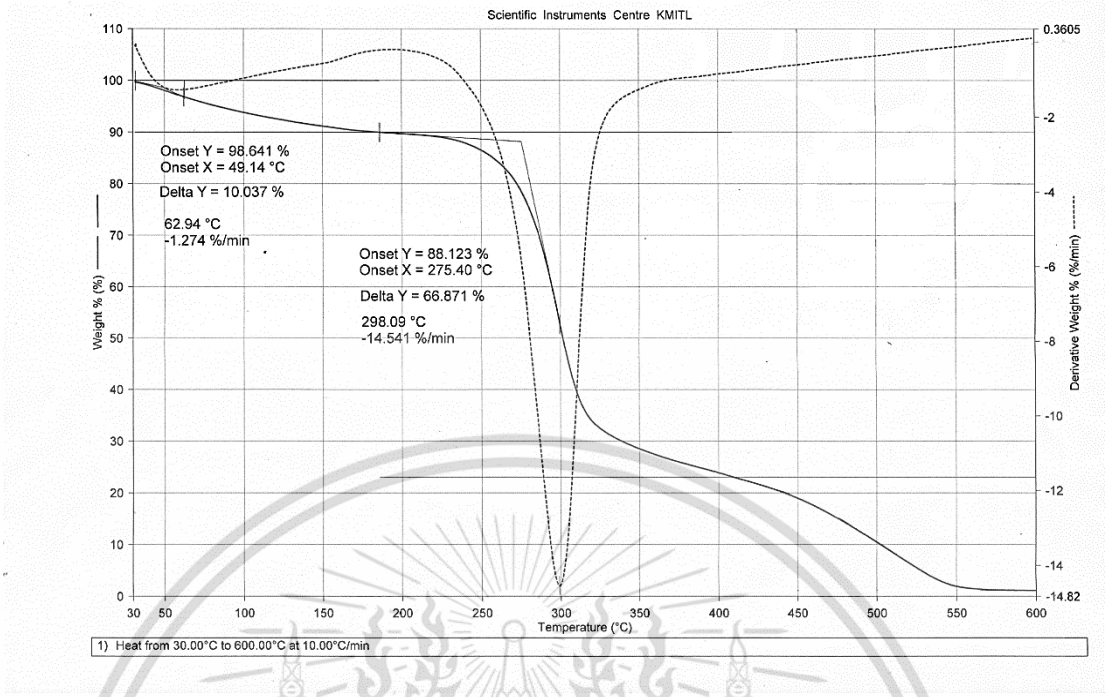

Figure B-9 TGA thermogram of OCS-BO

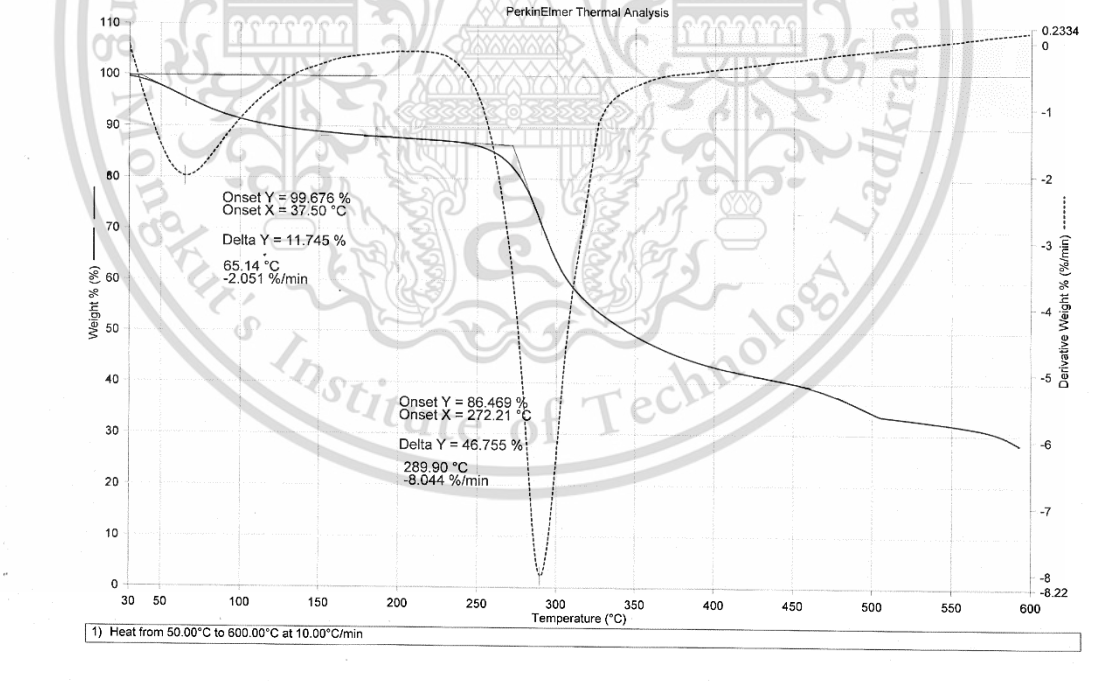

Figure B-10 TGA thermogram of OCS-BA

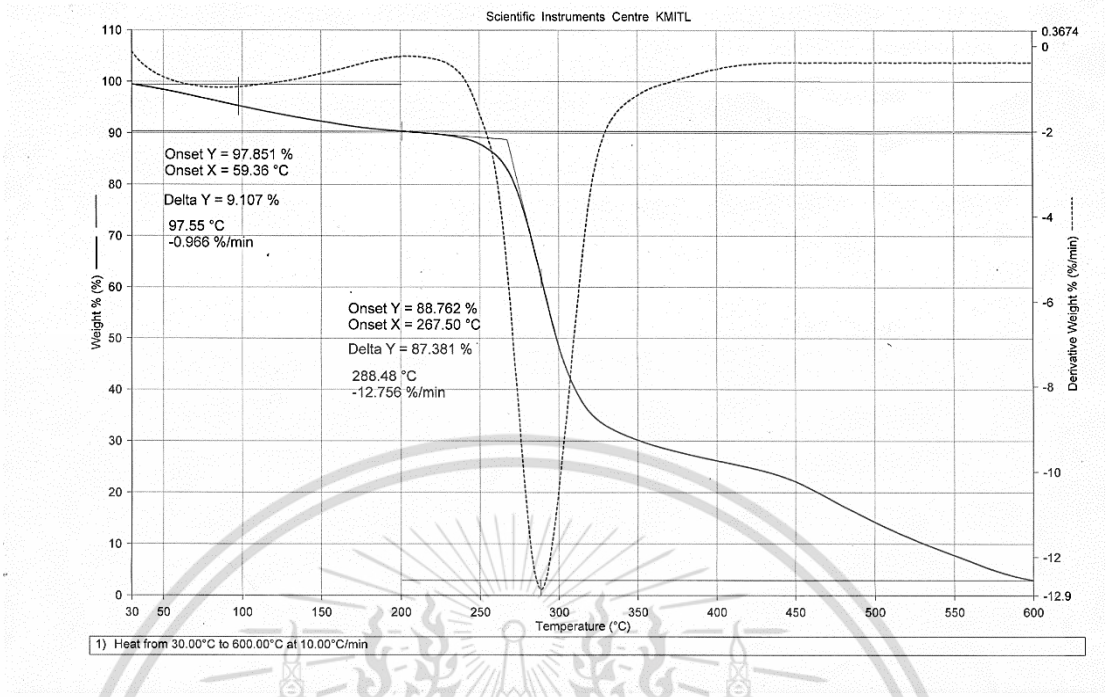

Figure B-11 TGA thermogram of OCS-ST

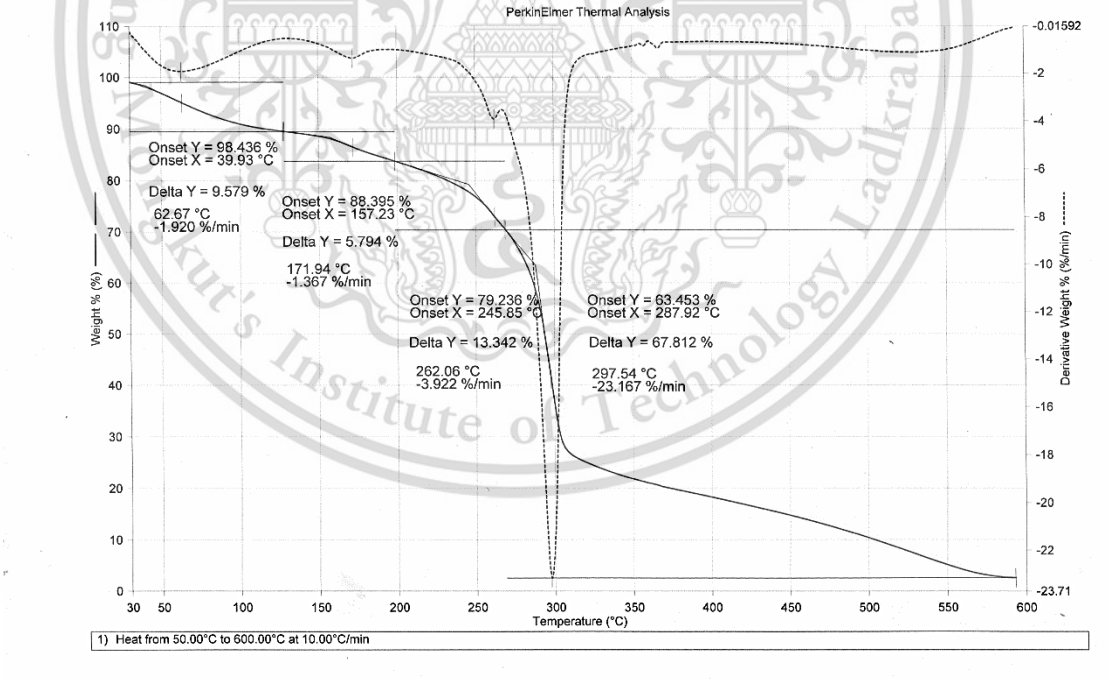

Figure B-12 TGA thermogram of NSF

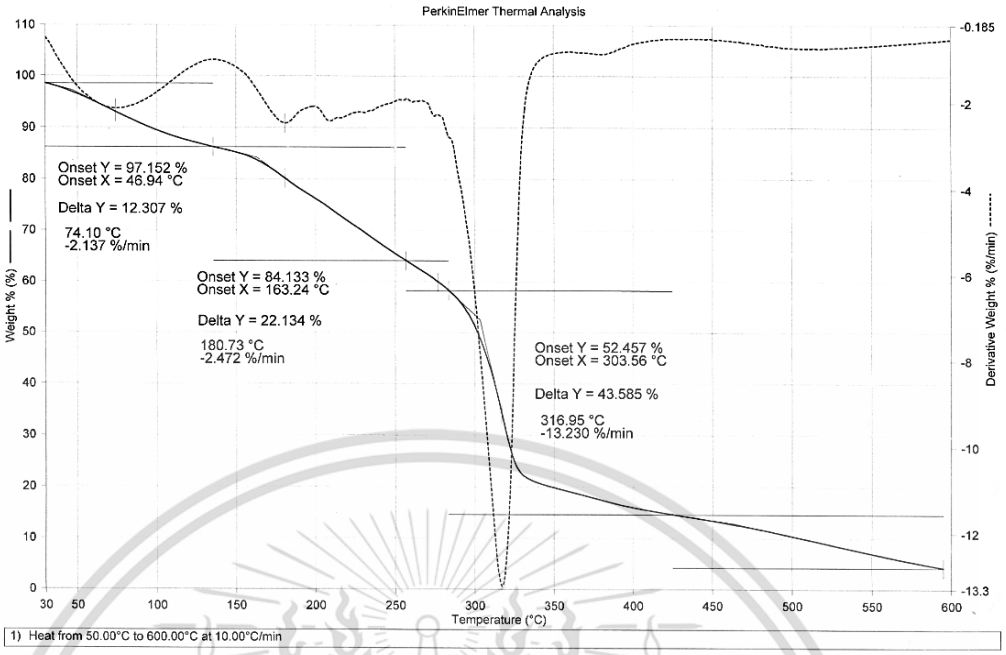

Figure B-13 TGA thermogram of CS-BOF

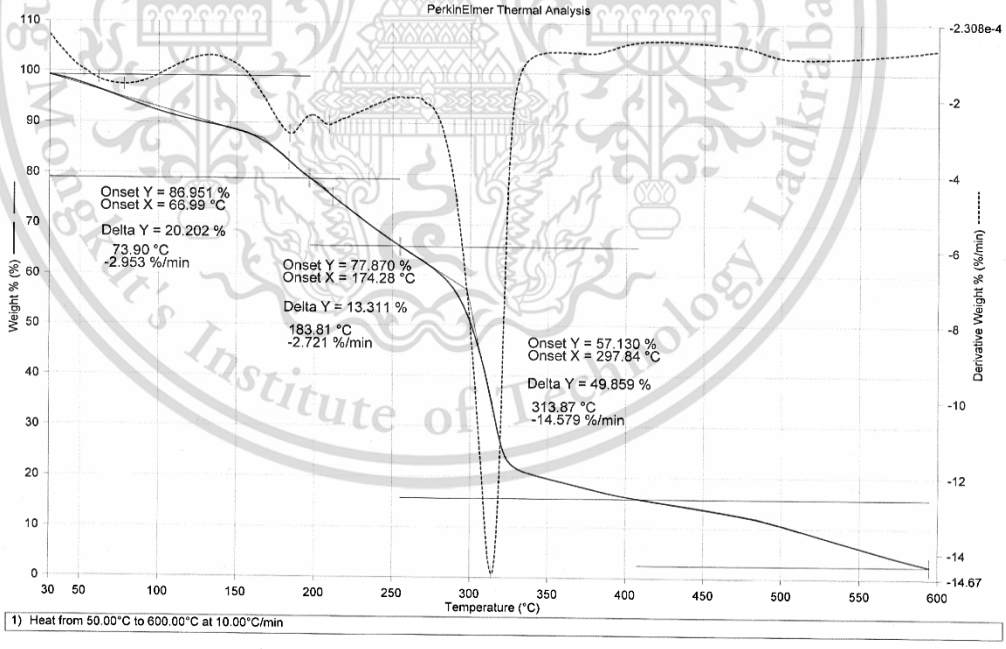

Figure B-14 TGA thermogram of CS-BAF

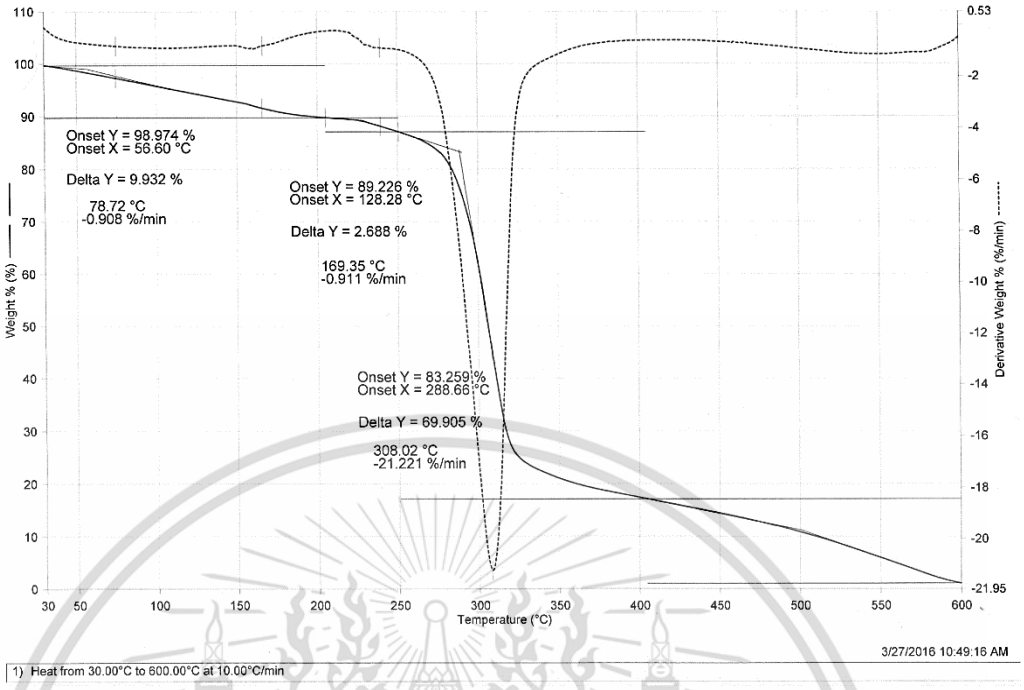

Figure B-15 TGA thermogram of CS-STF

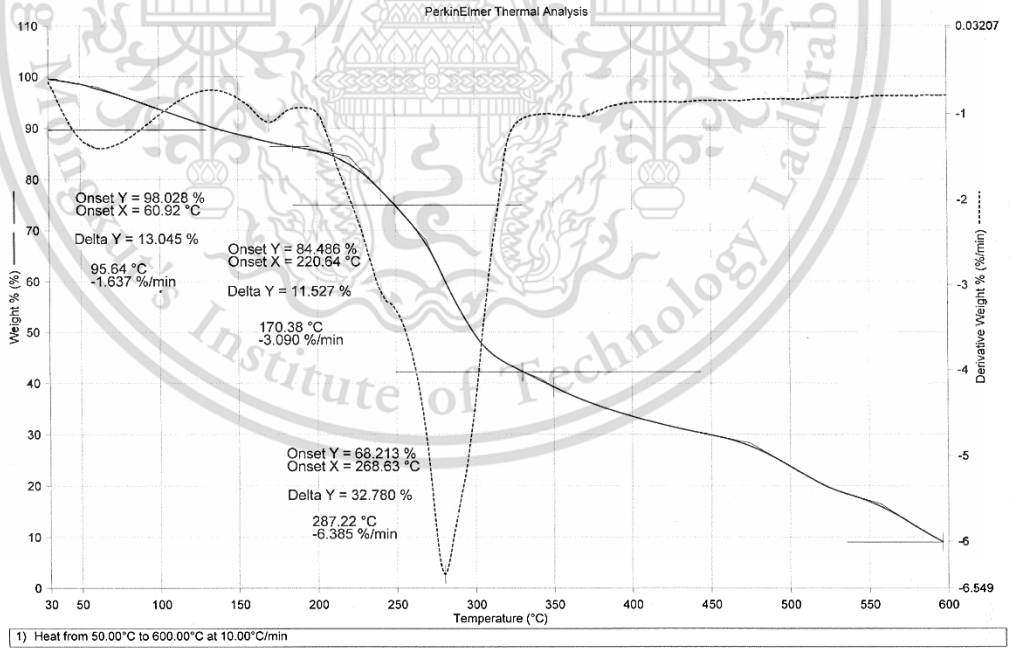

Figure B-16 TGA thermogram of OSF

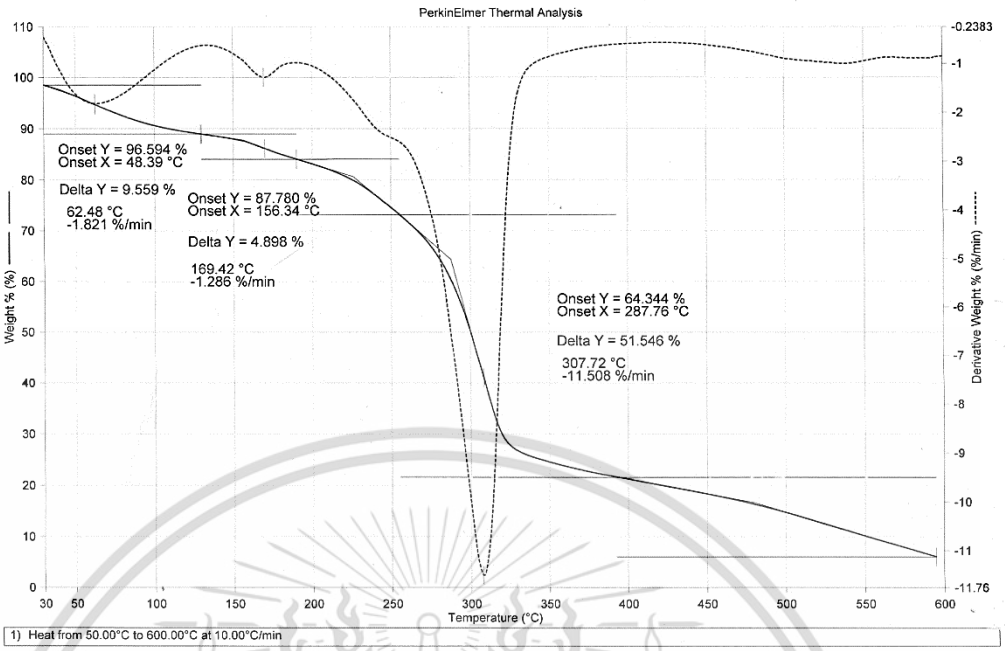

Figure B-17 TGA thermogram of COS-BOF

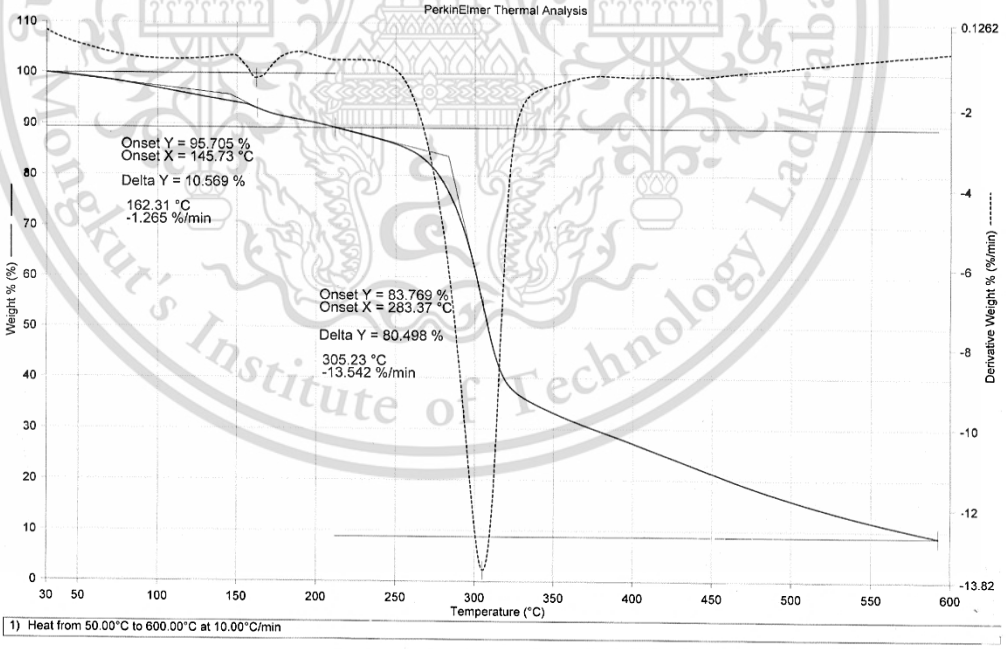

Figure B-18 TGA thermogram of COS-BAF

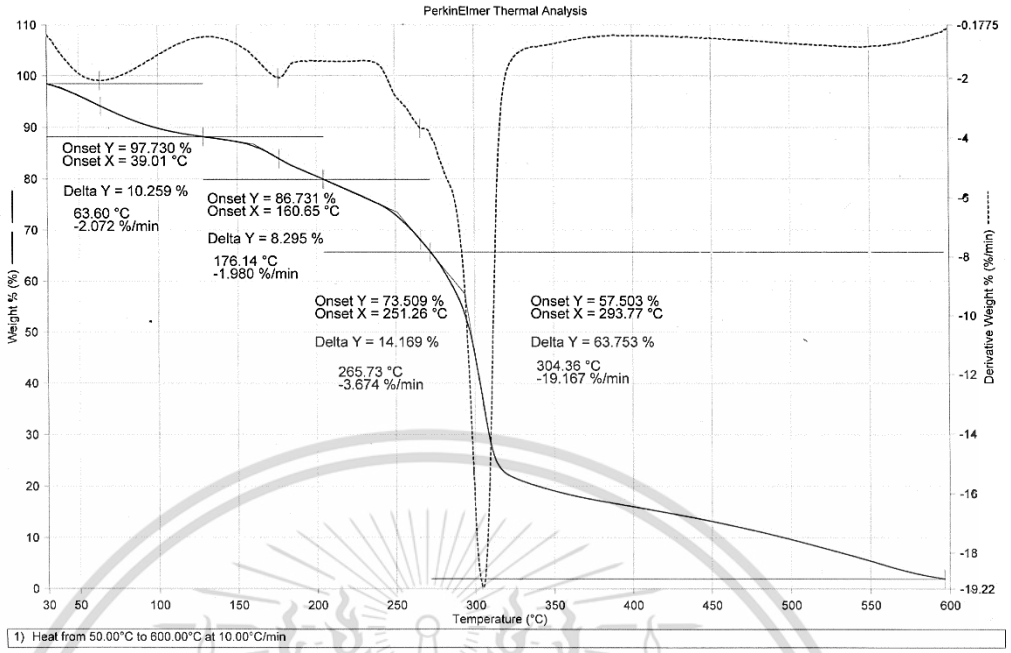

Figure B-19 TGA thermogram of COS-STF

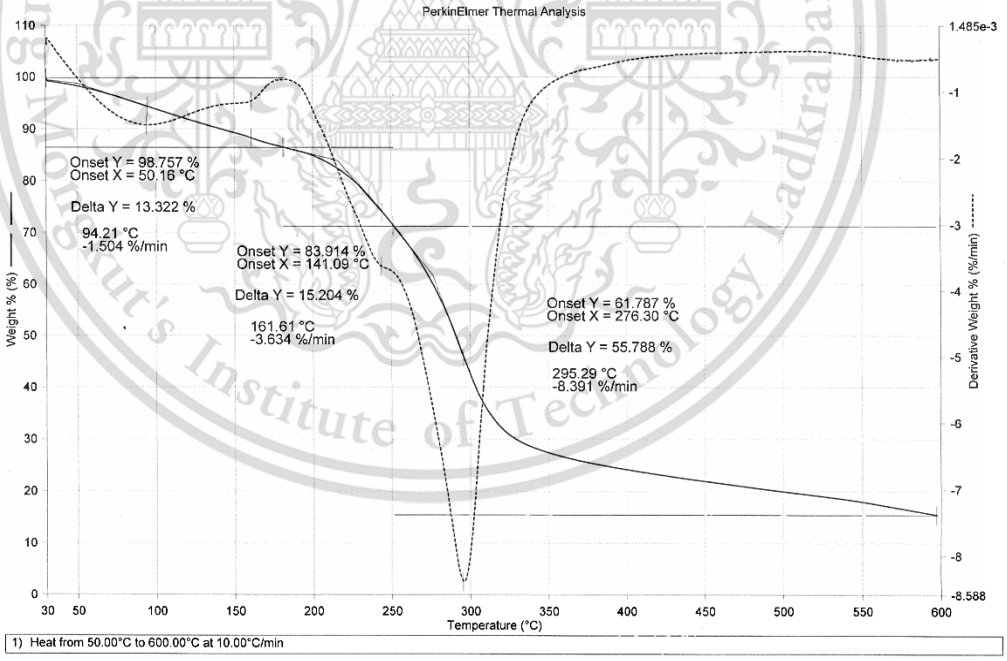

Figure B-20 TGA thermogram of OCS-BOF

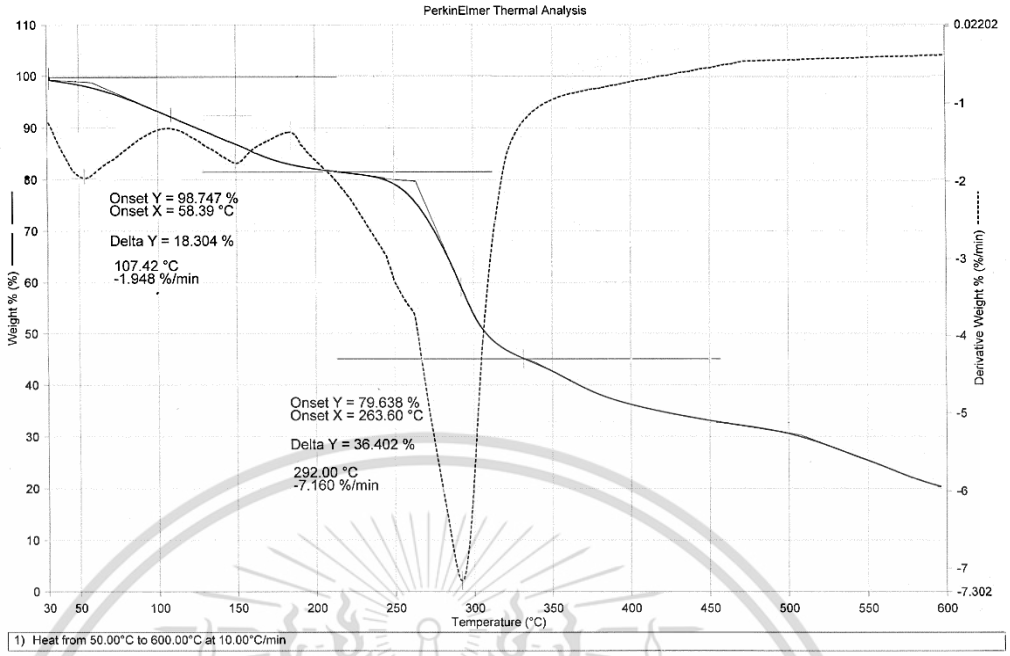

Figure B-21 TGA thermogram of OCS-BAF

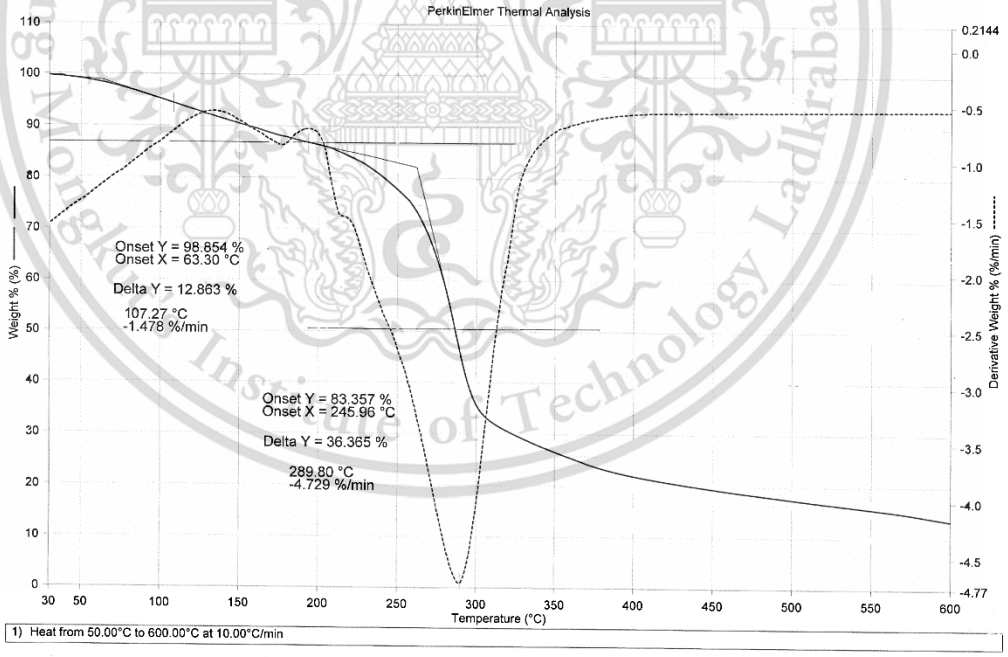

Figure B-22 TGA thermogram of OCS-STF

Appendix C

X-ray diffraction (XRD) study

X-ray diffractograms of NS film and various modified starch films

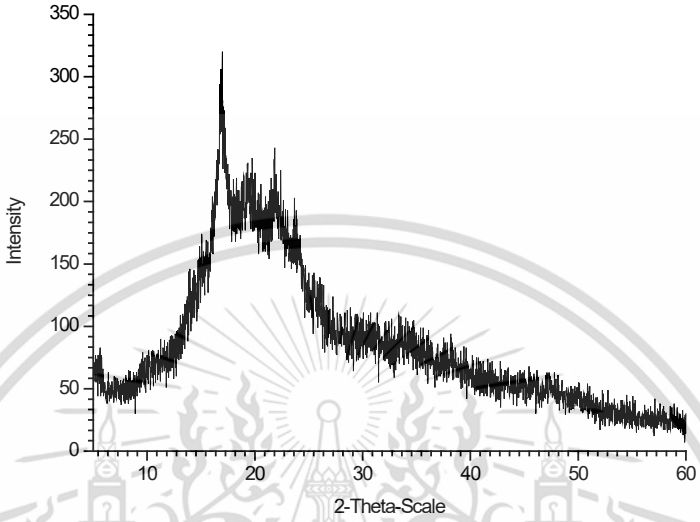

Figure C-1 X-ray diffractogram of NSF

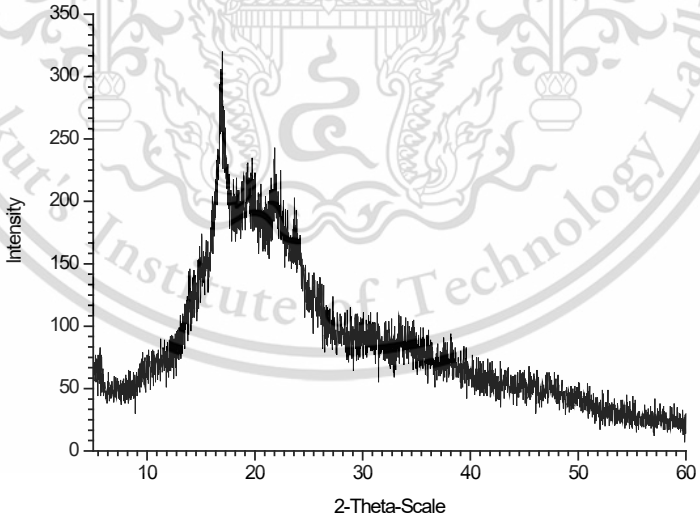

Figure C-2 X-ray diffractogram of CS-BOF

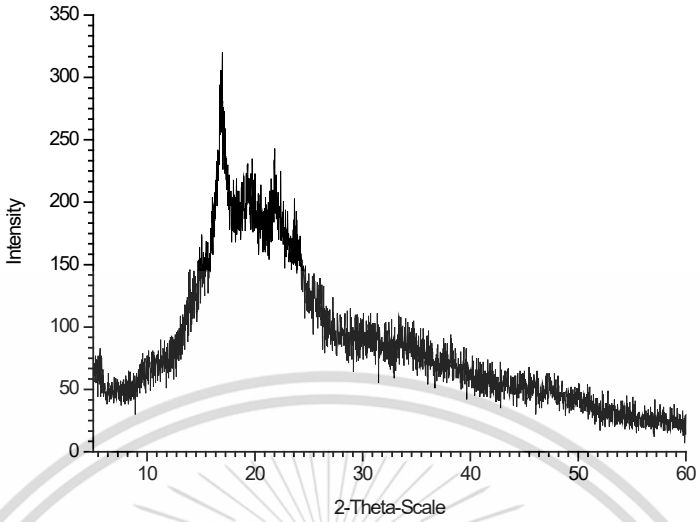

Figure C-3 X-ray diffractogram of CS-BAF

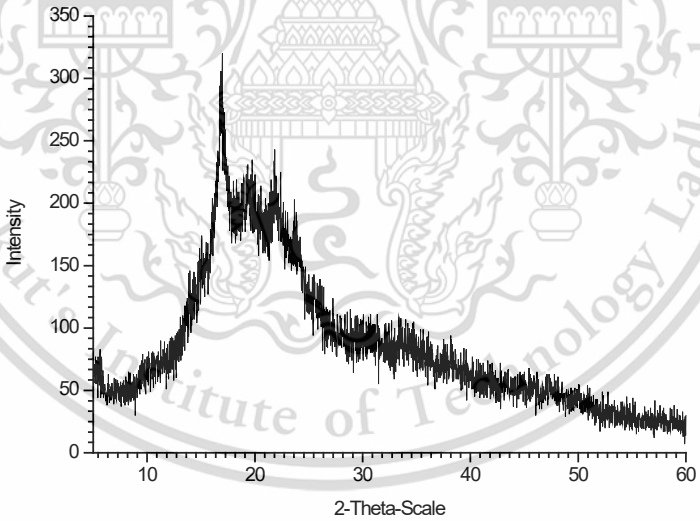

Figure C-4 X-ray diffractogram of CS-STF

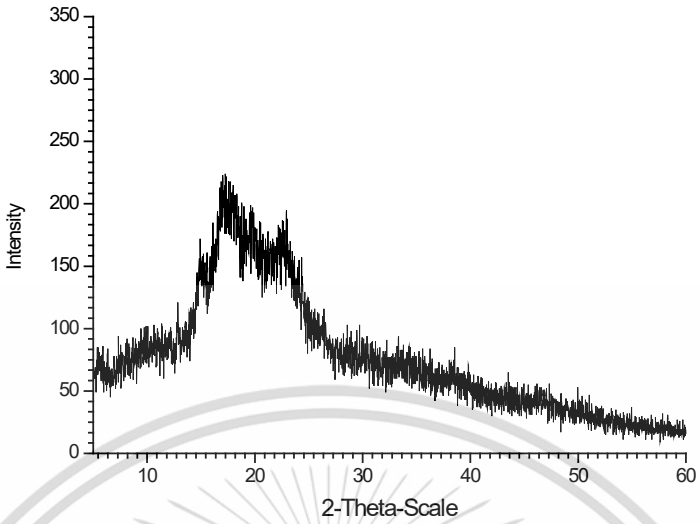

Figure C-5 X-ray diffractogram of OSF

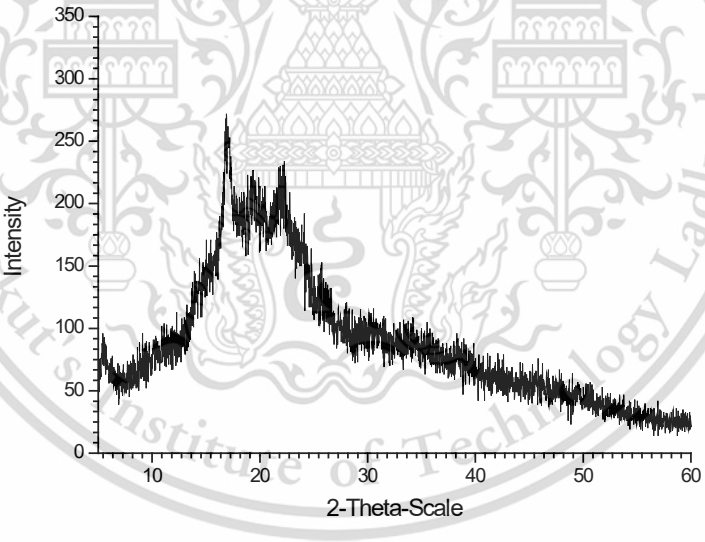

Figure C-6 X-ray diffractogram of COS-BOF

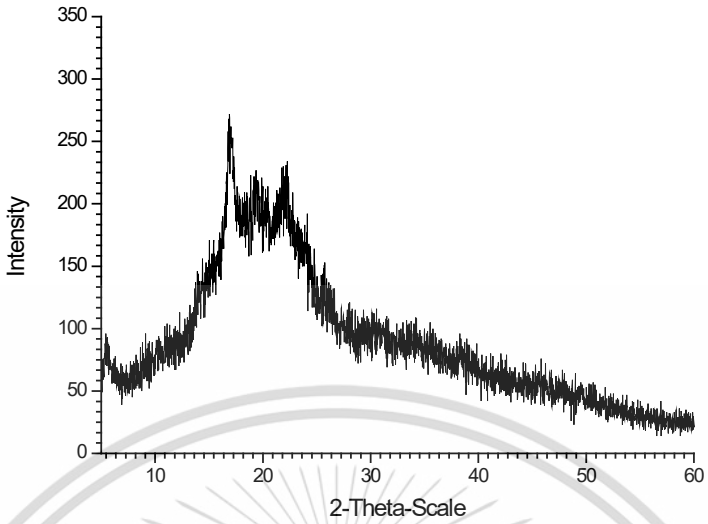

Figure C-7 X-ray diffractogram of COS-BAF

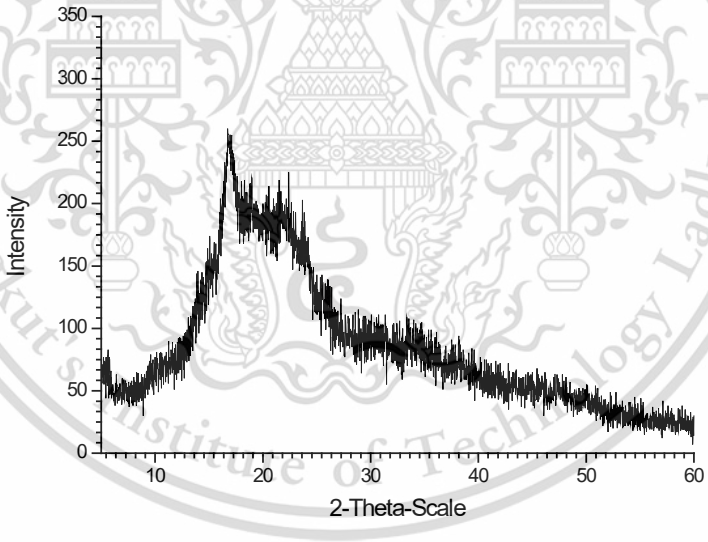

Figure C-8 X-ray diffractogram of COS-STF

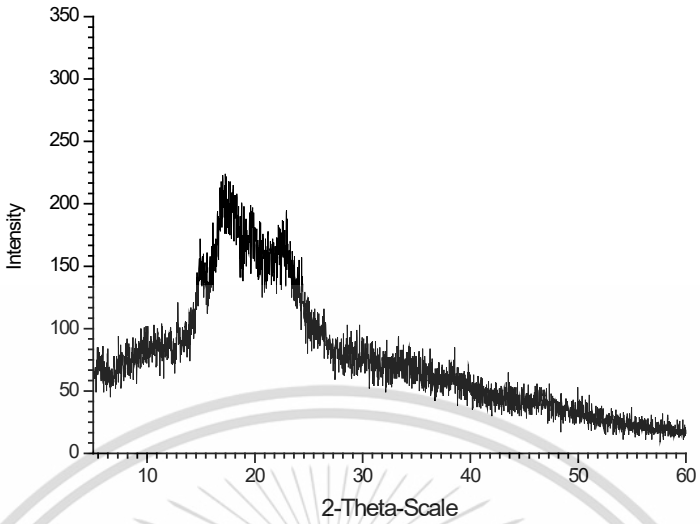

Figure C-9 X-ray diffractogram of OCS-BOF

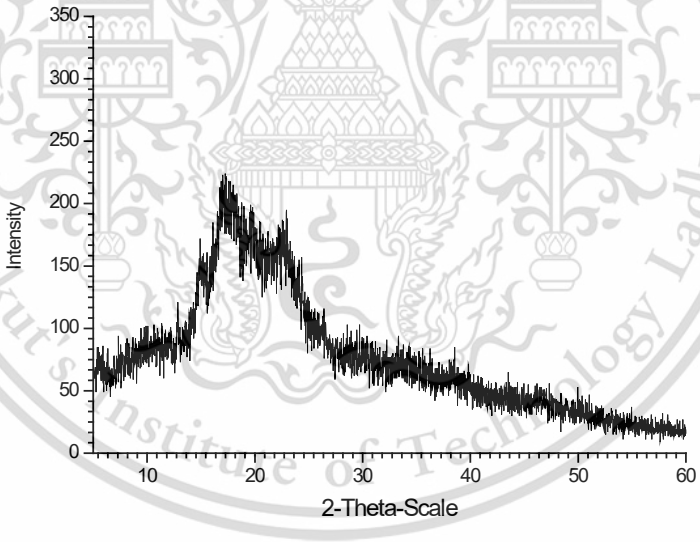

Figure C-10 X-ray diffractogram of OCS-BAF

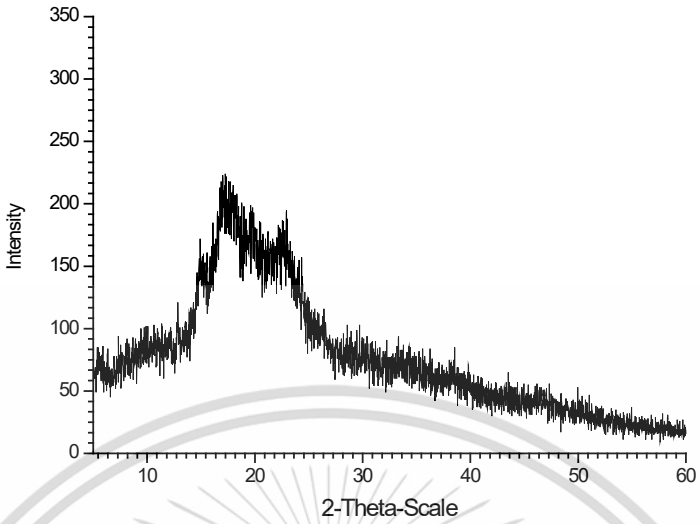

Figure C-11 X-ray diffractogram of OCS-STF

Appendix D

Degree of swelling

Table D-1 Degrees of swelling of various singly modified starch films for the immersion time of 1, 2, 3, 4, 5, 6 or 72 h

Time (h)	Degree of swelling (%)				
	NSF	CS-BOF	CS-BAF	CS-STF	OSF
0	0	0	0	0	0
1	260.15±3.12	200.20±2.34	220.56±1.23	230.12±2.11	246.23±4.21
2	320.24±2.07	258.23±4.21	270.45±2.34	280.34±2.45	290.45±2.33
3	340.67±1.24	270.56±2.60	280.23±2.40	290.56±2.65	307.12±2.16
4	360.23±1.21	280.53±1.23	290.12±1.32	298.45±3.12	315.33±1.34
5	380.34±1.43	290.32±1.65	300.67±3.25	314.21±3.23	320.43±2.55
6	400.23±1.34	295.12±2.21	315.87±2.11	330.06±3.19	340.01±2.65
72	430.23±1.69	300.90±3.45	320.45±1.34	340.12±1.12	360.77±2.71

Table D-2 Degrees of swelling of various COS films for the immersion time of 1, 2, 3, 4, 5, 6 or 72 h

Time (h)	Degree of swelling (%)		
	COS-BOF	COS-BAF	COS-STF
0	0	0	0
1	180.22±2.35	190.10±2.44	200.12±2.19
2	200.12±1.34	215.34±3.12	230.76±1.76
3	205.45±3.44	217.65±2.55	235.23±3.20
4	210.76±2.17	220.11±2.37	240.67±2.09
5	215.21±2.69	225.45±2.19	243.23±2.56
6	220.77±2.33	230.65±2.20	248.76±2.10
72	230.34±2.60	240.98±2.39	260.32±3.18

Table D-3 Degrees of swelling of various OCS films for the immersion time of 1, 2, 3, 4, 5, 6 or 72 h

Time (h)	Degree of swelling (%)		
	OCS-BOF	OCS-BAF	OCS-STF
0	0	0	0
1	190.78±2.14	227.12±3.41	240.80±2.17
2	240.54±3.78	262.54±3.00	275.65±3.09
3	260.12±3.03	272.13±2.34	283.11±2.12
4	267.54±1.30	280.31±1.45	290.12±3.56
5	276.54±1.12	286.75±2.09	295.43±3.03
6	280.32±2.34	291.34±2.33	302.31±2.45
72	285.12±1.88	307.12±1.11	320.29±1.15

Appendix E

The results of mechanical properties

Table E-1 Mechanical properties of various modified starch films

Sample	Mechanical properties		
	Stress at maximum load (MPa)	Young's modulus (MPa)	Strain at maximum load (%)
NSF	3.25±0.12	90.65±2.87	40.98±1.12
CS-BOF	9.16±0.29	590.87±3.21	15.67±1.67
CS-BAF	8.23±0.24	540.85±3.49	17.87±1.89
CS-STF	7.66±0.15	510.98±2.45	21.98±1.45
OSF	1.87±0.23	35.24±2.76	130.98±1.67
COS-BOF	7.65±0.21	240.56±3.40	43.56±0.35
COS-BAF	6.21±0.19	210.22±2.89	48.79±0.65
COS-STF	5.76±0.18	200.65±2.32	54.78±0.92
OCS-BOF	3.02±0.32	75.67±1.67	60.89±1.56
OCS-BAF	2.87±0.30	60.78±2.56	80.95±1.45
OCS-STF	2.65±0.16	50.87±0.76	90.67±4.23

Appendix F

Biodegradable property by the soil burial test

Table F-1 Mechanical properties of various modified starch films after the soil burial test for 5 and 10 days

Sample	Mechanical properties after the soil burial test for 5 day			Mechanical properties after the soil burial test for 10 day		
	Stress at maximum load (MPa)	Young's modulus (MPa)	Strain at maximum load (%)	Stress at maximum load (%)	Young's modulus (MPa)	Strain at maximum load (%)
NSF	2.00±0.22	55.00±2.76	30.45±1.45	1.56±0.02	32.46±1.33	20.98±1.32
CS-BOF	8.57±0.03	560.67±2.35	10.67±0.12	8.03±0.04	540.98±2.65	6.57±3.56
CS-BAF	6.63±0.04	520.45±2,23	14.56±1.45	5.43±0.03	490.76 ±1.21	13.53±1.23
CS-STF	6.13±0.12	450.35±1.32	17.87±1.56	4.90±0.01	440.34±3.21	15.33±0.45
OSF	1.24±0.15	12.35±2.34	122.45±0.36	0.57±0.03	5.67±2.45	115.53±1.24
COS-BOF	6.63±0.02	230.87±2.69	41.23±0.24	6.25±0.02	215.67±4.34	38.45±0.32
COS-BAF	5.54±0.12	195.23±4.34	45.65±0.23	5.04±0.05	182.75±3.21	39.87±1.45
COS-STF	5.02±0.02	180.34±1.12	45.23±0.34	4.42±0.03	165.64±2.12	40.34±0.45
OCS-BOF	2.54±0.08	70.96±2.37	55.12±0.42	2.13±0.08	65.76±0.34	49.53±1.21
OCS-BAF	2.32±0.03	54.32±1.23	74.56±1.45	1.90±0.05	48.03±0.85	68.73±2.34
OCS-STF	2.04±0.02	30.23±1.56	73.12±1.41	1.60±0.07	30.87±1.45	73.56±1.09

Figure F-1 Various modified starch films after the soil burial test for 10 days

Preparation and properties of oxidized starch using hydrogen peroxide as oxidizing agent

Yossathorn Tanetrungroj[1] and Jutarat Prachayawarakorn[1,2*]

[1]*Department of Chemistry, Faculty of Science,*
King Mongkut's Institute of Technology Ladkrabang (KMITL), Bangkok 10520, Thailand,
[2]*Advanced Materials Research Unit, Faculty of Science,*
King Mongkut's Institute of Technology Ladkrabang (KMITL), Bangkok 10520, Thailand

*e-mail: jutarat.si @kmitl.ac.th

Abstract: In the present work, native starch was modified by an oxidative chemical treatment with hydrogen peroxide. The oxidation reaction conditions were controlled with temperature, pH and molar concentration of hydrogen peroxide oxidizing agent. The reaction times were varied for 30, 60, 90 and 120 minutes. The native starch and oxidized starch were evaluated by carbonyl and carboxyl content, FT-IR, SEM and XRD techniques. The result showed that hydrogen peroxide could be used to oxidize the gelatinized starch into the oxidized starch with the carbonyl contents from 0.13 to 0.53 and the carboxyl contents from 0.05 to 0.48, depending on the reaction times. In addition, the oxidized starch contained more carbonyl groups than carboxyl groups. FT-IR spectrum of the oxidized starch showed the new peak position, characteristic of C=O groups. For SEM micrographs, the morphology of the oxidized starch was changed significantly. Moreover, the crystallinity of the oxidized starch was decreased with higher carbonyl and carboxyl contents.

1. Introduction

Among natural materials, starch is one of well-known biodegradable polymers and the main source of carbohydrate. However, native starch without modification possesses shows certain disadvantages, e.g., high water absorption, high viscosity and difficulty in controlling processing.

Chemical modification such as oxidation can be used as an alternative way for improving several properties of native starch. Oxidation reaction brings about structural alternation, the viscosity reduction and the production of new function groups. Oxidized starch is commonly prepared by reacting starch with oxidants under controlled temperature and pH. They are widely used in many applications, especially in paper and food industries.[1]

In recent time, the oxidation process of the native starch have been used many oxidizing reagents such as sodium hypochlorite, potassium permanganate, potassium dichromate, sodium periodate, nitrogen dioxide, sodium perborate and potassium nitrate.

Hydrogen peroxide is one of the reagents employed to produce the oxidized starch. Hydrogen peroxide has been used in commercial applications because it creates no harmful by products. Unlike sodium hypochlorite, hydrogen peroxide decomposes inevitably to oxygen, which is safe for the environment, and is preferred especially when a chlorine-free process is desired[2]. Normally, the oxidation reaction of starch using hydrogen peroxide requires a long reaction time, high temperature or high pH level[3]. However, there have been a few report on the oxidized starch prepared by using hydrogen peroxide as an oxidizing agent.[4]

This objective of this work was to evaluate the preparation and properties of native starch modified by hydrogen peroxide. The

samples were investigated on the carbonyl and carboxyl contents, Moreover, the functional group analysis, morphology, X-ray diffraction analysis were examined.

2. Materials and Methods

2.1 Materials

Cassava starch was obtained from Chaopraya Phuchrai 2999 Co.,Ltd. (Kamphaengphet, Thailand). Hydrogen peroxide (H_2O_2, 30%, w/v), analytical grade (99.5%), hydrochloric acid, and sodium hydroxide were purchased from Italmar (Thailand) Co. Ltd.

2.2 Preparation of oxidized starch

The oxidation process of native cassava starch was followed according methodology described by Shui-Dong Zhang.[2] 50.0 g of cassava starch was suspended in 250 mL water in a 1000 mL three-necked round-bottomed flask and heated at the temperature of 80 °C for 1 h with gentle stirring. After cooling the gelatinized starch to 35 °C, a further 200 mL distilled water, containing 70.2 mL of 30% (w/v) H_2O_2 -to give a H_2O_2: starch molar ratio of 0.7- was added dropwise to the mixture over a period of 1 h with continuous vigorous stirring; while, the temperature and pH were maintained at 25 °C and 10.0, respectively. After 24 h, the slurry was separated by slow-speed centrifugation and the precipitated product was washed with excess amount of distilled water before drying at the temperature of 50 °C for 24 h in a hot air oven. Furthermore, the reaction times were varied for 30, 60, 90 and 120 min.

2.3 Sample characterization

2.3.1 Carbonyl and carboxyl content

The carbonyl content was determined as described by R.J. Smith.[5] Starch sample (4 g) was suspended in 100 mL of distilled water. The slurry was gelatinized in a boiling water bath for 20 min, cooled to 40 °C and adjusted to pH 3.2 with 0.1 M HCl. Then 15 mL of hydroxylamine reagent was added. The flask was stoppered and agitated in a water bath at 40 °C. After 4 h, the sample was rapidly titrated to pH 3.2 with 0.1 M HCl. A blank determination with only hydroxylamine reagent was performed in the same manner. The hydroxylamine reagent was prepared by 25 g hydroxylamine hydrochloride in 100 mL of 0.5 M NaOH. The final volume was then adjusted to 500 mL with distilled water. Carbonyl content was calculated as follows:

$$\%\text{Carbonyl content} = \frac{[(\text{Blank-Sample})\ \text{mL} \times \text{Acid Normality} \times 0.028 \times 100]}{\text{Sample weight (g, dry basis)}}$$

The carboxyl content was determined as previously described by D. S. Kuakpetoon and Y.J. Wang.[6] Starch sample (5 g) was stirred in 25 mL of 0.1 M HCl for 30 min. The slurry was then filtered and washed with distilled water until free of chloride ions. The filtered cake was transferred to a 600 mL beaker, and the volume was adjusted to 300 mL with distilled water. The starch slurry was heated in a boiling water bath with continuous stirring for 15 min to ensure complete gelatinization. The hot sample was immediately titrated with 0.1 M NaOH using phenolphthalein as indicator. A blank determination was run on the original sample in the same manner but being stirred in 25 mL of distilled water instead of 0.1 M HCl. Carboxyl content was calculated as follows:

$$\frac{\text{Milliequivalents of Acidity}}{100\ \text{g Starch}} = \frac{[(\text{Blank-Sample})\ \text{mL} \times \text{Base Normality} \times 100]}{\text{Sample weight (g, dry basis)}}$$

%Carboxyl content =

$$\frac{\text{Milliequivalents of Acidity} \times 0.045}{\text{100 g Starch}}$$

2.3.2 FT-IR technique

A sample was characterized by FT-IR analysis on a Spectrum 2000 GX spectrometer (PerkinElmer, USA) using KBr disk technique with a resolution of 4 cm^{-1} using 16 scans per sample.

2.3.3 X-ray diffraction

Wide angle X-ray diffraction measurement was carried out using a D8 Advance X-ray diffractor (Bruker, Madison, USA), CuKα radiation (wavelength 0.1542 nm) operating at 40 kV and 35 mA. The scattering angle (2θ) covered the range from 3° to 60° (θ is the Bragg angle) with a step size of 0.02° and a sampling interval of 10 s.

2.3.4 Scanning electron microscopy

Morphology of a sample was observed by Scanning Electron Microscope (LEO 1450 VP). The sample was sputter-coated with a thin layer of gold to prevent electrical charging during the observation.

3. Results & Discussion

3.1 Carboxyl and carbonyl group contents

Table 1. The carbonyl and carboxyl contents of different oxidized starch

Reaction time (min)	Carbonyl content (%)	Carboxyl content (%)
30	0.13	0.05
60	0.30	0.13
90	0.42	0.27
120	0.53	0.48

Table 1 showed the carbonyl and carboxyl contents of different oxidized starch at the different reaction times. It was found that the carbonyl contents of the oxidized starch clearly increased from 0.13 to 0.53 when the reaction times increased from 30 to 120 minutes. In addition, when the reaction time increased, the carboxyl content of oxidized starch markedly increased from 0.05 to 0.48. It indicated that the increasing of reaction time for oxidation reaction with hydrogen peroxide progressively created more aldehyde groups than carboxyl groups.

3.2 FT-IR spectroscopic study

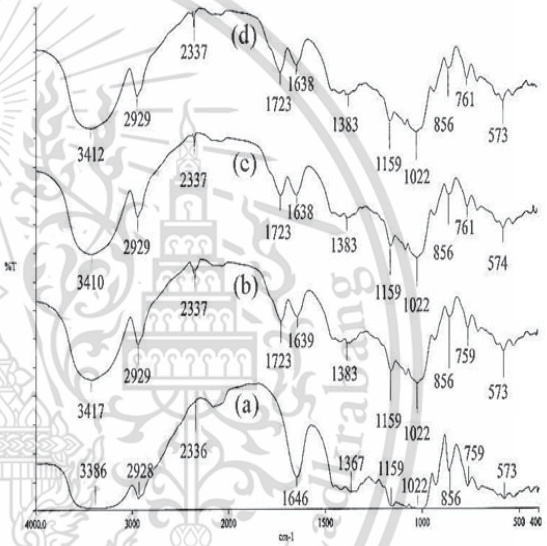

Figure 1. IR spectra of different oxidized starch at different carbonyl contents (a) 0% (b) 0.13% (c) 0.42% and (d) 0.53%

FT-IR spectra of different starch were shown in Figure 1. The broad band appeared at 3,250-3,500 cm^{-1} was attributed to O-H stretching. The wavenumber in the range of 2,800-3,000 cm^{-1} was assigned from C-H asymmetric stretching of $-CH_2-$. The bands in the range of 1,641-1,646 cm^{-1} and 1,450-1,475 cm^{-1} were assigned for bounded water presented in starch and $-CH_2-$ deformation, respectively. The peaks in the range of 1,070-1,275 cm^{-1} and 1,000-1,200 cm^{-1} were characteristic for C-O-C stretching and C-O-H stretching, respectively.[7] It was found from Figure 1 that all the starch showed the same IR peak positions since they still consisted of the

same chemical structure of polysaccharide structures. It should be noted that the spectra of different oxidized starch in Figures 1(b) – 1(d) showed the new peak position at 1723 cm^{-1} the characteristic of C=O stretching, arisen from the change of starch structure by oxidation creating carbonyl and carboxyl groups.[8]

3.3 X-ray diffraction

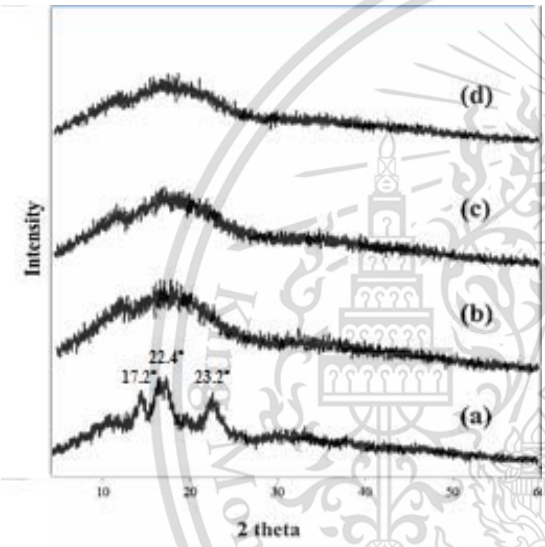

Figure 2. XRD diffractograms of different oxidized starch at different carbonyl contents (a) 0% (b) 0.13% (c) 0.42% and (d) 0.53%

XRD diffractograms of different oxidized starch were presented in Figure 2. Figure 2(a) shows B-type diffraction pattern of the native starch. It was found that the oxidized starch (Figures 2(b)-2(d)) showed V_h-type diffraction pattern, with the peak position at 2θ of 12.6°, 19.4° and 22.1°. When the carbonyl content of the oxidized starch increased, the intensity of peak at 12.6°, 19.4° and 22.1° seemed to decrease. This result indicated that the degree of crystallinity of oxidized starch was greatly reduced and clearly lower than that of the native starch. This observation could confirm the oxidation process occurred on the starch granules.

3.4 SEM Micrographs

SEM micrographs of various oxidized starch were shown in Figure 3. It can be seen in Figure 3(a) that the native starch consisted of the smooth granule; whereas, the oxidized starch in Figures 3(b)-3(d) presented different morphology. The granule characteristic was completely destroyed by the oxidation process. Furthermore, the surface of oxidized starch showed more apparently rough, especially with the increasing of carbonyl content caused by hydrogen peroxide.

4. Conclusion

It can be concluded that hydrogen peroxide could oxidize the gelatinized starch into the oxidized starch with different carbonyl contents from 0.13 to 0.53 and carboxyl contents from 0.05 to 0.48 depending on the reaction times. The oxidized starch contained more carbonyl groups than carboxyl groups. Moreover, the new IR peak position, the characteristic of C=O groups in carbonyl and carboxyl group of oxidized starch was observed. Moreover, the granule characteristic of the oxidized starch was completely destroyed after the oxidation reaction. Besides, the crystallinity of different oxidized starch was clearly lower than that of the native starch, as observed from the XRD diffractograms.

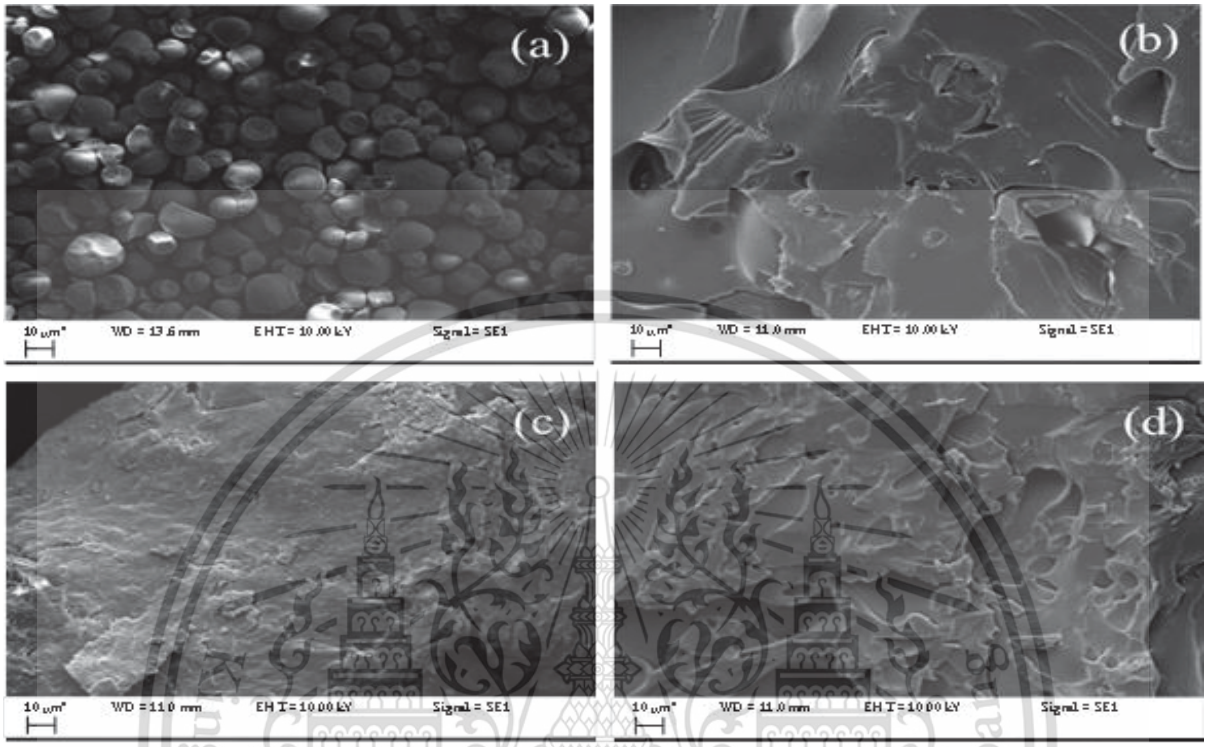

Figure 3. SEM micrographs of different oxidized starch at different carbonyl contents (a) 0% (b) 0.13% (c) 0.42% and (d) 0.53%

Acknowledgements

The authors express their sincere appreciation to KMITL Research Fund for supporting the study financially.

References

1. Scallet, B.L.; Sowell, E.A. in Starch Chemistry and Technology Vol.II. Eds. Whistler, R.L; Paschall, E.F.; Academic Press: New York, 1967; pp 237–251.
2. Zhang, S.D.; Zhang, Y.R.; Wang, X. L.; Wang, Y.Z. *Starch/Stärke* **2009,** 61, 646–655.
3. Sangseethong, K.; Termvejsayanon, N. Sriroth, K. *Carbohydrate Polymers* **2010,** 82, 446-453.
4. Hage, R.; Lienke. A. *Journal of Molecular Catalysis A: Chemical*, **2006**, 251, 150–158.
5. Smith, R.J.; Starch chemistry and technology (vol.2): New York, Academic press, 1967; pp 321-345.
6. Kuakpetoon, D. S.; Wang, Y. J. *Starch/Stärke* **2001,** 53, 211–218.
7. Bower, D.I.; Maddams, W.F. The Vibrational Spectroscopy of Polymer 2nd Edition, Cambridge University Press: Cambridge, U.K, 1996.
8. Para, A.; *Carbohydrate Polymers* **2004,** 57, 277–283.

BIOP-P8

Preparation and properties of crosslinked starch using borax as a crosslinking agent

Yossathorn Tanetrungroj[1] and Jutarat Prachayawarakorn[1,2*]

[1] Department of Chemistry, Faculty of Science, King Mongkut's Institute of Technology Ladkrabang (KMITL), Bangkok 10520, Thailand

[2] Advanced Materials Research Unit, Faculty of Science, King Mongkut's Institute of Technology Ladkrabang (KMITL), Bangkok 10520, Thailand

[*] E-mail: jutarat.si @kmitl.ac.th Tel +668-3298400 ext 6235

Abstract

Due to poor mechanical properties and high water absorption properties, in this study, native starch was chemically modified by crosslinking with borax. The crosslinked starches were prepared using the different contents of borax, i.e., 5, 10, 15 and 20% w/w of dried starch. The effects of different contents of borax on properties of crosslinked starches were investigated by degree of crosslinking, pasting, thermal and water absorption properties. It was found that the degree of crosslinking was increased with the increasing of borax content. Moreover, the decrease in peak viscosity of the crosslinked starches was observed by the pasting properties. The thermal and water absorption properties were improved by adding crosslinking agents into cassava starch. Furthermore, it was found that the highest degree of crosslinking, thermal stability and the lowest water absorption properties were obtained from the crosslinked starch with borax at the content of 20 % w/w.

Keywords: crosslinked starch, borax, modified starch

1. Introduction

Starch is a common material widely using in many food and several applications. However, the applications of native starch are limited due to low thermal stability, high retrogradation tendency, water absorption properties and low mechanical properties [1].

The chemical modification of starch can be achieved by a variety of different chemical reactions such as acid hydrolysis, oxidation, etherification, esterification and cross-linking. Among these methods, crosslinking has been commonly used to modify native starch and improve granule stability with new covalent bonds. Cross-linking reinforces the hydrogen bonds in the granule with chemical bonds that act as a bridge with at least two hydroxyl groups in a single polymer molecule or in adjacent molecules; thus, providing desired functional properties, increase in gelatinization temperature and decrease in retrogradation rate [2].

Crosslinked starch were used many applications, especially in the manufacture of foods to thicken, stabilize and provide texture. There has been investigated on the different crosslinking agents such as epichlorhydrin, glutaraldehyde, citric acid [3-4]. Borax or sodium borate is one of the most effective crosslinking agents. It is mineral, water soluble and less toxic. However, there have not been a few reports on the crosslinked starch prepared by using borax as a crosslinking agent.

Consequently, the objective of the present study was to evaluate the effect of borax contents on properties of crosslinked starch. The crosslinked starches were, then, characterized by the degree of crosslinking, pasting properties, as well as thermal properties, and water absorption properties.

2. Experimental methods

2.1 Materials

Cassava starch was purchased from Chaopraya Phuchrai 2999 Co.,Ltd. (Kamphaengphet, Thailand). Borax or sodium borate ($Na_2B_4O_7 \cdot 10H_2O$) were

obtained from Chemipan Co., Ltd. (Bangkok, Thailand), respectively.

2.2 Preparation of crosslinked starch

Crosslinked starches were prepared according to the method of Woo and Sei [5]. Cassava starch (50 g) was mixed with borax as a crosslinking agents with different contents of 5, 10, 15 and 20% weight (based on dry weight of starch) and dissolved in 70 mL distilled water, After that, the pH was adjusted to 10.0 with 0.1 M NaOH. The temperature of the slurry was maintained at 45°C and continuous stirring by magnatic stirrer for 2 hours. Then, the suspensions were neutralized to pH 7.0 with 0.1 M HCl, washed with distilled water four times, and finally dried at 50°C for 24 hours in an hot-air oven.

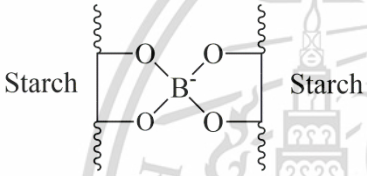

Figure 1 Schematic chemical structure of the starch crosslinked with borax.

2.3 Sample characterization

2.3.1 Determination of degree of crosslinking

The degree of crosslinking of modified starch was determined from the viscosity value, according to the procedure of K.Singh [5]. The peak viscosity of modified starch slurries (25% by weight) was measured from a rapid viscosity analyzer (RVA) (Newport Scientific Co.,Ltd., Warrie wood, Australia). A programmed heating and cooling cycles to obtain the peak viscosity was employed as follows: starch slurries were heated from 50 to 95 °C at 11 °C/min, and then held at 95 °C for 2 min. Afterwards, the paste was cooled down to 50 °C at 11 °C/min and finally kept at 50 °C for 2 min. The degree of crosslinking was calculated by using the equation below:

Degree of crosslinking (%) = (A-B)/A×100

where A is the peak viscosity of the control sample (native starch), and B is the peak viscosity of the crosslinked starch.

2.3.2 Pasting properties

A rapid viscosity analyzer (RVA) was used to measure viscosity change of starch during heating and cooling. The starch sample (3 g, dry basis) was added to distilled water (25 g) in a RVA vessel. The mixture was stirred at 960 rpm for 10 s and at 160 rpm by a plastic paddle in the vessel. After incubating for 1 min at 50°C, the sample was heated to 95°C in 3.7 min, maintained at 95°C for 2.5 min, cooled to 50°C in 3.7 min, and then held at 50°C for 2 min. The pasting parameters such as pasting temperature (PT), peak viscosity (PV), were determined. Peak viscosity was the highest viscosity during the heating step and pasting temperature was the temperature at which the viscosity curve leaved the baseline as the temperature rises during the initial heating process.

2.3.3 Thermogravimetric analysis

Thermogravimetric (TGA) and derivative thermogravimetric (DTG) thermograms of a sample were recorded by a thermogravimetric analyzer (Pyris 1, Perkin Elmer, Massachusetts, USA). The sample was tested under nitrogen atmosphere within a temperature range of 50-700°C at a heating rate of 10°C/min. Thermal decomposition temperatures (T_d) was reported by the maximum degradation temperature where the weight loss started to occur.

2.3.4 Water absorption properties

The specimen was dried at 105 °C for 3 h and, then, stored at 100% relative humidity at a temperature of 30 ± 2 °C prior to water absorption examination. The amount of water absorbed by the sample was determined until the constant weight was obtained. The percentage of water absorption was calculated as follows:

Water absorption = $(W_2 - W_1)/W_1 \times 100$

where W_2 and W_1 were the wet weight and the dried weight of the sample, respectively.

3. Results and discussions

3.1 Degree of crosslinking

Table 1 The degree of cross-linking of different crosslinked starch.

Crosslinked starch with different borax contents (% w of dry starch)	Degree of crosslinking (%)
0	0
5	11.59
10	44.85
15	53.78
20	66.76

The degree of cross-linking of starch modified by different amounts of borax (0, 5, 10, 15 and 20%) is presented in Table 1. It was found that the degree of crosslinking of the crosslinked starch clearly increased from 11.59 % to 66.76 % when the borax content increased from 5 to 20 %w. It could be explained that with the increasing borax content, more borax molecules could react with four hydroxyl group of the starch chains creating higher tetra-starch borate molecules (Figure 1).

3.2 Pasting properties

Table 2. Peak viscosities and pasting temperatures of crosslinked starch with different borax contents

Crosslinked starch with different borax contents (%w of dry starch)	Peak viscosity (mPa.s, cP)	Pasting Tempearature (°C)
0	6294±0.2	69.23±0.01
5	5564±0.2	72.60±0.05
10	3408±0.1	71.95±0.02
15	2909±0.1	71.00±0.09
20	2091±0.2	71.95±0.02

The results of the pasting properties of the different crosslinked starches as measured by RVA are presented in Table 2. It was observed that the peak viscosity of the crosslinked starches was clearly lower than the native starch. This result could confirm the successfully crosslinked of the native starch. Moreover, when the concentration of borax increased, the peak viscosity of crosslinked starch was significantly decreased. The decreasing of the peak viscosities of crosslinked starch could be due to the intermolecular bridge in crosslinking process, which reduced interactions of starch molecules with water molecules resulting in lower peak viscosity values when compared with native starch [6]. However, the pasting temperature of different crosslinked starches was comparable.

3.3 Thermogravimetric analysis

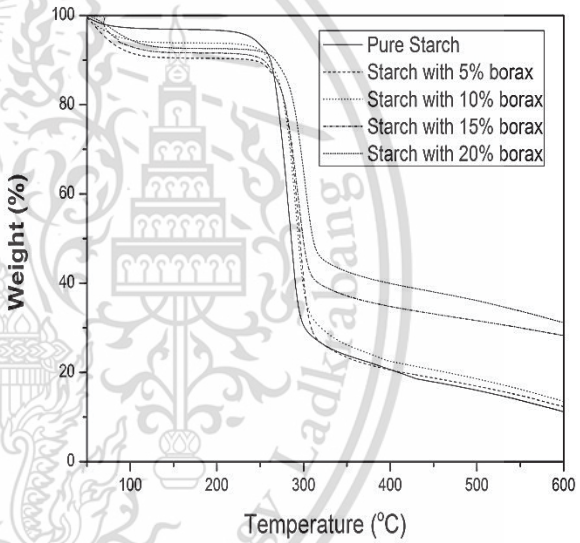

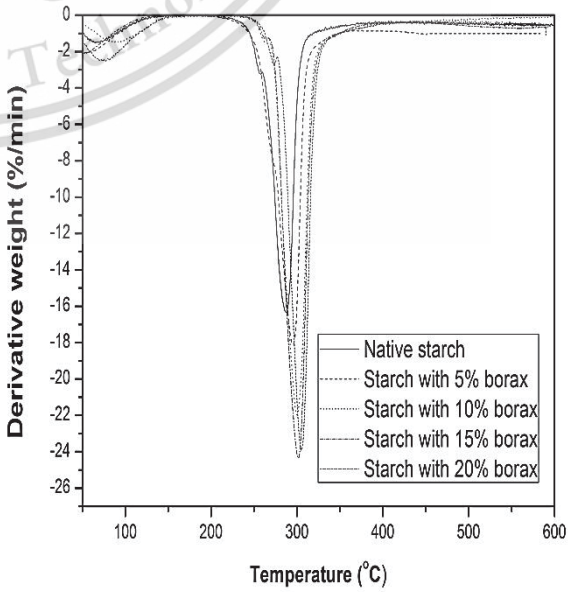

Figure 2. (a) TGA and (b) DTG thermograms of crosslinked starch with different borax contents

Table 3 Thermal decomposition temperatures of different crosslinked starches

Crosslinked starch with different borax contents (% w of dry starch)	Degradation Temperature (° C)
0	290.2
5	296.3
10	301.0
15	303.2
20	306.1

TGA and DTG thermograms of various crosslinked starches are shown in Figure 2 and Table 3. The two steps of weight loss were obtained. The initial step at around 100°C was merely due to evaporation of the absorbed moisture. The second stage in the range of 290 to 306 °C was due to the decomposition of the starch [7]. The result showed the improved thermal decomposition temperature of different crosslinked starch with the increasing of borax contents. This was due to the linkages between starch molecules provide higher thermal stability.

3.4 Water absorption properties

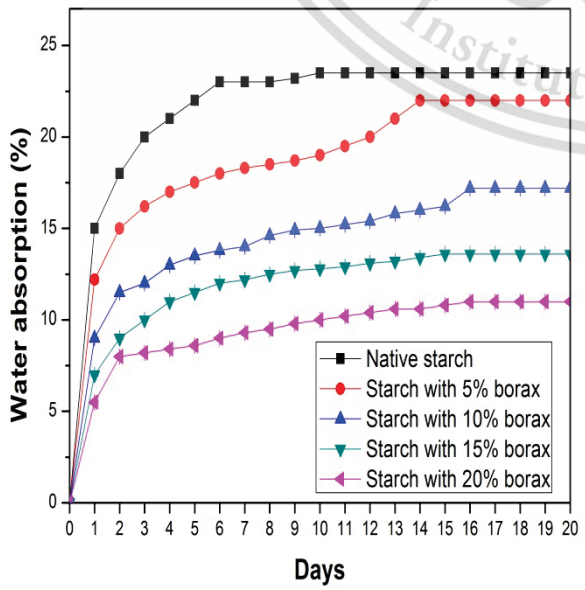

Figure 3 Percentage water absorption of crosslinked starches with different borax contents.

Water absorption properties of different crosslinked starches are presented in Figure 3. The result suggested that the crosslinked starch presented lower water absorption than native starch. In addition, when the borax contents increased from 5 to 20 %wt, the percentage of water absorption tended to decrease. This behavior could be explain that the decreasing of water absorption properties cause by a hydrophilic group (OH) of starch molecules decreased when the crosslinking reaction occurred. The interaction between starch and borax molecules could block the water absorption by restricting the mobility of starch chains in the amorphous region [8].

4. Conclusions

In this study, the influence of borax contents on properties of crosslinked starch was examined. The degree of the crosslinking increased with the addition of borax contents. From the pasting properties, the addition of borax caused the significant decrease in peak viscosity. Besides, the thermal degradation temperature and water absorption properties of crosslinked starches were clearly improved when the borax was added into the native starch. From the overall results, the highest thermal properties and lowest water absorption was obtained from the crosslinked starch modified by 20 %wt of borax content.

Acknowledgements

The authors express their sincere appreciation to the KMITL Research Fund for supporting the study financially.

References

[1] Scallet, B.L. and Sowell, E.A., "Production and used of hypochlorite oxidized starches", *in Starch Chemistry and Technology Vol.II (Eds. R.L. Whistler, E.F. Paschall),* Academic Press, New York : 237–251 (1967).

[2] Jayakody, L., and Hoover, R. "The effect of linterization on cereal starch granules", *Food Research International*, 665-680 (2002).

[3] Ratnayake, W. S., and Jackson, D. S. "Phase transition of cross-linked and hydroxypropylated corn (Zea mays L.) starches", *LWT - Food Science and Technology* : 346-358 (2008).

[4] Lim, S.T. and Seib, P. A. "Location of phosphate esters in a wheat starch phosphate by 31P-nuclear magnetic resonance spectroscopy." *Cereal Chemistry* : 145-15 (1993).

[5] Woo, K.S. and Seib, P. A. "Cross-linked resistant starch: preparation and properties." *Cereal Chemistry*, 819-825. (2002).

[6] Gamonpilas, C., Pongjaruvat, W., Methacanon, P., Seetapan, N., Fuongfuchat, A. and Klaikherd, A. "Effects of cross-linked tapioca starches on batter viscosity and oil absorption in deep-fried breaded chicken strips." Journal of Food Engineering : 262–268 (2013).

[7] Majzoobi, M., Beparva, P., Farahnaky, A. and Badi, F. "Physicochemical Properties of Cross-linked Wheat Starch Affected by L-Ascorbic Acid." Journal of Agricultural Science and Techmology :. 355-364. (2014).

[8] Zhang, X.Z., Zhuo, R.X., Cui, J.Z. and Zhang, J.T. "A novel thermo-responsive drug delivery system with positive controlled release", *International Journal of Pharmacy* : 43-50.(2002).

International Journal of Biological Macromolecules 120 (2018) 1240–1246

Contents lists available at ScienceDirect

International Journal of Biological Macromolecules

journal homepage: http://www.elsevier.com/locate/ijbiomac

Effect of dual modification on properties of biodegradable crosslinked-oxidized starch and oxidized-crosslinked starch films

Yossathorn Tanetrungroj [a], Jutarat Prachayawarakorn [a,b,*]

[a] Department of Chemistry, Faculty of Science, King Mongkut's Institute of Technology Ladkrabang (KMITL), Bangkok 10520, Thailand
[b] Advanced Materials Research Unit, Faculty of Science, King Mongkut's Institute of Technology Ladkrabang (KMITL), Bangkok 10520, Thailand

ARTICLE INFO

Article history:
Received 28 May 2018
Received in revised form 19 July 2018
Accepted 26 August 2018
Available online 29 August 2018

Keywords:
Crosslinked starch
Dual-modification
Oxidized starch

ABSTRACT

Due to poor properties of biodegradable native starch (NS) film; in this work, dual-modified starch films i.e. crosslinked-oxidized starch (C-OS) and oxidized-crosslinked starch (O-CS) films were prepared and compared to single-modified starch i.e. crosslinked starch (CS) and oxidized starch (OS) films. All modified starch films were oxidized and crosslinked using hydrogen peroxide and boric acid by casting technique. Degree of crystallinity and swelling behavior of both dual-modified starch films were found to decrease. Moreover, O-CS film showed smoother fractured morphology than C-OS and NS films. Both C-OS and O-CS films presented not only high stress at maximum load and Young's modulus but also high strain at maximum load, as compared to single-modified film. Furthermore, water vapor permeability, thermal property and biodegradability of all modified films were also studied.

1. Introduction

Starch is one of the interested biodegradable polymers due to its abundance, renewability and low cost. In recent time, biodegradable starch film has received much attraction for used in industrial applications due to excellent biodegradability. However, applications of native starch (NS) have been restricted for biodegradable film due to its high hydrophilic properties, poor mechanical properties, low stability and difficulty in controlling process [1]. Chemical modification of starch is an alternative way for improving several properties of biodegradable starch based film. Traditionally, differences in chemical modification of various modified starch have been affected on differences in physiochemical properties of the films [2]. Several researchers have tried to enhance their properties of starch-based films for food packaging by preparing modified starch including oxidized starch, crosslinked starch, hydroxypropyl starch, acetylated starch and heat-moisture treated starch [3–6].

Generally, crosslinked process is one of the chemical modifications for starch, which reinforces hydrogen bonds between starch molecules; thus, it can improve mechanical strength, thermal stability, resistance to solubility and swelling capability [2]. Previous study has been presented for crosslinked starch (CS) using citric acid [4], epichlorohydrin [7] glutaraldehyde [8] and boric acid [9]. However, most of the crosslinking agents were either toxic or expensive with low crosslinking efficiency. Boric acid has finally been selected because it can form starch borate structure between hydroxyl groups of the starch molecules. In addition, it is also important as a food additive with low toxicity [9]. It was reported that epichlorohydrin could enhance thermal and mechanical properties of starch-poly (vinyl alcohol) (PVA) blends by reinforcing the intermolecular bonding with the introduction of covalent bonds [7]. Starch was also crosslinked with PVA by boric acid. The result showed that starch films prepared by boric acid crosslinking showed excellent tensile strength and Young's modulus [9]. S.H. Koo et al. reported that cross-linking of starch by STMP/STPP (99:1 w/w) decreased solubility, swelling factor and paste clarity of corn starch [10]. Citric acid crosslinked starch film showed the improvement in tensile strength, thermal stability and dissolution in water and formic acid [4].

Alternatively, oxidation reaction leads to structural alternation, reduced viscosity, degradation of starch molecules and production of new function groups i.e. carbonyl and carboxyl groups. Several types of oxidizing agents have been used, e.g. sodium hypochlorite [11], organic acids (acetic, citric and lactic acid) [12], potassium permanganate [13] and bromine [14]. Among these chemicals, hydrogen peroxide is one of the attractive oxidizing agents used to prepare oxidized starch (OS) [15]. F.M. Bustos et al. reported that oxidation with organic acids (acetic, citric and lactic acid) generally decreased the maximum viscosity of oxidized potato starch [12]. Other studies by pasting property confirmed that the gelatinization temperature increased and gelatinization enthalpy decreased in OS oxidized by sodium hypochlorite [16]. Besides, morphology of the starch oxidized by sodium hypochlorite presented irregular surface [11]. Furthermore, compressed thermoplastic oxidized starch film was also prepared and studied. The result showed

* Corresponding author at: Department of Chemistry, Faculty of Science, King Mongkut's Institute of Technology Ladkrabang (KMITL), Bangkok 10520, Thailand.
E-mail address: jutarat.si@kmitl.ac.th (J. Prachayawarakorn).

https://doi.org/10.1016/j.ijbiomac.2018.08.137
0141-8130/

that oxidation with hydrogen peroxide led to the decrease of crystallinity, intrinsic viscosity and thermal stability [17].

Generally, many researchers have focused on using either crosslinked or oxidized method to improve properties of NS granules. Thus, dual modification is a new interesting choice for starch modification. Previous study has shown that crosslinked-oxidized (C-OS) maize starch granules oxidized by hydrogen peroxide and crosslinked by sodium trimetaphosphate enhanced the water-binding capacity [18]. The light transmittance and retrogradation properties of the C-OS were highly improved compared to NS [18]. For dual-modified rice starch with epichlorohydrin and sodium hypochlorite, it was found that C-OS exhibited lower swelling power and solubility and higher paste clarity in comparison with NS. In addition, crosslinked-oxidized rice starch presented the lowest tendency of retrogradation and the highest ability to resistant to shear compared with other modified starch [19]. Furthermore, OS, CS, oxidized-crosslinked (O-CS) and C-OS from yam starch were also prepared. C-OS and O-CS prepared by sodium trimetaphosphate and sodium hypochlorite. It was found that C-OS showed higher gelatinization peak temperature, lower retrogradation, better paste clarity, stronger moisture holding capacity than those of other modified starch. Besides, XRD result indicated that cross-linking showed no significant effect on X-ray pattern of NS [20]. Therefore, the dual modification using a boric acid and hydrogen peroxide as a crosslinking agent and oxidizing agent was selected for the preparation of starch films. Moreover, other studies have focused on the dual modification of NS granules, but the effect of crosslinked-oxidized and oxidized-crosslinked by hydrogen peroxide and boric acid on properties of starch film has never been reported.

The objective of the present study was to evaluate the effect of modified starch types on their relative properties of biodegradable thermoplastic starch films prepared from different modified starch, i.e. CS, OS, C-OS and O-CS. The modified films were, then, characterized for function group analysis by Fourier-transform infrared spectroscopy (FTIR), crystallinity by X-ray diffraction (XRD). In addition, morphology, water permeability, swelling, tensile properties, thermal property and biodegradation properties by soil burial test were also examined.

2. Materials and methods

2.1. Materials

Cassava starch was purchased from Chaopraya Phuchrai 1999 Co., Ltd. (Kamphaengphet, Thailand) and contained 16.4 wt% amylose and 83.6 wt% amylopectin. Boric acid and hydrogen peroxide (H_2O_2, 30% (w/v)), analytical grade (99.5%), were obtained from Italmar Co., Ltd. (Bangkok, Thailand). Glycerol was supplied from Lab System Co., Ltd. (Bangkok, Thailand).

2.2. Preparation of CS and OS

CS was prepared according to the method of K.S. Woo and P.A. Seib [21]. Cassava starch (50 g) was mixed with boric acid at the content of 20% weight (based on dry weight of starch) and dissolved in 70 mL distilled water. After that, pH was adjusted to 10.0 with 0.1 M NaOH. The temperature of the slurry was maintained at 45 °C and continuously stirred by a magnetic stirrer. The suspension was neutralized to pH 7.0 with 0.1 M HCl, washed with distilled water and dried at 50 °C for 24 h in a hot-air oven (Memmert, Germany). The degree of crosslinking was calculated by Rapid Visco Analyzer technique (RVA) from the viscosity values [10,22]. The crosslinked starch showed 66.81% degree of crosslinking.

The oxidation process of NS was followed according to S.D. Zhang and R.E. wing [17,23]. 50 g of cassava starch was suspended in 250 mL distilled water in a 1000 mL three-necked round-bottomed flask and held at 80 °C for 1 h with continuous stirring. After cooling to room temperature, 200 mL distilled water containing 24.6 mL of 30% (w/v) H_2O_2 with H_2O_2: starch molar ratio of 0.7:1 was added dropwise to the mixture for 1 h with continuous stirring while the temperature and pH were maintained at 25 °C and 10.0, respectively [24]. After 24 h, pH value was adjusted to 7.0 with 0.1 M HCl and; then, the slurry was separated by slow-speed centrifugation and washed with distilled water. The sample was dried at 50 °C for 24 h. The oxidized starch showed the carbonyl content of 0.53% and the carboxyl content of 0.48%.

2.3. Preparation of C-OS and O-CS

C-OS was synthesized by crosslinking with 20% weight of boric acid; followed by oxidation with hydrogen peroxide at H_2O_2: starch molar ratio of 0.7:1, pH was maintained at 10.0. After that, the solution was adjusted to pH 7.0 with 0.1 M HCl. C-OS showed the degree of crosslinking of C-OS was 65.93%; the carbonyl content of 0.35% and the carboxyl content of 0.27%.

Besides, O-CS was prepared by the following method. Firstly, cassava starch was oxidized with hydrogen peroxide and, then, followed by the crosslinking with boric acid at the same content of the oxidizing agent and crosslinking agent as mentioned above. The pH of O-CS solution was maintained at 10.0. Finally, pH of solution was adjusted to 7.0 with 0.1 M HCl. The carbonyl and the carboxyl content of O-CS were 0.52% and 0.46%, respectively. O-CS showed the degree of crosslinking of 19.24%.

2.4. Preparation of biodegradable modified starch films

A film was prepared by casting technique using glycerol as a plasticizer. NS or modified starch (10 g) was added into a beaker with 100 mL of distilled water, and followed by the addition of 30% (w/w) glycerol. After that, the mixture was heated on a hot plate (IKA, Germany) and stirred at 65 °C until pre-gelatinization occurred. After cooling to room temperature, the mixture was poured into a polyethylene plate. The thickness of the film was approximately 0.1–0.2 mm. The film was, then, dried in a hot-air oven (Memmert, Germany) at 50 °C for 6 h.

2.5. XRD

XRD measurement was performed by using a D8 Advance X-ray diffractometer (Bruker, Madison, U.S.A.) with CuKα radiation operating at 40 kV and 35 mA. The scattering angle (2θ, with θ being the Bragg angle) covered the range from 5° to 60° with a step size of 0.02° and a sampling interval of 10 s. Percentage crystallinity of each sample was determined by Eq. (1):

$$\text{Crystallinity}(\%) = \frac{A_c}{A_c + A_a} \times 100 \quad (1)$$

where A_c and A_a referred to the area of crystallinity region and the area of amorphous region of a sample on the diffractogram, respectively.

2.6. Swelling property

Degree of swelling for a film was tested. A film (20×20 mm^2) was dried at 105 °C for 2 h and immersed in distilled water at room temperature for 24 h. The weight of the wet film (W_2) was measured after removal of water from the surface with blotting paper. Each film was tested for three times. Percentage of swelling was calculated as follows:

$$\text{Swelling}\ (\%) = \frac{W_2 - W_1}{W_1} \times 100 \quad (2)$$

where W_2 and W_1 were the wet and the dried weights of the sample, respectively.

2.7. Water vapor permeability test

Water vapor permeability (WVP) was measured according to ASTM E96 with the gravimetric modified cup method (the desiccant method). WVP was calculated according to Eq. (3):

$$WVP = \frac{W \times X}{A \times t \times \Delta P} \quad (3)$$

where W/t was the slope of system weight gain vs. time (g/day), A was the area of the exposed surface of the film (32.15 cm^2), X was the average thickness of the film (mm) and ΔP = vapor pressure difference (KPa).

2.8. Morphology

Scanning Electron Microscope (FEI, Quanta 250, U.S.A.) was used to observe morphology of a sample. In order to prevent electric charge, the sample was sputter-coated with a thin layer of gold. Fractured surface of a sample was examined after immersed into liquid nitrogen.

2.9. Mechanical properties

Mechanical test was investigated according to ASTM D-882. A film was cut into rectangular strip of 15 mm × 100 mm. Prior to the test, a film was stored in a desiccator for 24 h before measurement at the temperature of 23 ± 1 °C and relative humidity of 60 ± 5%. The measurement was conducted using a Universal Testing Machine (Lloyd Instrument, LR 5 K, West Sussex, UK) with a load of 100 N and the crosshead speed was maintained at 50 mm/min.

2.10. Biodegradability

A specimen was buried in soil at a depth of approximately 10 cm from the surface. pH and temperature of soil were maintained at 7 ± 1 and 32 ± 2 °C, respectively. The moisture of soil was maintained in the range of 5–10%. After the test, the sample was removed from soil and, then, tensile properties were examined from ten independent samples.

2.11. Thermal properties

A sample approximately 10–12 mg was tested under nitrogen atmosphere within a temperature range of 50 to 600 °C at the heating rate of 10 °C/min using thermogravimetric analyzer (Pyris I TGA HT, PerkinElmer, U.S.A.).

3. Results and discussion

The schematic of molecular structure of both C-OS and O-CS is shown in Fig. 1. For the preparation of C-OS, hydroxyl groups of starch chains were crosslinked with boric acid to form starch borate structure. After the cross-linking reaction, remaining hydroxyl groups at C-2, C-3, and C-6 positions of starch could further oxidized with hydrogen peroxide via a radical chain reaction to form carbonyl and carboxyl groups. Simultaneously, the chain scission might occur in the oxidation process, which could produce lower molecular weight starch chains. Generally, chain scission by oxidation can occur under the influence of one or more environmental factors such as heat, light or chemicals such as acids, alkalis and some salts [25].

For O-CS, hydroxyl groups primarily at C-2, C-3, and C-6 positions were firstly transformed to carbonyl and/or carboxyl groups by oxidation with hydrogen peroxide via a radical chain reaction, causing the decrease of hydroxyl group on the starch chain. The oxidation reaction of starch not only transferred hydroxyl group to carbonyl and carboxyl groups, but also caused polymer chain scission and created low molecular weight starch chains. After that, the remaining hydroxyl groups could, further, crosslinked with boric acid. Finally, starch borate linkages were also generated in the starch chains.

3.1. XRD

Degree of crystallinity of different biodegradable modified starch films is presented in Table 1. It was found that the degree of crystallinity of CS film was similar to NS film. This was probably because crosslinking mainly occurs on amorphous regions of the starch granules [18–20]. Similar results were also reported that the XRD pattern of starch was not changed by cross-linking [18,26]. Nevertheless, OS film showed lower degree of crystallinity than NS film and this was because the chain scission and the disruption of hydrogen bonds in starch molecules during oxidation [12,18]. This observation could confirm the oxidation process occurred on the starch chains.

For dual-modified starch, C-OS film showed higher degree of crystallinity than O-CS film. This observation could be explained that crosslinked reaction with boric acid at the position of hydroxyl groups on starch chains did not change the crystalline structure of C-OS film. As a result, the remaining hydroxyl groups of starch chains after the crosslinking reaction could oxidize with hydrogen peroxide, presenting

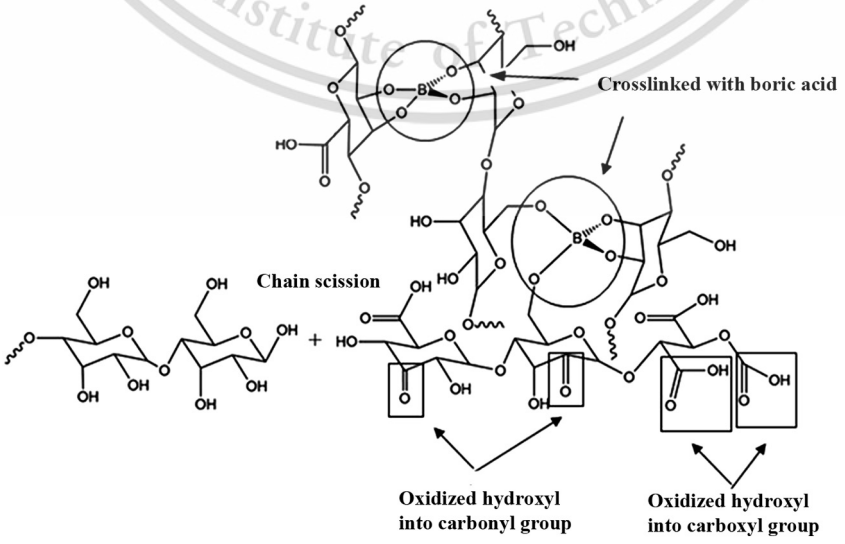

Fig. 1. Schematic of molecular structures of O-CS and C-OS.

Table 1
Degree of crystallinity, percentage of swelling and water vapor permeability of different modified starch films.

	Degree of crystallinity (%)	Swelling (%)			WVP ($g \cdot mm/m^2 \cdot day \cdot KPa$)
		Hour 2	Hour 4	Hour 6	
NS	49.26 ± 0.02	320	360	400	22.19 ± 0.04
CS	49.20 ± 0.02	280	289	293	19.15 ± 0.03
OS	38.36 ± 0.04	290	315	340	20.54 ± 0.04
C-OS	45.27 ± 0.04	215	220	230	15.95 ± 0.03
O-CS	38.74 ± 0.03	265	289	303	16.81 ± 0.02

the decrease of degree of crystallinity of C-OS film. As expected, O-CS film showed lower degree of crystallinity than C-OS film mainly caused by oxidation process. It should be note that the crystallinity of OS and O-CS films was similar because crosslinked reaction with boric acid did not change the crystallinity of the starch [18–20].

3.2. Swelling property

The swelling property of different modified films is presented in Table 1. All of the modified starch films showed lower percentage of swelling than NS film. Comparison between CS and OS films, CS film showed lower of swelling property because of the reduction of hydroxyl group of the starch chains caused by the crosslinking agent [9]. In addition, the oxidation also decreased the swelling power of starch. This could be due to a replacement of hydrophilic hydroxyl groups by more hydrophobic carbonyl groups created by oxidation [12].

For dual-modified films, C-OS film presented lower swelling behavior than O-CS film. This was because the oxidation of O-CS film caused the partial degradation of starch molecules (Fig. 1), leading to more hydrophilic properties than C-OS film. In addition, the crosslinking occurred first, followed by oxidation. This may lead to higher degree of crosslinking, resulting in lower swelling of C-OS film. It should be noted that percentage of swelling of both dual-modified starch films was lower than that of the single-modified starch film. This was because dual-modification by crosslinking and oxidation decreased hydroxyl groups in starch structure, causing lower hydrophilic properties. Our result was also in agreement with M.M.S. Rivera et al. (2006), who reported that the solubility of oxidized banana starch was clearly lower than NS [16]. From this study, the lowest and the highest of percentage of swelling were obtained from C-OS and NS film, respectively.

3.3. Water vapor permeability

Water vapor permeability of different modified starch films was investigated and shown in Table 1. WVP of the films related to the amount of water vapor that diffused through the film. It was found that water resistant properties of NS film could be enhanced by both single and dual modifications. CS film showed lower WVP than that of NS film. This was because the crosslinked modification caused the decreasing of hydroxyl group, leading to the decreasing in hydrophilic properties [27]. Moreover, OS film also exhibited lower WVP than NS film. The changes in WVP can be explained by oxidation reaction, creating the decrease of hydrophilic hydroxyl groups; therefore, the capacity of the film to absorb water vapor of OS film was reduced.

For dual-modified starch films, C-OS film showed lower WVP value than O-CS film. This could be because the crystalline structure of the film was not destroyed by crosslinking reaction (Table 1) and remaining hydroxyl group after crosslinking process could be further oxidized. The oxidation could create the partial chain scission of starch chains (Fig. 1), which could increase the hydrophilicity of starch molecules. When compared with single-modified films, WVP values of both dual-modified starch films were lower than those of single-modified starch films, caused by the decreasing of hydroxyl group in starch structure. The WVP results of all biodegradable films also related to the swelling properties. Furthermore, the lowest WVP was observed from C-OS film; while, NS film showed the highest of WVP value.

3.4. Morphology

Morphology of different modified starch films is shown in Fig. 2. The results demonstrated that different modified starch films presented different morphology. The morphology of NS film (Fig. 2(a)) was rather rough with the presence of some starch granules. Moreover, CS film (Fig. 2(b)) also showed more starch granules than NS film (Fig. 2(a)). Similar result was also found for the structural properties of chemically modified Chinese yam starch and their films [28]. On the other hand, OS film (Fig. 2(c)) showed relatively smooth and more homogeneous morphology than NS and CS films. This result caused by damaging of NS granules resulting from oxidation process [11,12].

When the dual-modified films were observed, C-OS film (Fig. 2(d)) showed rough fractured surface. This could relate to cross-linking reaction of C-OS film. In addition, O-CS film showed smoother surface (Fig. 2(e)) when compared with C-OS film caused by destruction of NS granules producing from oxidation process.

3.5. Mechanical properties

It was shown in Fig. 3 that stress at maximum load and Young's modulus of CS film were higher than those of NS, OS and O-CS films. On the other hand, percentage strain of maximum load of CS film was lower than those of the films. This result was caused by the crosslinking of starch. Boric acid cross-linker caused the restriction the molecular motion of starch molecules (Fig. 1), resulting in the stabilization of the starch molecule [4]. This was related to fractured surface morphology from SEM micrograph (Fig. 2(b)). The stress maximum of CS film was higher than that of NS film, related to morphology in Fig. 2. Similar result was reported for the structural properties of chemically modified Chinese yam starch and their films [28].

On the other hand, OS film showed the enhancement of the strain at maximum load, led to the drop of stress at maximum load and Young's modulus. The increment of strain at maximum load for OS film might be due to the reduction of degree of hydrogen bonding caused by hydroxyl groups, which allowed starch molecules to move easily. The result was related to increased flexibility of the chains in the amorphous region of the film by oxidation process [12].

Additionally, the dual-modified of C-OS and O-CS films showed better overall mechanical properties than the single-modified starch films of CS and OS. C-OS film showed the raise in stress at maximum load and Young's modulus when compared with NS film and the increase in strain at maximum load when compared to NS and CS films. This result was attributed to the stabilization of the starch molecule. Besides, O-CS showed the enhancing in strain at maximum load when compared with the NS and C-OS film. This observation was due to the disruption of hydrogen bonding of starch chain after oxidation process. The highest of stress at maximum load and Young's modulus was obtained from CS film. On the other hand, the highest of strain at maximum load was observed from OS film. From this study, both dual-modified starch films were found to show not only good strength but also elongation.

3.6. Biodegradability

Fig. 4 showed the effect of soil burial test on tensile properties of different biodegradable films. It can be seen that stress at maximum load, Young's modulus and strain at maximum load of different single- and dual-modified starch films significantly decreased with the increase of the burial time. The decrease of mechanical properties was due to the absorption of the water from soil and the degradation by microorganisms existed in soil. The moisture absorbing characteristics of starch sample led to the decrease in tensile properties [29].

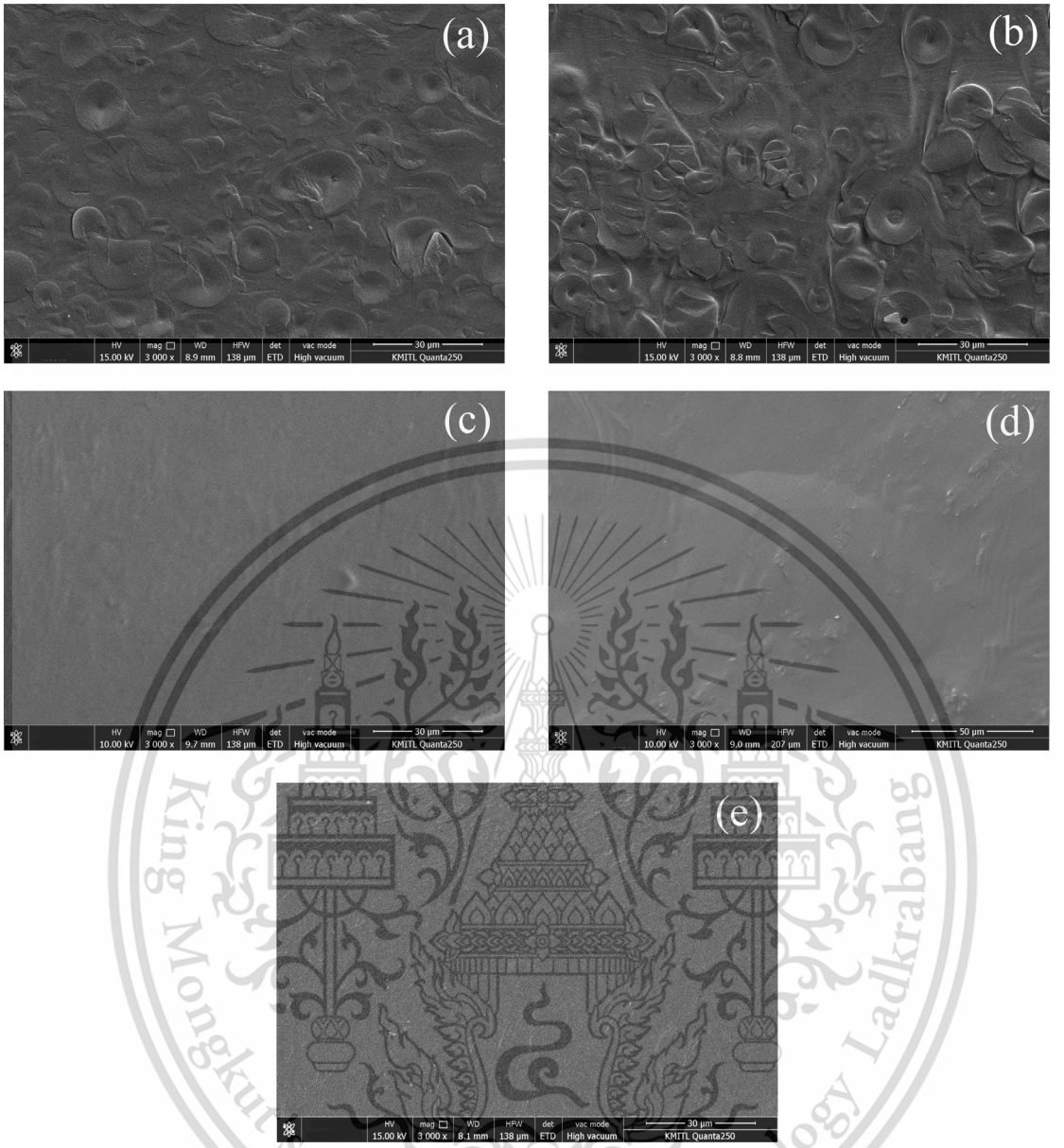

Fig. 2. Cross section morphology of different modified starch films at magnification 3000× (a) NS (b) CS (c) OS (d) C-OS and (e) O-CS.

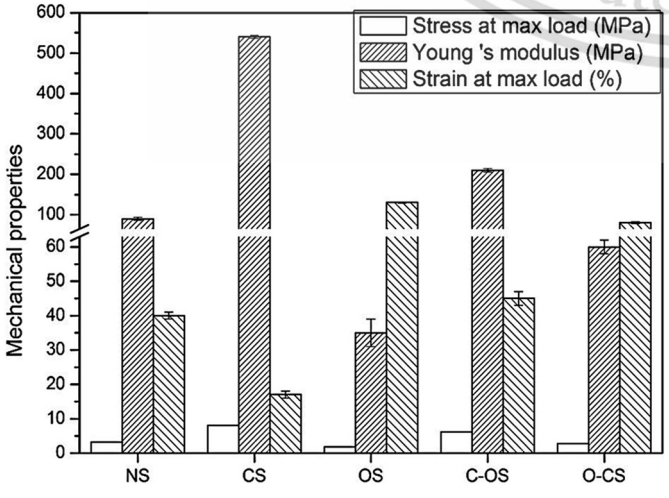

Fig. 3. Mechanical properties of different modified starch films.

3.7. Thermal properties

Thermogravimetric (TGA) and derivative thermogravimetric (DTG) thermograms of various modified starch films are shown in Fig. 5 and Table 2. The three steps of weight loss were obtained. The initial step lower than 100 °C was merely due to evaporation of the absorbed moisture. The second step at a temperature of about 150–200 °C was due to the decomposition of glycerol plasticizer. In addition, the degradation temperature of approximately 280–350 °C was due to the decomposition of starch. The result showed that CS film showed the higher thermal degradation temperature than NS film. This fact may be attributed to the increase in the intermolecular forces due to the presence of boric acid-crosslinked starch networks (Fig. 1) [30].

For OS film, the oxidation process led to the decrease of the main degradation temperature of starch as compared with NS film. This was attributed to a progressive reduction in inter-chain hydrogen bonding (or molecular weight) produced by replacement of hydroxyl groups with carbonyl and carboxyl groups and the disintegration of the starch structure (Fig. 1) [31].

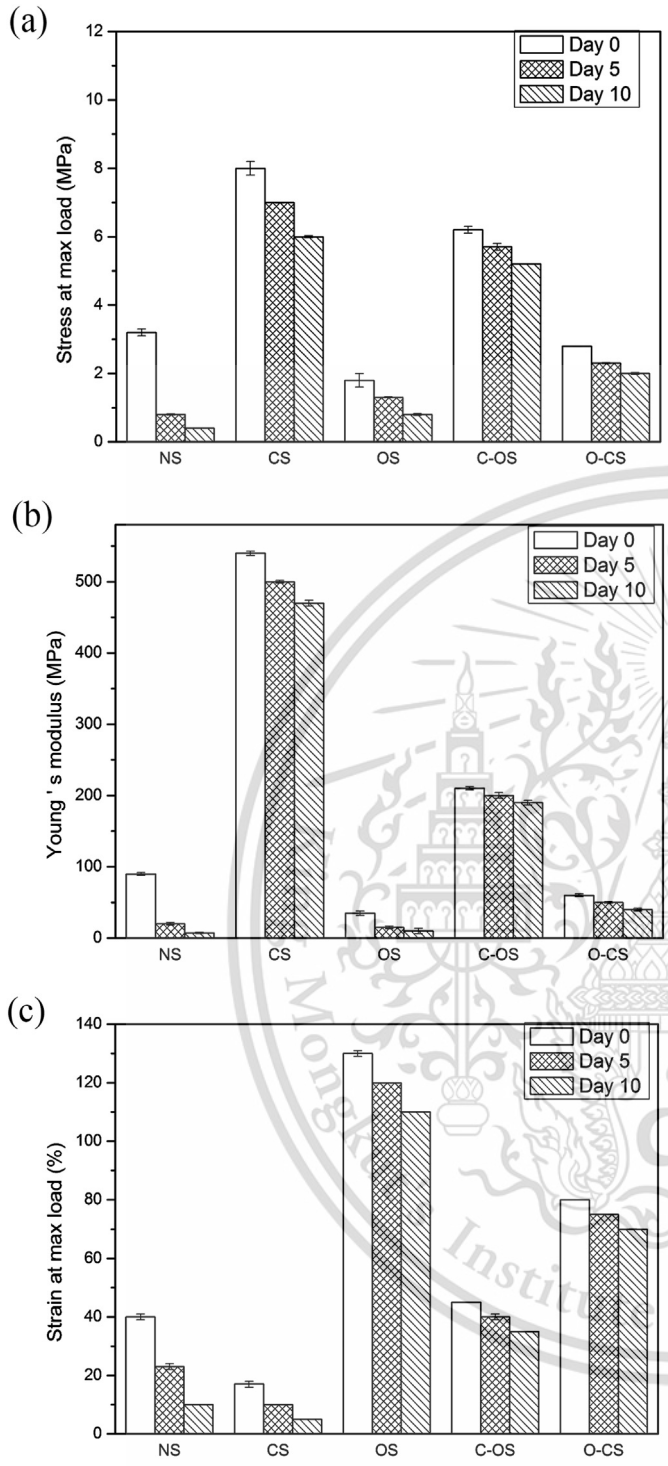

Fig. 4. Tensile properties after biodegradation tests for different modified starch films (a) stress at maximum load (b) Young's modulus and (c) strain at maximum load.

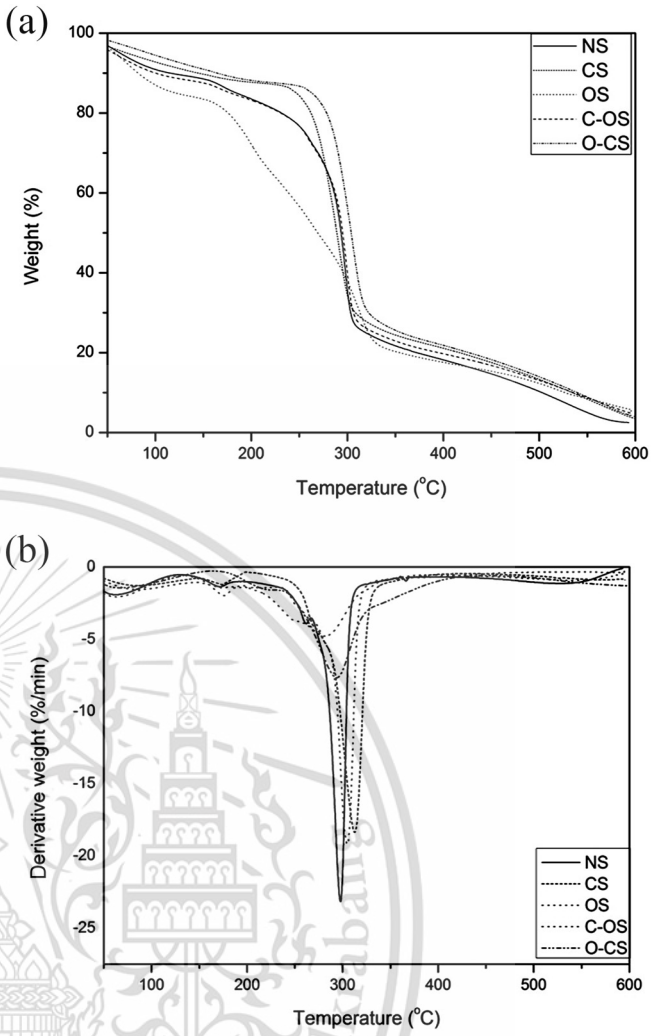

Fig. 5. (a) TGA and (b) DTG thermograms of different modified starch films.

4. Conclusion

Dual modification by crosslinking and oxidation for starch can improve various properties of NS film. The decrease of degree of crystallinity for O-CS and C-OS film was obtained after the modification processes. In terms of morphology, O-CS film was smoother than C-OS and NS film. Both dual-modified films showed the improvement of both strength and extendibility than NS film. As compared to NS and single-modified starch film, swelling and WVP results of the dual-modified starch films; i.e. C-OS and O-CS film were clearly lowered. Besides, C-OS film presented higher thermal degradation temperature than NS and OS film. From biodegradation test, all films, i.e. NS, single- and dual-modified starch films showed the ability to degrade. From this study, both C-OS and O-CS dual-modified films, especially for C-

Besides, C-OS film contained higher thermal degradation temperature than O-CS film, but lower than CS film. This was because crosslinking could strengthen the connection of starch granules (Fig. 1) and improve thermal stability of starch structure by producing new chemical bonds. On the other hand, O-CS film contained lower thermal degradation temperature than C-OS film, because the hydroxyl groups of O-CS film were degraded by the oxidation process, causing lower degradation temperature. The highest of thermal degradation temperature was obtained from CS film. In contrast, OS film presented the lowest of thermal degradation temperature.

Table 2
Degradation temperatures of different biodegradable films with various modified starch obtained from TG and DTG thermograms.

	Degradation temperature (°C)		
	Step 1	Step 2	Step 3
NS	62.6	171.3	297.5
CS	71.4	196.2	310.5
OS	91.8	198.1	287.4
C-OS	72.6	176.1	300.9
O-CS	97.7	152.6	292.0

OS film, presented not only greater strength but also elongation, lower swelling and lower WVP than those of CS and OS single-modified films.

Acknowledgements

The authors express their sincere appreciation to KMITL Research Fund (KREF 045612) for supporting the study financially.

References

[1] A. Jimenez, M.J. Fabra, P. Talens, A. Chiralt, Edible and biodegradable starch films: a review, Food Bioprocess Technol. 5 (2012) 2058–2076.
[2] F. Garavand, M. Rouhi, S.H. Razavi, I. Cacciotti, R. Mohammadi, Improving the integrity of natural biopolymer films used in food packaging by crosslinking approach: a review, Int. J. Biol. Macromol. 104 ((2017) 687–707.
[3] E.R. Zavareze, V.Z. Pinto, B. Klein, S.L.M. Halal, M.C. Elias, C. Prentice-Hernández, A.R.G. Dias, Development of oxidised and heat–moisture treated potato starch film, Food Chem. 132 (2012) 344–350.
[4] N. Reddy, Y. Yang, Citric acid cross-linking of starch films, Food Chem. 118 (2010) 702–711.
[5] W. Vorwerg, J. Dijksterhuis, J. Borghuis, S. Radosta, A. Kröger, Film properties of hydroxypropyl starch, Starch-Stärke 56 (2004) 297–306.
[6] R. Colussi, V.Z. Pinto, S.L.M. El Halal, B. Biduski, L. Prietto, D.D. Castilhos, E.D.R. Zavareze, A.R.G. Dias, Acetylated rice starches films with different levels of amylose: mechanical, water vapor barrier, thermal, and biodegradability properties, Food Chem. 221 (2017) 1614–1620.
[7] B. Sreedhar, D.K. Chattopadhyay, M.S.H. Karunakar, A.R.K. Sastry, Thermal and surface characterization of plasticized starch polyvinyl alcohol blends crosslinked with epichlorohydrin, J. Appl. Polym. Sci. 101 (2006) 25–34.
[8] X. Wang, Z. Gu, H. Qin, L. Li, X. Yang, X. Yu, Crosslinking effect of dialdehyde starch (DAS) on decellularized porcine aortas for tissue engineering, Int. J. Biol. Macromol. 79 (2015) 813–821.
[9] Y. Yin, J. Li, Y. Liu, Z. Li, Starch crosslinked with poly(vinyl-alcohol) by boric acid, J. Appl. Polym. Sci. 96 (2005) 1394–1397.
[10] S.H. Koo, K.Y. Lee, H.G. Lee, Effect of cross-linking on the physicochemical and physiological properties of corn starch, Food Hydrocoll. 24 (2010) 619–625.
[11] F. Zhou, Q. Liu, H. Zhang, Q. Chen, B. Kong, Potato starch oxidation induced by sodium hypochlorite and its effect on functional properties and digestibility, Int. J. Biol. Macromol. 84 (2016) 410–417.
[12] F. Martínez-Bustos, S.L. Amaya-Llano, J.A. Carbajal-Arteaga, Y.K. Chang, J.J. Zazueta.-Morales, Physicochemical properties of cassava, potato and jicama starches oxidised with organic acids, J. Sci. Food Agric. 87 (2007) 1207–1214.
[13] F.F. Takizawa, G.O. Silva, F.E. Konkel, I.M. Demiate, Characterization of tropical starches modified with potassium permanganate and lactic acid, Braz. Arch. Biol. Technol. 47 (2004) 921–931.
[14] L.J. Tornepor, A.C. Salomonsson, O. Theander, Chemical characterization of bromine oxidized potato starch, Starch-Stärke 42 (1990) 413–417.
[15] A.R.G. Dias, E.R. Zavareze, E. Helbig, F.A. Moura, C.G. Vargas, C.F. Ciacco, Oxidation of fermented cassava starch using hydrogen peroxide, Carbohydr. Polym. 86 (2011) 185–191.
[16] M.M.S. Rivera, G.M. Montealvo, C.N. Santiago, J.R. Millan, Y.J. Wang, L.A.B. Péreza, Physicochemical properties of banana starch oxidized under different conditions, Starch-Stärke 61 (2009) 206–213.
[17] S.D. Zhang, Y.R. Zhang, X.L. Wang, Y.Z. Wang, High carbonyl content oxidized starch prepared by hydrogen peroxide and its thermoplastic application, Starch-Stärke 61 (2009) 646–655.
[18] J. Liu, B. Wang, L. Lin, J. Zhang, W. Liu, J. Xie, Y. Ding, Functional, physicochemical properties and structure of cross-linked oxidized maize starch, Food Hydrocoll. 36 (2014) 45–52.
[19] S. Sukhija, S. Singh, C.S. Riar, Effect of oxidation, cross-linking and dual modification on physicochemical, crystallinity, morphological, pasting and thermal characteristics of elephant foot yam (*Amorphophallus paeoniifolius*) starch, Food Hydrocoll. 55 (2016) 56–64.
[20] F. Sun, J. Liu, X. Liu, Y. Wang, K. Li, J. Chang, G. Yang, G. He, Effect of the phytate and hydrogen peroxide chemical modifications on the physicochemical and functional properties of wheat starch, Food Res. Int. 100 (2017) 180–192.
[21] K.S. Woo, P.A. Seib, Cross-linked resistant starch: preparation and properties 1, Cereal Chem. 79 (2002) 819–825.
[22] L. Kaur, J. Singh, N. Singh, Effect of cross-linking on some properties of potato (*Solanum tuberosum* L.) starches, J. Sci. Food Agric. 86 (2006) 1945–1954.
[23] R.E. Wing, J.L. Willett, Water soluble oxidized starches by peroxide reactive extrusion, Ind. Crop. Prod. 7 (1997) 45–52.
[24] P. Tolvanen, A. Sorokin, P. Maki-Arvela, S. Leveneur, D.Y. Murzin, T. Salmi, Batch and semibatch partial oxidation of starch by hydrogen peroxide in the presence of an iron tetrasulfophthalocyanine catalyst: the effect of ultrasound and the catalyst addition policy, Ind. Eng. Chem. Res. 50 (2011) 749–757.
[25] R.L. Whistler, J.N. Bemiller, Alkaline degradation of polysaccharides, in: M.L. Wolfrom (Ed.), Advance in Carbohydrate Chemistry, Academic Press Inc. Publisher, New York 1958, pp. 315–317.
[26] F. Carlos-Amaya, P. Osorio-Diaz, E. Agama-Acevedo, H. Yee-Madeira, L.A. Bello-Perez, Physicochemical and digestibility properties of double modified banana (*Musa paradisiaca* L.) starches, J. Agric. Food Chem. 59 (2011) 1376–1382.
[27] B. Ramaraj, Crosslinked poly(vinyl alcohol) and starch composite films. II. Physicomechanical, thermal properties and swelling studies, J. Appl. Polym. Sci. 103 (2007) 909–916.
[28] L. Wang, X. Liu, J. Wang, Structural properties of chemically modified Chinese yam starches and their films, Int. J. Food Prop. 20 (2017) 1239–1250.
[29] H.C. Obasi, F.N. Onuoha, I.O. Eze, S.C. Nwanonenyi, I.O. Arukalam, P.C. Uzoma, Effect of soil burial on properties of polypropylene (PP)/plasticized potato starch (PPS) blends, Int. J. Eng. Sci. 2 (2013) 14–18.
[30] B. Sreedhar, M. Sairam, D.K. Chattopadhyay, P.A. Syamala Rathnam, D.V. Mohan Rao, Thermal, mechanical, and surface characterization of starch–poly(vinyl alcohol) blends and borax-crosslinked films, J. Appl. Polym. Sci. 96 (2005) 1313–1322.
[31] L. Zhang, P. Liu, Y. Wang, W. Gao, Study on physico-chemical properties of dialdehyde yam starch with different aldehyde group contents, Thermochim. Acta 512 (2011) 196–201.

Author Biography

Name	Mr.Yossathorn Tanetrungroj
Date of Birth	18 January 1989
Address	492/3 Itsarapap road, Siriraj, Bangkok noi, Bangkok 10700
Education	(2010) Bachelor of science in industrial chemistry (King Mongkut's Institute of Technology Ladkrabang)
	(2015) Bachelor of business administration (Sukhothai Thammathirat Open University)
	(2013) Master of science in polymer technology (King Mongkut's Institute of Technology Ladkrabang)
Scholarship	-
Academic Publications	

1. Y. Tanetrungroj and J. Prachayawarakorn. 2013. “Effect of arrowroot starch contents on properties of biodegradable thermoplastic starch and low-density polyethylene blends using injection molding technique 344-348. In The 39th Congress on Science and technology of Thailand (STT-39), Bangkok
2. Y. Tanetrungroj and J. Prachayawarakorn, 2015. “Effect of starch types on properties of biodegradable polymer based on thermoplastic starch process by injection molding technique” Songklanakarin Journal of Science and Technology, 37(2) : 193-199.
3. Y. Tanetrungroj and J. Prachayawarakorn, 2017. “Preparation and properties of oxidized starch using hydrogen peroxide as oxidizing agent.” 1451-1454 In Pure and Applied Chemistry international conference 2017 (PACCON 2017).
4. Y. Tanetrungroj and J. Prachayawarakorn, “Preparation and properties of crosslinked starch using borax as a crosslinking agent” 59-63. In International Polymer Conference of Thailand 2017 (PCT-7). Bangkok.
5. Y. Tanetrungroj and J. Prachayawarakorn, 2018. ”Effect of dual modification on properties of biodegradable crosslinked-oxidized starch and oxidized-crosslinked starch films” International Journal of Biological Macromolecules, 120: 1240-1246.
6. Y. Tanetrungroj and J. Prachayawarakorn.2019. “Influence of different crosslinking agents on property improvement of biodegradable dual-modified starch films prepared by

crosslinked-oxidized method" Innovative Food Science and Emerging Technologies (IFSET)." Submitted for publication